Ruthenium metallotherapeutics: A targeted approach to combatting multidrug resistant pathogens.

Nicole Sophie Britten

PhD 2023

Ruthenium metallotherapeutics: A targeted approach to combatting multidrug resistant pathogens.

Nicole Sophie Britten

A thesis submitted in partial fulfilment of the requirements of Manchester Metropolitan University for the degree of Doctor of Philosophy.

Department of Life Sciences

Manchester Metropolitan University

2023

Table of Contents

Contents

List of Figures

List of Tables

Abbreviations

ABD ATP binding cassette

AMR Antimicrobial Resistance

ATP Adenosine triphosphate

CFU Colony Forming Units

CLSI clinical and Laboratory Standards Institute

CORM Carbon Monoxide Releasing Molecule

DMEM Dulbecco's Modified Eagle Media

DMSO Dimethyl sulphate

DNA Deoxyribonucleic acid

DPBS Dulbecco's Phosphate-Buffered Saline

ECM Extracellular Matrix

EGF Epidermal Growth Factor

EGF Epidermal Growth Factor

EMEM Eagle's Minimum Essential Medium

ESPAUR English Surveillance ProGramme for Antimicrobial Utilisation and Resistance

EUCAST European Committee on Antimicrobial Susceptibility Testing

FBS Foetal Bovine Serum

FIC Fractional Inhibitory Concentration

GO Gene Ontology

IC_{50} Inhibitory Concentration 50%

IGF Insulin-like Growth Factor

IgG Immunoglobulin G

IL Interleukin

kDa KiloDalton

KEGG Kyoto encyclopaedia of genes and genomes

MBC Minimum Bactericidal Concentration

MFS Major Binding Facilitator

MGE Mobile Genetic Elements

MHA Mueller Hinton Agar

MHB Mueller Hinton Broth

MIC Minimum Inhibitory Concentration

MRSA Methicillin-Resistance *Staphylococcus aureus*

NETs Neutrophil Extracellular Traps

OD Optical Density

PBS Phosphate Buffered Saline

PDGF Platelet Derived Growth Factor

RMPI Roswell Park Memorial Institute

RNA Ribonucleic acid

RND Resistance-Nodulation-Division

ROS Reactive Oxygen Species

RT-qPCR Reverse Transcriptase quantitative Polymerase Chain Reaction

Ru Ruthenium

SEM Scanning Electron Microscopy

TGF-β Transforming Growth Factor Beta

VEGF Vascular endothelial growth factor

µg microGram

µL microliter

µM micromolar

Abstract

The discovery of antibiotics revolutionised healthcare practice. However due to overuse, inappropriate use, widespread prophylaxis therapy and the lack of new developments, the threat of antimicrobial resistance is now a major global threat to health. By 2050, it is estimated that mortality due to antimicrobial resistant infections will exceed 10 million people per annum, superseding cancer as the leading cause of global mortality. The use of drug repurposing to identify potential therapies which combat antimicrobial resistance is one potential solution. Metals have been used as antimicrobial agents throughout the history of medicine for a broad range of applications, including the use of Silver as an antimicrobial agent which dates back to antiquity. More recently, Ruthenium metallotherapeutic complexes have been shown to exhibit highly active antimicrobial properties by targeting a range of bacterial species, and in contrast to traditional antibiotics, these compounds are thought to elicit antibacterial activity at multiple sites within the bacterial cell, which may reduce the possibility of resistance evolution. This study aimed to evaluate the antimicrobial activity of a series of Ruthenium metallotherapeutic complexes against multidrug-resistant bacterial pathogens, with a focus on use within wound care applications.

Antimicrobial susceptibility assays identified two lead candidates, Hexaammineruthenium (III) chloride and [Chlorido(η6-p-cymene)(N-(4-chlorophenyl)pyridine-2-carbothioamide) ruthenium (II)] chloride which demonstrated activity against *Pseudomonas aeruginosa* and *Staphylococcus aureus* respectively with MIC values ranging between 4 µg mL^{-1} and 16 µg mL^{-1}. Furthermore, Hexaammineruthenium (III) chloride demonstrated antibiofilm activity in both a time and concentration-dependent manner. Synergy studies combining lead complexes with antibiotics demonstrated the

potential for use as resistance breakers. Subsequent *in vitro* infection modelling using scratch assays with skin cell lines, coupled with a 3D full thickness skin wound infection model was used to determine potential applied applications of Hexaammineruthenium (III) chloride for use as topical antimicrobial agent against *P. aeruginosa* infections.

Antimicrobial mechanistic studies demonstrated that Hexaammineruthenium (III) chloride targeted the bacterial cell ultrastructure of *P. aeruginosa* strain PAO1 as cell perturbations were observed when treated cells were analysed by scanning electron microscopy. Furthermore, exposure of *P. aeruginosa* PAO1 to Hexaammineruthenium (III) chloride also resulted in a concentration dependent membrane depolarisation, which further supported the antimicrobial mechanistic role.

Finally, global changes in gene expression following exposure of *P. aeruginosa* strain PAO1 to Hexaammineruthenium (III) chloride were explored by RNA sequencing. Genes involved in ribosome function, cofactor biosynthesis and membrane fusion were downregulated, which provided a further insight into the wider mechanisms of antibacterial activity.

The research conducted in the present study indicated the potential use of Hexaammineruthenium (III) chloride (and derivatives) as a potential treatment option for chronic wounds infected with *P. aeruginosa*, which could be applied as either a direct treatment or used within antimicrobial wound care applications.

Declaration and Copyright Statements

Declaration

No portion of the work referred to in this thesis has been submitted in support of an application for another degree or qualification of this or any other university or institute of learning.

Signed.....(candidate) Date.....

Statement 1

This thesis is being submitted in partial fulfilment of the requirements for the degree of PhD.

Signed.....(candidate) Date.....

Statement 2

This thesis is the result of my own independent work/investigation, except where otherwise stated. Other sources are acknowledged by explicit references.

Signed.....(candidate) Date.....

Statement 3

I hereby give consent for my thesis, if accepted, to be available for photocopying and for interlibrary loan, and for the title and summary to be made available to outside organisations.

The Author

The author has published successfully the following manuscripts during the PhD degree:

Lu, H., Butler, J.A., Britten, N.S., Venkatraman, P.D. and Rahatekar, S.S., 2021. Natural antimicrobial nano composite fibres manufactured from a combination of alginate and oregano essential oil. *Nanomaterials*, *11*(8), p.2062.

Britten, N.S. and Butler, J.A., 2022. Ruthenium Metallotherapeutics: Novel Approaches to Combatting Parasitic Infections. *Current Medicinal Chemistry*, *29*(31), pp.5159-5178.

Venkatraman, PD, Butler, JA, Britten, NS. (2023). Advances in medical textiles. In: Subhankar, M, Kunal, S, Pintu, P. (Ed). *Functional and Technical Textiles*. Kidlington: Woodhead Publishing. pp.31-70.

The author has presented at the following conferences:

British Society for Antimicrobial Chemotherapy Into Clinical Practice: Meeting the Challenges of Gram-negative Infection Management 2021, London 14th October 2021 In person

International Biodeterioration and Biodegradation Society's Symposium 'IBBS 18' Online where an award was received: Top Poster Presentation Award. 6-9th September 2021.

The Microbiology Society Annual conference 2022 Belfast 4-7th April 2022 In Person

COVID-19 Impact statement

The progress of this PhD was significantly impacted due to the COVID-19 pandemic. Access to the laboratory was restricted throughout this degree in both lockdowns, which overall resulted in 10 months of laboratory work being impeded. Although much as been done to rectify this, there are areas of this project that could not have been completed during the time frame overall resulting in a negative impact to the project and impacting on my ability to generate data for this thesis. Additional university restrictions have been implemented following construction of the building meaning that cellular facilities were inaccessible for months resulting in a loss of cells and shut down of certain areas resulting in further restrictions to the work conducted.

Acknowledgements

Firstly, I would to thank my supervisor Dr Jonathan Butler for the support and guidance during these past few years. For giving me the opportunity to continue my research and pursue this PhD. We have had many trials and triumphs together and it is with your help that I am where I am today. You have not only been my supervisor, but my friend and I look forward to collaborating in the future.

To the technical staff, you always assist students to the best of your ability and have been there when I was in need of assistance. I will forever be grateful and I hope you realise how valuable you are to us all. To my friends who have supported me all the way through this journey, even though you may not have understood it all fully, you still cheered me on and picked me up when I was down.

To Amelia, I couldn't have done this without you. You have been there through the good times and bad, helping me troubleshoot and generate new ideas thank you, especially for all your help with the wound model.

To Shaun, you have given me a home the last few years and have supported me through all of the ups and downs this journey has taken me through and provided guidance when I needed it. Thank you for everything.

Finally, I would like to thank my Mom and Dad. I could not have completed this journey without you. You have encouraged me through every step and allowed me to pursue it. You have been there to lend an ear when I have struggled, listened to me talk about ideas and supported me in every avenue. You are the reason why I am here today and are able to submit this work. I will be forever grateful of this opportunity, I cannot thank you both enough and I hope that I make you proud.

Chapter 1: Introduction

1.1 Background

Antibiotics have been a vital healthcare component since the discovery of penicillin in 1928 which revolutionised medical practices for combatting infectious diseases. Advances in medicine have seen more antibiotics being discovered leading to better treatments of bacterial infections, however overuse within the population and lack of research in this area has led to an increase in resistant bacterial strains. Antimicrobial resistance (AMR) contributes to more deaths in the US than HIV/AIDS, Parkinson's disease and homicide combined in 2006 (Cole, 2014). Currently, mortality associated with AMR is estimated at 25,000 people per annum in Europe (Blair *et al.*, 2015; Gajdács *et al.*, 2021) resulting in excess of €1.5 billion in healthcare costs (Cole, 2014). Deaths associated with AMR infections are expected to exceed 10 million by 2050, overtaking cancer as a leading cause of global mortality (Srivastava *et al.*, 2019).

Inappropriate overuse of antibiotics is the primary cause for the rise of AMR with an estimated 30-50% of prescriptions being incorrectly supplied (Ventola, 2015). Additionally a lack of drug development prevented resistant bacteria from being treated (Fig. 1). In 2016 over 60 tonnes of antibiotics were used in UK hospitals and overall consumption in the USA for both human and animal use totalled 8361 tonnes (Hardie, 2020). Prophylactic use of antibiotics in animals is another cause, building resistance in bacteria and can transmit resistant strains to humans through horizontal gene transfer (Džidic *et al.*, 2007). Antibiotics are used extensively in animal husbandry to improve animal health and produce larger yields of higher quality meat. In the USA, 80% of antibiotics sold are for prophylactic use in animals, significantly contributing to the resistance crisis (Ventola, 2015). Bacterial resistance may evolve towards such antibiotics and transmit to humans through the food chain (Nathan, 2004).

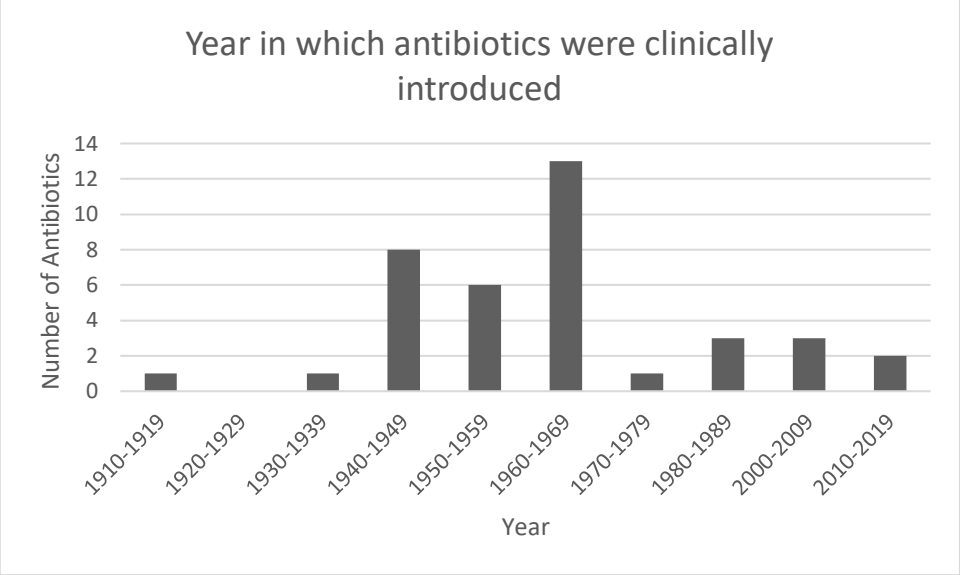

Figure 1. 1: Introduction of the number of antibiotics discovered over the past century adapted from (Hutchings et al, 2019).

Additionally as a result of the Severe Acute Respiratory Syndrome Coronavirus 2 (SARS-CoV-2) pandemic in 2020, antimicrobial prescribing has increased throughout the duration of this period (Rawson *et al*,. 2020), potentially increasing antimicrobial resistance in bacteria. In a study conducted by Russell *et al*, during the course of the pandemic out of 48,902 patients who tested positive for COVID-19 in the UK, 85.2% of patients received antibiotic treatment with only 2.2% actually having a bacterial infections, with *S. aureus* being one of the most commonly isolated pathogens (Russell *et al*., 2021).

1.2 Mechanisms of resistance

Bacterial resistance mechanisms have evolved to protect against antimicrobial therapy. There are five main mechanisms including antibiotic inactivation (Džidic *et al.*, 2008), drug target modification (Munita and Arias, 2016), creation/activation of efflux pumps (Cox and Wright, 2013), target bypass and changing the outer membrane to become less susceptible to the antibiotics (Džidic *et al.*, 2008). Bacterial mutations and horizontal gene transfer

greatly contribute to conferring resistance (Giedrotiene *et al.*, 2011). There is an urgent need to identify and develop novel antimicrobial complexes which can overcome such resistance mechanisms and be used to treat the most serious of AMR infections.

1.2.1 Resistance mediated by genetic mutations

Mechanisms of resistance caused by genetic alterations are pivotal in allowing the bacteria to become resistant. Spontaneous mutations may occur through errors during replication of the bacterial genome or failure of DNA repair mechanisms. Point mutations within the DNA can produce a resistance phenotype within the bacterium, affecting antibiotic targets or expression of certain porins (Džidic *et al*, 2008). Chromosomal mutations occur in bacteria; roughly 1 in $1x10^{6-8}$ (Giedratiene *et al*, 2011) and commonly confer resistance to structurally related components. For example, Rifampicin resistance occurs due to amino acid substitutions within the gene *rpoB* inhibiting enzymatic activity of DNA gyrase and topoisomerase IV, thus altering the DNA replication in the bacterium (Munita and Arias, 2016).

Hyper mutations are regulated by SOS inducible mutator DNA polymerase IV, which repairs DNA when damage and arrest of the cell cycle has occurred. Inactivation of *mutS* and *mutL* genes generate a resistant phenotype in the bacteria due to a defective mismatch repair system. This prevents the repair system eliminating biosynthetic errors (Džidic *et al*, 2008).

The final type of mutation is adaptive, occurring in slow and non-dividing bacterial cells caused by the selective pressures exhibited in the presence of non-lethal, favourable pressures (Džidic *et al*, 2008). The main cause of resistance originating under normal conditions (Giedratiene *et al*, 2011) is due to bacterial stress and errors encoded in DNA polymerase V and IV (Džidic *et al*, 2008).

1.2.2 AMR mediated by horizontal gene transfer

Horizontal gene transfer is able to confer resistance genes through viral transfer, plasmids and free DNA (Giedraitiene *et al*, 2011) which are incorporated into the bacterial chromosome through the process of recombination. Some genes are grouped together in clusters and are transferred with the assistance from integrons (Džidic *et al*, 2008). Within healthcare settings, plasmid conjugation is the most common form of transfer due to its efficiency and use of mobile genetic elements (MGEs) such as large plasmids and bacteriophages which share genetic material through cell-to-cell contact. Mobile gene cassettes are an efficient way of transferring new genes into the bacterial chromosome through integrons providing the necessary machinery to enable expression within the chromosome (Munita and Arias, 2016). An example of this is the β- lactamase encoding cassette found in bacteria such as *S. aureus* (Partridge *et al*., 2018).

1.2.3 Direct inactivation of antibiotics

Antibiotic inactivation occurs through three different processes: hydrolysis, group transfer and redox. Hydrolysis cleaves bonds in the antibiotics leading to the loss of activity (Džidic *et al*, 2008). A notable example of this is the resistance mechanism to penicillin by *Staphylococcus aureus*, where expression of the *blaZ* gene encodes a β-lactamase enzyme which hydrolyses the β-lactam ring structure (Lowy, 2003). Group transfer involves chemical substitution of either an adenylyl, acetyl or phosphoryl group to the antibiotic altering the ability to target Penicillin Binding Protein (PBP2) (Džidic *et al*, 2008). The *blaZ* gene is under the control of a repressor encoded by *blaI*. The presence of β-lactam antibiotics is detected by the *blaRI* encoded sensor, which causes the depression of *blaI* and subsequent expression of BlaZ and further BlaRI. Aminoglycoside based antibiotics are found to be particularly vulnerable to this process due to the increased exposure of hydroxyl and amide

groups present on the large molecule (Blair *et al*,. 2015). There are three classes of enzymes; phosphotransferases, acetyltransferases and nucleotidyltransferases which are found to alter the antibiotic frequently due to their ability to mimic the ribosomal binding cleft in their active sites (Romanowska *et al*,. 2013).

1.2.4 Bacterial target modification to reduce antibiotic activity

Target modification is a vital resistance mechanism carried by MGEs and can confer protection against antibiotics (Munita and Arias, 2016), thereby preventing correct antibiotic target binding with subsequent loss of antibiotic activity. An example of this mechanism is the alteration of peptidoglycan causing a change from alanine to lactate at the C-terminus which the antibiotic vancomycin fails to recognise (Džidic *et al*, 2008) and prevents crosslink blockages of the cell wall therefore the antibiotic cannot bind to its target site (Lowy, 2003). It may be caused by a mutation such as in the case of Rifampicin resistance or enzymes encoded by the *erm* genes in bacteria such as MRSA causing ribosome methylation resulting in macrolide resistance by enzymatic alteration of the target site (Munita and Arias, 2016). *Erm* methyltransferase enzyme catalyses S-adenosylmethionine methylation of N6 causing a loss of hydrogen bond properties and steric block of the antibiotic binding site (Wright, 2011). Protein synthesis interference occurs at the ribosome through the binding of macrolide antibiotics to the ribosome, this type of resistance is known as macrolides-lincosamides and streptogramins B (MLS(B)) type which prevents antibiotic binding to the 50S subunit (Džidic *et al*, 2008).

1.2.5 The role of efflux pumps in mediating AMR

Efflux pumps are effective at secreting an antibiotic out of the bacterial cell (Džidic *et al*, 2008). In *P. aeruginosa*, the role of the RND pump system termed MexAB-OprM is to export β-lactams and carbapenams out of the cell (Li *et al*, 2015). There are 5 different types of

efflux pump; including major facilitator super (MFS), ATP binding cassette (ABC), multidrug and toxic complex extrusion, small multidrug resistance and resistance-nodulation-cell division. All differing in structure, extrusion of substrates, bacterial organism and energy source (Munita and Arias, 2016). Due to the presence of slow porins, which produce slow permeation of solutes, such as OprF, the bacterial membrane has low outer membrane permeability. OprF and OprD porins for peptide and amino acid diffusion and OprB for glucose uptake are some responsible for the permeability (Li *et al*, 2015). The efflux pumps that are chromosomally encoded confer resistance against multiple antibiotics and generally utilise cellular energy to move the antibiotic against the concentration gradient (Cox and Wright, 2013).

1.2.6 Alterations in the cell ultrastructure to reduce antibiotic uptake

Outer membrane permeability changes occur in Gram-negative bacteria due to the presence of a phospholipid inner membrane which inhibits penetration of antibiotics. Therefore alternate entry methods are used, through the bilayer, porins or self-mediated uptake into the cell (Džidic *et al*, 2008). Protection against antibiotics can be conferred by the presence of a thick peptidoglycan cell wall consisting of teichoic acid polymers and proteins that are covalently bonded together providing strength and resisting changes in osmotic pressure in the cytoplasm. Gram-positive bacteria are able to withstand a permeability threshold of 30-57kDa molecules contributed by a large number of fatty acid chains whereas Gram-negative bacteria have a finer selectivity barrier that nutrients can enter through specialised porins as mentioned above (Cox and Wright, 2013) including *P. aeruginosa*.

1.3 Normal wound healing process

Wounds are caused by a few factors including injury, surgery, and extrinsic factors including burns, cuts and pressure and as a result of certain pathologies such as diabetes or vascular disease (Tottoli *et al*., 2020). Wounds can be categorised as either acute or chronic depending on the effectiveness of the healing process or underlying cause of the initial wound (Karimi *et al*., 2017). The normal wound healing process consists of four phases which begins immediately following injury in order to prevent exsanguination of the patient (Singh *et al*., 2017). Many differing factors affect the healing process including the patients age, disease presence, medications, lifestyle and hormones (Guo and DiPietro., 2010; Bielefeld *et al*., 2013).

1.3.1 Coagulation and Haemostasis

Haemostasis is a process that prevents haemorrhaging within the damaged blood vessel and involves six phases. The first mechanism involves vasoconstriction. Initially vasoconstriction ceases blood flow in affected blood vessels, preventing excess blood loss and the coagulation cascade is initiated with a primary aim to create a clot (Li. J *et al*., 2007). Mast cells during this process release histamine, causing an influx of inflammatory cells to the area (Singh *et al*., 2017). Circulating platelets, intrinsically by Hageman factor XII found in the blood and extrinsically by the wound releasing tissue factor, form a plug (Li. J *et al*., 2007). This is caused by exposing collagen which releases clotting factors to create a clot made of fibronectin, fibrin, thrombospondin and vitronectin (Opneja *et al*., 2019). The alpha granules of platelets are filled with growth factors and cytokines such as Transforming growth factor-β, platelet factor-4 and CXC chemokine ligand-4 which activate and attract endothelial cells, fibroblasts, neutrophils and macrophages to the affected area (Velnar *et al.*, 2009; Opneja *et al*., 2019). (Pallister and Watson, 2010).

The third phase of haemostasis involves the activation of the coagulation cascade. In the extrinsic cascade tissue factor (TF) binds to factor VII (FVII) and activates FX (Periahyah *et al*., 2017). The intrinsic pathway involves factors present in plasma and does not require tissue injury to be activated, instead can be activated through contact with foreign substances such as bacteria. Thrombin aids in the conversion of fibrinogen to fibrin, and additionally activates FXIII which causes fibrin to cross link and form a clot at the injury site (Figure 4.1) (Periahyah *et al*., 2017).

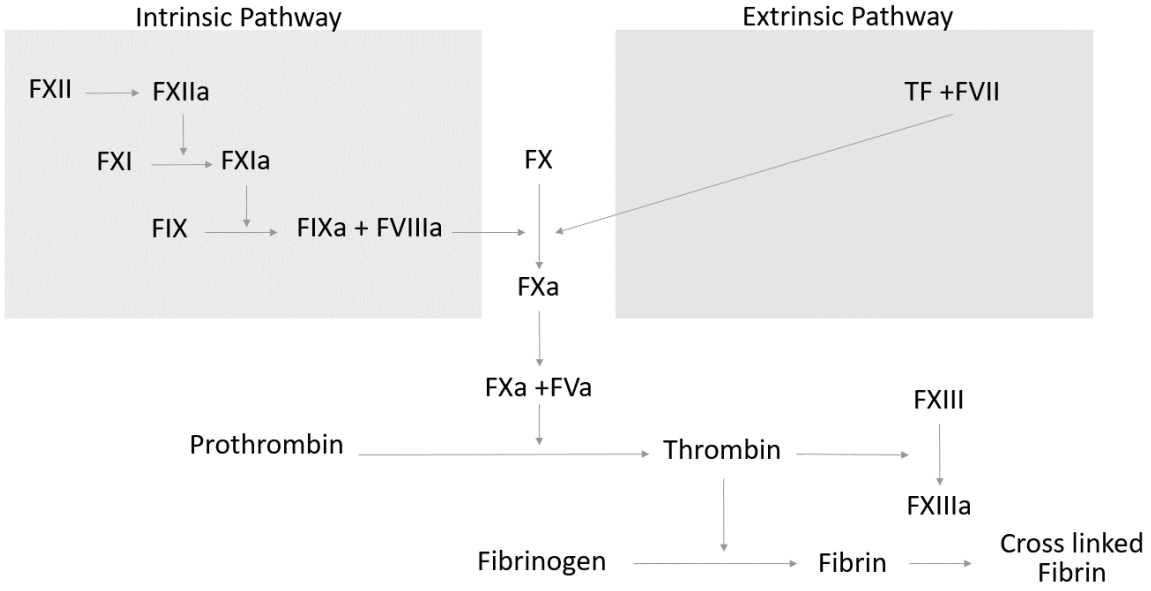

Figure 1. 2: Coagulation cascade demonstrating both intrinsic and extrinsic pathways used to cleave prothrombin to thrombin in order for clot formation to occur.

Upon formation of the fibrin clot, platelets contract their cytoskeleton comprised of actin or myosin. The actin network connects to integrin GpIIbIIIa and an internal receptor Fib, and the external section of GpIIbIIIa adheres to the fibrin clot, compacting and decreasing the volume of the overall clot (Periayah *et al*., 2017).

1.3.2 Inflammatory phase

During inflammation, cells such as neutrophils are recruited to the wound area by complement cascade activation and begin phagocytosis to remove debris and bacteria from the wound in order to prevent infection (Velnar *et al*., 2009). Chemotactic factors are released by mast cells and fibrinogen during the inflammatory response in which neutrophils perform phagocytosis for a few days, however contamination may prolong this response (Collington *et al*., 2011). Neutrophils have different mechanisms to remove bacteria and cellular debris including phagocytosis, degranulation which releases toxic substances such as cathepsin, lactoferrin, neutrophil elastase and proteases, NETs (Gibson and Cohen., 1999; Singh *et al*., 2017) and reactive oxygen species. Neutrophils additionally release pro-inflammatory cytokines to activate keratinocytes and fibroblasts as well as matrix metalloproteinase 8 which is a collagenase that removes wound debris and type 1 damaged collagen (Opneja *et al*., 2019).

Endothelial cells are proliferated through a highly mitogenic epidermal growth factor (EGF) and can additionally stimulate the synthesis of fibronectin, and the control the activity of processes such as angiogenesis, collagenase and fibroplasia (Qing., 2017). Additionally endothelial cells secrete chemokines that enhances adhesion to cease the rolling and allow the neutrophils to migrate in between endothelial cells through a process called diapedesis (Li. Z *et al*., 2020). Once phagocytosis is complete the neutrophils are eliminated by apoptosis, and the remaining cell debris is phagocytosed by macrophages (Velnar *et al.*, 2009).

Macrophages gather at the wound site at 48-72 hours after injury, where they release growth factors paramount to the inflammatory process including TGF-β, EGF, PDGF, Insulin like growth factor 1 (IGF1) and VEGF allowing for angiogenesis, cellular proliferation and

granulation tissue formation (Singh *et al*., 2017; Krzyszczyk *et al.,* 2018; Vannella and Wynn., 2017). M1 pro-inflammatory macrophages aid in the removal of debris and bacteria alongside neutrophils and as the repair continues, they transition to anti-inflammatory M2 macrophages and help the migration of proliferative cells such as fibroblasts, keratinocytes and epithelial cells. (Ogle *et al*., 2016; Krzyszczyk *et al*., 2018)

Monocytes migrate to the wound site forty eight hours after wound injury (Velnar *et al*., 2009) under the influence of monocyte chemoattractant protein 1 and macrophage inflammatory protein 1 (J. Li *et al*., 2007). Monocytes differentiate into macrophages to continue the role of phagocytosis and provide sufficient quantities of growth factors, mainly TGF-β, to activate keratinocytes, endothelial cells and fibroblasts (Velnar *et al*., 2009; Schreml *et al*., 2010).

Lymphocytes enter the wound site seventy two hours after injury under the influence of complement molecules, Immunoglobulin G (IgG) breakdown products and Interleukin (IL) 1 (IL-1) which promotes collagen remodelling (Schreml *et al*., 2010).

1.3.3 Proliferative phase

The proliferative phase occurs seventy two hours after initial injury, continuing up to around two weeks, and results in new extracellular matrix being deposited at the wound site, comprising of granulation tissue and fibroblasts (Velnar *et al*., 2009).

Cell morphology changes following signals from multiple pathways assisting in cell migration and polarity. Carried out by controlling the membrane of the cells and creating protrusions that extend and retract (Welf and Haugh., 2011). Migrating cells must attach to a solid surface controlled by integrins acting as receptors for extracellular matrix proteins to attach. The process of adhesion is inversely proportional to the rate of cell migration, resulting in

faster endothelial cell movement. Granulation tissue which replaces the fibrin matrix, eventually over time causes scar tissue (Velnar *et al*., 2009). There are three stages that occur during this phase:

1.3.3.1 Angiogenesis

Angiogenesis and a formation of granulation tissue occurs. Endothelial cells respond to angiogenesis factors including vascular endothelial growth factor (VEGF), fibroblast growth factor and TGF-β by initiating mitosis which stimulates host endothelial cells to produce growth factors such as PDGF and VEGF (J. Li *et al*., 2007). Endothelial cells produce proteases such as matrix metalloproteinases (Goicovich *et al*., 2003) which degrade the basal lamina, causing chemotaxis of cells and proliferation in order for remodelling and differentiation to take place. The new capillaries invade the wound site providing subsequent new blood supply to the area (Enoch and Leaper., 2008).

1.3.3.2 ECM formation

Fibronectin is vital in the final stages of wound healing (Alberts *et al*., 2008). There are two forms of fibronectin, plasma synthesised by hepatocytes and cellular fibronectin which is synthesized by endothelial cells, fibroblasts and keratinocytes (To and Midwood., 2011). Plasma fibronectin is discovered at the wound site within 3 hours of injury and increased within 48 hours, this is essential for epithelial cells to allow migration and adhesion at the site. Keratinocytes can upregulate the actin and fibronectin binding and additionally fibroblast migration is dependent on the presence of fibronectin as shown in a study conducted by Greiling and Clark (1997) where without fibronectin there was a migration decrease of 80% (Lenselink., 2015). Fibronectin indirectly mediates wound contraction by providing a scaffold for collagen and myofibrils to adhere (Li *et al*., 2017; Lenselick, 2015).

1.3.3.3 Re-epithelialisation

Keratinocyte migration is a vital part of this process, basal and suprabasilar keratinocytes become polarized and undergo mitosis (Raja *et al*., 2007). Additionally during keratinocyte migration growth factors increase in concentration such as TGF-β, TNF- alpha, IL-1, IL-6 and IL-22 (Bandyopadhyay *et al*., 2006). TGF-β and EGF influence the formation of a digested fibrin matrix tunnel, which allow the keratinocytes to migrate efficiently (Rouselle *et al*., 2019; Ronfard and Barrandon., 2001) and deposit cellular fibronectin, laminin and tenascin C (ECM proteins) which enables re-epithelialisation to occur (Rouselle *et al*., 2019). Fibroblast growth factor additionally is released from damaged endothelial cells, specifically FGF-7 (keratinocyte growth factor) is increased in response to skin wounds (Raja *et al*., 2007). Fibronectin promotes the activation of macrophages for debris removal at the wound site as well as being part of the preliminary scaffold with fibrin to a tissue and fibronectin scaffold which contains proteoglycans and crosslinked collagen eventually forming granulation tissue allowing keratinocyte interactions (Rousselle *et al*., 2019). Fibronectin assembles using a process called fibrillogenesis which produces a 3D matrix that is critical for ECM organisation and the retention and deposition of collagen I and thrombspondin (Masden *et al*., 2013). Following the formation of granulation tissue, dermal reconstruction can begin around 3-5 days following injury (Roussselle *et al*., 2019).

1.3.3.4 Remodelling phase

Wound remodelling occurs when scar tissue and new epithelium forms, thus covering the wound site. A process called epithelial-mesenchymal transition (EMT) causes epithelial cells to become motile and move across the wound boundary. A change in cytokine concentration may cause the epithelial cells to become proliferative instead of mobile in order to complete the wound healing process (Singh *et al*., 2017). Collagen increases in size with other components such as fibronectin and hyaluronic acid being degraded by

macrophages; increasing the strength of the new tissue (Velnar *et al*., 2009). Fibronectin is replaced by collagen I (Ashcroft *et al*., 2012) but the overall tissue strength does not reach that found in non-injured tissue (Ashcroft *et al*., 2002). The cell content and blood flow are subsequently reduced (Harding *et al*., 2002).

Impairment of this process can lead to a chronic wound and a prolonged inflammatory state of the wound (Zhao *et al*., 2016). This can occur due to the presence of an infection at the site from opportunistic bacteria (James *et al*., 2008) such as *S. aureus*.

Staphylococcus aureus is a Gram-positive opportunistic pathogen which can cause a plethora of infections including those at wound sites therefore delaying the rate of wound healing leading to chronic wound infections (Serra *et al.*, 2015). This coagulase positive, coccoid and non-motile pathogen (Lee *et al.,* 2018) is the most common cause of surgical site infections (SSIs) resulting in 30-50% of SSIs after clinical procedures, increasing recovery time, healthcare costs and mortality (Ramirez *et al.*, 2013). *S. aureus* commonly colonises diabetic, HIV and children wounds (Lin *et al*., 2017) and is the predominant isolate in diabetic foot infections. *S. aureus* produces four types of haemolysins (alpha, beta, gamma, and delta), lipases, nucleases, collagenase and protease which all contribute to tissue invasion (Shettigar and Murali, 2020). These virulence factors contribute to impaired wound healing by increasing the number of inflammatory cells in the wound area, decreased cell migration and an absence in growth of skin cells, thus leading to a chronic wound (Giurato *et al*., 2017).

1.4 *Pseudomonas aeruginosa*: an overview of the pathogen

P. aeruginosa is a Gram-negative opportunistic pathogen which predominantly affects immunocompromised patients (De Oliveira *et al*., 2020). Antimicrobial resistance in *P. aeruginosa* is very high with multiple classes of antibiotic being rendered ineffective. Multi-drug resistant variants of *P. aeruginosa* are isolated frequently from intensive care units with in excess of 51,000 healthcare associated infections being caused by the pathogen in the US alone (Azam and Khan, 2019). Infections may occur at wound and burn sites or in the lungs of patients with respiratory compromise such as those with cystic fibrosis (Cuthbertson *et al.*, 2016). Burn sites colonised by *P. aeruginosa* can become significantly infected leading to systemic disease and death. In lung infections, *P. aeruginosa* uses exotoxin-S to damage to the lung epithelium. Other enzymes such as lipase, elastase and protease and additionally exotoxins such as ExoA, ExoS, ExoT, ExoU, and ExoY which can be injected via Type 3 secretion systems (T3SS) needle-like apparatus into the host cells. This then leads to loss of lung capacity and is associated with high morbidity and mortality (Curran *et al.*, 2018).

P. aeruginosa has low membrane permeability with the outer cell membrane comprised of an asymmetric phospholipid and LPS bilayer which blocks most antibiotics from entering the cell, coupled with efflux pumps such as OprF to remove antibiotics (Delcour, 2009). OprF is a major porin vital in the virulence of *P. aeruginosa* which regulates secretion of T3SS effectors and produces other virulence factors such as elastase, exotoxin A, lectin PA-1L and pyocyanin (Moussini, *et al*., 2021).

The invasive nature of *P. aeruginosa* infections is mediated by many different virulence factors such as multiple iron uptake systems to allow infections and subsequent

multiplication within the host. Two siderophores, pyover-dine and pyochelin, are secreted by *P. aeruginosa* which chelate ferric ions contributing to enhance pathogenicity of *P. aeruginosa*. There are 30 different Ton-B dependent receptors located on the outer membrane allowing for successful uptake of siderophores produced by other commensal microorganisms for additional iron uptake (Minandri *et al.*, 2016). *P. aeruginosa* has a large genome which can also encode for the virulence factor lipopolysaccharide O biosynthesis which may allow the alteration of the *P. aeruginosa* outer membrane during infection, thus persisting in wounds. It has additionally been determined that during soft tissue infection, type II and III secretion systems are upregulated to enhance colonisation (Turner *et al.*, 2014*). P. aeruginosa* infections are exacerbated by two quorum sensing systems which allow for efficient colonisation of a wound site and expression of virulence factors within the pathogen (Pastar *et al.*, 2013).

Enzymes additionally are present within the bacterium which alter the chemical structure of the antibiotics to render them ineffective. New emerging extended spectrum β-lactamases are now making an appearance, conferring resistance to third generation cephalosporins (El-Shouny *et al*., 2018) and fourth generation cefepimes resistance are also making an occurrence (Saravanan *et al*., 2018).

There are four classes of β-lactamases dependent on amino acid sequence, classes A, C and D cause hydrolysis through a serine active site whereas class B is a metalloenzyme which requires zinc irons to be present for hydrolysis to occur (Bush and Bradford., 2020). In 2009 a study conducted demonstrated that *P. aeruginosa* mutants *mutT* and *mutY* caused increased the frequency of mutations and higher oxidative damage compared to the wild-

type, and the expression of β-lactamase and the efflux pump MexCD-OprJ increased, leading to the conference of resistance (Mandsburg et al., 2009).

Rağbetli *et al.* (2016) tested clinical isolates of *S. aureus* for resistance and established only four antibiotics were effective at eliminating the bacteria; vancomycin, linezolid, levofloxacin and daptomycin. *P. aeruginosa* however is resistant to most antibiotics including β-lactams and penem classes, acquiring further resistance mechanisms to multiple classes of antibiotics, including fluoroquinolones and aminoglycosides (Pachori *et al.*, 2019).

Infections associated with *P. aeruginosa* are challenging to treat due to a number of resistance mechanisms. *P. aeruginosa* can also become resistant to antibiotic through the formation of a biofilm which acts as a diffusion barrier to treatments as well as the acquired resistance through mutations such as altered antibiotic target sites (Pang *et al.,* 2019).

P. aeruginosa biofilms are formed of aggregated bacteria encased in extracellular polymeric substances to allow for more efficient survival against unfavourable conditions. The biofilm can evade host-immune responses and become more resistant to antimicrobial treatment, thus causing issues in cases of cystic fibrosis (Oluyombo *et al*., 2019), medical device (Ghafoor *et al*., 2011) and equipment of the food industry infections (Coughlan *et al*., 2016). The biofilm matrix comprises of polysaccharides, proteins, lipids and extracellular DNA which accounts for 90% of the biomass and allows for the adhesion to a multitude of surfaces, cellular signalling and provides nutrients, enzymes and proteins essential for bacterial survival (Strempel *et al*., 2013). There are three specific exopolysaccharides that are vital for cell adhesion. PsI, a neutral pentasaccharide comprising of l-rhamnose, d-glucose and d-mannose moieties (Byrd *et al*., 2009) is responsible for sessile cell adhesion and cell-to-cell interactions (Jones and Wazniak., 2017). PeI is a cationic polysaccharide

polymer comprised of *N*-acetyl-d-glucosamine and *N*-acetyl-d-galactosamine which have been partially deacetylated and is essential in nonmucoid strain matrix, biofilm integrity maintenance and initiation of surface adhesion (Jennings *et al*., 2015). Alginate is produced in mucoid strains due to a *mucA22* allele mutation, typically found in cystic fibrosis isolates. This mutation confers maturation of the biofilm, protection from opsonisation and phagocytosis and decreases the ability of antibiotics to diffuse through the biofilm (Hay *et al*., 2013).

The development of a *P. aeruginosa* biofilm begins with the adherence of cells to a surface through the use of cell appendages such as type IV pili and flagella (Thi *et al*., 2020) which can be a material specific activity, where the presence of specific proteins of *P. aeruginosa* PAO1 and altered quantities are as a result of sensing to given surfaces (Guilbaud *et al*., 2017). Once attached the cells can change from reversible attachment to a surface to irreversibly adhering, in which propagation of attached bacteria occur to create a more structured form known as a microcolony. These microcolonies further develop as they mature into three-dimensional structures before the central portion of the microcolony (matrix cavity) is disrupted through the process of cell autolysis to liberate dispersed cells (Thi *et al*., 2020) where the transition between sessile and planktonic growth is observed allowing for the biofilm cycle to repeat (Rasamiravaka *et al*., 2015).

New treatment options such as wound dressings, topical agents or nebulised antimicrobials are urgently needed to reduce the impact of *P. aeruginosa* and *S. aureus* infections. Silver wound dressings are used in current treatments and contribute to the overall cost of wound dressings in the UK by 18% (Nice, 2021). Current options for dressings include the use of alginate due to its haemostatic properties (Venkatraman *et al*., 2023), ability to maintain a

moist environment to allow for wound healing (Casey., 2000) and drug delivery properties (Lee and Mooney., 2012). In recent studies electrospun alginate nanofibers impregnated with oregano essential oil demonstrated increased antimicrobial activity against *K. pneumoniae* 13883 and MRSA with an increase in concentration from 2 to 3% suggesting effective delivery of the antimicrobial (Lu *et al*, 2021). Ruthenium has been addressed for use in a medical dressing where *S. aureus* VRSA (CCM 1767) infected wounds were fully healed in 15 days in murine models with a Ruthenium-Schiff Base-Benzimidazole complex (Sur *et al*., 2020).

To combat antibiotic resistance, new cellular targets must be identified with new methods of identifying potential agents from the soil or marine environments, combination therapy with different antimicrobials, phage therapy or drug repurposing (Taneja *et al*, 2019). One method, potentiation, could overcome the effectiveness of the bacterial membrane by manipulating non-essential areas of the bacteria to cause antibiotic sensitivity such as efflux pump inhibitors. The active uptake mechanism has also been investigated to combat antimicrobial resistance, by using sugar transporters in the bacterial membrane to enter the cell such as the antibiotic fosfomycin. The main transporter target is iron, to enable easy entry into bacterial cells due to the requirement being high for bacterial survival. Bacteria have evolved over time to acquire iron in numerous ways including, stripping from the host via siderophore release and ingestion of the bound iron-siderophore complexes (Baker *et al*., 2018). This has been completed previously however optimization is needed to allow for cell penetration (Lorca *et al*., 2007). Vaccines could additionally be a promising avenue in order to prevent bacterial proliferation, reduction of symptoms associated with antimicrobial ingestion and prevent infections overall (Rappuoli *et al*., 2017). Some are in development including vaccines against *Mycobacterium tuberculosis, P. aeruginosa, S.*

aureus and *C. difficile* however are not available without vigorous testing (Delany *et al*., 2014). Therefore, antimicrobial options should still be considered, should vaccines not be effective and metallotherapeutics could be a way to combat antimicrobial resistance against highly pathogenic bacteria.

1.5 Metals as antimicrobial agents

1.5.1 Historical use of metals in medicine

Metals have been used as antimicrobial agents for centuries, for example the Persians used copper and gold to disinfect water supplies and preserve food. In medicinal cases, silver (in the form of silver nitrate) was used to treat eye infections in 1880 (Moore and MacDonald, 2015) caused by gonorrhoea in new-born children and as foil to prevent wound infections following surgery (Gold *et al.*, 2018). Arsenic complexes such as Salvarsan were used in the early 19th Century to treat syphilis, however these were highly cytotoxic. As research continued less toxic alternatives were identified including tribromophenatebismuth (III) which reduced the number of colonising bacteria for the treatment of wounds (Mjos and Orvig, 2014).

Due to the emergence of organic therapies such as traditional antibiotics, research into organometallic drugs declined. However, with antibiotic resistance becoming more prevalent within society, metal complexes are now being re-explored for medical use (Lemire *et al.*, 2013). Metals are being used more frequently in the medical field as surface coatings such as on prosthetic and indwelling implants (Table 1.1). Some metals exhibit many different mechanisms of antimicrobial action such as generating oxidative stress, inhibiting protein function and mediating membrane damage against bacteria at low concentrations and at low cytotoxicity to the host. Metal coatings disrupt biofilm formation, which is a major issue with medical devices (Hobman and Crossman, 2015). Antibiotics are

less successful at treating some infections due to drawbacks such as non-continuous drug delivery, antibiotic diffusion through the biofilm is limited and resistance can occur which could be transferred to other bacteria within the biofilm (Sultana *et al.*, 2015). Alternative methods to prevent biofilm formation have been studied, for example using metal coatings of internal devices such as implants, due to their ability to disrupt bacterial cellular processes and prevent infection of the site. Some elements, which are effective antimicrobial agents at low concentrations, such as lead, arsenic, mercury and cadmium (Koechler *et al.*, 2015) are also highly cytotoxic. Generally, transition metal elements such as silver, titanium, copper, chromium, zinc, platinum and ruthenium are considered less cytotoxic but the concentration of metal/metal complex required for sufficient antimicrobial activity varies depending on target organism, chemical structure and application.

Table 1. 1: Metals as antimicrobial agents.

Metal	Medical application
Silver	Surface coatings, topical gels, hygiene and grooming products (Deodorant, shavers, contact lenses) (Sim *et al*., 2018) Coatings for dressings, catheters, breathing tubes (Silver, 2003; Ip *et al*., 2006; Silver *et al*., 2006; Chopra, 2007; Mijnendonkx *et al.*, 2013)
Mercury	Antifungal Treatment of sexually transmitted infections (Hobman and Silver, 2007) Psoriasis, ring worm Dental amalgam fillings (Franke, 2007)
Copper	Antiseptic, antifungal, socks for athletes foot (Borkow and Gabbay, 2009) Syphilis and tuberculosis (Grass *et al.*, 2011)
Arsenic	Trichomoniasis, malaria, ulcers and syphilis (Liu *et al.*, 2008)
Antimony	Leishmaniasis, schistomiasis/bilharziasis, trypanosomiasis, smallpox, syphilis (McCallum, 1977)
Titanium	Anti-biofilm agent (TiO_2) (Jesline *et al.*, 2015) Joint endoprostheses and osteosyntheses (Hempel *et al.*, 2014) Dental polymers (Chambers *et al.*, 2017) Orthopaedic implants (Jäger *et al.*, 2017) Food packaging (Siripatrawan *et al.*, 2018)
Cadmium	Anti-cancer (Heidari, 2016) Electroplating, alloys (Nessa *et al.*, 2016) Nanoparticles (Zhu *et al.*, 2019)

	Anti-fungal (Malarkodi *et al.*, 2014)
Iron	Hydrogel anti-biofilm (Konwar *et al.*, 2016) Siderophore (Lamb, 2015) Nanocomposite (reclaim metal ions from solution) (Zhou *et al.*, 2014) Nanoparticles (affect cell integrity, create ROS, damage DNA) (Arias *et al.*, 2018)
Chromium	Leather coating, Diabetic shoes, laundry applications, deodorant (Xia *et al.*, 2018) Nanoparticles (Raghunath and Perumal, 2017)
Cobalt	Prosthetic implants (Aherwar *et al.*, 2016) Sterilization of medical equipment (Bashir *et al.*, 2016)
Zinc	Coatings, wood preservatives, eye treatments, antifungals (Giachi *et al.*, 2013) Toothpaste (Pal *et al.*, 2017)

1.5.2 Mechanisms of antimicrobial action of metals

Metals can enter the bacterial cells via several methods including, molecular mimicry (such as ruthenium mimicking iron) Xand co-transport by binding to peptides, amino acids and phosphates where they can exhibit their antimicrobial action within the cell (Lemire *et al.*, 2013). In a study conducted by Yasuyuki *et al*., (2010), cobalt, copper, nickel, zinc, zirconium, molybdenum and lead all demonstrated significant antibacterial effects against both *S. aureus* and *Escherichia coli* due to metal ion dissociation. Metals can be used in nanoparticle format in which the smaller particles have more efficient antimicrobial capability due to the increased production of reactive oxygen species (ROS) (Table 1.2) that can target cellular DNA, proteins and lipids thus damaging the bacterial cell (Slavin *et al.*, 2017). Some metal-

based complexes exhibit multiple mechanisms of antimicrobial action at different bacterial cellular targets (Table 1.2). One notable example being carbon monoxide (CO) Releasing Molecule-3 (CORM-3), a ruthenium-based complex which targets thiol-groups in proteins and inhibits bacterial respiratory chains (Southam *et al*., 2017). Having multiple bacterial cellular target reduces the risk of antimicrobial resistance evolution.

Table 1. 2:Mechanisms of antimicrobial activity of metals such as silver, copper, cobalt and nickel against bacterial cells.

Target site	Action	Metals and References
Cytosol	Bind to enzymes and DNA inhibiting replication and division or causing gene upregulation, disrupt ATP production, inhibition of respiratory and metabolic pathways.	Silver (Sondi *et al*., 2004; Morones *et al*., 2005) and gold nanoclusters (Zheng *et al*., 2017)
Protein synthesis inhibition	Thiol group binding on proteins by metal ions impair binding of apoenzymes by cofactors and impair folding of the protein.	Nickel, cadmium, zinc (Harrison *et al*., 2007) Ruthenium (Southam *et al*., 2017)
Cell membrane	Bind electrostatically to the phospholipid bilayer and cause membrane disruption. Cationic metals can interact with the overall negatively charged bacterial membrane with high affinity.	Silver, oxides including magnesium, iron, cooper and titanium (Beyth *et al*., 2015) and iron and ruthenium (Abd-El-Aziz *et al*.,

		2017)
Production of Reactive Oxygen Species (ROS)	Causes oxidative stress within cells resulting in damage to DNA, lipids, proteins, enzymes and cell membrane creating pores and causing intracellular leakage. An imbalance of free radicals and production of ROS can cause antioxidant depletion additionally and overwhelm the defence system.	Copper and iron (Nathan *et al*., 2013) Silver (Sondi *et al*., 2004), Zinc, cadmium, copper, iron and arsenic (Valko *et al*., 2016) Aluminium, copper, cobalt, titanium and zinc (Pan *et al*., 2010)
Inhibition nucleic acid synthesis	Platinum ions intercalate with DNA and can form covalent bonds with the N7 region of adjacent purine bases causing cytotoxicity to the bacteria and cleavage of DNA.	Platinum (Sobha *et al*., 2012)
Metabolic process interference	Membrane transporters are competitively inhibited due to metal ions blocking binding sites and interfering with the potential of the membrane.	Copper, zinc, nickel, cadmium (Harrison *et al*., 2007) Ruthenium (Southam

		et al., 2017)
Inhibition of biofilm formation	Metal cations can bind to respiring cells and cause cell death in others through other mechanisms which can alter the pH of the microenvironment which contribute to metal ion accumulation.	Zinc, cadmium, copper, silver, mercury, manganese (Harrison *et al*., 2007)

1.5.3 Ruthenium complexes as antimicrobial agents

Ruthenium (Ru) was first discovered in 1844 by Karl Karlovich Klaus (Southam *et al*., 2017) and is a transition metal (atomic number 44) found in Group 8 of the periodic table, with an atomic mass of 101.07. Ru has three accessible oxidation states of 2+, 3+ and 4+ with the initial two being inert and octahedral in shape (Li *et al.*, 2015). Such variable states mean that Ru has a propensity for coordination chemistry, which allows for chemical design and synthesis of a range of diverse complexes centred around a mono, di or tri nuclear Ru core.

Over 50 years ago, an Ru (II) mononuclear complex with bidentate phenanthroline ligands termed $[Ru(Me_4Phen)_3]^{2+}$ was the first synthesised Ru complex to demonstrate antimicrobial activity (Dwyer *et al*., 1969). With the development of organic antibiotics, very little further research was conducted into developing Ru-based antimicrobial complexes. However, Ru metallotherapeutics continued to be investigated for anticancer applications (Alessio and Messori., 2019).

A number of Ru based anti-cancer complexes have been formulated including NAMI-A, KP1019, NKP1339 and TLD1443 and thus far none are in clinical use however they have advanced to clinical trials (Lee *et al*., 2022). Each complex has been found to exhibit

different actions with NAMI-A demonstrating anti-metastatic and anti-angiogenic activity against secondary tumours (Sanna *et al*., 2002). NAMI-A ([ImH][trans-RuCl4(dmso-S)(Im)] (dmso-S = sulphur-bonded dimethyl sulfoxide, Im = imidazole) was the first studied ruthenium-based anticancer complex used in humans for the treatment of non-small cell lung cancer (Leijen *et al*., 2015). In animal models, treatment of platinum resistant chemically induced autochthonous colorectal cancer was treated which simulated the human cancer very closely, demonstrating effectiveness when other treatment options have failed. However, NAMI-A is non-cytotoxic against solid tumour cell lines, due to its ability to transform and only interact with the tumour cell walls instead of being internalised (Webb and Walsby., 2013). The mechanism of action involves the Ru complex binding with high affinity to DNA and RNA (Hostetter *et al*., 2011) causing an arrest in cell cycle at the G2 or M phase in mitosis (Frausin *et al.*, 2011) and inhibiting the release of matrix metalloproteinases MMP-2 and MMP-9 which affects cellular uptake (Alessio., 2017). NAMI-A additionally interacts with model proteins including lysozyme, carbonic anhydrase and H-chain ferritin. With lysozyme the Ru ions bind to carboxylate groups of different aspartate residues, Asp 101 and 1090 via coordinative bonds, carbonic anhydrase the Ru ion binds to the imidazole group of histidine His 64 and for ferritin His 105 (Alessio and Messori., 2019). KP1019 has been found to have a broad spectrum of activity against primary tumours (Kapitza *et al*., 2005). KP1019 ((IndH)[*trans*-$RuCl_4(Ind)_2$], Ind = indazole) has been used for the treatment of platinum-resistant colorectal cancers due to its cytotoxic nature, whereas NAMI-A (((ImH)[*trans*-$RuCl_4$(dmso-S)(Im)], Im = imidazole) is non-cytotoxic and has been used as an anti-metastatic drug. Both have the ability to coordinate to DNA irreversibly, with NAMI-A binding faster than KP1019 and forms bifunctional adducts on the DNA causing a termination in RNA synthesis (Thompson *et al*., 2012). KP1019 which was shown to target

guanine residues in DNA molecules via hydrophobic interactions (Alessio and Messori., 2019). It is thought, the complexes enter the cancer cells through the non-covalent binding to serum albumin, effective due to cancer cells need for excess iron. An increased soluble complex NKP1339 was formulated to overcome solubility issues of KP1019 as a sodium salt allowing for higher doses to be administered to patients (Thompson *et al*., 2012) and TLD1443 has entered phases 1 and 2a clinical trials for bladder cancer treatment with photodynamic therapy (Monro *et al*., 2018).

Half sandwich arene-Ru complexes containing 1,3,5-triaza-7-phosphatricyclo-[3.3.1.1]decane (PTA) ligands (known as RAPTA complexes) can be adapted through ligand modification to allow for pharmacological changes (Ang *et al*., 2011). Dichlororuthenium (II) (*p*-cymene) (1,3,5-triaza-7-phosphaadamantane) (RAPTA-C) has been used as an anti-metastatic cancer treatment for triple negative breast cancer. It comprises of an Ru(II) centre with arene, chloride and phosphine ligands with each having its own specific role. The arene ligand size determines the cytotoxicity and DNA damage of the complex, chloride ligands allow for activation of the drug when in contact with water and phosphine increases the water-solubility (Blunden *et al*, 2012). It was discovered that RAPTA-C caused pH dependent DNA damage by coordinating to the DNA of cancer cells via labile chloride ligand loss so the oligomers can wrap around the central Ru forming multiple coordination bonds thus distorting the oligonucleotide. In addition to this action RAPTA-C has the ability to decrease the density of microvessels through its strong anti-angiogenic activity and will not accumulate in vital organs due to its fast renal excretion (Weiss *et al*., 2014). RAPTA-C additionally can cause cell cycle arrest in the G2/M phase and cause cancer apoptosis. A downside of this complex was its low solubility and rapid degradation (Blunden *et al*, 2013) which can be overcome through encapsulation with micelles (Lu *et al*., 2016). Overall the

complex has high metastatic activity with IC_{50} values ranging above 500 x 10^6 $_M$ and was enhanced by combining RAPTA-C with micelles (Lu *et al*., 2017).

Other Ru complexes have been studied including a redox organoruthenium complex RDC11 with linked two acetonitriles, one phenanthroline, and one 2-phenylpyridine has been studied for anticancer capability. The complex is highly cytotoxic with and IC_{50} between 1-5 μM on multiple cell lines, including platinum resistant models however has been successfully used in mouse syngeneic mouse models and xenographic human models by inducing the p53 dependent and endoplasmic reticulum stress pathways. Following 6 h treatment acetylation of the histone H3 was increased however decreased over a 24 h period in contrast with cisplatin however the genes associated with ER stress- and oxidative stress are elevated at 24 h (Licona *et al*., 2017).

There is now renewed interest in repurposing anticancer Ru complexes and indeed developing novel complexes for antimicrobial applications. Many Ru-based complexes have potent antimicrobial activity (Southam *et al*., 2017) and this is an emerging area of antimicrobial research and discovery. Ru-mediated antimicrobial mechanisms of activity can be enhanced by modifying attached ligands to improve lipophilicity and solubility such as with [Chlorido(η^6-toluene)(*N*-(4-fluorophenyl)-2-pyridinecarbothioamide)ruthenium(II)] chloride (Meier *et al.*, 2017).

As well as being repurposed for bacterial infections, some Ru complexes have been used for anti-parasitic applications. Ruthenium metallotherapeutic agents have been documented to be highly effective at targeting a range of key parasites, including the causative agents of amoebiasis, leishmaniasis, malaria, toxoplasmosis and trypanosomiasis as well as other orphan diseases, whilst demonstrating lower cytotoxicity profiles than current treatment

strategies. Generally, such compounds demonstrate multi-site activity within parasites, including alterations to metabolic pathways, cell membrane perturbation and inhibition of enzyme function (Britten and Butler, 2022).

For example for the treatment of malaria, a trinuclear complex comprised of [Ru(p-cymene)Cl_2]$_2$ containing polypyridyl ester ligands (monodentate donors) and benzene-1,3,5-tricarboxylic acid tripyridin-4-ylmethyl ester proved effective with low cytotoxicity against HEK cell lines, proving to have a 4.5 fold increased effect on the parasites than the currently used drug chloroquine (Chellan *et al*., 2014). Additionally RAPTA complexes which contain a monodentate 1,3,5-triaza-7-phospaadamantane (PTA) and η^6 arene ligand coupled to a Ru core forming [Ru(η^6-p-arene)Cl2(P-TA)] exhibits antiparasitic activity due to the protonation in low pH environments including in the digestive vacuole of the parasite. The IC_{50} values observed of following exposure to (η^6-p-cymene)(N-(2-((5-fluoro-2-hydroxyphenyl)methylimino)propyl)-7-chloroquinolin-4-amine)PTA ruthenium(II) hexafluorophosphate, where values of 0.10 µM ± 0.069 (*P. falciparum* strain NF54) and 3.8 µM ± 0.68 (*P. falciparum* strain K1), compared to chloroquine alone (0.031 µM ± 0.004 and 0.36 µM ± 0.07 respectively). With cellular cytotoxicity against a CHO cell line was low at >100 µM (Stringer *et al*., 2019).

Leishmania species were additionally targeted with complexes with a general formula *cis*-[RuII(η^2-O_2CR)(dppm)$_2$]PF_6, where dppm = *bis*(diphenylphos-phino)methane and R = 4-butylbenzoate (bbato), have demonstrated high levels of activity through covalently interacting with the parasitic DNA with an IC_{50} of 7.52 µM with *L. amazonesisis* and low cytotoxicity of 8.73 µM with RAW 264.7 macrophages (Costa *et al*., 2017). Chelating ligands are exchanged with the chloride groups causes an increase in the complexes biological

activity by increasing the overall molecular positive charge, therefore allowing covalent interactions with DNA more readily (Britten and Butler., 2022).

In addition to parasites some Ru complexes have been investigated for anti-viral capability. A Ru complex $Na_7[Ru_4(\mu_3\text{-}O)_4(C_2O_4)_6]$ has exhibited 98% viral inhibition of the HIV-1 R5-tropic strain at a concentration of 5 μM, which was 10-fold more effective against the HIV-1 reverse transcriptase compared with the commonly used inhibitor 3'-azido-3'-deoxythmidine-5'-triphosphate (Wong *et al*., 2006; Munteanu and Uivarsoi., 2021).

Most active Ru complexes are dinuclear and the metal ion alters electronic and stereochemical properties, paving the way for new mechanisms of action against bacteria. Ru complexes such as tris(homoleptic) ruthenium(II) complexes of 2-(1-**R**-1*H*-1,2,3-triazol-4-yl)pyridine have been found to exhibit high antimicrobial action against MRSA strains, by disrupting the cytoplasmic membrane, causing uneven distribution of cell contents and leakage of the cell membrane thus causing cell death (Kumar *et al.*, 2016). However, many complexes continue to have high cytotoxicity profiles against mammalian cell types. The activity of Ru based complexes is determined by the lipophilicity, charge and separation of the charge which affect the overall antimicrobial capacity and uptake into the bacterial cell (Pandrala *et al*., 2013; Frei., 2020).

An initial complex, $[Ru(phen)_3]^{2+}$, had little to no activity against bacteria including *S. aureus, M. tuberculosis* and *S. pneumoniae*, however upon addition of methyl groups to bidentate phenanthroline ligands (creating $[Ru(Me_4Phen)_3]^{2+}$) caused a significant increase in antibacterial activity. This was most notably against Gram-positive bacteria such as *S. aureus, M. tuberculosis, S. pneumoniae* and *C. perfringens*. It was also demonstrated that resistance generation was less likely when compared to traditional antibiotics (Dwyer *et al*.,

1969). Subsequent studies discovered that the complex binds to the major groove of DNA thus causing the antimicrobial activity (Metcalfe and Thomas., 2003). More recently, dinuclear polypyridylruthenium(II) compounds have been investigated, including 2,2'-bipyrimidine [bpm], 1,4,5,8,9,12-hexaazatriphenylene, 4,6-bis(2-pyridyl)pyrimidine [dppm], 2,3-bis(2-pyridyl)benzo[*g*]quinoxaline [dpb], 2,3-bis(2-pyridyl)pyrazine [2,3-dpp], 3-pyrazin-2-yl)*as*-triazino[5,6-*f*]-1,10-phenanthroline, tetrapyrido[3,2-*a*:2',3'-*c*:3'',2''-*h*:2''',3'''-*j*]phenazine, bis[4(4'-methyl-2,2'-bipyridyl)]-1,*n*-alkane, 2,9-bis(2-imidazo[4,5-*f*][1,10]phenanthroline-1,10-phenanthroline, 11,11'-bis(dipyrido[3,2-*a*:2',3'-*c*]phenazine [dppz(11,11')dppz], 1,10-phenanthroline-5-(2 mercaptoethyl ether)-5-1,10-phenanthroline, mainly due to their higher affinity for DNA, with subsequent increased DNA binding ability. These compounds were found to be highly active against *S. aureus* and *E. coli* (Li *et al*., 2015). Four Rubb complexes based on [{Ru(phen)2}2{μ-bbn}]4+ {Rubbn; where phen = 1,10-phenanthroline and bbn = bis[4(4'-methyl-2,2'-bipyridyl)]-1,n-alkane had high antimicrobial activity against both *S. aureus* and *E. coli* with MIC's ranging between 1 μg mL^{-1} and 16 μg mL^{-1} due to the complexes ability to bind to DNA and increased lipophilicity. Additionally the Rubb complexes exhibited low cytotoxicity against eukaryotic red blood cell and THP-1 cells with HC_{50} and IC_{50} values ranging between 22 μg mL^{-1} - 1024 μg mL^{-1} and 78 μg mL^{-1} – 400 μg mL^{-1} for each cell line respectively (Li *et al*., 2011).

Additionally a promising Ru complex $[Ru(bb_7)(dppz)]^{2+}$ (bb_7 = bis[4(4'-methyl-2,2'-bipyridyl)]-1,7-alkane) was found to exhibit antimicrobial activity against both Gram-positive and Gram-negative pathogens. MIC values for *S. aureus* and MRSA were found to be at 2 μg mL^{-1} and 8 μg mL^{-1} for *E. coli* MG1655 (a laboratory strain) and two avian *E. coli* strains APEC and UPEC and 16 μg mL^{-1} for *P. aeruginosa* strain PAO1. Cytotoxicity was evaluated against the cell lines ACHN (kidney cancer cell), HEK-293 (healthy kidney cell), HepG2 (liver cancer cell)

and L02 (healthy liver cell) over a 48 h period IC_{50} values were low (22.8 µM, 29.5 µM, 4.9 µM, 71.4 µM respectively) however when in comparison to the MIC data overall toxicity was directed towards the bacteria and not the cell lines therefore having potential as a therapeutic agent.

There are four main classes of Ru-based complexes which target bacterial cells including structural, functional, photo-activated synthetic complexes and carrier complexes (Southam *et al*., 2017).

Structural complexes containing Ru ions have an overall cationic charge and contribute to the overall conformation of the complex, with attached ligands providing increased lipophilicity to mediate bacterial cell entry. Some inert mononuclear complexes have low antimicrobial activity against bacteria such as *S. aureus, P. aeruginosa* and *E. coli*, however introducing methyl groups to the complex increases lipophilicity and subsequent antimicrobial activity (Li et al., 2011; Paez et al., 2013). Dinuclear Ru complexes demonstrate greater antimicrobial activity due to the increased overall ionic charge of the complex, which enables higher affinity for negatively charged bacterial DNA and proteins (Southam *et al.*, 2017). complexes such as $([Ru(phen)_2(BPIP)]^{2+}$ where BPIP = 2,5bis(1-phenyliminoethyl)pyrazine) otherwise known as RuBP inhibit *S. aureus*, by causing cell membrane perturbation. This has been confirmed by an increase in the electrical conductivity of the bacterial suspension following the Ru treatment die to increased permeability of the cell membrane. Additionally, DNA and RNA synthesis is targeted by the complex binding to bases as proved by emission spectroscopy, along with the cell membrane (Sun *et al.*, 2015).

Ru ions can be used as carriers in complexes to transport an active drug such as some antimalarial treatments for example $[RuCl_2(CQ)]_2$, where CQ= chloroquine, a Ru (II) chelate chloroquine complex used for the treatment of *Plasmodium* species in mice. Here, the Ru ion assists in providing enhanced stability to the original complex, increasing the lipophilicity of the drug and the ionic charge allowing subsequent binding to DNA guanine bases. Additionally it may assist in the formation of carbonyl carbon monoxide releasing molecules (CORMs) (Southam *et al.*, 2017).

Functional Ru-based complexes contain ligands such as chloro, ammine and carboxyl which facilitate cellular uptake and also contribute to intracellular activity, such as targeting guanine bases with DNA or by generating intracellular Reactive Oxygen Species (ROS). This occurs due to Ru complexes ability to activate the cellular stress response, which is responsible for the generation of ROS as demonstrated through the anti-cancer Ru complex $Ru(diimine)_3(ClO_4)_2$ (Luo *et al*., 2014). In a *Caenorhabditis elegans* model, the ERSE response is activated in response to abiotic stress from components such as ethanol and the iron chelator phenanthroline, this in turn correlated with the increase in ROS concentration (Tjahjono *et al*., 2020).

Such complexes may also interfere with nutrient assimilation and metal homeostasis, meaning that efflux of the complex from the bacterial cytoplasm is challenging. This is the most destructive form of complex as membrane function is impaired, DNA damage occurs and ROS generation inhibits the vital respiratory enzyme cytochrome C oxidase. However, there is little evidence proving whether the amount of ROS generated can completely inhibit bacterial growth alone. Chlorido ligands present in some Ru complexes can reversibly form covalent bonds with the intracellular target (Southam *et al*., 2017) such as between the N7

region of guanine forming a chelate with N7 and O6 atoms. This occurs in ligands commonly found within most Ru complexes such as $H_5Ru\text{-}CH_3$, $H_5Ru\text{-}NH_2$, $H_5Ru\text{-}OH$, $H_5Ru\text{-}Cl$, $H_5Ru\text{-}PH_3$, and $H_5Ru\text{-}SH_3$ (Adenlyl and Ajibade, 2015).

Photoactive Ru complexes cause bacterial death by generating carbon monoxide from light activated CORM molecules. Cells become inactivated by the photosensitized generation of ROS which causes lipid, protein and DNA destruction (Feng *et al.*, 2019). There is an extensive research base regarding the use CORMs as antimicrobial agents; however these are generally highly cytotoxic to the host eukaryotic cell and the feasibility of using such complexes for medicinal applications is debatable (Southam *et al.*, 2017). For example two CORM producing Ru complexes $[Ru(CO)_3Cl_2]_2$ and $[Ru(CO)_3Cl(glycinate)]$ have been reported to exhibit antimicrobial activity with multiple bacterial species including *S. aureus, Lactobacillus lactis, E. coli, P. aeruginosa* and *S. enterica* (Munteanu and Uivarosi., 2021) due to the effect of CORM's causing membrane damage (Wilson *et al*., 2015). This is thought to be due to the CORM's ability to undergo ligand exchange to form protein-$Ru(CO)_2$ adducts which when decomposed released CO (Seixas *et al*., 2015).

1.6 Ruthenium complexes

Four structurally different Ru complexes Hexaammineruthenium (III) chloride (**1**), Hexaammineruthenium (II) chloride (**2**), Pentaamminechlororuthenium(III) chloride (**3**) and [Chlorido(η6-p-cymene)(N-(4-chlorophenyl)pyridine-2-carbothioamide)ruthenium(II)] chloride (**4**), were used within this project (Table 1.3), all of which have a mononuclear core but with different coordinated ligands. Additionally two other ammine chloride containing complexes were examined for comparison of antimicrobial efficacy including Hexaamminecobalt(III) Chloride (**5**) and Diammineplatinum (II) chloride (**6**). These

complexes were chose due to its varying number of amine groups ranging from zero to four, the effect of ruthenium as the central metallic ion and effect against Gram species.

Table 1. 3: Ru complexes used in the present study.

Name	Abbreviation	Molecular formula	Molecular weight	Structure
Hexaammineruthenium (III) chloride	**1**	$[Ru(NH_3)_6]Cl_3$	309.61	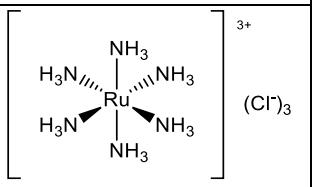
Hexaammineruthenium (II) chloride	**2**	$[Ru(NH_3)_6]Cl_2$	273.15	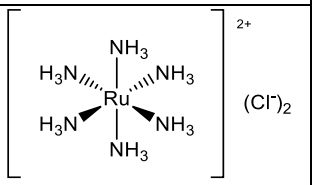
Pentaamminechlororuthenium (III) chloride	**3**	$[Ru(NH_3)_5Cl]Cl_2$	292.58	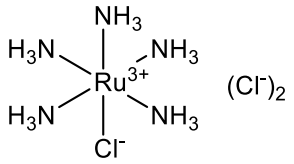
[Chlorido(η6-p-cymene)(N-(4-chlorophenyl)pyridine-2-carbothioamide) ruthenium(II)] chloride	**4**	$C_{22}H_{23}Cl_3N_2SRu$	554.92	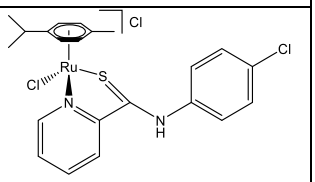
Hexaamminecobalt (III) Chloride	**5**	$[Co(NH_3)_6]Cl_3$	267.48	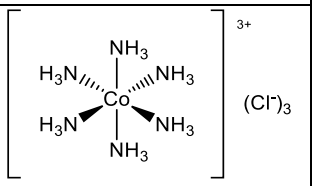
Diammineplatinum (II) chloride	**6**	$Pt(NH_3)_2Cl_2$	300.05	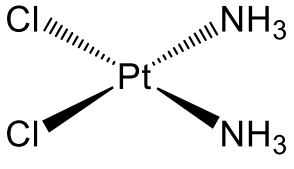

1.6.1 Hexaammineruthenium (III) chloride (**1**)

1 is octahedral in shape with labile ligands and is an electron donor and π acceptor (Lopes *et al*., 2010). This complex has a molecular weight of 309.61 Da and has the ability to efflux through porins of Gram-negative bacteria such as *P. aeruginosa* (Manchester *et al*., 2012) thus inhibiting the growth of *P. aeruginosa* strain PAO1 at 32 μg mL^{-1} and has potent bactericidal activity where after 6 h all *P. aeruginosa* cells were rendered non-viable. This complex additionally lacked activity against Gram-positive bacteria. **1** has been used in previous studies as a DNA binding signaller in cancer detection at low levels of miRNA-21 in human serum, demonstrating good selectivity, stability and high sensitivity without the need for extraction and purification of the miRNA's (Hong *et al*., 2019). Additionally, this complex inhibited calcium transport within mitochondria and the cell membrane, in addition to binding to phospholipids, acidic peptides, DNA and RNA as demonstrated through vertebrate mouse *in vivo* modelling (Luft, 1971). **1** selectively binds to imine areas on biomolecules through protein coordination to histidyl imidazolenitrogens or bind to the N7 region on purines mainly guanine and nucleic acids.

1.6.2 Hexaammineruthenium (II) chloride (**2**)

2 has labile ligands and alternatively to **1**, is a π donor however this complex is unstable and can decompose in air and water to **1**, Ru^0 and ammonia (Lopes *et al*., 2010). **2** is widely used as an electrochemical couple for redox reactions (Wang *et al*., 2011). Additionally it is used as an electrochemical sensor for neurodegenerative conditions due to its low redox potential eliminating interfering signals and increased sensitivity when combined to titanium oxide (Özdemir *et al*., 2019). **2** was used to observe telomerase activity by attaching to nicked double helixes, thus creating an amplified signal, increasing its affinity to DNA (Wang *et al*., 2015). **2** has a positive charge which allows for electrostatic binding to the

anionic phosphate in DNA, thus allowing for the detection of cancer as a biosensor (El Aamri *et al*., 2020). The complex is also used for the detection of miRNA of cancer including lung (Kannan *et al*., 2020) and breast due to the electro-reduction of **1** into **2** which produced a ratio metric signal (Gai *et al*., 2017).

1.6.3 Pentaamminechlororuthenium(III) chloride (**3**)

3 has an octahedral configuration with one chloro and five ammine ligands surrounding the central Ru(III) atom at differing bond lengths of 2.343 and 2.108 Å respectively (Hambley *et al,* 1991). It has been found to specifically bind to double stranded DNA through base pair intercalation (García *et al*., 2011). Therefore it has mainly been used previously as a probe like in a study where the complex has been tested previously for its antifungal ability against *Candida* species. As a lone complex at a concentration of 1mg cm^{-1}, antifungal activity was detected in one strain of *Candida albicans* through disc diffusion assays testing with a diameter of 11.5 mm, however combined with catecholamines such as isoproterenol then diameters increased and activity with other species were additionally found demonstrating that having **3** as a base allows for activity to occur with effective ligands (de Lima *et al.,* 2003). Additionally **3** has been used as an electrochemical probe, such as in a study evaluating apoptosis through the interaction of Annexin V and phosphatidylserine where the probe is sensitive to reduced proteins and can bind covalently. However, it was also discovered that phosphatidylserine inhibits electron transfer between the probes due to coating the surface (Liu *et al*., 2009).

1.6.4 [Chlorido(η6-p-cymene)(N-(4-chlorophenyl)pyridine-2carbothioamide)ruthenium(II)] chloride (**4**)

4 is comprised of an arene group which has been found to target DNA nucleotides, specifically guanine, and forms monofunctional adducts (Hoeschele *et al.*, 2007). Additional Ru(II) (η6-p-cymene) complexes have been found to intercalate with CT-DNA and have good antimicrobial activity against *B. subtilis* and *E. coli* (Mustafa *et al*., 2020). Ru-arene complexes such as this has been shown to induce cell cycle arrest in the G1 phase (Hartinger and Dyson, 2008). Ru(II) (η6-p-cymene) complexes have previously been evaluated for anticancer studies where it was found to be less toxic than cisplatin (a common anticancer agent) and are stable in acidic conditions (Arshad *et al.*, 2017). **4** contains a dimethylsulfoxide (DMSO) ligand and other Ru complexes which contain similar ligands have potent antimicrobial activity against Gram-positive bacteria (Li *et al.,* 2015) by inducing cytoplasmic membrane damage and inhibiting nucleic acid processing at ribosomes (Southam *et al.*, 2017). In recent studies, **4** was highly active at inhibiting growth of MRSA at 8 µg mL^{-1} and has potent bactericidal activity where after 4 h, all MRSA cells were rendered non-viable. This complex had specific efficacy against Gram-positive bacteria and lacked notable antimicrobial activity against other Gram-negative ESKAPE pathogens.

1.6.5 Hexaamminecobalt (III) Chloride (**5**)

The central cobalt ion in Hexaammine (III) is a low-spin octahedral atom, and the tight binding of the amine groups to cobalt means that protonation does not occur readily however the ammonia ligands do interact with nucleic acids through hydrogen binding with oxygen atoms of phosphate groups. The positive three charge of the central cobalt allows for interactions to take place more strongly compared to 2+ charged metallic groups and the metal ions are responsible for the folding and function of RNA (Rowinska-Zyrek *et al*., 2013).

Additionally **5** is responsible for the conversion of DNA (Todd and Rau., 2008) in its usual B-form to covert to A or Z form and form five hydrogen bonds with guanine O6 and N7 as well as phosphate oxygen for better stabilisation (Gessner *et al*., 1985; Rowinska-Zyrek *et al*., 2013). **5** has previously been used as an anion receptor due to its hydrogen bond donor groups, positively charged central ion for electrostatic interactions and a strong framework, additionally it is easy to synthesize in large quantities (Bala *et al*., 2007). It is additionally a magnesium channel blocker, which has been previously applied to yeasts such as *Candida albicans* and an inhibitor of mitochondrial ROS generation (Kwun and Lee., 2020).

1.6.6 Diammineplatinum (II) chloride (**6**)

In the 1960's initial observations of electrodes comprised of platinum mesh inhibited cell division in *E. coli* (Rosenburg *et al*., 1965), from there cisplatin was developed. Cisplatin is a world leading anti-cancer agent, which inhibits cellular division through binding to cellular DNA in multiple cancers (Ishida *et al*., 2002) such as small cell lung cancer, ovarian and testicular cancer (Ghosh., 2019). Cisplatin diffuses through the membrane of cells and actively transported through copper mediated transport proteins (Ishida *et al*., 2002), once inside the cell, a chloro ligand is replaced by water creating a positive charge and thus an inability to leave the cell. The platinum ion then binds to guanine bases in DNA forming a monofunctional adduct and causes DNA distortion and cell apoptosis (Alderden *et al*., 2006). Cisplatin has additionally been found to degrade the copper transporters that allow it into the cell, stopping efflux out of the cell and accumulation of platinum ions. Cisplatin induces ROS generation, as well as exhibiting DNA damage, to induce apoptosis (Dasari and Tchounwou., 2014. The extrinsic pathway of apoptosis involves activation of the Fas ligand through phosphorylation and production of ROS (Gupta *et al*., 2012). Calcium homeostasis is

disrupted upon cisplatins entry into the cell by initiating lipid peroxidation and inhibition of enzymes associated with homeostasis (Dasari and Tchounwou., 2014).

1.7 Aim and objectives

With global antimicrobial resistance (AMR) rates increasing, new antimicrobial complexes are essential in order to treat more challenging infections. Metal-based complexes are increasingly being examined for their efficacy against AMR infections. Previous studies have demonstrated the selective nature of certain Ru complexes, where some preferentially target either Gram-positive or Gram-negative bacterial cells. This study aimed to investigate the selective antibacterial effects of a series of Ru complexes, determine cytotoxicity profiling and validate lead complexes for potential use as topical or systemic treatment options against clinically relevant bacterial pathogens.

This was achieved through the following objectives:

(1) Validate the antimicrobial activity of each Ru-based complex against a range of antimicrobial resistant clones of each respective target pathogen.
(2) Validate lead complexes for use in topical treatment applications via *in vitro* and *in vivo* cytotoxicity studies and infection modelling based off data from Chapter 2.
(3) Understand the molecular mechanisms underpinning the selective antimicrobial activity of each complex.

Chapter 2: Antimicrobial activity of metallotherapeutic complexes

2.1 Introduction

2.1.1 Gram-negative bacterial pathogens

Infections mediated by Gram-negative pathogens are notoriously challenging to clinically treat due to the presence of an outer membrane as part of the cell ultrastructure, which reduces antimicrobial uptake into cell (Gupta and Datta., 2019). There are several key bacterial species which form the WHO priority list where antibiotics are urgently needed (Shrivastava *et al*., 2017). These include the ESKAPE pathogens comprising *Enterococcus faecium*, *Staphylococcus aureus*, *Klebsiella pneumoniae*, *Acinetobacter baumannii*, *Pseudomonas aeruginosa*, and *Enterobacter* species (Mulani *et al*., 2019). Due to increased mutations these pathogens are highly resistant to many classes of antibiotic including one of the last lines of defence, carbapenem. Carbapenem resistance has evolved due to the introduction of carbapenemase genes in bacterial plasmids, causing reduction in porin encoding genes thus resulting in fewer porins for antibiotic access and an overexpression of efflux pump genes for subsequent removal of antibiotic if present within the bacterial cell (Nordmann and Poirel., 2019). These mechanisms of resistance may cause cross-resistance in other species and antibiotic classes, contributing to the rise of antibiotic resistant bacteria (Moyá *et al*., 2012). In the USA, carbapenem resistant *A. baumannii* and *P. aeruginosa* infections contributed to 44.8 % and 14.2 % of community acquired infections respectively (Cai *et al*., 2017) and *S. maltophilia* was the most commonly carbapenem-resistant isolated pathogen in nosocomial pneumonia patients globally (Gales *et al*., 2019). It was discovered in Europe that 70.7 % of carbapenem-resistant *K. pneumoniae* cases produced carbapenemase and only 29.3 % were resistant through other mechanisms such as efflux as described previously (Grundmann *et al*., 2017).

Gram-negative pathogens including *P. aeruginosa, A. baumannii* and *S. maltophilia* are involved in numerous infections including urinary tract infections, pneumonia, skin and soft tissue infections including necrotizing fasciitis (De Oliveira *et al*., 2020). Mortality rates vary between the species of ESKAPE bacteria with *K. pneumoniae* necrotizing and soft tissue infections equating up to 47 % mortality (Krapp *et al*., 2017), *A. baumannii* associated pneumonia and bloodstream infections have a 35 % mortality (Antunes *et al*., 2014) and *P. aeruginosa* associated bacteraemia provided the highest mortality figure with 67 % (De Oliveira *et al*., 2020). Although *A. baumannii* infections have lower mortality compared to the other ESKAPE pathogens, the number of multidrug resistant infections were higher, exceeding rates in *P. aeruginosa* and *K. pneumoniae* by over four times (De Oliveira *et al*., 2020).

Data from the English Surveillance ProGramme for Antimicrobial Utilisation and Resistance (ESPAUR) demonstrated that there was a rise in the number of Gram-negative infections specifically within the bloodstream with the incidence increasing from 2015 to 2019 (Figure 3.1). Additionally the report showed the number of antibiotic resistant infections increased by 32 % over 4 years with an overall number of 18,110 antibiotic resistant infections in 2019 (Public Health England., 2019). *E. coli* is the more prominent Gram-negative infection however cases of *K. pneumoniae* and *P. aeruginosa* were increasing over the time period.

Additionally, *Pseudomonas aeruginosa* is a commercial issue, affecting both businesses and the end user through contamination of products and environments. The bacteria can infect equipment and products, potentially producing a threat to human health through consumption (Lundov *et al*., 2009) or application through products including make-up, mouthwash and hand lotion. *P. aeruginosa* can contaminate fuels, raw materials and

pharmaceuticals due to its ability for xenobiotic environment survival (Weiser *et al*., 2019). Contamination of high temperature and pressure environments have occurred such as in disinfectants, leather-making chemicals, crude oil and the Antarctic showing that in this setting *Pseudomonas* is resilient (Green *et* al., 2018). Usually to prevent contamination of products alcohols, acids and preservatives are used (Steinberg., 2010) however due to resistance emergence and in *P. aeruginosa* isolates these barriers are failing. Non-clinical strains of *P. aeruginosa,* including NCTC 12903 and ATCC 9027, have a larger genome than regular environmental strains with sizes of an average of 7.0 Mb and 6.5 Mb respectively due to the presence of a megaplasmid which is associated with highly stress-resilient phenotypes (Weiser *et al*., 2019). There is now an urgent need for biocidal products to overcome contamination and continue production of good quality products.

One of the reasons behind the prevalence in industry is due to the ability of *P. aeruginosa* to form biofilms. These biofilms are surrounded by an extracellular polymeric matrix comprised of lipids, nucleic acids, polysaccharides and proteins that provide protection against biocides and provide biofilm stability (Azam and Khan., 2019). Persister cells are more prevalent in Gram-negative based biofilms due to their cell membranes containing lipopolysaccharide (LPS) which halts the penetration of antimicrobials and nutrients into the biofilm thus leading to reduced metabolism (Sultana *et al*., 2016). *Pseudomonas* species found in the industrial setting cause additional issues including contamination of the surrounding areas from by-products where the bacteria can thrive and cause increasing damage (Kumar *et al*., 2019). Due to the high nutrient and idealistic environments of industrial work, horizontal gene transfer between the non-clinical and non-industrial pathogens could occur thus conferring resistance genes, making treatment more difficult. (Divya *et al*., 2018; Talmulden *et al*., 2021).

Necrotising fasciitis is a fast-progressing soft tissue infection with high mortality rates, even when treated with aggressive surgical intervention and antibiotic treatment (Bodansky *et al*., 2020). The bacteria involved in necrotising fasciitis vary with *Klebsiella, Pseudomonas, Staphylococcal, Streptococcal* species *and E. coli* being found in case studies (Marks *et al*., 2019). Necrotising fasciitis is caused by Gram-negative rods, *Streptococcal* and polymicrobial species of bacteria (Arif *et al*., 2016). Gram-negative associated necrotising fasciitis has the highest mortality rate, under optimal treatment conditions mortality can be as high as 44% with multiple organ failure occurring within 24 h (Leiblein *et al*., 2018).The incidence of necrotising fasciitis is additionally increasing, with incidence in the UK in the past decade reaching 500 cases per year (Diab *et al*., 2020) and with the additional rise in antimicrobial resistance, misdiagnosed cases are being left untreated for longer, contributing to the mortality rates. In the UK between the years 2002-2017, 14,659 patients were admitted to hospital for necrotising fasciitis infections with a 16 % mortality rate (Bodansky *et al*., 2020). In 2017 there was an increase in the frequency of Gram-negative cases due to an increase in the isolation of *E. coli* and *K. pneumoniae* species however *Pseudomonas* species are additionally involved (Yahav *et al*., 2014). Initially the infection starts from a break in the skin from a scratch, bite or abrasion (Bodansky *et al*., 2020), predominantly this disease affects immunocompromised patients such as in diabetes and HIV cases (Leiblein *et al*., 2018). Current treatments involve debridement and antibiotic therapy depending on the bacteria identified and its resistance profiling with the most common combination involving ampicillin with clindamycin or metronidazole (Misiakos *et al*., 2014). However due to an increase in the number of Gram-negative resistant infections (Public Health England., 2019) this can make treatment difficult. Resistance patterns in known cases include *A. baumannii* resistant to amoxicillin, ciprofloxacin and clavulanic acid (Harika *et al*., 2020), *P. aeruginosa*

was only sensitive to colistin, amikacin and tazobactam with resistance to other antibiotics (Coppola *et al*., 2020; Gautam *et al*., 2019) and *K. pneumoniae* study with samples taken from a variety of patients and infections including necrotising fasciitis showed that isolates were resistant to ceftazidime, cefotaxime, cefepime, and imipenem (Tiwana *et al*., 2020). In order to combat this, new novel antimicrobial treatments need to be found against Gram-negative species, to allow for more treatment options against this disease.

Additionally synergistic antimicrobial combinations could be used to combat skin infections including necrotising fasciitis. Drug repurposing can allow for antibiotic resistant infections to be treated again without the need of time-consuming research into developing novel antibiotics (Sun *et al*., 2016). Repurposing removes the need for entry into clinical trials due to the antibiotics already being approved thus reducing the time for development further (Zheng *et al*., 2018). Combining antibiotics have a beneficial effect, for example combining β-lactam antibiotics such as penicillin with a β-lactamase inhibitor thus enabling the β-lactam class of antibiotics to exhibit action against previously resistant species of bacteria (Aldeyab *et al*., 2008). Using antibiotics in combination also allows for antibiotics with reduced efficacy to work efficiently (Sun *et al*., 2016b) by using this method of phenotypic screening against current antibiotics and those in combination can allow for the success of treatment in a quick and timely manner.

2.1.2 Importance of antimicrobial evaluation

Evaluating antimicrobials for efficacy is vital for developing new diagnostic interventions. Upon diagnosis of the patients, the required antibiotic is identified, then a second epidemiological assessment is carried out in order to determine the pathogens epidemiology and evolution of resistance mechanisms as well as monitoring the pathogens

dissemination to assist with control mechanisms to cease the spread (van Belkum *et al*. 2019. This data can lead to an antibiogram machine learning programme to predict suitable antibiotic candidates for treatment and follow the resistant trends in species (Paul *et al*., 2006).

However, due to the increasing number of bacteria becoming resistant to many classes of antibiotics and decreased number of efficient antibiotics, there is a need for antimicrobial testing to highlight potential treatments which could prove beneficial. Surveillance of resistance patterns within the laboratories is vital for monitoring mutations within bacterial species (Sawatzky *et al*., 2015). Typical methods of assessing antimicrobial activity include disc diffusion and Minimum inhibitory concentration (MIC) (Bayot and Bragg., 2019). Antimicrobial susceptibility testing is used to determine the activity of potential antimicrobial complexes, determine the likelihood of resistance development to lead complexes and estimate *in vivo* efficacy (Haney *et al*., 2019; Mercer *et al*., 2020). Susceptibility methodologies currently cause a broad range of results due to only testing a single species against a single antimicrobial (Mouton *et al*., 2019)

2.1.3 Amine functional groups as antimicrobial ligands

Novel antimicrobial agents containing an amine group have been identified as having potent antimicrobial properties. In 1999 an extensive study on a library of amine derived peptoids against *S. aureus* and *E. coli* demonstrated increased antimicrobial activity when a primary or hydrophobic amine group was attached (Ng *et al*., 1999). Another example a tertiary amine bonded covalently to a polystyrene fibre was found to exhibit antimicrobial activity against Gram negative pathogens. Upon treatment with the fibre for 10 minutes, the bacterial viability of multiple species of bacteria including *E. coli, P. aeruginosa, S. aureus* and *C. albicans* decreased by 2-fold on tryptone soya agar and appeared to affect the

bacterial cell membranes by causing membrane perturbation (Endo *et al*., 1987). Additionally, a hydantoin amine derivative, poly(3-allyl-5,5-dimethylhydantoin-co-vinylamine) (P(ADMH-co-VAm)), chlorinated and bonded to a polyamide membrane demonstrated significant antimicrobial action against *E. coli* with additional N-C groups present causing an increase in antimicrobial activity and high regeneration capability. This is due to the amide group maintaining high membrane permselectivity in the presence of hydrogen bonding and its ability to interlink with chlorine (Wang *et al*., 2018).

It is known that amine-oxide derivatives are commonly used in personal care products therefore are acceptable for human use. Additionally, there are no known carcinogenic incidences as well as no developmental or reproductive toxicity in human studies (Fagnani *et al*., 2021). The antimicrobial activity of amine-oxides against the Gram-positive MRSA isolates increase as the length of the carbon chain increases (Devínsky *et al*., 1990; Fagnani *et al*., 2021). This is due to the complexes propensity to form aggregates (Battista *et al*., 2019). Amine groups are vital for antimicrobial activity to occur, a study conducted tested 1,3-bis(aryloxy) propan-2-amine complexes in which antimicrobial activity was observed, however upon substitution with azide, hydroxyl or mesyl group resulted in loss of antimicrobial activity (Serafim *et al*., 2019), demonstrating that the amine group is an integral part of antimicrobial complexes. Complexes such as the ones in the present study all have multiple amine groups and therefore have the potential to exhibit antimicrobial activity against bacterial pathogens. Complexes **4** and **6** has the least amount of amine groups with only 2 being present in the structures, whereas **3** has 5 amine groups and the remaining complexes have 6, meaning the potential for membrane perturbation was possible.

In summary, more must be done to tackle the challenging complications of Gram-negative infections. Additionally in cases of necrotising fasciitis where, although rare cases occur, the consequences of infection are devastating due to its rapid progression and antimicrobial resistance. Using ruthenium-based complexes could be a solution to tackling these issues due to its multiple mechanisms of action and the addition of amine groups which potentially enhances the antimicrobial activity. Activity against Gram-negative pathogens were explored to determine the potential use as an effective agent.

2.2 Aims and Objectives

2.2.1 Aim

The aim of this chapter was to use a range of standard assays to determine the antimicrobial activity of mononuclear ruthenium metallotherapeutic complexes containing amine functional groups. This was achieved through the following objectives.

2.2.2 Objectives

- Determine the resistance profiles of a series of commonly used antibiotics against different bacterial species and multiple clinical isolates of *Pseudomonas aeruginosa*.
- Evaluate the antimicrobial activity using disc diffusion assays, minimum inhibitory concentration (MIC) assays, minimum inhibitory concentration (MBC) assays and measuring effects on bacterial growth dynamics against clinical isolates of *Acinetobacter baumannii*, *Stenotrophomonas maltophilia*, *Klebsiella pneumoniae*, *Salmonella enterica* serotype Typhimurium, *Pseudomonas aeruginosa*, *Staphylococcus aureus*, *Micrococcus luteus*, *Staphylococcus epidermidis* and *Listeria monocytogenes*.
- Identify synergistic combinations of relevant clinically used antibiotics with lead Ru complexes against *P. aeruginosa*.

2.3 Methods

2.3.1 Bacterial strains and growth conditions

Cultures were grown on cationic adjusted Mueller Hinton-2 (MH) agar or broth (Oxoid, UK) and incubated at 37 °C for 24 h, with agitation at 200 rpm for broth cultures only. All cultures used in the present study were obtained from glycerol stock, cultured on MH agar and checked for contamination using visual appearances and bacterial identification. The bacteria used are outlined in Table 2.1.

Table 2. 1: Bacterial strains used in the present study.

Gram-negative species	*Acinetobacter baumannii* NCTC 12156 *Acinetobacter baumannii* LEEDS *Stenotrophomonas maltophilia* S1 *Klebsiella pneumoniae* 13883 *Klebsiella pneumoniae* LEEDS *Salmonella enterica* serotype Typhimurium strain 14028 *Pseudomonas aeruginosa* PAO1 *Pseudomonas aeruginosa* NCTC 12903 *Pseudomonas aeruginosa* ATCC 9027
Gram-positive species	MRSA *Staphylococcus aureus* USA300 *Micrococcus luteus* strain 15307 *Staphylococcus epidermidis* NCTC 11047 *Listeria monocytogenes* strain Scott A

Methicillin Resistant *Staphylococcus aureus* (MRSA) strain USA300 and *Pseudomonas aeruginosa* strain PAO1 were used as multidrug resistant (MDR) laboratory reference strains. All other strains of MRSA and *P. aeruginosa* were obtained from clinical isolates (kindly donated by Professor M. Enright) and stored in glycerol at -80 ˚C.

2.3.2 Preparation of Ruthenium complexes

1 (Hexaammineruthenium (III) chloride, Mr = 309.61), **2** (Hexaammineruthenium (II) chloride, Mr = 273.15) and **3** (Pentaamminechlororuthenium (III) chloride, Mr = 292.58) (Sigma-Aldrich, UK) was stored at 4 °C away from direct light and **3** stored at room temperature. Whereas **4** ([Chlorido(η6-p-cymene)(N-(4-chlorophenyl)pyridine-2-carbothioamide) ruthenium(II)] chloride, Mr = 554.92) (synthesised by Professor C. Hartinger, University of Auckland, NZ), **5** (Hexaamminecobalt (III) Chloride, Mr = 267.48) and **6** (Diammineplatinum (II) chloride, Mr = 300.05) (Sigma-Aldrich, UK) were stored away from direct light at room temperature until use. Complexes **1**, **2** and **3** was solubilised in distilled H_2O, complexes **4** and **5** was solubilised in neat analytical grade dimethylsulfoxide (DMSO) (Sigma-Alrich, UK) and **6** solubilised in ammonia creating stock solutions of 256 µg mL^{-1} stored at 4 °C.

2.3.3 Bacterial strain resistance profiling

In order to determine the sensitivity levels of each bacterial strain to current antibiotic treatments, resistance profiling was completed on every strain of *P. aeruginosa*. The Kirby-Bauer disk diffusion susceptibility protocol was followed from Hudzicki, 2009. Colonies of bacteria was suspended in a saline solution and were inoculated onto MHA using the lawn plating method and left to dry (McFarland). Antibiotic impregnated mast rings (Mast group) were then placed onto the agar and incubated overnight at 37 ˚C. Mast group M26 Mast rings were used for *P.* aeruginosa strains respectively. M26 Mast rings contained 25 µg ampicillin, 50 µg chloramphenicol, 100 µg colistin sulphate, 30 µg kanamycin, 30 µg nalidixic acid, 50 µg nitrofurantoin, 25 µg streptomycin and 100 µg tetracycline (Mast Group, 2020). The following day results are analysed by measuring the diameter of the zone of inhibition

and compared in accordance with CLSI guidelines to determine whether the bacteria are sensitive, resistant or intermediate. *N* = 3 per condition.

2.3.4 Disc diffusion assays

Following the Kirby-Bauer disc diffusion specified by EUCAST guidelines, an overnight culture of bacterial strains was adjusted to an optical density of 0.5 in sterile saline and inoculated onto pre-dried 25 mL Mueller-Hinton Agar (MHA) plates using a sterile swab. Sterile filter paper discs and 2x2 cm Melolin wound dressings (MedicalDressings, UK) were placed in triplicate on the plate and 20 µL of respective Ru complexes were added to saturate the disc (Matshwele *et al*., 2020; Hudzicki., 2009). The agar plates were incubated overnight at 37 ˚C and the zone size diameter was measured using digital callipers. *N* = 3 per condition.

2.3.5 Minimum Inhibitory Concentration (MIC) assay

All Ru compounds were screened for antimicrobial activity against a range Gram-positive and negative bacterial strains and 40 multidrug resistant clinical strains of *S. aureus* and *P. aeruginosa* and other Gram-negative bacteria using a broth microdilution assay in sterile 96-well flat-bottom plates (Sarker *et al*., 2007). This was conducted in order to determine if antimicrobial activity was shown across a wide range of strains of species. Each plate was initially inoculated with 200 µL of MHB around the outside border to prevent plate evaporation. Column 11 contained 180 µl of MHB and 100 µL MHB was added to columns 10 to 2. Column 11 B, C, D was inoculated with 20 µL of the respective Ru complexes at a starting concentration of 256 µg mL^{-1} (in well 11) and column 11 E, F, G was inoculated with 20 µL of DMSO or sterile water for all strains of *Staphylococcus* and *Pseudomonas* strains

respectively as a control measure. A serial dilution was then carried out with the final concentration in well 3 of 1 µg mL^{-1}.

Briefly, bacterial cultures were grown for 18 h in MHB and adjusted to an Optical Density of 0.05 at 600nm (OD_{600}) using the sterile broth. The bacterial culture was then added to each well at a volume of 100 µL and sealed with parafilm. All plates were incubated at 37 °C for 24 h and the MIC results were recorded as the lowest concentration which inhibited visible growth of the bacterial species. *N* = 3 per condition.

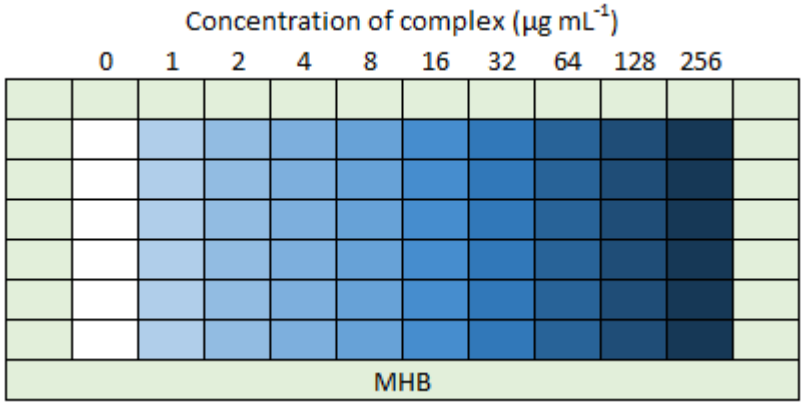

Figure 2. 1: Plate layout of the MIC assay.

2.3.6 Minimum Bactericidal Concentration (MBC) assay

Following MIC analysis, the MBC was determined using a multi-replicator plate where the culture from the 96-well plate was inoculated on to MHA and allowed to dry. These were incubated for 24 h at 37 ˚C and the MBC was recorded as the lowest concentration where bactericidal effects were observed. *N* = 3 per condition.

2.3.7 Growth dynamics

Following a similar method to Krishnamurthi *et al.*, an overnight culture of three Gram-negative bacteria grown in Mueller-Hinton Broth (MHB) was adjusted to an OD_{600} nm of 0.1

and plated in triplicate in a 96 well plate with a full range of concentrations of **1** (4 to 256 µg mL^{-1}). This was placed in a microplate reader and continual readings of the top of the plate were taken at 600 nm every 30 minutes for 24 h (Krishnamurthi *et al*., 2021). *N* = 3 per condition.

2.3.8 ATP leakage

P. aeruginosa strain PAO1 was incubated in 10 mL tryptone soya broth (TSB) overnight at 37 ˚C with shaking at 200 rpm. A 100 mL universal of bacteria was incubated with three concentrations of **1** at 8 µg mL^{-1}, 16 µg mL^{-1} and 32 µg mL^{-1}, colistin at 1 mg mL^{-1} and Triton-X-100 at 1% at 37˚C for 10 minutes and aliquots of 100 µL were taken. Samples of the culture were taken at intervals of 2 minutes and centrifuged for 5 minutes at 9000 x *g*, with the supernatant removed and the samples were kept on ice until use. All samples were then re-suspended in a boiling mixture of 100 mM Tris and 4 mM of EDTA at a pH of 7.4 where it was boiled at 100 ˚C for 2 minutes to ensure lysis of cells. Centrifugation at 9600 x *g* was carried out for 2 minutes before using an ATP bioluminescence kit (Invitrogen, Eugene, Oregon, USA) in accordance with manufacturer's instructions (Yasir *et al*., 2019). *N* = 3 per condition.

2.3.9 Crystal violet biofilm assay

In this thesis, a biofilm is classed as a community of *P. aeruginosa* singular strains grown overnight to adhere to the plate. The protocol, adapted from Cristensen *et al.* (1985), involved preparing an overnight culture of *P. aeruginosa* strain PAO1 in MHB and diluting the following morning by a 1:100 ratio using sterile MHB. A 96-well plate was inoculated with aliquots of 200 µL of culture with a comparable number of samples were a negative control of sterile MHB. The plates were incubated overnight at 37 ˚C. Following this the

plates were emptied and rinsed using sterile water and then varying sub-lethal concentrations of **1** (32 µg mL^{-1}, 16 µg mL^{-1}, 8 µg $mL^{-1}$and 4 µg mL^{-1}) were added at a ratio of 20 µL of complex with 180 µL MHB and incubated for 4 time points, 1, 2, 3 and 4 hours. Rinsing with water occurred before staining with 200 µL of 0.1% crystal violet (Sigma-Aldrich, UK) diluted in water and incubated at room temperature for 10 minutes, before being rinsed with water and blot dried 3 times in a category 2 hood. 96 % ethanol (Fischer chemicals, UK) was added at a volume of 200 µL to all the wells and refrigerated overnight before quantifying with a plate reader at 570 nm. *N* = 3 per condition.

2.3.10 Synergy studies

Using a 96 well plate, a combination of the Ru **1** and antibiotics used previously for the antibiotic resistance profiling was tested for synergistic properties (Andrade *et al.*, 2020). A serial dilution of the complex was conducted across the 96 well plate with the Ru complex being diluted in 1-12 wells and the antibiotic in the A-H wells similar to the 96 well plate MIC protocol. An overnight bacterial culture of *P. aeruginosa* strain PAO1 was diluted to an $OD_{600\ nm}$ of 0.05 and 100 µL will be added to each well and left overnight at 37˚C. Results was analysed to determine MIC values. The *P. aeruginosa* strain PAO1 was tested using **1** and colistin (Fluka Analytical, UK), gentamicin (Acros Organics, UK), streptomycin (Sigma-Aldrich, UK) and tetracycline (Sigma, UK). Concentrations of the antibiotic was found through journal articles as shown in the Table 2.2. *N* = 3 per condition.

The fractional inhibitory concentration index (FICI) was calculated using the formula (Spoorthi *et al*., 2011):

$$\frac{A}{MIC_A} + \frac{B}{MIC_B} = FIC_a + FIC_B$$

Where A and B was the MIC of the Ru complex and antibiotic respectively in combination (in a single well), and MIC_A and MIC_B was the MIC of each drug individually. Synergy is proven if the sum of the FIC values are < 0.5, additive or indifference with a FIC value 0.5-4 and antagonistic > 4 (Spoorthi *et al.*, 2011). This test can additionally determine whether the compounds can cause a resistance break among some antibiotics that the bacteria are normally resistant against.

Table 2. 2: Antibiotic concentrations used for the synergy studies along with the corresponding ruthenium complex.

Antibiotic	Concentration (µg mL^{-1})					Reference
Ciprofloxacin	8	16	32	64	128	Roudashti *et al*., 2017; Abdolhosseini *et al*., 2019
Colistin	50	100	200	400	800	
Gentamicin	5	10	20	40	80	Gupta *et al*., 2017; Das *et al*., 2016
Streptomycin	12.5	25	50	100	200	
Tetracycline	50	100	200	400	800	

All results were analysed using Graphpad Prism version 7.0 to determine significant differences between samples, with p <0.05 being considered as statistically significant in all cases. The data was presented as mean, standard error of the mean and standard deviation with t-tests and one-way and two-way ANOVA's being used to determine differences between the data.

2.4 Results

2.4.1 Resistance profiling

All bacterial strains in this chapter were tested for resistance to commonly used antibiotics using disc diffusion assays with Mast Rings. For all Gram-negative species there were no zones (0 mm) for Ampicillin (25 µg), Nalidixic Acid (30 µg) and Nitrofurantoin (50 µg). *A. baumannii* LEEDS was the most resistant strain, only having zones of inhibition with Colistin Sulphate and Kanamycin, whereas *P. aeruginosa* strain PAO1 was the most sensitive with an average zone size for all antibiotics being 59 mm (Table 2.3). Multiple t-tests proved the zone sizes of all bacterial strains were significant with $p<0.05$ and a two-way ANOVA demonstrated $P<0.0001$ for the bacterial strains, antibiotic used and the interaction of the two.

Table 2. 3: Zone sizes of Gram-negative bacteria following disc diffusion assay with Mast rings (N = 3). No EUCAST guidelines were available at the time of writing.

Antibiotic	**Tetracycline 100µg**		**Streptomycin 25µg**		**Chloramphenicol 50µg**		**Colisitin Sulphate 100µg**		**Kanamycin 30µg**	
Strain	ZOI (mm)	SD	ZOI (mm)	SD	ZOI (mm)	SD	ZOI (mm)	SD	ZOI (mm)	SD
***S. enterica* serotype Typhimurium strain 14028**	68.16	0.65	58.88	1.08	63.52	5.58	65.43	3.07	37.12	3.75
***P. aeruginosa* ATCC 9027**	79.53	2.15	31.63	0.20	57.82	1.68	79.95	3.42	34.38	2.60
***P. aeruginosa* NCTCC 12903**	44.92	2.47	50.87	2.02	0	0	57.15	1.05	0	0
***P. aeruginosa* PAO1**	78.64	2.74	37.40	4.44	64.73	1.01	82.34	3.58	31.89	4.85
***S. maltophilia* S1**	68.59	5.00	0	0	81.38	7.79	29.05	0.81	0	0
***K. pneumoniae* LEEDS**	57.34	4.09	0	0	33.64	5.26	85.02	4.52	29.67	3.55
***K. pneumoniae* 13883**	82.71	2.34	49.29	2.77	71.38	2.26	80.27	3.20	0	0
***A. baumannii* LEEDS**	0	0	0	0	0	0	65.55	6.31	53.36	2.64
***A. baumannii* NCTC 12156**	82.94	1.83	48.48	1.67	75.21	1.61	74.89	6.79	0	0

Whereas the Gram-positive bacteria were resistant to erythromycin, fusidic acid, oxacillin, novobiocin and penicillin G (0 mm). Two of the species *L. monocytogenes* and *S. epidermidis* was also resistant to Streptomycin (0 mm) however *M. luteus* and *S. aureus* USA 300 had small zones of 28.17 mm (SD = 1.08) and 39.23 mm (SD = 6.21) respectively. Two antibiotics, tetracycline and chloramphenicol both had zones ranging between 56.98 mm to 67.69 mm for all of the Gram-positive bacteria. Two-way ANOVA analysis suggests the bacteria, antibiotic and the interaction between the two was highly significant $p<0.0001$.

In order to compare the complexes in this study for efficacy, commonly used antibiotics were tested for their action against *P.* aeruginosa strain PAO1 using zones of inhibition testing as described previously. *P. aeruginosa* strains had a different profile with Ampicillin, Nalidixic Acid and Nitrofurantoin having no effect against the bacteria, concluding with a ZOI of 0 mm. Chloramphenicol created an average ZOI with two strains VTK:106177 and VTK:111070 of 5.72 mm and 8.42 mm respectively. Kanamycin additionally had effect with two strains VTK:106705 and VTK:111053 with a ZOI of 9.45 mm and 9.94 mm respectively. Streptomycin and Tetracycline both had effect against multiple strains of *Pseudomonas* with tetracycline affecting 13 strains with an average ZOI of 10.08 mm compared with Streptomycin affecting only 7 with an average ZOI of 11.52 mm. Colistin Sulphate was the only antibiotic to have effect against all of the *P. aeruginosa* strains tested with an average ZOI across species of 20.49 mm (Table 2.4).

One way ANOVA analysis revealed that there is significant difference between the susceptibility of bacterial strains to different antibiotics used in this study ($p<0.001$). *P. aeruginosa* proved to have a significant difference between the different antibiotic ($p<0.001$) and between bacteria insignificant results was shown with a p value of 0.989.

Table 2. 4: Resistance profiling of 20 *P. aeruginosa* strains with 5 antibiotics that produced a ZOI result (N = 3).

Strain	Chloramphenicol 50 µg		Colisitin Sulphate 100 µg		Kanamycin 30 µg		Streptomycin 25 µg		Tetracycline 100 µg	
	Mean ZOI (mm)	SD	Mean ZOI (mm)	SD	Mean ZOI (mm)	SD	Mean ZOI (mm)	SD	Mean ZOI (mm)	SD
VTK:106167	0	0	17.87	0.27	0	0	0	0	0	0
VTK:106176	0	0	19.16	0.51	0	0	0	0	0	0
VTK:106177	5.72	4.95	21.28	0.95	0	0	0	0	9.83	2.43
VTK:106188	0	0	23.23	0.06	0	0	17.11	1.50	9.22	0.22
VTK:106705	0	0	21.35	0.97	9.45	1.43	7.93	0.88	10.91	0.66
VTK:111050	0	0	20.81	0.26	0	0	0	0	2.84	4.92
VTK:111053	0	0	20.41	0.25	9.94	0.37	17.68	0.92	8.40	0.52
VTK:111055	0	0	20.67	0.72	0	0	0	0	10.92	0.66
VTK:111070	8.42	0.72	19.25	0.46	0	0	10.45	0.69	11.49	0.28
VTK:111074	0	0	18.88	0.58	0	0	11.77	0.56	9.37	1.19
VTK:111091	0	0	19.67	0.45	0	0	12.13	0.98	12.01	1.03
VTK:111124	0	0	20.29	1.00	0	0	6.55	0.21	14.19	0.74
VTK:111139	0	0	20.85	0.34	0	0	0	0	0	0
VTK:115480	0	0	20.28	0.56	0	0	0	0	0	0
VTK:115482	0	0	21.64	0.21	0	0	0	0	10.17	1.30
VTK:115489	0	0	22.42	0.41	0	0	0	0	10.34	0.99
VTK:115508	0	0	18.80	1.66	0	0	0	0	11.36	1.16
VTK:115529	0	0	22.06	0.44	0	0	0	0	0	0
VTK:115530	0	0	19.99	0.77	0	0	0	0	0	0
VTK:115531	0	0	20.83	0.44	0	0	0	0	0	0

2.4.2 Antimicrobial activity of Ru complexes against bacterial pathogens

Conducting a disc diffusion assay against a wide range of bacterial species was done through spread plating bacteria adjusted to a McFarland standard of 0.5 on MHA and placing filter discs impregnated with 32 µg mL^{-1} of each complex to be incubated overnight. **1** caused the largest zones with bacteria compared to the other complexes, especially **4** in which exposure only resulted in growth inhibition against MRSA and *P. aeruginosa* strain PAO1 with average zones of 19.403 mm (SD= 0.945) and 23.367 mm (SD= 2.606) respectively (Figure 2.2). Overall when **1** was added to *P. aeruginosa* PAO1 the zone sizes appeared larger in comparison with the other complexes, especially **4** in which majority of bacteria did not exhibit a zone size with the exception of MRSA and *P. aeruginosa* strain PAO1 with zone sizes of 19.403 mm (SD= 0.945) and 23.367 mm (SD= 2.606) respectively. The largest average zone recorded was when *P. aeruginosa* strain NCTC 12903 was exposed to **1** where a mean diameter of 40.453 mm (SD= 3.940) was recorded. Other bacterial strains when incubated with **1** had a range of zones between 28.110 – 40.453 mm with the exception of *S. enterica* serotype Typhimurium strain 14028 which had no zone. **2** all strains had a zone, ranging between 27.750 – 37.887 mm and **3** between 20.620 – 38.075 mm with the exception of *P. aeruginosa* strain PAO1 thus suggesting the ruthenium complexes have an antimicrobial effect against a plethora of bacterial strains. Two-way ANOVA analysis confirmed that the addition of the complexes, the bacterial strain and the interaction between the bacterial strain and complex have a $p<0.0001$ identifying that each individual complex and bacteria have significant zone sizes when exposed.

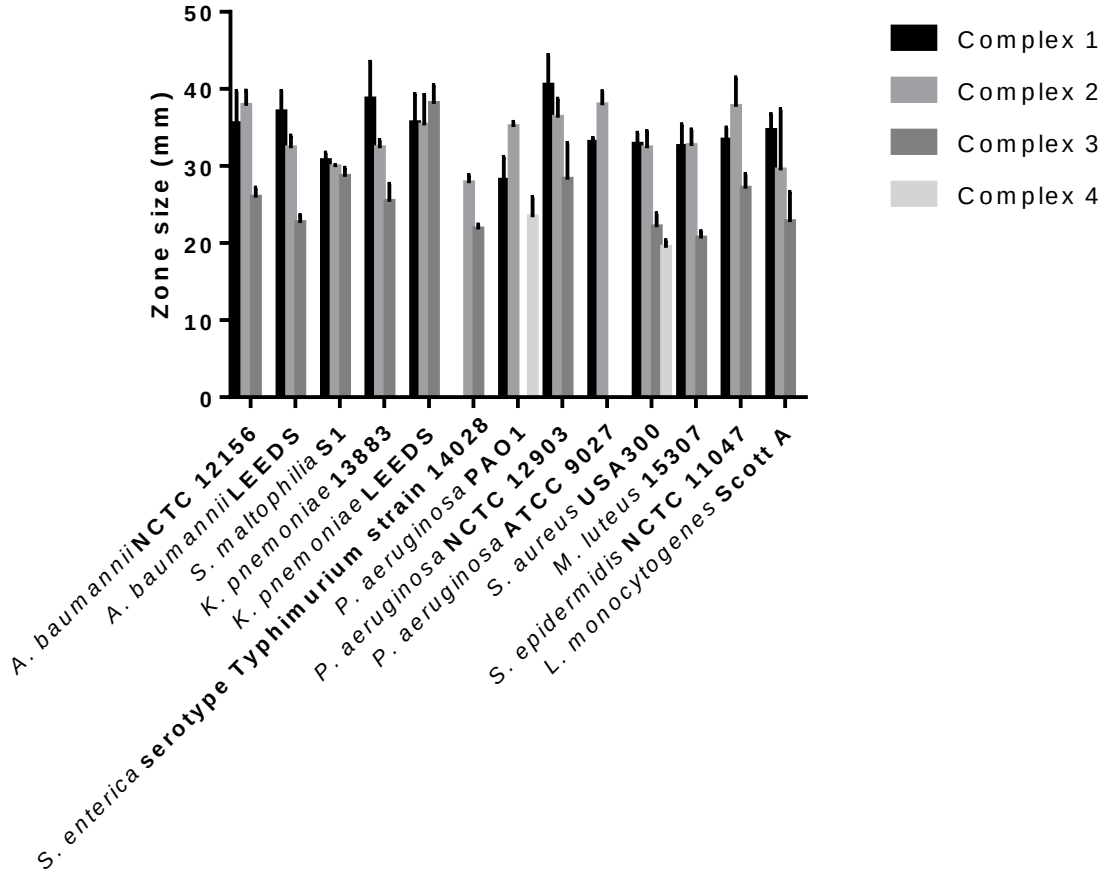

Figure 2. 2: Zones of inhibition of multiple Gram-positive and Gram-negative species of bacteria with four ruthenium complexes 1, 2, 3 and 4. Error bars represent standard error of the mean (*N*=3).

To determine efficacy of the **1** in this study, disc diffusion assays were conducted on MHA in triplicate, following an overnight incubation, zones were measured. The zones of inhibition of *P. aeruginosa* strain PAO1 increased in size with an increase in concentration of **1** (Figure 2.2; Figure 2.3; Figure 2.4). On average the zone size for 4 µg mL^{-1} was 16.291 mm (SD = 1.076) Fig. 2.3 a, 8 µg mL^{-1} 21.073 mm (SD= 1.372) Fig. 2.3 b and 16 µg mL^{-1} 26.691 mm (SD = 1.727) Fig. 2.3 c; Fig. 3.4. Over the three concentrations assessed the zone size increased

by 63%. Multiple t-tests between all concentrations gave a *p* value of 0.00896 and is therefore significant.

Figure 2. 3: Disc diffusion assay of *P. aeruginosa* strain PAO1 following exposure with 1 at a) 4 µg mL-1, b) 8 µg mL-1 and c) 16 µg mL-1 in triplicate (*N* = 3).

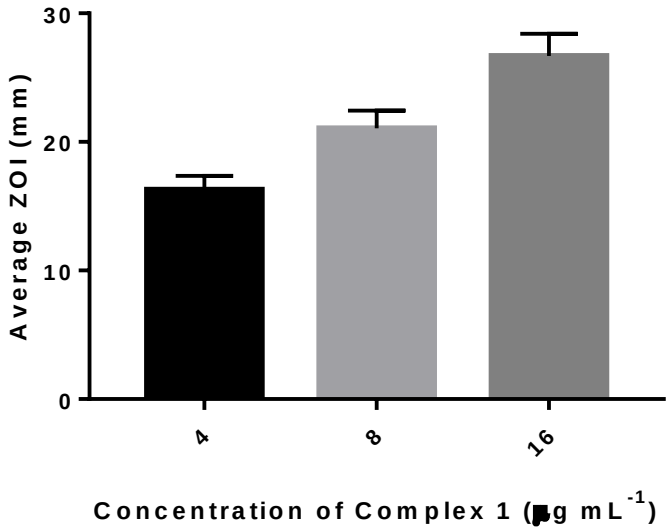

Figure 2. 4: Average zone size (*N* = 3) of differing concentrations of 1 (4 µg mL^{-1}, 8 µg mL^{-1} and 16 µg mL^{-1}) on filter discs with *P. aeruginosa* strain PAO1 with an error bar depicted as standard error of the mean (*N*=3).

Additional disc diffusion assays were carried out on 2x2 cm Melolin wound dressings to determine the efficacy of **1** in a real-world application which at concentrations of **1** at 4 µg mL^{-1}, 8 µg mL^{-1} and 16 µg mL^{-1} produced an average zone size of 40 mm, 46mm and 49mm

respectively (Figure 2.5). In which one-way ANOVA demonstrated significance with a *p* value of 0.0347 between the different treatments. Thus, this demonstrates an increased antimicrobial effect with an increase in concentration, even at sub-lethal concentrations there is still a large effect in diameter.

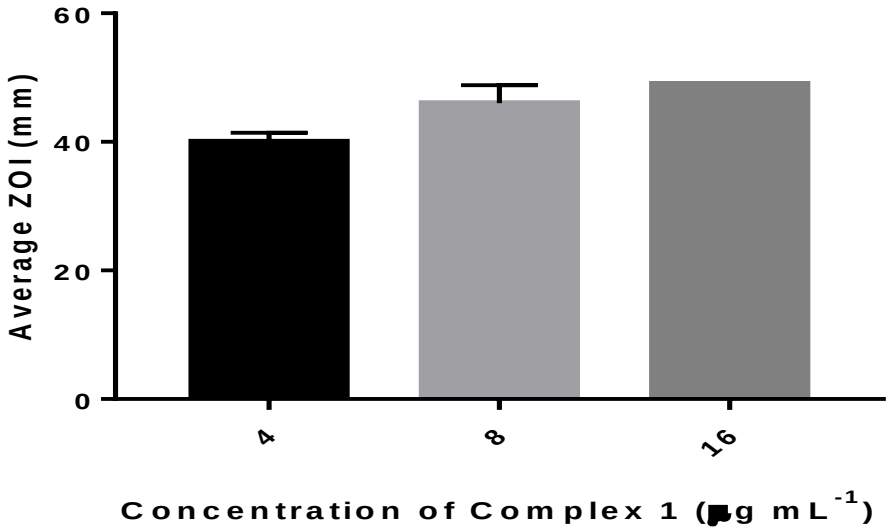

Figure 2. 5: Average zone size of *P. aeruginosa* strain PAO1 with wound dressings incubated with varying concentrations of 1 at 4 µg mL^{-1}, 8 µg mL^{-1} and 16 µg mL^{-1}. *N* = 3, error bars represent standard error of the mean (*N*=3).

2.4.3 MIC and MBC

Following disc diffusion assays, MIC and MBC assays were conducted using a broth microdilution method. Gram-negative bacterial strains including *Acinetobacter baumanii* NCTC 12156, *A. baumanii* LEEDS, *Stenotrophomonas maltophilia* S1 (hospital isolation) *Klebsiella pneumoniae* 13883 (Quality control strain), 13368 (antimicrobial resistant test) and LEEDS (multidrug resistant), *Salmonella enterica* serotype Typhimurium strain 14028, *P.*

aeruginosa strains PAO1, and non-clinical strains NTCT 12903 and ATCC 9027 and Gram-positive bacteria *Staphylococcus aureus* USA300, *Micrococcus luteus* strain 15307, *Staphylococcus epidermidis* NCTC 11047 and *Listeria monocytogenes* strain Scott A was used to determine the effectiveness of **1**, **2**, **3**, **5** and **6** with results shown in Table 2.5.

Table 2. 5: Average MIC and MBC values of alternative Gram-negative and Gram-positive bacteria when exposed with all 6 complexes (*N* = 3). SD and SE for all conditions was 0.

Strain	Mean MIC (μg mL^{-1})	Mean MIC (μM)	Mean MBC (μg mL^{-1})	Mean MBC (μM)
1				
A. baumannii NCTC 12156	16	51.6779	64	206.7117
A. baumannii LEEDS	128	413.4233	128	413.4233
S. maltophilia S1	32	103.3558	32	103.3558
K. pneumoniae 13883	32	103.3558	32	103.3558
K. pneumoniae 13368	128	413.4233	128	413.4233
K. pneumoniae LEEDS	256	826.8467	256	826.8467
S. enterica serotype Typhimurium strain 14028	>256	>826.8467	>256	>826.8467
P. aeruginosa PAO1	4	12.9195	8	25.8390
P. aeruginosa NCTC 12903	128	413.4233	128	413.4233
P. aeruginosa ATCC 9027	128	413.4233	256	826.8467
MRSA	256	826.8467	256	826.8467
M. luteus strain 15307	32	103.3558	32	103.3558
S. epidermidis NCTC 11047	128	413.4233	256	826.8467
L. monocytogenes strain Scott A	>256	>826.8467	>256	>826.8467
2				
A. baumannii NCTC 12156	16	58.5759	64	234.3035
A. baumannii LEEDS	128	468.6070	128	468.6070
S. maltophilia S1	32	117.1517	32	117.1517
K. pneumoniae 13883	128	468.6070	128	468.6070
K. pneumoniae LEEDS	256	937.2140	256	937.2140
S. enterica serotype Typhimurium strain 14028	256	937.2140	256	937.2140
P. aeruginosa PAO1	8	29.2879	8	29.2879
P. aeruginosa NCTC 12903	128	468.6070	128	468.6070
P. aeruginosa ATCC 9027	256	937.2140	256	937.2140
MRSA	128	468.6070	128	468.6070
M. luteus strain 15307	64	234.3035	64	234.3035
S. epidermidis NCTC 11047	256	937.2140	256	937.2140
L. monocytogenes strain Scott A	128	468.6070	128	468.6070

3				
A. baumannii NCTC 12156	64	218.7436	64	218.7436
A. baumannii LEEDS	256	874.9744	256	874.9744
S. maltophilia S1	64	218.7436	64	218.7436
K. pneumoniae 13883	256	874.9744	256	874.9744
K. pneumoniae LEEDS	>256	>874.9744	>256	>874.9744
S. enterica serotype Typhimurium strain 14028	256	874.9744	256	874.9744
P. aeruginosa PAO1	32	109.3718	64	218.7436
P. aeruginosa NCTC 12903	256	874.9744	256	874.9744
P. aeruginosa ATCC 9027	>256	>874.9744	>256	>874.9744
MRSA	32	109.3718	64	218.7436
M. luteus strain 15307	64	218.7436	64	218.7436
S. epidermidis NCTC 11047	128	437.4872	256	874.9744
L. monocytogenes strain Scott A	128	437.4872	128	437.4872
4				
A. baumannii NCTC 12156	256	461.3278	256	461.3278
A. baumannii LEEDS	>256	>461.3278	>256	>461.3278
S. maltophilia S1	>256	>461.3278	>256	>461.3278
K. pneumoniae 13883	>256	>461.3278	>256	>461.3278
K. pneumoniae LEEDS	>256	>461.3278	>256	>461.3278
S. enterica serotype Typhimurium strain 14028	>256	>461.3278	>256	>461.3278
P. aeruginosa PAO1	>256	>461.3278	>256	>461.3278
P. aeruginosa NCTC 12903	>256	>461.3278	>256	>461.3278
P. aeruginosa ATCC 9027	>256	>461.3278	>256	>461.3278
MRSA	8	14.4165	16	28.8330
M. luteus strain 15307	64	115.3319	64	115.3319
S. epidermidis NCTC 11047	128	230.6639	128	230.6639
L. monocytogenes strain Scott A	128	230.6639	128	230.6639
5				
A. baumannii NCTC 12156	2	7.4772	2	7.4772
A. baumannii LEEDS	4	14.9544	4	14.9544
S. maltophilia S1	8	29.9088	16	59.8176
K. pneumoniae 13883	16	59.8176	16	59.8176
K. pneumoniae LEEDS	16	59.8176	16	59.8176
S. enterica serotype Typhimurium strain 14028	8	29.9088	8	29.9088
P. aeruginosa PAO1	16	59.8176	16	59.8176
P. aeruginosa NCTC 12903	8	29.9088	8	29.9088
P. aeruginosa ATCC 9027	4	14.9544	8	29.9088
MRSA	32	119.6351	64	239.2702
M. luteus strain 15307	8	29.9088	8	29.9088
S. epidermidis NCTC 11047	16	59.8176	16	59.8176
L. monocytogenes strain Scott A	16	59.8176	16	59.8176
6				

A. baumannii NCTC 12156	128	426.5956	128	426.5956
A. baumannii LEEDS	256	853.1911	256	853.1911
S. maltophilia S1	256	853.1911	256	853.1911
K. pneumoniae 13883	128	426.5956	128	426.5956
K. pneumoniae LEEDS	128	426.5956	128	426.5956
S. enterica serotype Typhimurium strain 14028	128	426.5956	128	426.5956
P. aeruginosa PAO1	128	426.5956	128	426.5956
P. aeruginosa NCTC 12903	128	426.5956	128	426.5956
P. aeruginosa ATCC 9027	128	426.5956	128	426.5956
MRSA	64	213.2978	64	213.2978
M. luteus strain 15307	128	426.5956	128	426.5956
S. epidermidis NCTC 11047	128	426.5956	128	426.5956
L. monocytogenes strain Scott A	256	853.1911	256	853.1911

DMSO and water controls are not shown as there is no effect on bacterial growth (data not shown). However, MIC testing conducted with an ammonia control proved to have an antimicrobial effect on certain strains possibly contributing to the high antimicrobial activity of **5** (data not shown).

There is significant difference of MIC and MBC values as calculated by two-way ANOVA between the bacterial species and complex used to treat (p<0.0001). As the MIC and MBC data demonstrated in Table 3.1, *A. baumannii* NCTC 12156, *S. maltophilia* S1*, P. aeruginosa* PAO1*, K. pneumoniae* strain 13883 and *M. luteus* strain 15307 are susceptible to **1**. **1** demonstrated activity against the quality control strain of *K. pneumoniae* 13883 however not against the antimicrobial resistance test strain nor the multidrug resistant strain suggesting perhaps efflux pumps that are present in these resistant strains are removing **1** out of the bacterial cell. *S. maltophilia* S1 has comparable MIC and MBC values to majority of the strains of *P. aeruginosa* tested previously and *A. baumanii* NCTC 12156 is comparable with a couple of VTK strains as shown in Table 2. One way ANOVA analysis demonstrates

that this data is highly significant with a *p* value <0.0001 with activity being demonstrated with **1** and Gram-negative pathogens.

2 showed similar results with the same bacteria as **1** with *P. aeruginosa* strain PAO1 having a MIC of 8 μg mL^{-1} again with a significance of $p<0.0001$ however 69 % of strains had a MIC above 128 μg mL^{-1} and **3** had a slight effect on *A. baumannii* NCTC 12156 and *S. maltophilia* strain S1 with a MIC value of 64 μg mL^{-1} with the most effective being against PAO1 at 32 μg mL^{-1} ($p<0.0001$). Complexes 1, 2 and 3 all have amine and chloride ligands present within their chemical structure however a different number of ligands. Complexes 1 and 2 both have 6 amine ligands however **1** has 3 chloride ions in comparison with **2** which only has 2. **3** however has 5 amine ligands and 1 chloride ligand attached to the Ru core. The difference in MIC and MBC between the three complexes suggests that an increase in the amine groups has significant effect on the activity of the complex against the different bacteria with **3** being the least effective on multiple bacteria (MIC >256 μg mL^{-1}).

5 proved effective against all strains both Gram positive and negative with MIC values not exceeding 32 μg mL^{-1}. Between all conditions tested including cobalt and platinum complexes there was a high significance proven through a one-way ANOVA $p=0.0002$. There was highly significant difference between the MIC and MBC values upon bacterial exposure to complexes 5 and 6 $p<0.0001$ this is due to **6** having an increase in MIC values with majority (69%) having an MIC value of 128 μg mL^{-1} with the lowest MIC being 64 μg mL^{-1} with MRSA. In contrast **5** has a highest MIC of 32 μg mL^{-1} with MRSA with all other bacteria exhibiting MIC's and MBC's lower than 16 μg mL^{-1}. Between **5** and **1** $p= 0.0014$ significance was found due to similar MIC values with 38 % of bacteria treated with **1** exhibiting 32 μg mL^{-1} and less and 100% of cobalt exhibiting 32 μg mL^{-1} and less. Overall, **1** and **5** exhibited

lower MIC and MBC values compared to the other complexes tested in this study. With the most effective for *P. aeruginosa* strain PAO1 being **1** with a MIC value of 4 μg mL^{-1} and **4** with USA300 with 8 μg mL^{-1}.

Further MIC and MBC assays demonstrated the antimicrobial activity of both **4** and **1** against multiple clinical strains of *S. aureus* and *P. aeruginosa* respectively. 90 % of the *S. aureus* strains had an average MIC and MBC value of 8 μg mL^{-1} with the exception of strains ARI12 and CDC16 which had an average MIC and MBC of 16 μg mL^{-1} and 4 μg mL^{-1} respectively. One-way ANOVA with a Dunnett's post hoc analysis demonstrated these strains were significantly more resistant and sensitive respectively than the model strain MRSA (p <0.05), which had MIC and MBC values of 8 μg mL^{-1} and 16 μg mL^{-1} respectively. **1** was proven effective at inhibiting or killing multiple strains of *P. aeruginosa* with 60 % of MIC and MBC values of 8 μg mL^{-1} and the highest MIC being 16 μg mL^{-1} (Table 2.6) for 30% of the strains tested.

Table 2. 6: Average MIC and MBC values of **4** against the multiple strains of *S. aureus* (A) and **1** against *P. aeruginosa* strains (B) *N* = 3.

Strain	Mean MIC (μg mL^{-1})	SD	SE	Mean MBC (μg mL^{-1})	SD	SE
(A) *S. aureus*						
USA300	8	0	0	16	0	0
H65	8	0	0	8	0	0
98.4823.x	8	3.46	2.00	8	3.46	2.00
99ST18131	8	2.31	1.33	8	0	0
AR O650 784	8	4.62	2.67	8	2.31	1.33
H182MRSA	8	0	0	8	0	0
UK 96/32010	8	2.31	1.33	8	0	0
NottmA2	8	2.31	1.33	8	2.31	1.33
ARI12	16	5.66	4.00	16	5.66	4.00
57/92	8	4.62	2.67	8	4.62	2.67
BK59	8	0	0	8	0	0
CDC16	4	6.93	4.00	4	2.83	2.00
E2260	8	2.31	1.33	8	2.31	1.33
Btn2299	8	2.31	1.33	8	2.31	1.33
Btn2289	8	0	0	8	0	0
CDC201114 USA300	8	2.31	1.33	8	0	0
CDC980193 USA800	8	2.31	1.33	8	2.31	1.33
CDC960758 USA200	8	0	0	8	0	0
HO 5096 0412	8	2.31	1.33	8	0	0
Sweden AO17934/97	8	6.11	3.53	8	4.62	2.67
NJ992 (CDC4)	8	4.62	2.67	8	0	0
(B) *P. aeruginosa*						
PAO1	32	0	0	64	0	0
VTK:106167	8	2.31	1.33	8	4.62	2.67
VTK:106176	4	2.31	1.33	16	6.93	4.00
VTK:106177	8	2.31	1.33	16	0	0
VTK:106188	2	0	0	8	2.31	1.33
VTK:106705	8	2.31	1.33	8	5.66	4.00
VTK:111050	8	2.31	1.33	16	9.24	5.33
VTK:111053	8	4.62	2.67	8	4.62	2.67
VTK:111055	8	0	0	8	5.66	4.00
VTK:111070	8	0	0	8	0	0
VTK:111074	8	2.31	1.33	16	0	0
VTK:111091	16	14.0	8.11	16	0	0
VTK:111124	16	12.2	7.06	16	9.24	5.33

VTK:111139	16	12.2	7.06	16	0	0
VTK:115480	16	13.9	8.00	16	9.24	5.33
VTK:115482	16	13.9	8.00	16	0	0
VTK:115489	8	7.02	4.06	8	0	0
VTK:115508	8	6.11	3.53	8	0	0
VTK:115529	8	4.62	2.67	8	5.66	4.00
VTK:115530	8	4.62	2.67	8	0	0
VTK:115531	16	12.2	7.06	16	5.66	4.00

2.4.4 Growth Curves

Growth kinetics using two Gram-negative bacteria *P. aeruginosa* PAO1 and *S. maltophilia* S1 over a 24 h period was conducted with varying concentrations of **1** and the absorbance monitored every 30 min. The absorbance was adjusted by measuring the absorbance of the media alone and subtracting from the overall results. The results indicate without incubation the bacteria grow to an absorbance at 600 nm of a maximum of 2.214 and 2.468 for *P. aeruginosa* PAO1 (Figure 2.6a) and *S. maltophilia* S1 (Figure 2.6b) respectively. As the concentration of **1** increases the OD of each bacteria decreases, indicating the higher concentrations of **1** causes bacterial death and inhibition of growth. Two-way Anova analyses for both bacteria are highly significant with a *p* value <0.0001 with both time and concentration thus indicating that the increased concentration of **1** has a significant effect upon bacterial growth with the higher concentration inhibiting growth and the time the bacteria is incubated over 24 h is highly significant to the growth of the bacteria at all concentrations.

a)

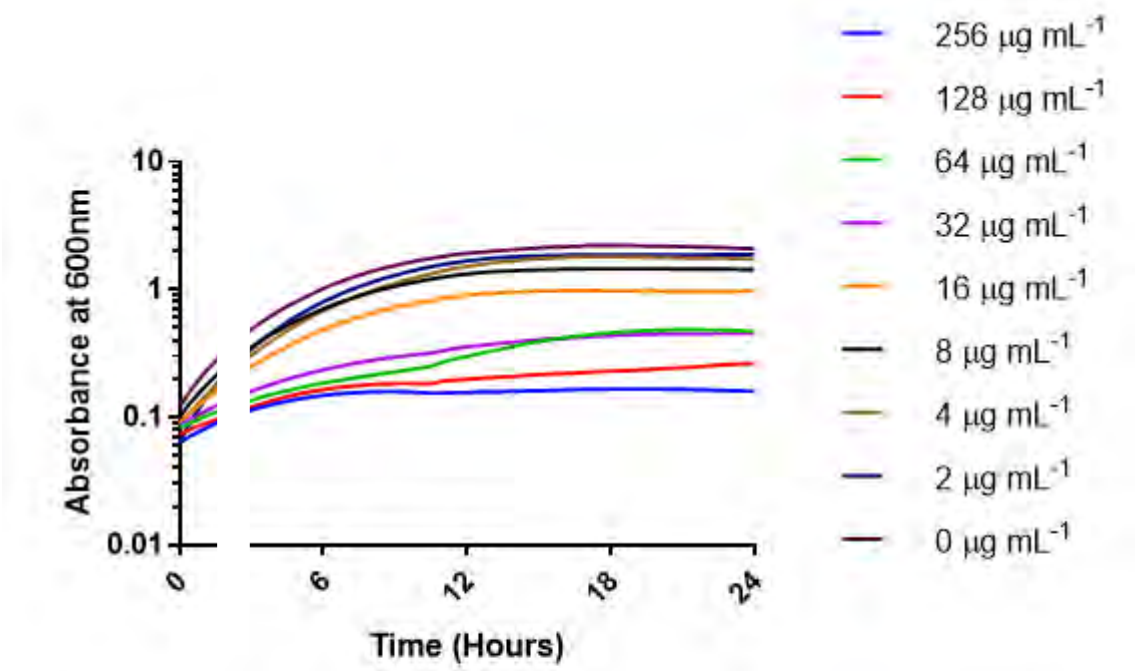

b)

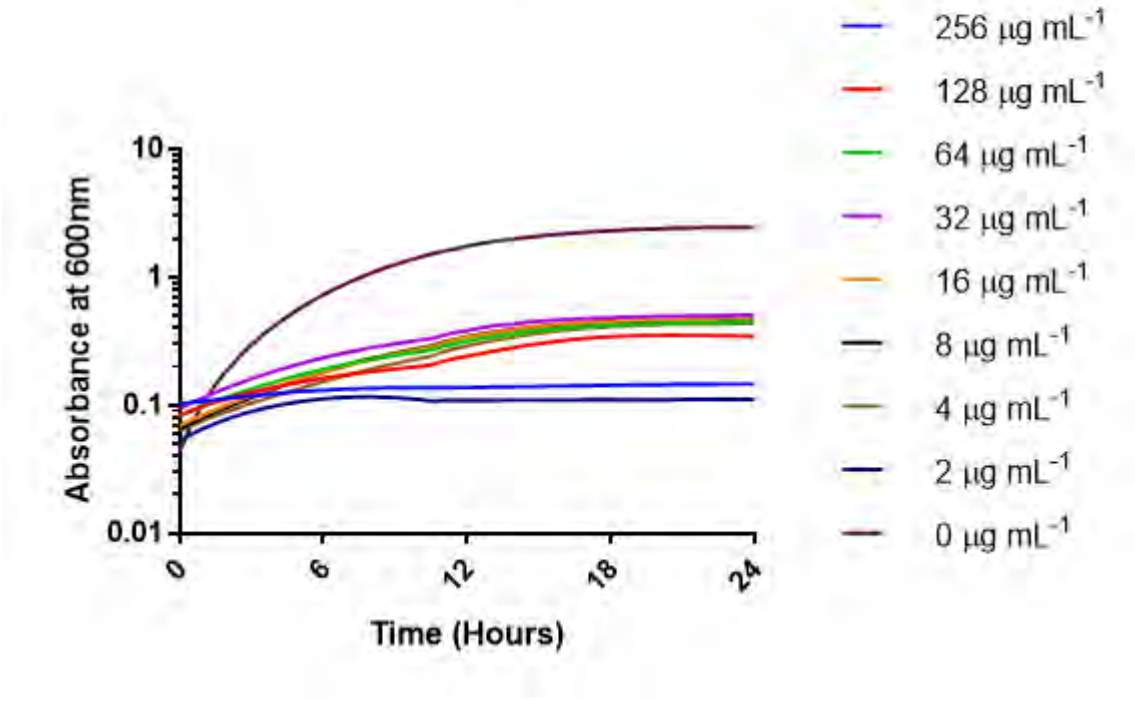

Figure 2. 6: Logarithmic growth curve of a) *P. aeruginosa* PAO1 and b) *S. maltophilia* S1 over a 24 h period with varying concentrations of **1** from 0 µg mL^{-1} to 256 µg mL^{-1} (*N*=3).

2.4.5 ATP Leakage

To determine cell viability, the measurement of ATP of metabolically active cells was measured using the luminescent cell viability assay over a 2 h period with the luminescence of the cells measured during this course. The assay demonstrated *P. aeruginosa* strain PAO1 bacterial cell viability decreased over time when incubated with the complex as demonstrated by the decrease in the luminescence of ATP with an increased concentration of **1** ($p<0.0001$). The luminescence increased over the time period ($p<0.0001$) without treatment by 266.4 % from 190.67 to 698.67 Relative light units (RLU) whereas upon incubation with MIC concentration of **1** a 44.6 % decrease (223.11 to 123.56 RLU) and upon incubation with post MBC concentration of **1** equated a 54.3 % (170.22 to 77.78 RLU) in cell viability. In comparison to a colistin control where an 83.4 % decrease in cell viability (477 to 79.33 RLU) which is greater than the highest concentration tested with **1** (Appendix Table 8.1; Figure 2.7). Two-way ANOVA analysis suggest that incubation with **1** has a highly significant effect on cell viability over time with the interaction between the two variables ($p<0.0001$). Using multiple t-tests to compare 0 and 120 minutes, significance was found with colistin, triton and 0 μg mL^{-1} and following treatment with 8 μg mL^{-1} and 32 μg mL^{-1} all with $P<0.0001$, however 16 μg mL^{-1} was found to be non-significant with a p value of 0.169.

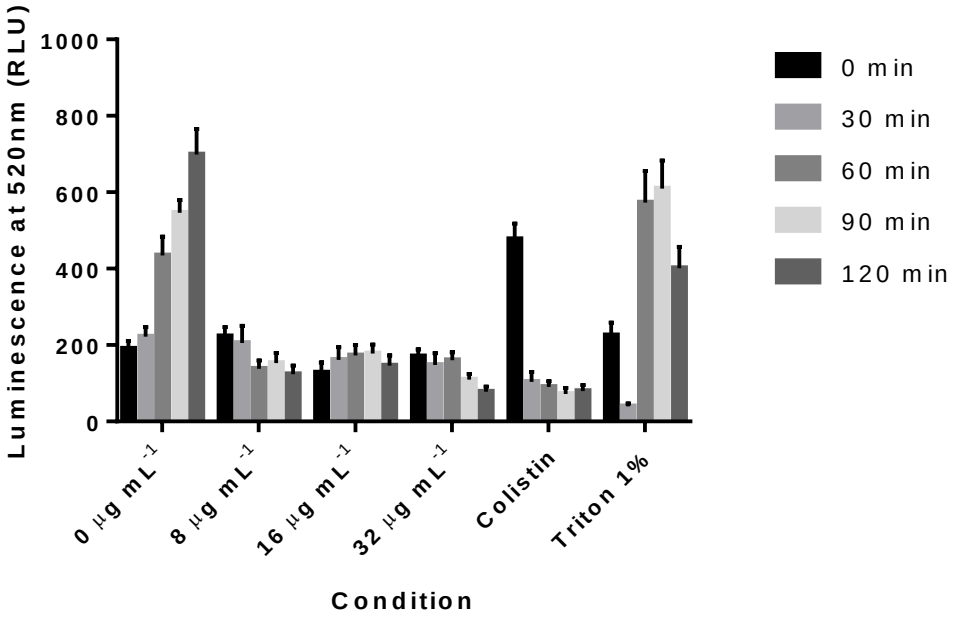

Figure 2. 7: Luminescence of *P. aeruginosa* strain PAO1 at 520 nm upon incubation with **1** at varying concentrations and controls colistin and triton X-100 for 2 h (*N*=3).

2.4.6 Biofilm eradication study

Following a 24 h incubation with bacterial culture to form biofilms and incubated over a 24 h period with **1** results were obtained through the staining with crystal violet and subsequent optical density measurement at time intervals. Following a 1 h incubation with **1**, the biofilm OD had decreased by 0.212 when incubated with 0 µg mL^{-1} compared with 128 µg mL^{-1} **1** with 2 h decreasing by 0.180, 3 h 0.163, 4 h 0.104, 6 h 0.225 and 24 h 0.203. Between 1 to 4 h, a decrease of 49% in the OD value of the biofilm for incubation until 6 h where it increased as shown in Appendix Table 8.2; Figure 2.8.

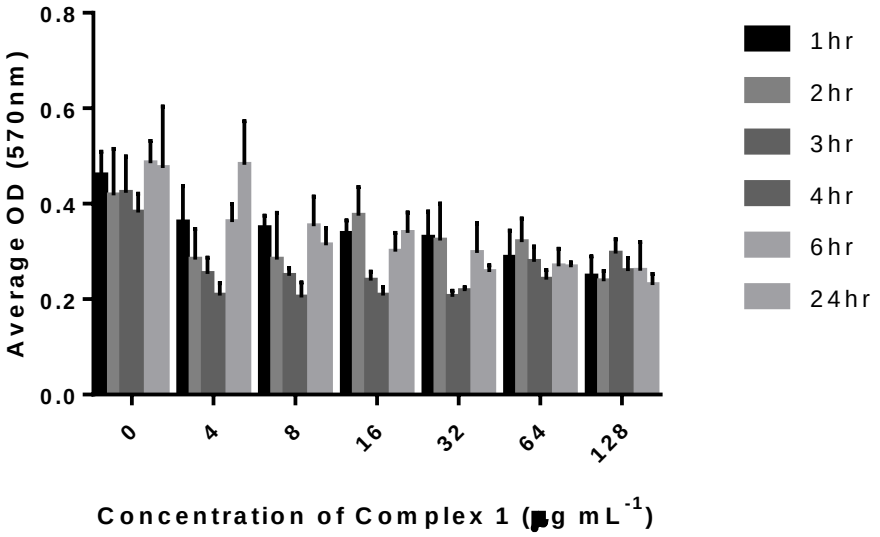

Figure 2. 8: Average OD values of the *P. aeruginosa* PAO1 biofilm with an increased concentration of **1** over 24 h (*N*=3).

Normal distribution analysis demonstrated that all apart from the biofilms treated with 0 µg mL^{-1} complex were not normally distributed ($p>0.05$) therefore the Kruskal-Wallace test was performed where the medians grouped by concentration were significant ($p<0.0001$) and additionally the same result was obtained for grouping with time of complex exposure ($p<0.0001$).

Correlation analysis additionally found that there was a negative correlation between the OD of *P. aeruginosa* strain PAO1 with both concentration and time with values of -0.607 ($p<00001$) and -0.117 ($p = 0.075$) thus indicating that that **1** has a negative impact on biofilm growth.

2.4.7 Crystal Violet Biofilm Assay with non-clinical strains of *P. aeruginosa*

The *P. aeruginosa* non-clinical strains were treated the same as the medical strain *P.* aeruginosa PAO1 with optical density measuring over a 24h period with crystal violet. The non-clinical strain *P. aeruginosa* ATCC 9027 without treatment the OD reading of crystal violet increased by 58.7 % over a 24 hour period whereas upon incubation with a sub-inhibitory amount of **1** biomass was reduced by 53.8 %. Both MIC and post MBC values remained similar in percentage decrease with 45.0 % and 49.5 % respectively. The time had little to do with the decrease in bacteria as shown with a *p* value of 0.012, however the concentration of **1** had a highly significant difference to the OD of the biofilm with $p<0.0001$ thus demonstrating the effectiveness of **1** at inhibiting biofilm formation. The interaction between the two variables time and concentration of **1** was slightly significant with a *p* value of 0.0366.

Another non-clinical strain *P. aeruginosa* NCTC 12903 grows quicker than the ATCC 9027 strain, over a 24h period biomass increases by 291 %. Upon incubation with **1** at concentrations 64 µg mL^{-1}, 128 µg mL^{-1} and 256 µg mL^{-1} the decrease in biomass was consistent with a deduction of 44.6, 38.8 and 44.0 % respectively. The factor of time was not significant for the deduction in biomass with a *p* value of 0.2386 however the combination of time and concentration was significant with a *p* value of 0.0022 suggesting the increased concentration has more of an effect on the biomass than time alone. Incubation with the concentration alone reflected a significant decrease in biomass with a highly significant result with $p<0.0001$, thus indicating in both non-clinical strains, the effect of the concentration of **1** is greater than the incubation time (Appendix Table 8.3; Figure 2.9).

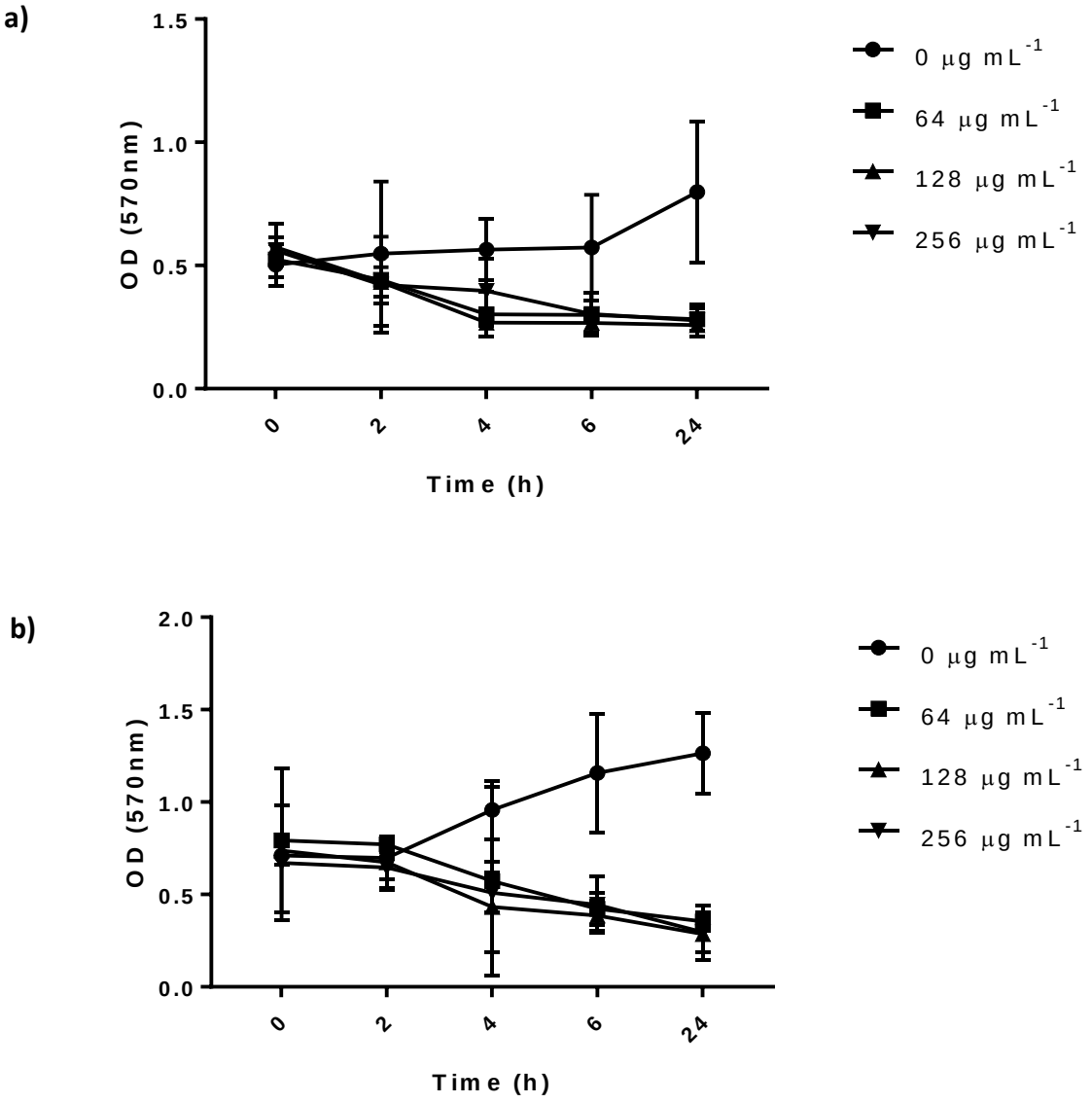

Figure 2. 9: Decrease in biomass observed with two *P. aeruginosa* non-clinical strains a) ATCC 9027 and b) NCTC 12903 over a 24h period with three concentrations of **1** (*N*=3).

2.4.8 Synergy study

Using the serial broth microdilution method similar to the MIC, both **1** and commonly used antibiotics were diluted and incubated with *P. aeruginosa* strain PAO1 for 24 h. As shown with the previous MIC results for **1** and *P. aeruginosa* strain PAO1, the MICs remained at 8 µg mL^{-1} with the exception of **1** and Tetracycline with an average of 6.667 µg mL^{-1}. Only one of the antibiotic combinations proved to be synergistic, **1** and Tetracycline with a fractional inhibitory complex of 0.4 whereas 80 % of the combinations were indifferent upon addition of an antibiotic with majority having a FIC value of 1.125 and **1** and Colistin with 2.125 (Table 2.7).

Table 2. 7: Synergistic combinations of **1** and antibiotics with the overall FIC value and synergistic status (*N*=3).

1 antibiotic Combination	**MIC of complex A (Ru) alone (µg mL^{-1})**		**MIC of complex B (Antibiotic) alone (µg mL^{-1})**		**MIC complex A in combination (µg mL^{-1})**		**MIC complex B in combination (µg mL^{-1})**		**ΣFIC**	**Synergistic status**
	Mean	SD	Mean	SD	Mean	SD	Mean	SD		
Colistin	8	0	50	0	1	0	100	0	2.125	Indifferent
Gentamicin	8	0	5	0	1	0	5	0	1.125	Indifferent
Streptomycin	8	0	200	0	1	0	200	0	1.125	Indifferent
Tetracycline	6.667	2.309	800	0	1	0	200	0	0.400	Synergistic
Ciprofloxacin	8	0	64	0	1	0	64	0	1.125	Indifferent

2.5 Discussion

2.5.1 Antimicrobial activity of Ruthenium containing metallic complexes against multidrug-resistant pathogens

Emerging resistance to current antibiotic treatments has demonstrated the need for new novel antimicrobials to be developed especially against Gram-negative species.

For *P. aeruginosa*, all clinical isolates examined had significantly lower (P <0.05) MIC and MBC values than the model strain *P. aeruginosa* PAO1. Comparing antibiotic resistance profiles of each clinical isolate to stain *P. aeruginosa* strain PAO1 would provide an insight into the antimicrobial resistance mechanisms of each isolate. Comparing the clinical pathology and location of each isolate compared to strain *P. aeruginosa* strain PAO1 would provide a useful comparison.

Validation of antimicrobial complexes against isolates from different infection sources is important in order to progress complexes as potential treatment options against the respective bacterial pathogens. It is essential that novel antimicrobial complexes function against different strains of the same species, irrespective of source and traditional antibiotic resistance profile (Sanchez and Martinez, 2019).

A diverse range of antibiotic resistant bacterial clones of *S. aureus* and *P. aeruginosa* were examined for susceptibility to **4** and **1** respectively. This study demonstrated that the majority of strains had similar susceptibility profiles to MRSA and *P. aeruginosa* PAO1, demonstrating that the antimicrobial activity of both complexes is not limited to model laboratory strains. Indeed, only one isolate of *S. aureus* (ARI12) was significantly more resistant to **4** than strain MRSA (p<0.05). It is plausible that this strain may express further efflux pumps which can exclude the complex from the cell or has altered resistance factors

which account for this phenotype. Comparing antibiotic resistance profiles between *S. aureus* strains ARI12 and MRSA may provide an insight into this phenomenon.

This demonstrated that *S. aureus* is susceptible to these complexes however with the same complexes *P. aeruginosa* proved to be resistant suggesting that similar to the two complexes 1 and 4 tested in the present study, the ruthenium complexes could display selective antimicrobial mechanisms with Gram positive and Gram-negative bacteria. In a study conducted by de Souza *et al.,* 2018, the MIC values of *S. aureus* range from 500 and 250 µg mL^{-1} for *cis*-$[Ru(bpy)_2(clbzpy)(Cl)](PF_6)$, *cis*-$[Ru(bpy)_2(4\text{-}bzpy)(Cl)](PF_6)$ respectively, however there was no detected antimicrobial action with *cis*-$[Ru(bpy)_2(4\text{-}bzpy)(CO)](PF_6)_2$.

Ru chelate complexes have additionally been tested for their antimicrobial activity. Among the complexes tested, Ru-nf $[Ru(nf)_2Cl_2]Cl{\cdot}4H_2O$ (nf = norfloxacin) was the most active against an MRSA strain 1263 and another complex Ru-enro $[Ru(enro)_2Cl_2]Cl{\cdot}5H_2O$ (enro = enrofloxacin) was the most active against the non-MRSA *S. aureus* strain ATCC25923 with an MIC of 7.81 and 31.25 respectively. Ru (III) complexes were also tested in this study with Ru-nf-DMSO $[RuCl_3(nf)_2(DMSO)]{\cdot}H_2O$ (nf = norfloxacin), Ru-levof-DMSO $[RuCl_3(levof)_2(DMSO)]{\cdot}DMSO{\cdot}8H_2O$ (levof = levofloxacin) and Ru-of-DMSO $[RuCl_3(of)_2(DMSO)]{\cdot}H_2O$ (of = ofloxacin). The Ru (III) complexes had excellent MIC values compared to other bacterial strains with a MIC value of 15.62 µg mL^{-1} for MRSA (Uivarosi *et al.,* 2017).

One study compared the effects of multiple Ru(II) polypyridal complexes supplemented with Ca^{2+} and CAMHB against *S. aureus,* MRSA, *B. subtilis, E. coli* and *P. aeruginosa*. The complexes tested were proven to have antimicrobial effect against all pathogens stated except *B. subtilis* with ranging MIC values from 0.97-64.47 µM. Activity was determined to

be due to the flexible alkane linkage present in all complexes and the bimetallic structure which allowed for subsequently low and effective MIC values. Whilst the Ru complexes tested proved to be effective at inhibiting the growth of MRSA the same could not be said for the non-resistant *S. aureus* strain with only 5 Ru(II) polypyridal complexes out of 15 Ru complexes having a MIC value. (Li *et al.,* 2012; Mital and Ziora, 2018).

An additional study conducted by Balakrishnan *et al*., 2015 built on the use of mono, di and tri-nuclear Ru(II) polypyridal complexes with the most antimicrobial complex being tri-nuclear against Gram-positive bacteria including *B. subtilis, E. lentum* and *S. aureus*. This could be due to an increase in the number of imidazole moieties compared with the other Ru complexes tested (Balakrishnan *et al*., 2015; Mital and Ziora, 2018). In comparison to **4** which is a Ru(II) complex and has similar activity to the MIC and MBC data in 2.5 studies could demonstrate that Ru(II) complexes are more effective at inhibiting the growth of Gram-positive bacteria due to the increased stability and lower oxidation states causing accumulation within the cell (Southam *et al*., 2017) .

In another study eighteen Ru complexes were tested where 56% produced a MIC of 128 μg mL^{-1} and 5 complexes *fac*-$[Ru(hexpytri)_3](PF_6)_2$, *mer*-$[Ru(hexpytri)_3](PF_6)_2$, *fac*-$[Ru(octpytri)_3](PF_6)_2$, *mer*-$[Ru(octpytri)_3](PF_6)_2$ and $[Ru(Me_4phen)_3](PF_6)_2$ all produced a MIC <8 μg mL^{-1} with the latter complex showing a MIC value of 0.5 μg mL^{-1} similar to the MIC of gentamicin (16 μg mL^{-1}) additionally conducted in this study against *S. aureus* strain ATCC 25923. These complexes have shown a similar activity to **4** and **1** with a MIC of 8 μg mL^{-1} showing that these are viable complexes for antimicrobial activity in addition to the study finding that activity of the complexes was lowered with Gram negative bacteria, this could

be due to a mechanism of action disrupting the cell membrane which is blocked by the outer membrane in Gram negative species (Kumar *et al*., 2016).

In contrast, upon testing Ru based complexes [Ru(η^6-p-cymene)(L^1)Cl_2], [Ru(η^6-p-cymene)(L^2)Cl_2] and [Ru(η^6-p-cymene)(L^3)Cl_2] on *S. aureus* and *P. aeruginosa* among other clinically relevant pathogens, activity was lower than the current antimicrobial treatment options (Obradović *et al*., 2020). These complexes have the same η^6-p-cymene ligand as **4**. However **4** exhibited greater antimicrobial activity against both the study complexes and current antibiotics with MIC values ranging between 8 and 16 μg mL^{-1} thus suggesting the additional ligands in the complex may have had additional antimicrobial effect than the η^6-p-cymene ligand alone.

The MIC values for 2 Ru complexes for both *P. aeruginosa* was 500 μg mL^{-1} at all the time points tested (24, 48 and 72 h) with p,t-[Ru(CO)(PPh_3)(tren)]Cl_2 and with another complex p,t-[Ru(CO)(P{p-tol}$_3$)(tren)]Cl_2 the MIC was 150 μg mL^{-1}. The second Ru complex proved more effective than chloramphenicol and the first Ru complex tested in this study which demonstrated efficacy over a commonly used antibiotic (Fagundes *et al.,* 2016). The Ru complexes tested in this study proved to have efficacy against *P. aeruginosa* at low MIC readings compared with both the Ru complexes in the Fagundes study. Another complex cis-[Ru(bpy)$_2$(Met)](PF_6)$_2$ demonstrated an MIC value of 62.5 μg mL^{-1} with *S. aureus* however no activity against *P. aeruginosa* was observed in this study. Activity was surprisingly discovered with *Escherichia coli* (de Sousa *et* al., 2020). Limited activity against Gram-negative species could be explained by the addition of a lipopolysaccharide outer membrane which potentially could be inhibiting the Ru complex from entering the cell.

However, the activity the Ru complexes **2**, **1** and **3** have upon *P. aeruginosa* could be due to Ru targeting the outer membrane thus overcoming that resistance mechanism.

A Ru ion solution demonstrated effectiveness against multiple Gram-negative species including *A. baumannii, K. pneumoniae* and *E. faecium* which the MIC values respectively shows 7.81 mg L^{-1}, 15.62 mg L^{-1} and 31.25 mg L^{-1} (Vaidya *et al*., 2019). These values are lower than the ones discovered in this study however both demonstrate activity against multiple Gram-negative species. This could be due to the metal ions attracting to the outer membrane of the bacterium due to the differing charges of the membrane and the Ru ions (Abd-El-Aziz *et al*., 2017).

In another study Ru complexes against Gram negative species *E. coli* and *K. pneumoniae* ranged between 0.15 and 1.0 mg mL^{-1} with the ruthenium complexes [(p-cymene)$RuL^1Cl]PF_6$ and [(benzene)$RuL^1Cl]PF_6$ being the most effective out of the ruthenium complexes tested (Lapasam *et al*., 2020). These complexes tested have higher MIC values than **1** and **3** tested in the present study however the addition of the chlorine ligands could be vital to antimicrobial activity. This could be due to the ability for chlorine to elicit an oxidative stress response in bacteria as proved by other Gram-negative bacteria *E. coli, E. faecalis* and *P. aeruginosa* by a 2.3 fold increase in ROS production (Jin *et al*., 2020). Additionally other ruthenium (II and III) based complexes with chlorine ligands demonstrated 10 and 15 mg mL^{-1} MIC values with *K. pneumoniae* and inactive with a multidrug resistant strain (Matshwele *et al*., 2020), similar to this study where the MIC and MBC values was 256 µg mL^{-1} with **1, 2** and **3**, thus relatively inactive.

The antimicrobial activity silver ions against *P. aeruginosa* strain MTCC demonstrated 8-10 mm inhibition whereas silver nanoparticles were smaller with a zone of 7-8 mm (Bose and

Chatterjee., 2016). **1** in this study had a greater zone of inhibition at double the size at 4 µg mL^{-1} at 16.291 mm. Other metals additionally provide large zones of inhibition comparable to ruthenium, for example zinc-doped copper oxide nanoparticles in 20 % DMSO produced a zone size of 16 ± 0.21 mm with *P. aeruginosa* (Khalid *et al*., 2021). Additionally ionic gold particles demonstrated efficacy across multiple strains of *P. aeruginosa* with zones of inhibition ranging between 13.69 and 26.89 mm (Torres *et al*., 2021), equivalent to the results with ruthenium **1** and increased zones of inhibition against other metal ions including zinc doped copper oxide and silver (Torres *et al*., 2021). In another study using other Gram-negative pathogens including *A. baumannii* and *K. pneumoniae* zones observed using a ruthenium ion solution of 8 mm and 10.66 mm respectively (Arumugan *et al*., 2018). Both smaller than the zones observed with **1** and *P. aeruginosa.*

2.5.2 Antimicrobial activity of Cobalt based metallic complexes.

Hexaamminecobalt (III) chloride **5** in the present study which demonstrated low MIC values with both Gram-positive and Gram-negative species with the highest MIC value being 64 µg mL^{-1} with MRSA. This could be due to a reduction in polarity of the cobalt ion and partial positive charge sharing with donor groups causing delocalisation of π-electron in the chelate ring thus causing increased bacterial lipid membrane penetration and subsequent killing. Cobalt(III) Schiff bases have been tested for antimicrobial activity against a range of Gram-positive and Gram-negative bacteria. The complex $[Co^{III}(L^2)(4\text{-Mepy})_2]PF_6$ was found to have efficient antimicrobial activity with the lowest MIC value being 125 µg mL^{-1} with *S. aureus* however Gram-negative bacteria *E.coli* and *Salmonella typhi* exhibited MIC values of 1250 and 1500 µg mL^{-1} respectively (Taherlo and Salehi., 2014). Hexammine cobalt has been discovered to inhibit the gene CorA which regulates metal influx in bacteria such as *M.*

tuberculosis (Quezada *et al*., 2019) this could explain why our complex exhibited low MIC values due to the inhibition of the gene, subsequently allowing additional metal ions into the bacterial cell and exhibit antibacterial action. The transport activity of CorA with *T. maritima and M. jannaschii* was not inhibited significantly by **5** however a competition assay of CorA discovered a preference for cobalt ions indicating that CorA of *T. maritima* might be a cobalt specific channel (Stetsenko and Guskov., 2020). Additionally **5** is similar to **1** with the mechanism of action. The cobalt complex has a lower EC_{50} for DNA and heparin binding than **1** however it is lower than other metallic complexes with a 2+ charge with **5** exhibiting an EC_{50} of 689 ± 17 µM compared to **1**'s 853 ± 156 µM (Katner *et al*., 2018) demonstrating a high affinity to DNA causing damage to bacteria more efficiently than **1** suggesting the difference in MIC values.

Cobalt ferrites with zinc have been found to be very potent with disc diffusion analysis against a wide range of bacterial pathogens ranging zone sizes between 11 and 15 mm with bacteria including *Aerococcus viridians, Enterococcus columbae* and *Staphylococcus* strains *aureus, lentus, sciuri and vitulinus*. Similarly, to **1** the addition of the nanoparticles caused a structural change to the bacteria creating a rough shape, it is though the overall positive charge of the nanoparticles electrostatically adheres to the cell wall of the bacteria and destroy it (Maksoud *et al*., 2019). Another study investigating zinc-doped cobalt ferrite nanoparticles suggest bacteriostatic activity due to the increase of ROS and membrane damage caused by the metal ions (Naik *et al*., 2019), whilst membrane damage appears to be the cause behind most antibacterial activities of metal ions, with increased ROS production by cobalt ion derivatives could enhance the antibacterial activity as exhibited by **5**.

Cobalt-based metal organic frameworks have higher antimicrobial activity compared to silver nanoparticles due to the release of cobalt ions into the bacterial solution (Aguado *et al*., 2014) and disruption of bacteria cell walls and entering the bacterial cell through lipid peroxidation (Hatamie *et al*., 2019). Combined with graphene oxide the antimicrobial activity of cobalt frameworks are increased compared to each separate component however notably higher with the Gram-positive bacteria *S. aureus* compared to *E.coli* due to the presence in the peptidoglycan layer of lipoteichoic acid acting as a chelating agent to prevent of lipid peroxidation thus allowing membrane damage to take place (Zhuang *et al*., 2012). **5** however had an increased effect against Gram-negative species compared to Gram-positive with the average MIC's at 8 µg mL^{-1} and 16 µg mL^{-1} respectively. The difference between Gram-species could be due to the increased attraction of the cobalt ions to the positively charged bacterial membrane allowing additional membrane damage compared to Gram-positive species. Other reasons behind this action could be due to interference during the translation and transcription processes or disruption of metabolic pathways (Chidurala *et al*., 2016), additionally cobalt ions can be released from nanoclusters to interact with bacterial enzyme via the thiol groups and cause DNA damage within the bacteria (Alahmadi *et al*., 2017).

2.5.3 Investigating the drug repurposing properties of the commonly used cancer treatment cisplatin as an antimicrobial agent

Cisplatin has been found to have low MIC values against *P. aeruginosa* with values of 6.25 µM being recorded, in contrast to this study where the MIC value was high at 128 µg mL^{-1}. This could be due to the upregulation of the gene recA vital for DNA repair in the bacterial cell as well as other genes associated with DNA modification, recombination and replication with additional pyocyanin synthesis being disrupted. (Yuan *et al*., 2018). Previous work

completed demonstrated cisplatin and *E.coli* where genes associated with energy metabolism and the interference with the stress response in bacteria ultimately causing cell death (Stefanopoulou *et al*., 2011).

Most strains including *E. coli, S. aureus* and majority of *Pseudomonas* strains apart from PAO1 and PA14 (MIC 50 µg mL^{-1}) were above 100 µg mL^{-1} similar to cisplatin in this study where MIC values were mainly 128 µg mL^{-1}. Cisplatin's efficacy is due to its action as an alkylating agent and enhanced ROS production due to the presence of the platinum ion. Similarly to cisplatin with *P. aeruginosa* PAO1 this study found that cisplatin was not more susceptible as an antimicrobial. The mechanisms of action have been determined to be through the direct cross-linking of DNA (Chowdhury *et al*., 2016), the additional cross-linking of multiple types of RNA including tRNA, siRNA and rRNA (Dedduwa-Mudalige and Chow, 2015) and inhibition of the DNA repair genes UvrA and RecA responsible for nucleotide excision repair and SOS repair (Chowdhury *et al*., 2016). Additionally platinum (II) complexes have been found to induce filamentation and bacterial lysis (Johnstone *et al*., 2014).

Intrinsic cytotoxicity is an issue for repurposing anti-cancer drugs as antimicrobial agents however low concentrations of cisplatin have been discovered to combat sepsis in mice models through the activation of peritoneal macrophages (Li *et al*., 2014) thus combination with current antimicrobials could be beneficial through inhibition of metabolic and dormant persistor cells.

The action of cisplatin against Gram-negative bacteria has been known for over 55 years (Rosenburg *et al*., 1965) with one particular study in 2010 showing 16 µg per disc produced zone sizes of 7-15 mm for a range of bacteria including *Bacillus brevis, cereus, subtilis, Streptomyces lividans,* three strains of *E. coli* and *Serratia marcescens* (Joyce *et al*., 2010).

However research emerged suggesting resistance to cisplatin was identified in strains of *E. coli* with a mutation in the gyrase gene *gyrA* leading to cross-resistance with nalidixic acid and cisplatin. Other mechanisms deduced included a decrease in the platinum ion binding to DNA, increased glutathione concentration and increased DNA repair capacity (Bouayadi *et al*., 1993). Platinum resistance has additionally been documented in later years with a 2021 study demonstrating the strain *P. aeruginosa* PAO1 has inherent resistance to platinum based antimicrobials due to an overexpression of quorum sensing through the gene *lasR* as a mechanism to overcome the production of ROS generated by the metal nanoparticles (Li *et al*., 2021). This could be why the MIC activity of cisplatin is higher with the bacteria used in the present study compared with the ruthenium and cobalt complexes (complexes **1**-**5**). Due to the resistance being discovered over 20 years ago this could have allowed time for cross-resistance to occur explaining the increased MIC values in comparison to older studies. There is a possibility that the bacteria have gained the ability to efflux the platinum ions out of the bacterial cell as described by (Ma *et al*., 2016). There have only been a few studies since 2014 that have described antibacterial activity of platinum complexes and one study recently tested 63 platinum based complexes with only 43% exhibiting antimicrobial activity against at least one bacterial strain or fungi with majority of activity ranging above 20 µM against ESKAPE pathogens (Frei *et al*., 2021). The bacteria investigated in the present study with **6** exhibited increased MIC values, this could be due to an increase in the number of platinum efflux pumps present that was inherited causing an increased resistance to platinum, limited platinum complexes have antimicrobial effect however **6** in the present study has some effect which could be due to the ROS generation not being inhibited.

2.5.4 Time dependent killing of *P. aeruginosa* with ruthenium chloride complexes

To observe the effects of ruthenium based antimicrobials against two Gram-negative pathogens, growth curve kinetics were completed to determine the effects of multiple concentrations of **1** over a 24 h period.

Silver nanoparticles have been shown to demonstrate similar time killing patterns as ruthenium. Multiple Gram negative pathogens including *E. coli* and *K. pneumoniae* were discovered to have similar time killing patterns to **1** within 2 h of incubation at 2 to 8 log higher than the MIC value (7.8 - 62.4 μg mL^{-1}). This study demonstrated that silver nanoparticles have broad spectrum antimicrobial capacity against multiple species of Gram-negative pathogens (Loo *et al*., 2018). The **1** analysed in this chapter demonstrated more efficient killing over the same period of time with lower MIC values with multiple species as shown by the growth curves, exhibiting the same broad spectrum activity as the silver nanoparticles in the study conducted by Loo *et al*.

Similar results have been discovered using colloidal silver as an antimicrobial complex against a wider range of Gram-negative species including *P. aeruginosa* and *A. baumannii* which displayed similar results to the ones found with ruthenium complexes in this chapter. Where complete killing of the bacteria occurred at MIC value after 8 h of incubation for *P. aeruginosa* PAO1 and 2 h for *A. baumannii* (MIC values 4 mg mL^{-1} for both bacteria) (Domínguez *et al*., 2020). The MIC values in the present study are however growth of bacteria is inhibited after 12 h for both bacteria at a concentration of 8 μg mL^{-1} following a similar pattern demonstrating that metal complexes have an adverse effect on multiple Gram-negative species of bacteria.

A study investigating $[RuCl(MePhtpy)(dpp)]^+$ with *E. coli* over a 6 h period found at a concentration of 25 µM there was no significant change in bacterial growth comparing to the untreated bacteria however when the concentration was increased to 50 µM after 4 h of exposure caused a shift in the growth curve through to be due to interaction with the bacterial DNA (Jain *et al*., 2022). Similarly with **1** for both *P. aeruginosa* PAO1 and *S. maltophilia* S1, at MIC concentration for both began to shift the growth curve, lowering the absorbance. This decreases further with an increase in concentration of **1** and it is thought the mechanism of action similarly is DNA interaction.

Another study investigating Ru oxide nanoparticles made from 0.1 M ruthenium chloride $[RuCl_3{\cdot}xH_2O]$ with four bacteria, *E.coli, P. aeruginosa, S. marcescens* and *S. aureus* where the growth rate decreased upon an increase in concentration with maximum inhibition of growth obtained at 100 µL (Kannan and Sundrarajan., 2015). This is identical to the findings in the present study where **1** caused a decrease in growth rate upon an increase in concentrations however maximum inhibition of growth was a little higher at 128 µg mL^{-1} showing that **1** acts similarly to other reported Ru complexes.

2.5.5 Metallic ions against biofilms

Many studies including one conducted by Wong *et al*., 2015 reported that in wound microbiota prevalence in Malaysia, *S. aureus* and *P. aeruginosa* were the most prevalent at 23.3% and 14.8% respectively (Rahim *et al*., 2017). Another study found that *Staphylococcal* species were the most prevalent, proving to be 30.7% of the overall species found with *S. aureus* being the most prevalent with 18.6%. *Staphylococcal* species were followed by *Corynebacterium* at 14.1% and then Pseudomonas at 9.7% (Haiko and Westerlund-Wikström., 2013).

Biomass of *P. aeruginosa* PAO1 biofilms decreased as a result of the addition of **1** over the course of 24 h. Although not all of the biofilm was eradicated, **1** decreased the biomass by 49% over 4 h, and additionally decreased over the concentrations. The negative correlation is promising, indicating that as the time incubated with the compound increases the biomass decreasing, proving to be a promising alternative to current treatment options.

A Ru(II) complex ($C_{24}H_{34}B_{10}FeRuS_2$) was shown to reduce the adherence of a *P. aeruginosa* biofilm compared to a normally growing biofilm cells over a 12 and 24 h period using 8 µg mL^{-1}. This was determined to be due to a decrease in expression of extracellular matrix proteins (Li *et al*., 2013). Different types of Ru complexes have varying effects on biofilm formation. In a study conducted by O'Reilly *et al* (2021), two Ru (II) complexes with a btp ligand (2,6-bis(1,2,3-triazol-4-yl)pyridine) with a general structure $[Ru{\cdot}(L)_2]Cl_2$ were created. One compound 7Man ($C_{42}H_{54}N_{14}O_{20}Ru^{2+}$) had little effect on biofilm eradication however 8Gal ($C_{66}H_{102}N_{14}O_{32}Ru^{2+}$) significantly reduced biofilm formation. Compound 8Gal had chains comprised of triethylene glycol which allows for flexibility of the compound thus 80% reduction in biofilm formation (O'Reilly *et al*., 2021). **1** is able to inhibit biofilm formation due to interactions between Ru and lectin. Another study demonstrated similar findings using $RuCl_3$ and Ru (IV) type complexes which resulted in a reduction in biofilm compared to planktonic cells and a control, reducing the biomass by 69% and 80% respectively (Czerwonka *et al*., 2019). The Ru (IV) complex reduced the biomass significantly due to an increased affinity to adhesins on *P. aeruginosa* strain PAO1 which prevents initial bacterial adhesion to a surface thus affecting biofilm adherence (Haiko and Westerlund-Wikström., 2013) and high toxicity (Southam *et al*., 2017). However Ru (IV) complexes are highly toxic, binding to DNA causes an unfavourable enthalpy, heat capacity change and a subsequent water release from the non-small cell lung carcinoma H358 in mice (Sudhindra *et al*., 2015)

Ru complexes are effective at preventing biofilm formation is due to CORMs with CORM-3 previously proving effective against *P. aeruginosa* with Ru allowing entry (Southam *et al*., 2018). A study testing the effect of CORM molecules coupled with Ru ($Ru(DMSO)_4Cl_2$) demonstrated CORM-2 had significant effect against the growth of biofilms in a crystal violet study with a reduction in biomass observed after 1 h and prevents additional bacterial growth and biofilm maturation (Murray *et al*., 2012). This is due to CORMs ability to bind to respiratory components within a bacteria, one example of this is CORM-3 which binds to haem containing proteins and terminal oxidases which impairs respiration within the cells and additionally detoxifies nitric oxide. Additionally ROS are generated as well as hydroxyl radicals through the reduction of oxygen by Ru^0 and Ru-H species (Nobre *et al*., 2016). Due to the multiple actions CO producing molecules can exhibit on bacterial cells this is promising in the inhibition of biofilms and could additionally be a reason why an increase in concentration of **1** could exacerbate the effects to reduce biofilm formation further.

Other Ru compounds have been found to release nitric oxide in response to a photosensitizer. Ru (II) coupled with boronic acid was found to release 85.4 % NO following irradiation for 20 minutes, faster than controls without boronic acid. Additionally adhesion to lipopolysaccharide or peptidoglycan is facilitated through the addition of the boronic acid through boron–polyol based boronolectin chemistry. Cell membrane zeta values were determined to prove the hypothesis of this compound targeting bacterial cells over mammalian which increased from -23.55 mV to -18.75 mV which was important for biofilm removal in which 90% of biomass was eradicated following incubation with the compound (Zhao *et al*., 2021). Although **1** has not been examined for photosensitivity, once **1** interacts with the internal *P. aeruginosa* PAO1 environment it has the potential to release NO similar

to the complex in this study, again explaining why bacterial biomass is eradicated upon incubation.

Overall there are many potential reasons why **1** is able to eradicate biomass and further studies are needed to determine the exact mechanism of action against *P. aeruginosa* PAO1 biofilms.

2.5.6 Ruthenium based antimicrobials as a solution to industrial applications in a timely application

In the food industry, organic alternatives are being examined for potential antimicrobial use due to the bacteria's ability to from biofilms under stress. One study investigating pathogenic food bacteria demonstrated a crude extract of *Adiantum philippense* against *E. coli, S. aureus, Shigella flexneri* and *P. aeruginosa* where an increased MIC value was found against the latter two pathogens in comparison to *E. coli* and *S. aureus* of 500 and 250 µg mL^{-1} for *S. flexneri* and *P. aeruginosa* respectively. Exceeding MIC values time-dependent killing was observed with all bacteria due to physiological factors within the cell thus demonstrating a delayed lag phase of growth and slow logarithmic growing phase (Adnan *et al*., 2020). The increased MIC values of *P. aeruginosa* could be suggested by increased resistance genes such as *MexB* and therefore additional efflux pumps to remove the antimicrobial from the bacterial environment, protecting the cell subsequently more than other bacterial strains. Similarly in this case where other Gram-negative bacteria exhibited lower MIC and MBC values than the non-clinical *Pseudomonas* strains.

The non-clinical strains of *Pseudomonas* have a higher MIC and MBC than the medical *P. aeruginosa* strain PAO1, however the time kill data is similar with complete killing observed after 24 h with the *P. aeruginosa* strain ATCC 9027. This strain may be more resistant due to its effective quorum sensing. There is a lack of genes encoding T3SS (Freschi *et al*., 2019)

however the virulence of the strain is determined by the exlBA operon which expresses a two-component exolysin (Reboud *et al*., 2016; García-Reyes *et al*., 2021). However belonging to the PA7 clade, this strain produces quorum sensing dependent virulence factors such as pyocyanin (Grosso-Becerra et al., 2016).

When exposed to industrial reagents such as benzisothiazolone and phenoxyethanol it was found in a study that the genes associated with the efflux pump MexPQ-OpmE was upregulated, this could contribute to the increased MIC values to **1** complex compared to the medical strain of *Pseudomonas*. If the frequency of efflux pumps increased then the ruthenium ions would be unable to exhibit antimicrobial action inside the cell (Green *et al*., 2018).

Additionally Ru ions are photoactive, complexes such as $[Ru(bpy)_3]^{2+}$ have been extensively studied due to this property with enhanced $\pi \rightarrow \pi^*$ intraligand transitions. Upon excitation with 450 nm optical light causes a transition into Ru(dπ)→bpy(π*) metal to ligand transfer transitions where the electron is excited and spin flips rapidly in order for the energy transfer of molecular oxygen to singlet oxygen to occur thus cleaving DNA backbones (Li *et al*., 2018). However due to the outer membrane in Gram negative bacteria, these oxygen ions cannot pass through easily leading to diminished antimicrobial activity in comparison to Gram-positive bacteria (Jain *et al*., 2021). Previous *E. coli* studies with monochloramine stress induced the alteration of the bacterial genomic profile causing ROS neutralization and repair. Genes such as *AhpC* and *AhpF* in *P. fluorescens* are up-regulated for alkyl hydroperoxide reductase, these genes are additionally peroxide scavengers using NADH and NADPH to activate AhpC through donation of an electron in response to oxidative stress (Lipus *et al*., 2019). Thus the *Pseudomonas* strains tested may have inherited the response

to upregulate the same genes to produce increased number of peroxide scavenging enzymes to dampen the activity of ROS and additionally repair damage, causing an increase in the amount of **1** needed to exhibit an antimicrobial effect.

2.5.7 Ruthenium based antimicrobials as industrial biofilm eradication agents

Bacterial strains isolated from industrial settings including *P. aeruginosa* strain W10, *B. licheniformis* CAN55 and *S. capitis* SH6 was tested for biofilm formation where the latter two pathogens had a more effective formation of biofilms compared with *Pseudomonas*. Addition of rhammolipid W10 after 48 h biofilm formation demonstrated a 60% inhibition at a low concentration of 0.04 mg mL^{-1} with *B. licheniformis* and *S. capitis* and increased with an increase of concentration with 90 % inhibition being achieved. *P. aeruginosa* additionally experienced a 90 % reduction in biomass with an increased concentration of rhammolipid. This could be due to the removal of the extracellular polymeric substance (EPS) protecting the biofilm and the disruption of the biofilm environment leading to inhibition. Biosurfactants may also be able to induce energy alternation and anchor into the membrane of the cell wall thus increasing cell fluidity and causing leakage of intracellular components (Chebbi *et al*., 2017). The addition of **1** could additionally affect the EPS of the biofilms causing a decrease in biomass with both concentration and time.

Research has suggested a way to disrupt biofilm formation could be to target surface lectins LecA and LecB, which demonstrates specific binding for galactosides and fucosides respectively, with carbohydrate-appended molecules (Yu *et al*., 2019). One such molecule based on a calix[4]arene scaffold containing units of galactose and fucose which was found to inhibit biofilm formation (Boukerb *et al*., 2014). Adding a ruthenium ion additionally helps the biofilm inhibition process with complexes consisting of Ru(II) glycoclusters at a low concentration of 5 mM over the course of 24 h. Ruthenium ions can be used as a scaffold for

glycoclusters which are more effective than the metallic ions themselves (O'Reilly *et al*., 2021).

Highly valent ruthenium based complexes which contain carboxylic acids and heterocyclic alcohols exhibit moderate anti-biofilm activity with Ruthenium (IV) acting as a counter ion (Czerwonka *et al*., 2019) however Ru (III) and Ru(IV) oxidation states have additionally been found to have weaker activity possibly due to the N,)-donor ligands (Rogala *et al*., 2019). Ruthenium chloride complexes such as $[RuCl_4(CH_3CN)_2]$ exhibited anti-biofilm activity by causing *Pseudomonas* aggregation into microcolonies, making it more susceptible (Jabłońska-Wawrzycka *et al*., 2020). The presence of **1** could be causing microcolonies to be formed instead of the hardier biofilm allowing for subsequent inhibition at MIC values of the non-clinical strains and more effective inhibition at higher concentrations.

2.5.8 Current antimicrobial status of *P. aeruginosa* and what can be done to alleviate

The identification of bacteria is essential to being able to treat patients effectively with resistance profiling becoming more important to allow for treatments to be adapted in order to negate infection (Kelley, 2017).

A study testing 242 *P. aeruginosa* isolates from UTI patients found 31 % of isolates were resistant to penicillins (Tumbarello *et al*., 2020), similar to this study where ampicillin had no ZoI. Additionally it was discovered that only 4 isolates were resistant to colistin, closely resembling this study where none of the isolates tested were resistant to colistin sulphate (Tumbarello *et al*., 2020). *P. aeruginosa* in UK cystic fibrosis patients was found to be 97 % susceptible to colistin at <4 mg L^{-1} (Pitt *et al*., 2003).

Testing 135 clinical isolates that were independently related had resistance against the antibiotics ceftazidime, ciprofloxacin, meropenem and tobramycin. Aminoglycoside-

modifying enzymes were discovered in 36 % of the isolates and between 2 and 6 different enzymes in majority of the isolates (Khaledi *et al*., 2016). Additionally 158 *P. aeruginosa* isolates tested against 17 antibiotics, where >85 % of the isolates were resistant to Amoxacillin-clavulanic acid, ceftriaxone, tigecycline and sulfamethoxazole (Castañeda-Montes *et al*., 2018). Similarly in resistance profiling conducted in this thesis where 35% of the isolates tested were resistant to 4 out of the 5 antibiotics tested. This could be due to the presence of antibiotic-degrading enzymes that have been passed between the isolated via plasmids.

Chloramphenicol resistance is well documented, with one study testing *Pseudomonas* strains found that 16 % of the 6 isolates tested was susceptible to chloramphenicol. It was determined that the susceptible phenotype had the *MexB* gene deleted whereas the other strains were overproducers of other Mex operons (Borselli *et al*., 2016), leading to subsequent efflux of chloramphenicol out of the bacterial cell. This could be why only two of the 20 strains profiled were sensitive to chloramphenicol, the outer membrane could be more permeable to the antibiotic (Idowu *et al*., 2019) and there may be an under-expression of Mex efflux pump systems resulting in zones of inhibition being observed.

Aminoglycoside resistance involving antibiotics, such as kanamycin and streptomycin of which 18 and 13 isolates respectively tested were resistant to, could occur due to the presence of aminoglycoside-modifying enzymes, 16S rRNA methytransferases, translation machinery interference, limited diffusion from the outer membrane (Bolard *et al*., 2017; Khan *et al*., 2020) and the presence of Mex efflux systems such as a mutation in *MexZ* which increased the MIC to aminoglycosides by up to 8 fold (El'Garch *et al*., 2007). The enzymes involved in *N*-acetylation *O*-adenylylation and *O*-phosphorylation that recognise

aminoglycoside antibiotics and modify the antibiotic include aminoglycoside acetyltransferases, aminoglycoside nucleotidyltransferases aminoglycoside phosphotransferases respectively (Bacot-Davis *et al*., 2016). Modification of the bacterial ribosome additionally confers resistance due to N7 methylation of the ArmA, RmtB and NpmA through 16S rRNA methyltransferases thus affecting the binding site (Doi *et al*., 2016; Cox *et al*., 2018). The *Pseudomonas* isolates tested could have had the target site modified to aminoglycosides thus Kanamycin has no zone of inhibition when tested, out of the clinical isolates tested only 2 were susceptible meaning they lack the mutation however due to horizontal gene transfer, this could change rapidly and contribute to the increase in drug resistance.

Other antibiotics that had an inhibitory effect on the *Pseudomonas* isolates included streptomycin and tetracycline with 7 and 13 out of the 20 isolates susceptible respectively. Tetracycline resistance occurs due to the overexpression of efflux pumps in *pseudomonas* and one particular efflux pump the resistance-nodulation-division (RND) is present which only effluxes antibiotics through reutilising energy from proton motive force across the inner membrane of the bacteria (Kanai and Haldar., 2020). Due to the increased number of susceptible isolates in this study could suggest the lack of the RND efflux pump, specific for antibiotics allowing for 65% of isolates to be killed with an average zone size of 10.08 mm suggesting effective antimicrobial action.

P. aeruginosa isolates were susceptible to **1** with ranging MIC's of 2-32 μg mL^{-1}. The varying degree of sensitivity to **1** could be due to the resistance profiling. Six strains which had an MIC value for **1** of 16 μg mL^{-1} were all sensitive to colistin sulphate and additionally all resistant to chloramphenicol and kanamycin. Additionally strains with a MIC value of 8 μg

mL^{-1} to **1** was sensitive to tetracycline as well as colistin (Britten., 2020, RD2 unpublished). This could be due to similar mechanisms of action. The mechanism of action of colistin involves interacting with the lipopolysaccharide outer membrane of *P. aeruginosa* where positively charged colistin is attracted to the negatively charged membrane and displaces Ca^{2+} and Mg^{2+} ions leading to disruption and increased permeability culminating in bacterial cell leakage and death (Bergen *et al*., 2012).

The combination of antibiotics can be used to evade resistance to one antibiotic and eliminate the possibility of resistance evolution. Having synergy occur between two different kinds of antibiotics can allow for efficient action against bacteria in difficult infections (Wright, 2016) and potentially could allow for the re-use of abandoned antibiotics due to increased antimicrobial activity (Möhler *et al*., 20118).

There are currently six models created for antibiotic synergism mechanisms being bioavailability modulation, regulation modification, mutual stabilisation, sequential blockade, parallel pathway inhibition and inhibitor inhibition (Sullivan *et al*., 2020) as proven by multiple studies outlined.

Bioavailability modulation is defined as one drugs bioavailability is increased due to the activity of the other drug by facilitating entry into the cell or decreasing the degradation or efflux of the second drug (Brennan-Krohn *et al*., 2018). This could be due to the increased concentration of a complex causing a favourable binding to internal binding sites thus causing antibiotic retention and an increase in antibiotic activity (Chevalier *et al.,* 2010).

Regulation modification is where the transcriptional response of one drug on the cell impacts the effects of the second drug (Chevereau and Bollenbach, 2015). In the case of colistin and vancomycin on *S. aureus*, colistin causes alterations in the bacterial phenotype

and gene expression such as changing the overall charge of the bacterial cell wall and a reduction in autolysis which in turn reduces the bacterial susceptibility to vancomycin (Haaber *et al.,* 2015).

Mutual stabilisation is where each drug allows the other drug to be more stable when binding to their target site (Harms *et al*., 2004). An example of this is through the synergistic potentiation of trimethoprim and sulfamethoxazole disrupting a metabolic feedback loop and dihydrofolate inhibition resulting in the enhanced interaction of trimethoprim with its target dihydrofolate reductase and additionally resulting in the decreased concentration of the tetrahydrofolate cofactor in *E. coli* (Minato *et al*., 2018).

Sequential blockade where both drugs have the same target which bypasses biological redundancies or increase the effectiveness of one or both drugs (Masters *et al*., 2003; Minato *et al.*, 2018). Parallel pathway inhibition where the drugs have different targets on parallel pathways (Maifiah *et al*., 2017) and knowing the synthetic legality of two genes can determine whether the two drugs will be synergistic hypothetically (Weinstein *et al.*, 2017). This pathway is demonstrated with *A. baumannii* treated with colistin and doripenem due to a decrease in the metabolites used to create peptidoglycan and LPS additionally the antibiotics alter the pathways for cell envelope biosynthesis (Maifiah *et al.,* 2017).

Inhibitor inhibition one drug causes the sequestering of antibiotic inhibitors allowing the other drug to act as normal (Maryam and Khan, 2018; Maryam and Khan, 2017). In *P. aeruginosa* studies, treatment with rifampicin and conessine allow for this synergistic mechanism to occur, with conessine potentially being an efflux pump inhibitor, more specifically MexAB-OprM which allows for the antibiotic to exhibit its action effectively (Siriyong *et al*., 2017).

Tetracycline proved to be synergistic with **1** which is in contrast to the study conducted by Andrade *et* al., 2020 where the ruthenium based complex RuNN (*cis*-$[RuCl_2$ (dppb) (bqdi)$]^{2+}$) reported no synergistic activity with the same antibiotic however with *S. aureus* and *S. epidermidis*. This could be due to the ability of **1** to efflux through porins similar to the action of tetracycline and additionally target other areas of the bacteria including RNA which tetracycline interacts with the 30S ribosomal sub-unit and halts translation (Luft, 1971; Grossman, 2016). Additionally another study that did show synergism between Ru complex $[Ru(phen)_2(ETPIP)](ClO_4)_2$ and kanamycin has been documented which is a similar antibiotic to streptomycin used in this study, potentially proving that Ru complexes could enhance the effect of aminoglycoside antibiotics (Liao *et* al., 2020).

Tetracycline additionally has synergy with silver nanoparticles with two studies showing an increase in antimicrobial activity (Panáček *et al*., 2016; Wypij *et al*., 2018). The efficacy of silver nanoparticles have been demonstrated with checkerboard assay with Amikacin where a fold change of 2 and 8 occurred for *S. aureus* and *P. aeruginosa* respectively and the nanoparticles combined with ampicillin with a 1 and 32 fold change for each pathogen respectively. The study proved to be effective against other species of bacteria including *E. coli, A. baumannii* and *K. pneumoniae* (Lopez-Carrizales *et al*., 2018). Silver nanoparticles additionally have been tested for synergism with ebselen which proved highly effective with MICs ranging between 5 and 40 μM in comparison with other commonly used antibiotics such as gentamicin, geneticin, kanamycin and tetracycline which ranges between 40-160 μM (Zou *et al*., 2018).

A chromium(III) complex $[Cr(phen)_3]^{3+}$ demonstrated synergism with ciprofloxacin against *E. coli* producing an FIC value of 0.032 at a concentration of ciprofloxacin 0.016 µg mL^{-1} which was 15 fold less than the initial tested antibiotic MIC (Páez *et al*., 2013).

A study conducted tests to determine the synergistic activity of zinc (Zn) nanoparticles with doping with other metals. The combinations of metals proved to be more synergistic than Zn nanoparticles alone with clinical isolates of *S. aureus* and *P. aeruginosa* with the most synergistic combination being with ciprofloxacin 10 % iron (Fe) doping with an FIC value of 0.33 ± 0.08 and 1 % cobalt (Co) with a value of 0.21±0.06 for *S. aureus* and *P. aeruginosa* respectively. Other combinations that were synergistic for *S. aureus* includes 10 % manganese (Mn), 10 % copper (Cu) and 1 % Co with FIC values ranging between 0.38 and 0.48. *P. aeruginosa* also had synergism exhibited with FIC values ranging between 0.38 and 0.46 with 1 % Fe, 10 % Mn and 1 % Cu. *P. aeruginosa* showed synergy with 1 % Fe, Mn and Cu with values ranging between 0.44 and 0.5 and a FIC value of 0.45 with 10% Cu doping (Sharma *et al*., 2016). Potentially the addition of other metallic nanoparticles could lead to additional synergistic mechanisms being displayed and more effective antimicrobial activity against pathogenic bacteria. This could be investigated in the future using Ru complexes to determine if the same could be done with similar positive effect.

2.6 Conclusion

The number of Gram-negative infections are rising, including those associated with bloodstream infections and soft tissue, including rare diseases such as necrotising fasciitis. Novel antimicrobials need to be assessed for efficacy to treat Gram-negative infections or potentially cause a resistance break for existing antimicrobials. Classes of amine derived complexes are used currently in non-medicinal application and therefore are deemed suitable for human use.

These derivatives have been discovered to effect against multiple species of Gram-negative and Gram positive pathogens with low MIC and MBC values with hexaammineruthenium complexes and **5** compared to another amine **3** and **6**. In comparison with other Ru complexes tested with various studies, **1** exhibits lower MIC values against multiple strains of species of *P. aeruginosa* with MIC values ranging between 4 and 16 μg mL^{-1}. Additionally antibiotic activity is mimicked across strains of species making it a plausible option for antimicrobial treatment irrespective of the strain of bacteria. However an intriguing conclusion to draw is that a lot of the complexes have selective antimicrobial activity against Gram-negative bacteria. This could be due to the addition of a cell wall on Gram-negative bacteria providing a protective barrier against the Ru complexes. Zones of inhibition testing demonstrated an increased inhibitory effect with *P. aeruginosa* PAO1 compared to other ruthenium complexes with an increase of 63% from 4 μg mL^{-1} to 16 μg mL^{-1}. A reason behind thus could be due to the reduction of the virulence factor pyocyanin, preventing quorum sensing thus conferring sensitivity to **1**.

Growth kinetics demonstrate high efficacy with **1**, achieving complete stasis of growth within a 24 h period at all concentrations however an increased concentration above MIC

value lead to faster rates of stasis across both species of bacteria. Additionally a decrease in biomass was observed within the same timeframe, demonstrating the potential for **1** to be applied as a biocide as higher concentrations can be used in comparison to medicinal applications.

Resistance profiling of *P. aeruginosa* isolates showed that across strains colistin sulphate was the most effective producing inhibitory zones with all strains compared to other antibiotics in which only a couple of strains were susceptible. Compared with the zones created by **1** which even at sub-lethal concentration the zones are greater than the zones of currently used antibiotics. Whilst more analysis is needed to determine the cell interaction with the Ru complexes to determine the potential mechanism of synergism, the results show promise for potentially allowing the susceptibility of otherwise resistant antibiotics to be altered allowing for effective activity. This could help slow the antimicrobial resistance problem, instead of trying to find new antibiotics which may be ineffective or have cytotoxic complications, the use of other complexes to allow for more commonly used antibiotics to be used without issue is a promising idea. Other metallic complexes have been studied for synergism proving to be promising as well potentially leading to a new era of combined treatments to allow for more effective infection resolution.

All three amine complexes have been proven to be effective against Gram-negative species with **1** being the most effective against the species. Following this research, toxicity must be determined for real-world application both *in vitro* and *in vivo.* However the research conducted here is promising with low MIC and MBC levels which could be beneficial to low toxicity.

Chapter 3: Evaluating the *in vitro* cytotoxicity of Hexaammineruthenium (III) chloride ($_1$)

3.1 Chronic Wounds

If the normal wound healing mechanism fails, the wound will result in being non-healing or chronic wounds. These affect many people and is associated with substantial cost to healthcare services (Posnett and Franks., 2008; Gould *et al*., 2015). On average £5.3 billion was invested within the National Health Service (NHS) during 2013 for treating wounds in the elderly with an average age of 69 (Guest *et al.*, 2015) and due to increasing longevity within the population, this issue is likely to increase in the future. Chronic wounds affect 120 in 100,000 people between the ages of 45 and 65 and rises significantly to 800 in every 100,000 over the age of 75 (Velnar *et al.*, 2009).

Chronic wounds are formed when the normal wound healing process is disrupted and remains in an inflammatory state (Zhao *et al.*, 2016) due to an excess in the number of inflammatory mediators such as C-reactive protein, IL-6 and IL-8 (Howcroft *et al.*, 2013). An increase in the concentration of angiotensin II and angiotensin I receptor blockers additionally inhibit re-epithelialization (Gould *et al.*, 2015). Development of chronic wounds are often caused by excessive and persistent inflammation or infection at the wound site. Neutrophils, a chronic wound marker, can cause an overproduction of ROS and release collagenase which prevents the repair of the extracellular matrix (ECM) (Zhao *et al*., 2016). ECM is present in excess at wound borders and can prolong the expression of pro-inflammatory cytokines (Rodero and Khosrotehrani., 2010) potentially contributing to the development of a chronic wound.

Chronic wounds can be identified through the manifestations of exudate, infection and tissue necrosis. The exudate represents the wound microenvironment and can additionally be detrimental to the wound healing process by metalloproteinases (MMP), specifically MMP-9s which causes ECM degradation (Jahromi *et al*., 2018).

Pro-inflammatory macrophages persist in the wound site which causes the impairment of repair, they are unable to phagocytose dead neutrophils which in turn causes the accumulation and inflammatory environment (Hesketh *et al*., 2017). The neutrophil clearance normally would initiate the conversion of M1 to M2 macrophages, however as clearance is not achieved in chronic wounds, M1 macrophages are unable to convert (Krzyszczyk *et al*., 2018). Additionally there is a low expression of markers CD16 and CD35 which indicate the presence of mature macrophages and those areas with high concentrations were near the vasculature of the wounds which could suggest the presence of microenvironments within the wound site which in turn prevent the activation of macrophages (Krzyszczyk *et al*., 2018). Accumulation of AGEs causes and increase in the production of inflammatory cytokine TNFα, which impairs epithelialisation (Qing., 2017)

Advanced glycation end products (AGEs) have a high affinity to AGE receptors on neutrophils, as a consequence of this there is an increase in the polymerization of actin, decreased migration capacity and an increase in the concentration of intracellular calcium. This in turn causes transendothelial cell migration to decrease in neutrophils (Glowacka *et al*., 2002; Qing., 2017). A large inflammatory zone is found within the wound due to limited migration to the basal area of the wound (Tian *et al*., 2016).

Fibroblasts in diabetic patients have impaired VEGF production due to the increased production of MMP-9 and additionally an impairment in NO secretion, vital for normal wound healing (Sivitz *et al*., 2010; Qing., 2017).

3.2 Infections of chronic wounds

Infection is often found in chronic wounds due to the idealistic environment. This includes a continual inflammatory phase, low oxygen tension and the presence of necrotic debris (James *et al*., 2008) Bacterial attachment is usually facilitated by the physiochemical and electrostatic properties between the surface of cells and the envelope of bacteria (Persat *et al*., 2015) with chronic wounds requiring specific interactions between the receptors and ligands. Overall there is a net negative charge on both cellular and bacterial walls therefore a virulence factor of bacteria, such as pili and flagella, are needed to overcome the force and attach (Alsharif *et al*., 2015).

Chronic wounds are inhabited by multiple species of bacteria, around 93% are polymicrobial (Walcott *et* al., 2016). A study found that normal skin surfaces contain 37% *S. aureus,* 17% *P. aeruginosa,* 10% *Proteus mirabilis,* 6% *E. coli and 5% Corynebacterium* species (Bessa *et al*., 2015), therefore skin wounds are likely to have bacteria from the normal flora present. In a study conducted by Dowd *et al*. (2008) 16S rDNA analysis confirmed that 27 different bacteria colonised within a chronic wound biofilm including *Acinetobacter baumannii, Enterococcus faecalis*, *Staphylococcus aureus, Staphylococcus epidermidis*, *Stenotrophomonas maltophilia, Prevotella bivia, Proteus mirabilis*, *Pseudomonas aeruginosa* and many other species. Additionally, more studies including one conducted by Wong *et al*. (2015) reported that microbiota present in chronic wounds, *S. aureus* and *P. aeruginosa* were the most prevalent at 23.3% and 14.8% respectively in Malaysian patients. (Rahim *et al*., 2017)

Biofilms can form within chronic wounds due to polymicrobial infections (Omar *et al*., 2017). There are four stages of biofilm formation including surface attachment, formation of a

microcolony, maturation and dispersal and detachment of the biofilm (Bjarnsholt., 2013;Wu *et al*., 2019)).

Biofilms contribute to inflammation within a chronic wound due to the numerous interactions with the immune system. The presence of a biofilm causes a release in growth factors and inflammatory cytokines such as EGF, PDGF, IL6, IL8 and TNFα (Prabhakara *et al*., 2011). TNFα is released excessively within chronic wounds due to the release from fibroblasts, keratinocytes and leukocytes thus increasing the activity of a converting enzyme of TNF (TACE) and a deficiency in the inhibitor (Wu *et al*., 2019)

Presence of *P. aeruginosa* starting biofilm has been linked to an increase in the number of neutrophils present (Fazli *et al*., 2011). It may additionally use the host immune system to leverage neutrophil derived polymers composed of actin and DNA that are necrotic in order to begin biofilm formation (Walker *et al*., 2005; Wu *et al*., 2019). *S. aureus* within a biofilm attract macrophages and causes the activation into M2 macrophages which migrate less and have limited microbicidal activity (Xu *et al*., 2013)

The colonisation of wounds with *P. aeruginosa* occur due to the many virulence factors it possesses including LPS, exotoxins, extracellular enzymes, secretion systems and pili (Haiko and Westerlund-Wikström., 2013). An essential virulence factor, pyoverdine, utilises iron bound in haemoglobin and causes an increase in the expression biofilm formation related genes (Kruczek *et al*., 2012; Brandenburg *et al*., 2019). The secretion systems assist with mammalian cellular damage through secretions of enzymes such as phospholipases, proteases and exotoxins directly into the cells. Pro-inflammatory cytokine expression is elevated in the epidermis upon infection (Garcia *et al*., 2018), prolonging inflammation and potentiating the likelihood of chronic wound development. Additionally, the formation of

biofilms is a contributing factor towards chronic wound prevalence in which extracellular polymeric substances protect the bacterial cells from immune system mechanisms and antimicrobial treatments (Flemming and Wingender., 2010).

3.3 Metals as wound healing agents

Metal complexes have been previously studied for use as treatment in wound cases. The development of metal-organic frameworks, which are porous crystalline polymers made of metal ions and organic ligands, have multiple active sites, low skeleton density and thermal stability, among other useful characteristics to release metal ions into the environment. Additionally copper ions have been used in chronic wound healing treatments including H-HKUST-1 with cell migration promoted through scratch assays with human epithelial keratinocytes cell line at low doses due to the increases cytotoxicity of the ions. Apoptosis does not occur and has been found to allow for adequate wound healing in diabetic mice with angiogenesis improved and collagen deposition increased by 377.9% from 11.3 vessels per mm^2 to 54.0 with the copper complex, copper benzene tricarboxylate $Cu_3(BTC)_2$ (Xiao *et al*., 2016). Copper incorporated into the frameworks provides effective antimicrobial activity against *S. aureus* and *E. coli* with effective proliferation of epidermal tissue and promotion of cell migration (Xiao *et al*., 2016; Wang *et al*., 2020). Zinc ions have been discovered to be effective against both *S. aureus* and *E. coli* with log reductions greater than 7 and a specific focus on fibroblast proliferation and migration and the reduction of inflammation (Abednejad *et al*., 2019; Yuan *et al*., 2019).

Silver oxide functionalised bioactive glass has an ability to treat both *P. aeruginosa* and *S. aureus* after 24-48 hours with a 6-log reduction to *P. aeruginosa* after a 30-minute treatment which has been used previously in wound models. Biofilms created by both

bacteria were additionally inhibited with a concentration of 0.6%. When added to a porcine wound model, the biofilm was reduced in thickness compared to untreated samples and additionally the host tissue damage was reduced by an increase in the collagen turnover at the biofilm interface (Wilkinson *et al*., 2018). Silver nanoparticles with a biocompatible γ-cyclodextrin metal-organic framework have been shown to be a promising solution to chronic wound injuries through release of reactive oxygen species disrupting bacterial DNA replication with MIC values of 16 μg mL^{-1} and 32 μg mL^{-1} MBC for *E. coli* and 64 μg mL^{-1} MIC and 512 μg mL^{-1} MBC for *S. aureus*. However murine wound healing was observed with a 62.2% decrease in wound size over 6 days with rat models and a 90% decrease in size after 10 days, complete re-epithelization had occurred in the tissue following 14 days incubation, with inflammatory markers TNF-α, IL-1-β and IL-6 decreased thus allowing for the normal would healing process to continue (Shakya *et al*., 2019). Other silver-based metal-organic frameworks have extensive anti-bacterial activity against multiple bacteria including *P. aeruginosa* through the release of silver ions and reactive oxygen species (Chen *et al*., 2021).

3.3.2 Ruthenium as a wound healing agent

Ru complexes have been identified previously in wound environments. One complex $[Ru(L^{1})(H_2O)Cl_3]$ where L is 2,10-dimethyl-8-(3-methyl-5-phenyl-1*H*-pyrazol-1-yl)-4-phenylpyrido[2',3':3,4]pyrazolo[1,5-*a*]pyrimidine identified in cancer trials was found to exhibit gradual inhibition of the SK-OV-3 cancer cell line when compared to a non-treated control at a lower concentration that the IC_{50} value of 5.0 μM using a cellular migration assay (Gu *et al*., 2022).

In contrast one complex has been found to exhibit improved wound healing in BLAB/c mice models where upon incubation over seven days, the wound of the Ru nanosystem HA-Ru

NFs/GOx (hyaluronic acid, ruthenium nanoframe consisting of a $RuCl_3{\cdot}xH_2O$ solution and glucose oxidase) treated mice had healed with new pink skin being observed whereas the control wound remained open. In addition to healing there was a reduced number of inflammatory cells in the area and the presence of new hair follicles could be seen within the wound site (Liu *et al*., 2021).

When coupled with selenium based nanoparticles, ruthenium complexes were highly compatible and effective at both selective antimicrobial activity and wound healing (Jain *et al*., 2022). Mouse models (BALB/cA-nu) infected with *S. aureus* and *E. coli* and treated using the Se@PEP-Ru2 (Selenium nanoparticles with D/L-[Ru (phen) 2 (p-HPIP)]$(ClO_4)_2 \cdot 2H_2O$ added) exhibited healing, with no ulceration of the wound site, thicker granulation and development of hair follicles were observed, in contrast to the untreated control. The nanoparticle complex exhibited a stronger ability to heal wound infections with *S. aureus* compared to *E. coli* and additionally cell cytotoxicity was not enhanced in the presence of the complex with mouse embryonic fibroblasts with cell viability remaining at 80% at a concentration of 128 μg mL^{-1} (Huang *et al*., 2017).

Another Ru nanoparticle variant, mesoporous Ru nanoparticles (comprised of ruthenium trichloride) coupled with ascorbic acid, encapsulated in hyaluronic acid and modified with the enzyme MoS_2 to create AA@Ru@HA-MoS_2 caused bacterial cells to secrete hyaluronidase (Jain *et al*., 2022). This in turn caused the release of the Ru and ascorbic acid thus generating a bactericidal response with *S. aureus* and *P. aeruginosa* where a concentration of 12 μg mL^{-1} elicited bactericidal rates of 89.2% and 81.9% respectively. Additionally in mouse models when a catheter was inserted and incubated with *S. aureus* and incubated for seven days exhibited swelling and purulence in a non-treated control.

Whereas when treated with AA@Ru@HA-MoS_2 and NIR radiation had no ulceration and displayed signs of gradual healing with no inflammatory response as determined by histological analysis. A similar texture was found compared to healthy tissue in the muscle. Reduced biofilm formation was exhibited in another mice model infected with *P. aeruginosa* which was measured over a 10 day period. No ulceration was found however tissue scarring was evident with reduced wound size of 37% after day four. By day 10 the treated wounds had healed completely with new hair follicles in place (Liu *et al*., 2019).

The complex $[RuL^{1\text{-}2}(PPh_3)(NO)Cl_2(PF_6)]$ additionally demonstrated wound healing capability within 36 h. The complexes ability releases NO into the wound environment, allowing for tissue regeneration however if the release is too high over an extended period keloids may develop thus impairing the wound healing. The Ru complex was added to wounds inflicted in mice skin cells (B16F1) at a concentration of 50 μg mL^{-1}, where significantly increased rate of wound healing occurred with the additional benefit of being antimicrobial against *E. coli* ATCC 25922 with 90% of bacterial cells being killed (Singh *et al*., 2022).

Metal complexes are a proven way to promote wound healing, reduce inflammation and prevent the occurrence of chronic wounds as proven with silver and ruthenium complexes. In addition to this Ru complexes have been used in mouse modelling in recent years, in order to understand the impact of Ru complexes such as **1** on human wound healing, various tests against human cell lines including human dermal fibroblasts WS1, human EA.hy926 endothelial cells, human keratinocytes HaCaT and human macrophages U937 was conducted in this chapter.

3.2 Aims and Objectives

3.2.1 Aims

The aim of this chapter was to use cell culture modelling to determine the *in vitro* cytotoxicity of **1** against a range human-associated cell lines which are directly involved within the wound healing process.

3.2.2 Objectives

- Use metabolic dye indicators to evaluate the cytotoxicity of **1** against fibroblasts (WS1), macrophages (U937), keratinocytes (HaCaT) and endothelial cells (EA.hy926).
- Assess *in vivo* cytotoxicity by inoculating *Galleria mellonella* modelling with **1**, coupled with infection modelling using *P. aeruginosa* strain PAO1.
- Identify the wound healing potential of **1** using *in vitro* scratch assays against human cell lines involved in the wound healing process.
- Determine the effects of **1** on host-pathogen interactions.
- Use *in vitro* 3D full thickness skin wound modelling to determine closure rates following exposure to **1**, coupled with infection modelling with *P. aeruginosa* strain PAO1.

3.3 Methods

3.3.1 Preparation of cell culture medium

Initially, Foetal Bovine Serum (FBS) (Sigma-Aldrich, UK) and penicillin-streptomycin (Sigma-Aldrich, UK) was thawed in a 56 ˚C water bath for 30 minutes. Roswell Park Memorial Institute (RPMI)-1640 (L-Glutamine, 25 mM HEPES) (ThermoFischer, UK) for U937 monocytes (ATCC, UK), Eagle's Minimum Essential Medium (EMEM) (ThermoFischer, UK) for WS1 fibroblasts (ATCC, UK) and Dulbecco's Modified Eagle Medium (DMEM) (ThermoFischer, UK) for EA.hy926 (ATCC, UK) and HaCaT cells (AddexBio, USA). The respective medias was prepared aseptically by supplementing with 10 % FBS and 100 mL^{-1} pen-strep before culturing the cells.

3.3.2 Cell culture

All cell lines were cultured aseptically and incubated at 37 ˚C and 5 % carbon dioxide. Cell suspensions were defrosted from liquid nitrogen storage and centrifuged with 9 mL of respective medium at 500 x *g* for 7 minutes and supernatant removed. Cells were re-suspended in 10 mL medium and transferred to a T25 flask to incubate for 2-3 days depending on cell type. Subsequent cell splitting was carried out by removing the media and placing in a 50ml flacon tube, 2 mL trypsin EDTA (Life Technologies, USA) was added and incubated with the cells at 37 ˚C and 5 % CO_2 for 5 minutes for cells to detach before 2 mL respective media was added. The cells were placed in the falcon tube containing media and centrifuged at 500 x *g* for 7 minutes before re-seeding. Before experimentation began, cell viability was assessed using sterile filtered trypan blue in a 1:1 ratio with cells and counted using a haemocyter (Bio-Rad, USA) with cells being used above 80 % viable.

3.3.3 Cytotoxicity of **1** against diverse mammalian cell lines

WS1 fibroblasts (Primary dermal fibroblasts (ATCC PCS-201-012)) were thawed and grown in EMEM media for two weeks. Cells were propagated at 5×10^5 cells mL^{-1} and 100 µL were added to each well of a 96 well plate and incubated for 24 h at 37 ˚C in 5 % CO_2 until 70 – 80 % confluent as described Slate *et al.,* (2018). Cells were washed and 100 µL of either media (negative control), 70 % ethanol (positive control), **1** at 4 µg mL^{-1}, 8 µg mL^{-1} and 16 µg mL^{-1} respectively were added. Exposed cells were incubated at 24 h in 5 % CO_2 and all experiments were repeated in triplicate. Finally, cells were washed, 100 µL of media and 20 µL of MTS solution for cell viability was added and colour changes were monitored over a 4 h period. The absorbance was measured at a wavelength of 490 nm and stopped when the negative control had reached a saturation of 1. A similar protocol was followed using U937 monocytes, EA.hy926 (ATCC CRL-2922) endothelial cells HaCaT keratinocytes (AddexBio T0020001). *N* = 6 per condition.

3.3.4 Scratch assay

Adapting the protocols described by Liang *et al*., 2007 and Mouritzen and Jenssen, 2018, the cell lines described in 3.3.1 were seeded into wells of a 12 well plate at a concentration of 1 × 10^5 cells mL^{-1} and incubated for 24h until confluent. On the day of the experiment, cells were washed with their respective medias and an additional 1 mL of media was added, with 3 of the 6 wells receiving treatment with **1**. This was incubated for an hour before a scratch was made using a 200 µl pipette tip. The scratch was marked with a pen on the plate in order to take the image from the same location. Images were taken continuously using GXCam – U3 series camera until cells had migrated to close the scratch wound and images were analysed using the software used to capture the images. *N* = 4 per condition.

3.3.5 Host-Pathogen Assay

3.3.5.1 Differentiation of U937 monocytes into M0 macrophages

U937 monocytes following culture are checked for viability using sterile filtered trypan blue at a 1:1 ratio, a viability of 80% was used for the experiment. Cells at a concentration of 1 × 10^6 cells mL^{-1} were differentiated into M0 macrophages in a 24 well plate using 50 ng mL^{-1} phorbol 12-myristate 13-acetate (PMA) (Sigma-Alrich, UK) in RMPI media and incubated for 24 h at 37 °C and 5 % CO_2. The cells were washed twice with RMPI media and incubated for a further 48 h in PMA-free media (Rios de la Rosa *et al.*, 2017).

3.3.5.2 Host-pathogen interaction with *P. aeruginosa* PAO1

M0 macrophages in the 24-well plate had the media aspirated and triplicate wells were treated with 4 µg mL^{-1}, 8 µg mL^{-1} and 16 µg mL^{-1} of **1** in antibiotic-free media for 24 h at 37 ˚C and 5 % CO_2. Wells were additionally prepared with RMPI media with no macrophages and a negative control of macrophage containing wells at 1 × 10^{-7} M bovine serum albumin (BSA) (Sigma-Alrich, UK) in antibiotic-free media were prepared and incubated for the same time as the treated cells in triplicate.

The supernatant was removed before inoculating all wells with 1 x 10^4 CFU mL^{-1} of *P. aeruginosa* strain PAO1 in 100 µL of antibiotic-free media for 3 h at 37 ˚C and 5 % CO_2 to enable phagocytosis to occur. Following this the supernatant of each well was collected before releasing the M0 cells from the wells using 450 µL trypsin EDTA and incubating for 3 minutes. This was then neutralised by 450 µL of antibiotic-free media and added to the previously collected supernatant and mixed thoroughly. Aliquots of 100 µL were added to

nutrient agar plates in triplicate and incubated overnight at 37 ˚C. The CFU mL^{-1} was counted the following day to determine bacterial recovery. *N* = 3 per condition.

3.3.5.3 Imaging host-pathogen interaction

Silicon wafers with an area of 1 cm^2 were washed in Dulbecco's phosphate-buffered saline (DPBS) (Fischer Scientific, UK) for 10 minutes and placed in 12-well plates. M0 macrophages were generated in the 12-well plates on the wafers before being exposed to treatments of varying concentrations of **1** as described in 2.17.2 and with the negative controls of BSA. The cells were then incubated with 1 x 10^4 CFU mL^{-1} of *P. aeruginosa* strain PAO1 for 3 hours at 37 ˚C and 5 % CO_2. Following the incubation the wafers were collected and incubated overnight at 4 ˚C in 2.5 % glutaraldehyde in DPBS and washed twice in DPBS the following day. The samples were dehydrated as described in in 2.8 with ethanol and stored in a desiccator until analysis a scanning electron microscope (Zeiss, Germany) (El Mohtadi *et al*., 2020). *N* = 3 per condition.

3.3.6 *Galleria mellonella in vivo* modelling

Initial testing involved inoculating *Galleria mellonella* wax moth larvae (Livefoods, UK) with different concentrations of the bacterial strains *P. aeruginosa* strain PAO1 (Thomaz *et al*., 2020) and MRSA to determine a suitable inoculum prior to addition of compounds. Ten larvae were used for each bacterial concentration and completed in triplicate. Using a Hamilton syringe coupled with a 34 gauge needle, 10 µL aliquots of bacteria at different concentrations as determined by OD_{600} nm were injected into the rear left proleg (Debois and Coote, 2011). Larvae were then incubated in 37 ˚C overnight and survival counts were performed at 24 h intervals for a 72 h total duration. *N* = 10 per condition as biological

replicates, 3 technical replicates were conducted. Bacterial viability was determined in parallel using standard Miles and Misra techniques using the following equation:

Colony forming units per mL (CFU mL^{-1}) = [number of colonies x sample size (20 µL) x dilution factor].

3.3.7 3D wound model

An *in vitro* 3D full thickness skin tissue wound infection model was used (Mattek, USA) (Kim *et al*., 2011) to generate preliminary data to evaluate the effectiveness of compounds for wound treatments, prior to considering future *ex vivo* wound modelling.

Upon arrival, the tissue was removed from the packaging and 2.5 mL medium was added to each well. The gauze covering the tissues was removed using sterile forceps and transfer the tissue into the plate containing the media ensuring the agarose didn't adhere to the insert and the media had full contact with the underside of the model with no air bubbles. The tissue is then equilibrated overnight at 37 ˚C at 5 % CO_2 and incubated with 5 drops of NucBlue cell stain reagent (Invitrogen, USA) which binds to the nucleus in the cells. Following the incubation the media is aspirated and replaced with fresh media as specified by the manufacturer.

Each tissue model was subjected to a biopsy punch (1 mm in diameter) with 12 models inoculated with 20 µL of *P. aeruginosa* strain PAO1 at 1×10^3 CFU mL^{-1} and incubated for 2 hours. Following the incubation, 4 infected models were incubated with **1** at a concentration of 8 µg mL^{-1} and 4 models with 64 µg mL^{-1} of ciprofloxacin (Fluka Analytical, UK) and incubated for a further 4 h. Controls of 2 models each MHB, **1**, Ciprofloxacin, *P. aeruginosa*

strain PAO1 and 4 models with a biopsy punch alone to compare infected and treated models to.

After treatment, the wound centre of 6 models; 2 of each condition *P. aeruginosa* PAO1 alone, *P. aeruginosa* PAO1 and **1** after 6 h incubation and *P. aeruginosa* PAO1 with ciprofloxacin at 64 μg mL^{-1} was obtained using a 2 mm diameter biopsy punch and vortexed in 7 mL of 0.85 % saline. Serial dilutions was carried out on MHA and incubated at 37˚C for 24 h to determine bacterial colony counts (Kim *et al*., 2011; Wheeler *et al*., 2019).

The remaining 16 models were imaged at 2 h intervals, using z-stack microscopy using the Leica Thunder microscope, the excitation wavelength was set to 360 nm to visualise the NucBlue stain. The images demonstrated wound closure rates, cell proliferation and death in the presence of **1** and bacteria. At the 24 h time point, the final images were taken and tissues were sectioned using the Thermo microtome with water collector where 5 mm sections were collected onto glass slides and stained using hematoxylin and eosin and fixed by placing tissue samples in 10 % formalin and dehydrated in graded alcohols, cleared in xylene, and embedded in paraffin. The slides were then imaged using the thunder microscope. *N* = 2 per condition.

All results were analysed using Graphpad Prism version 7.0 to determine significant differences between samples, with $p < 0.05$ being considered as statistically significant in all cases. The data was presented as mean, standard error of the mean and standard deviation with t-tests and one-way and two-way ANOVA's being used to determine differences between the data and log-rank analyses being conducted for the *Galleria mellonella* study.

3.4 Results

3.4.1 Investigating the effect of **1** on mammalian cell cytotoxicity

Four different cell lines were grown to an appropriate confluency and seeded in a 96 well plate. **1** was added at varying concentrations for 24 h and analysed using the MTS assay. On average at 4 μg mL^{-1} the average percentage viability across all four cell lines was 55.5 %. In response to **1** at 8 μg mL^{-1} and 16 μg mL^{-1} cell lines, excluding U937 macrophages, had a percentage viability higher than 100 %. The results show a gradual increase in viability proportional to the increase in complex concentration including WS1, HaCaT and EA.hy926 P5 cell lines all results are displayed in Figure 3.1. U937 macrophages experienced an increase in viability with an increase in concentration however the viability decreased upon incubation with 16 μg mL^{-1} by 2 % when compared with 8 μg mL^{-1}.

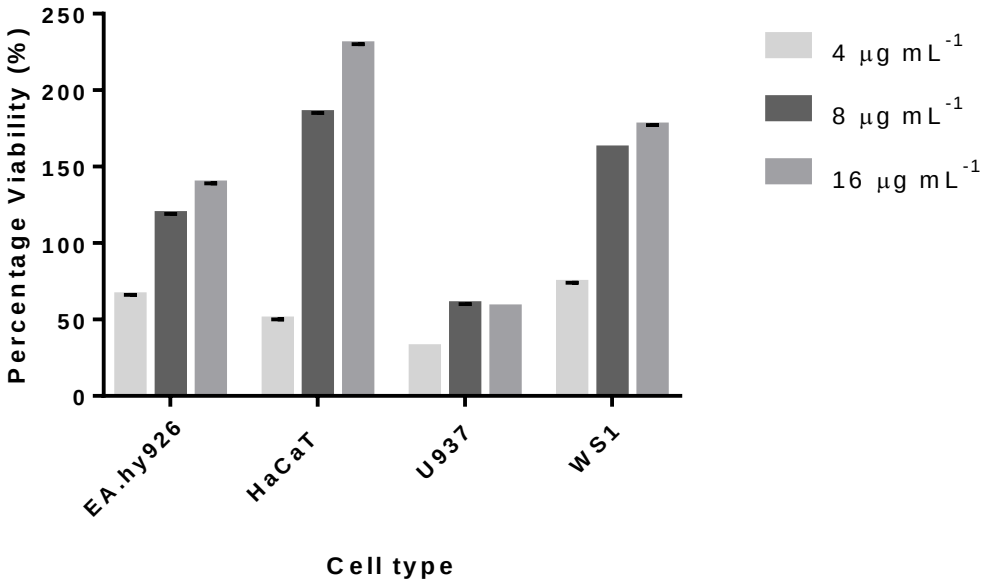

Figure 3. 1: Percentage viability of the cell lines EA.hy926, HaCaT, U937 and WS1 upon incubation with three concentrations of **1** at 4 μg mL^{-1}, 8 μg mL^{-1} and 16 μg mL^{-1} for 24 h (*N*=3).

Controls with **1** and MTS incubated together was completed and had no effect (data not shown)

There was highly significant difference between each cell type and concentration of the complex used $p<0.0001$ through two-way ANOVA analysis where an increase in concentration of **1** causes an increase in cell viability.

3.4.2 The determination of cell migration through Scratch assay applications when incubated with **1**

Scratch assays were used to determine the effect of exposure of **1** towards mammalian cell lines. All cell lines were seeded on a 24 well plate and grown to confluency. Either cells incubated in media alone or varying concentrations of **1** was added over 24 h. A scratch was then created using a 200 µL pipette tip and the migration of the cells was analysed over a 24 h period using a microscope. The distance migrated was calculated using Image J. EA.hy926 endothelial cells migration (Figure 3.2; Appendix Table 8.4) is not affected by the highest concentration of **1** tested (32 µg mL^{-1}) with all concentrations achieving full scratch closure after 40 minutes. Two way ANOVA analysis demonstrated high significance with the time, demonstrating that the length of time is vital for wound closure to occur with $p<0.0001$ and low significance with the concentration of **1** $p=0.0234$, the complex alone has little effect on cell migration rates and is therefore similar to cell migration without treatment. Rates of migration consisted of 2.502, 2.453, 2.621, 2.327 µm h^{-1} respectively for 0 µg mL^{-1}, 8 µg mL^{-1}, 16 µg $mL^{-1}$and 32 µg mL^{-1}.

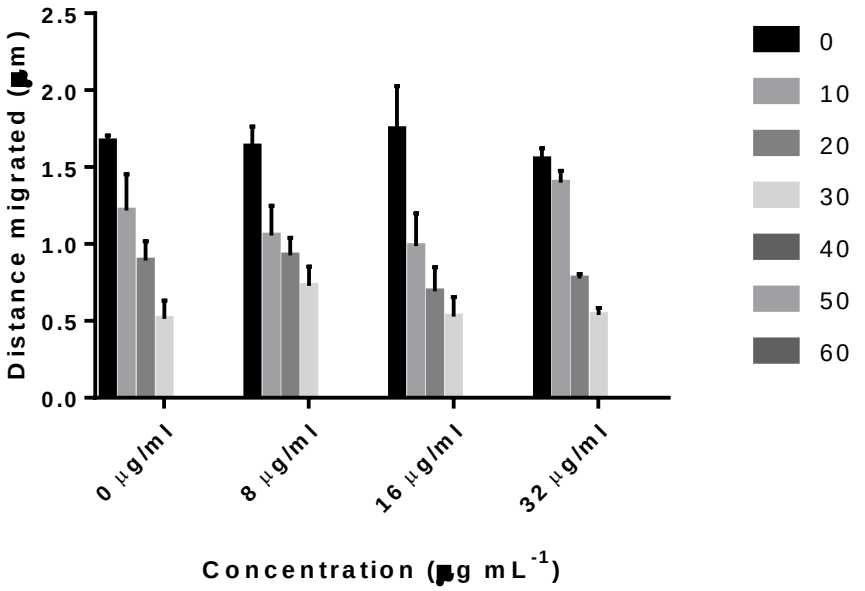

Figure 3. 2: Migration rates of EA.hy926 cells over an hour period with varying concentration of **1** at 0 µg mL^{-1}, 8 µg mL^{-1}, 16 µg mL^{-1} and 32 µg mL^{-1} with all conditions fully closing at 40 min (*N*=3).

With HaCaT (Table 3.1; Figure 3.3) all cells achieved complete closure of the scratch within 1 h with migration rates of 0.538, 0.316, 1.158 and 1.047 µm h^{-1} respectively for the increasing concentrations of **1** at 0 µg mL^{-1}, 8 µg mL^{-1}, 16 µg mL^{-1} and 32 µg mL^{-1}.

Table 3. 1: Percentage closure of HaCaT cells following incubation with 8 µg mL^{-1}, 16 µg mL^{-1} and 32 µg mL^{-1} **1** for 2 h (*N*=3).

Time (h)	T = 0			T = 1			T = 2		
	Width (µm)	SD	%	Width (µm)	SD	%	Width (µm)	SD	%
0 µg mL^{-1}	0.538	0.0288	0	0	0	100	0	0	100
8 µg mL^{-1}	0.316	0.0295	0	0	0	100	0	0	100
16 µg mL^{-1}	1.158	0.0528	0	0	0	100	0	0	100
32 µg mL^{-1}	1.047	0.222	0	0	0	100	0	0	100

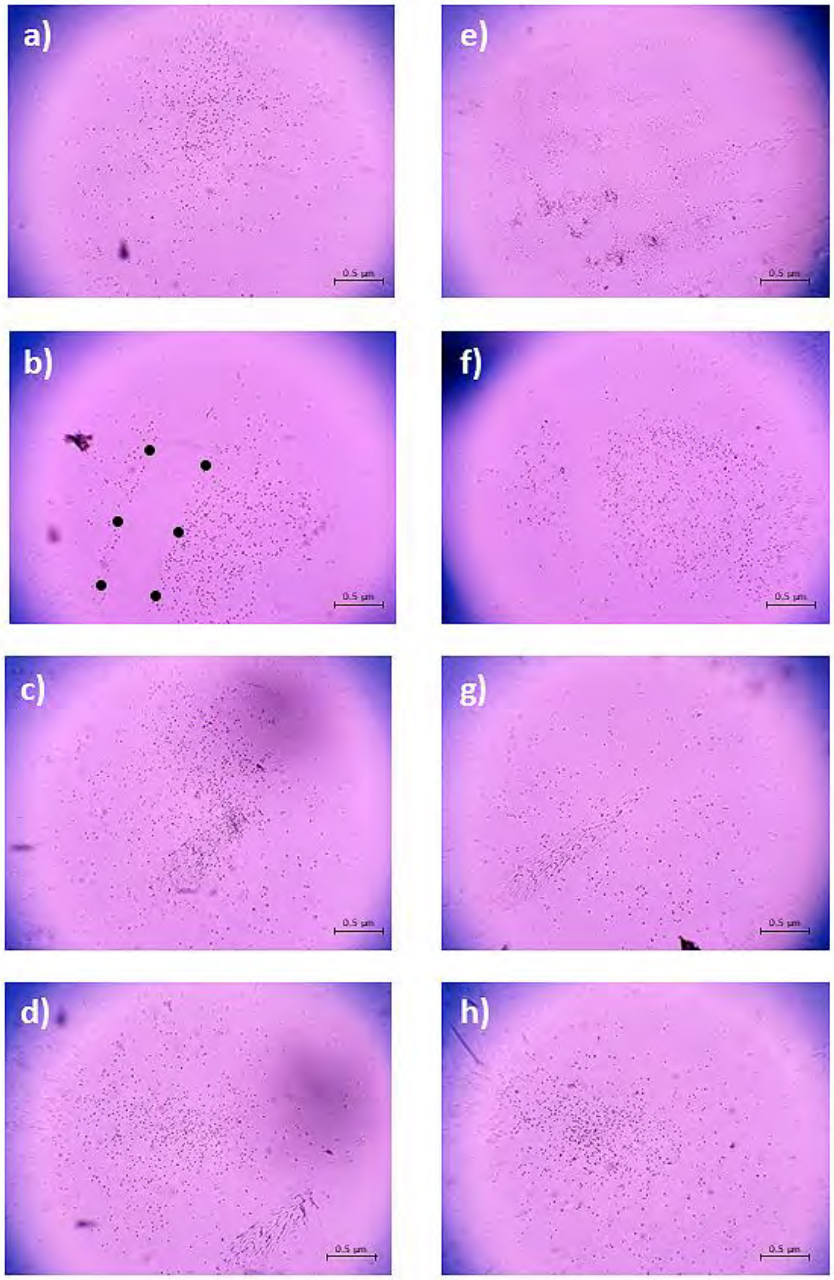

Figure 3. 3: Scratch closure with HaCaT cells following 24 h incubation with both untreated cells a) Pre-scratch, b) 0h, c) 1h, d) 2h and treated with 8 µg mL^{-1} 1 e) Pre-scratch, f) 0h, g) 1h, h) 2h. The dots on figure b) represent measuring points used for calculations of scratch closure (*N*=3).

Over the course of 6 h, the scratch reduced in size by 0.946 µm and 0.880 µm for WS1 cells and WS1 treated with 8 µg mL^{-1} **1** respectively. The speed of migration was 0.158 µm h^{-1} and 0.147 µm h^{-1} for control and treated cells respectively. A paired T-test was conducted on the cell migration distances at the start and end of the closure where a low significance was found of p=0.0338 between the treated and untreated cells meaning that **1** has little effect on the migration of WS1 fibroblasts. By 1 h the untreated cells had closed by 18.4 % and the treated cells by 4.7 % with that increasing to 68.9 % and 64.1 % respectively after 6 hours with full closure observed at 24 h post scratch (Appendix Table 8.5; Figure 3.4 and 3.5).

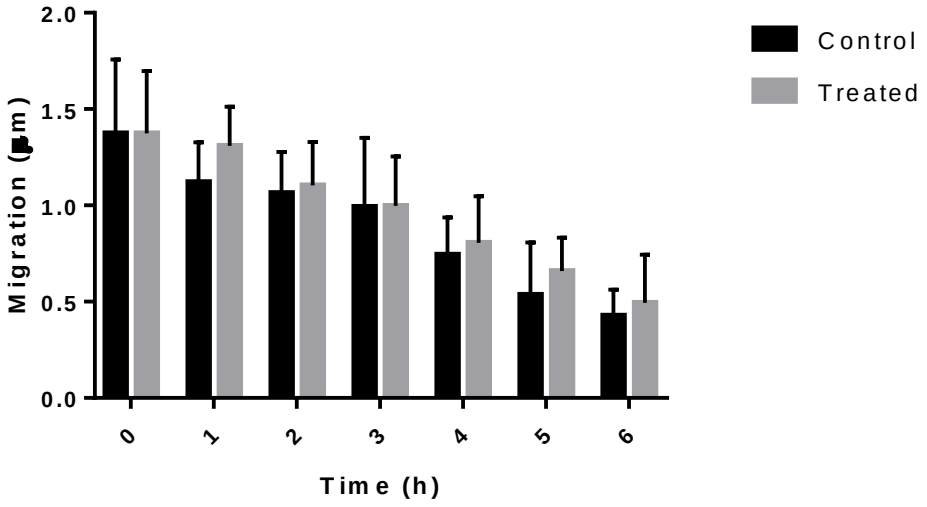

Figure 3. 4: Migration rates of WS1 fibroblasts over a 6 h period with both untreated and treated conditions of **1** at 0 µg mL^{-1} and 8 µg mL^{-1}. Error bars show standard deviation of cell distances (µm) (N=3).

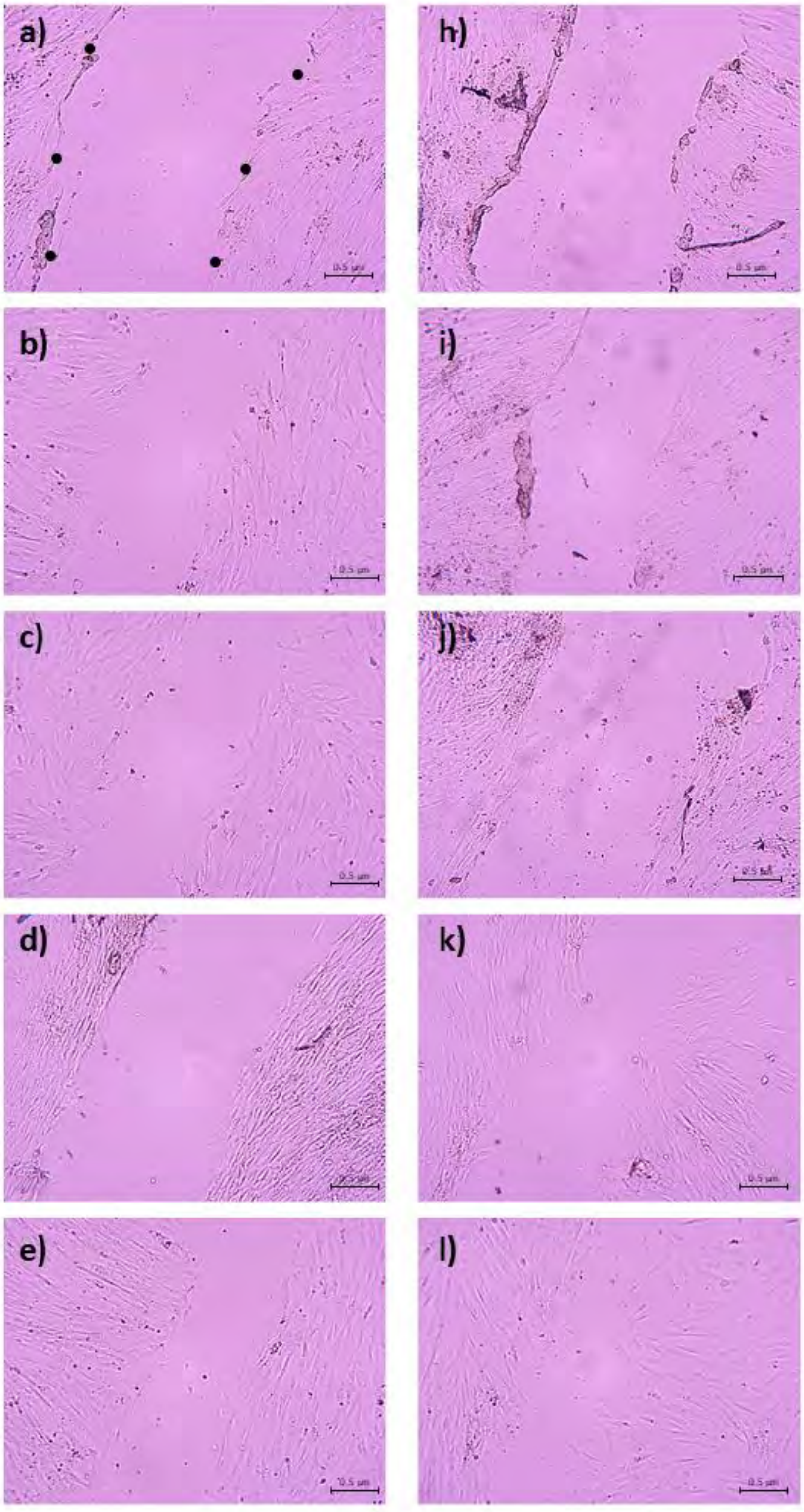
a)
h)
b)
i)
c)
j)
d)
k)
e)
l)

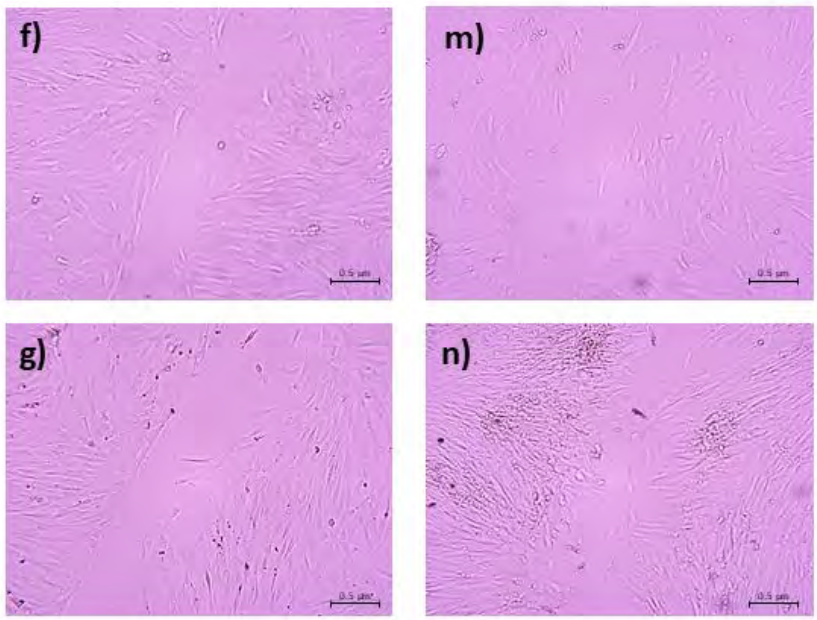

Figure 3. 5: Scratch closure of WS1 fibroblasts over a 6 h period with both untreated a) 0h, b) 1 h, c) 2 h, d) 3 h, e) 4 h, f) 5 h and g) 6 h and treated with 8 µg mL^{-1} **1** at h) 0 h, i) 1 h, j) 2 h, k) 3 h, l) 4 h, m) 5 h and n) 6 h. The dots on image a) represent measuring points used for wound closure (*N*=3).

3.4.3 Host-Pathogen Assay

To determine the effect of **1** on the phagocytic capability of macrophages, U937 monocytes were differentiated into M0 macrophages and incubated with varying concentrations of **1** for 24 h. Cells were washed to remove excess complex and *P. aeruginosa* strain PAO1 was added at a concentration of 1 x 10^4 CFU mL^{-1} was added to the cells and incubated before performing a bacterial recovery assay. With no compound being incubated with the macrophages the bacterial cell count was 3.28 x10^7 CFU mL^{-1} which decreased following incubation with 4 µg mL^{-1}, 8 µg mL^{-1} and 16 µg mL^{-1} where the *P. aeruginosa* strain PAO1 bacterial cell count was 9.17x10^6 CFU mL^{-1}, 5.02x10^6 CFU mL^{-1} and 2.01x10^6 CFU mL^{-1} respectively (Figure 3.6). After incubation with Bovine serum albumin (BSA), a known

macrophage inhibitor, the bacterial cell count increased to 7.90×10^8 CFU mL^{-1}. One-way ANOVA analysis suggests addition of **1** was highly significant for reducing the mean bacterial count (p<0.0001) in comparison with untreated macrophages and multiple t-tests between each concentration proved highly significant additionally demonstrating an increase in concentration of **1** had a significant impact on the number of *P. aeruginosa* PAO1 recovered (p<0.0001). SEM analysis showed upon incubation with **1**, macrophage pseudopodia are extended and bacteria are being phagocytosed in increasing numbers proportional to an increased concentration of **1** whereas macrophages treated with BSA (Figure 3.7b), do not have extended and bacteria are gathered around the macrophage without phagocytosis taking place.

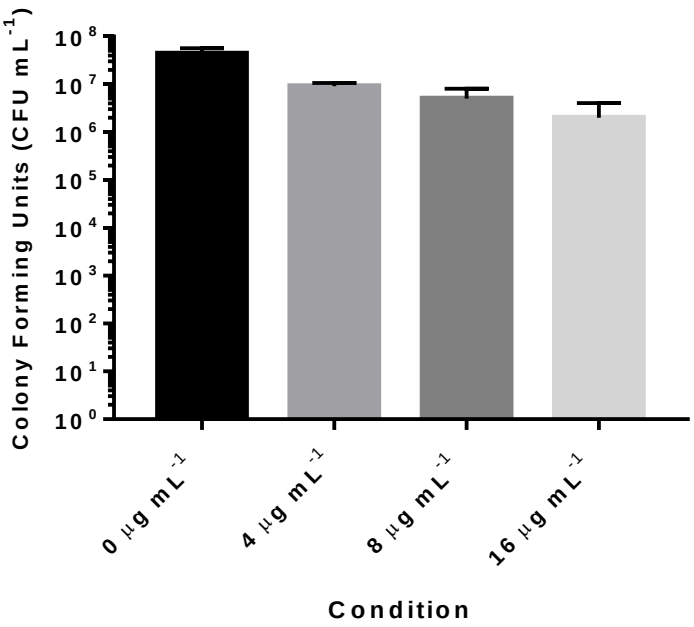

Figure 3. 6: Reduction in the viability of *P. aeruginosa* strain PAO1 when incubated with U937 macrophages and treated with various concentrations of **1** ranging from sub-MIC and Post-MBC concentrations (N=4).

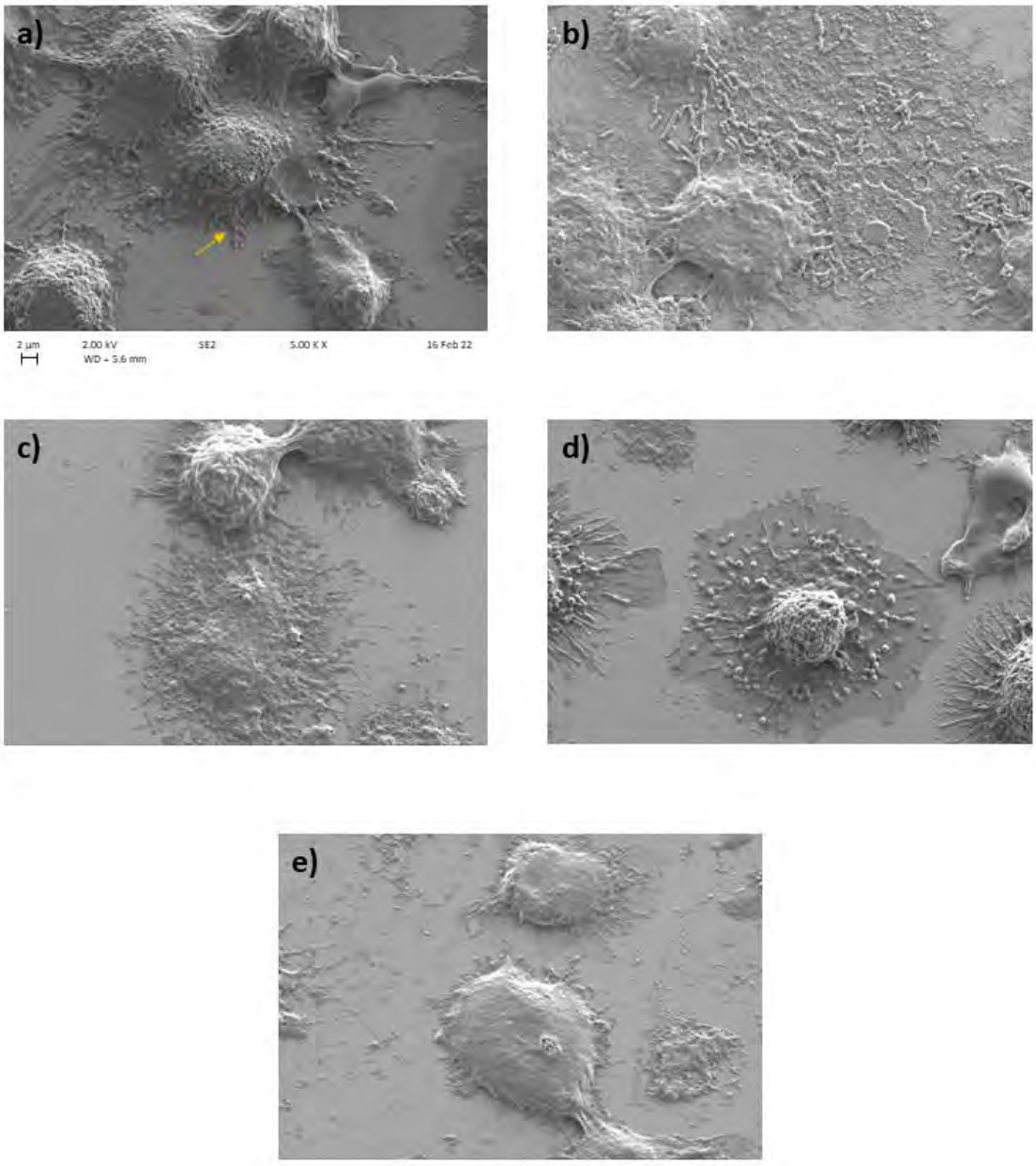

Figure 3. 7: SEM analysis of U937 differentiated M0 macrophages upon exposure demonstrating extended pseudopodia (yellow arrow) in response to a) no compound, b) Bovine Serum Albumin, and **1** at the concentrations of c) 4 µg mL^{-1}, d) 8 µg mL^{-1} and e) 16 µg mL^{-1} . All images had the same magnification properties as indicated by image a) (N=4).

3.4.4 *In vivo Galleria mellonella* model to determine cytotoxicity of **1**

G. mellonella were injected with a range of concentration of *P. aeruginosa* strain PAO1 to determine starting value however due to the toxins produced by the bacteria after 24 h 100 % of *G. mellonella* were deceased even at a low OD_{600} of 0.02. Studies were conducted to determine if **1** could prevent the death of the *G. mellonella* as a preventative treatment. The concentrations of **1** alone had increasing mortality with an increase in concentration. *P. aeruginosa* PAO1 alone had 100% mortality following a 24 h incubation and combinations of varying concentrations of **1** injected before the bacteria additionally had 100 % mortality after 24 h (Table 3.2; Figure 3.8). The no injection control demonstrated a 10 % mortality following 72 h incubation and the water only control only 30 % mortality after 24 h. Statistical analysis with the Log-Rank test demonstrates highly significant results with $p<0.0001$ demonstrating that injection with *P. aeruginosa* PAO1 causes mortality within 24 h.

Table 3. 2: Survivability in vivo of **1** and *P. aeruginosa* PAO1 both separate and in combination over a 72 h period with percentage survival calculated (N=3 technical replicates with 10 biological replicates).

Condition	24 h	48 h	72 h
No Injection	100	100	90
Water	70	70	70
2 mg kg^{-1}	90	90	70
4 mg kg^{-1}	60	20	10
8 mg kg^{-1}	60	10	0
***P. aeruginosa* PAO1**	0	0	0
2 mg kg^{-1} + *P. aeruginosa* PAO1	0	0	0
4 mg kg^{-1} + *P. aeruginosa* PAO1	0	0	0
8 mg kg^{-1} + *P. aeruginosa* PAO1	0	0	0

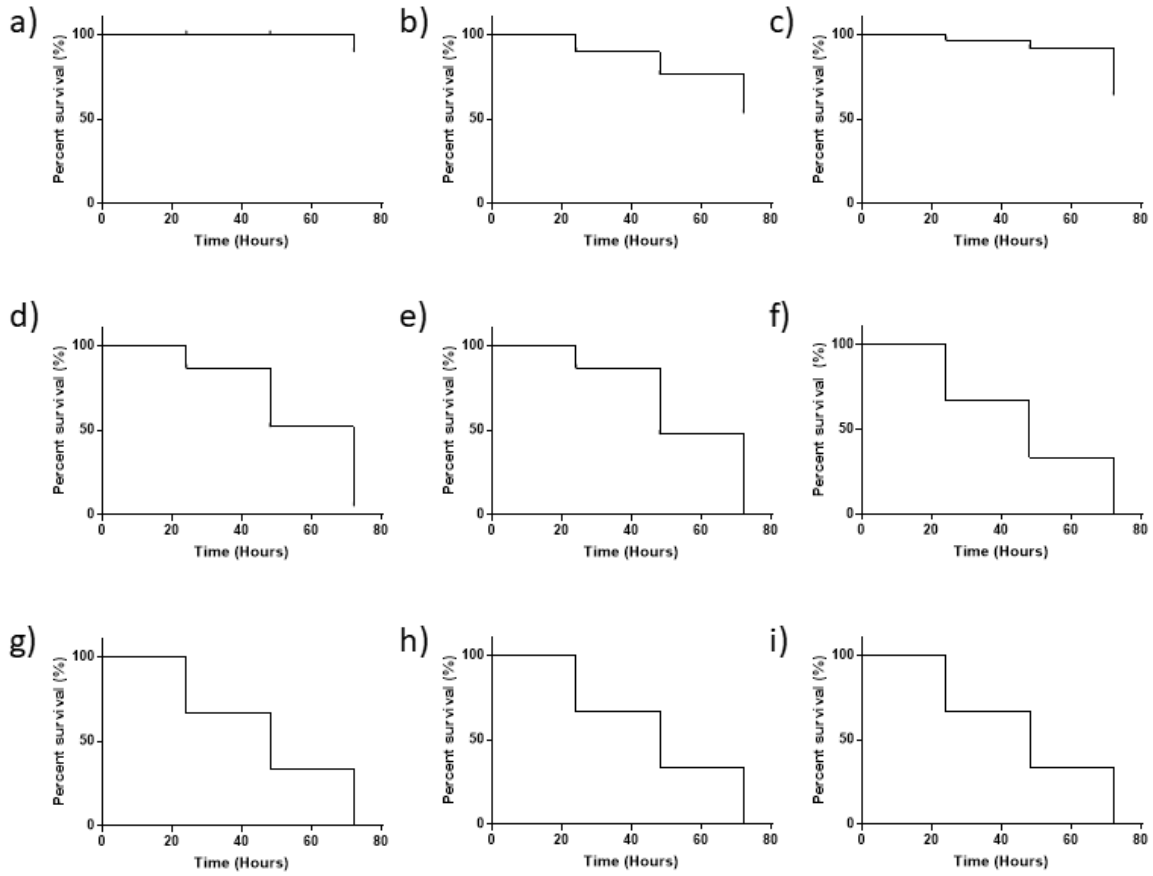

Figure 3. 8: Survival of G. mellonella with varying concentrations of **1** and P. aeruginosa PAO1. a) No injection b) Water, c) 2 mg kg^{-1}, d) 4 mg kg^{-1}, e) 8 mg kg^{-1}, f) P. aeruginosa strain PAO1, g) **1** 2 mg $kg^{-1}$and P. aeruginosa strain PAO1, h) **1** 4 mg $kg^{-1}$and P. aeruginosa strain PAO1, i) **1** 8 mg kg^{-1} and P. aeruginosa strain PAO1.

3.4.5 Application of a novel 3D wound infection model to determine the effects of **1** on the wound healing response.

A 3D full thickness skin wound model (Mattek, EpiDermFT) was used to determine the *in vitro* cytotoxicity levels of **1** during infection modelling with *P. aeruginosa* strain PAO1. This model contains layers of human epidermal keratinocyte and human dermal fibroblast cell types arranged into a substratum of 8-12 cell layers plus the stratum corneum with a surface area of 1 cm^2 and is designed to represent a biologically relevant assay for wound healing

and cytotoxicity evaluation. Wounds were established within the model by using a 5 mm biopsy punch directed into the centre of each model. The wounds were inoculated with *P. aeruginosa* strain PAO1 and incubated for 2 h, before the addition of either ciprofloxacin (64 μg mL^{-1}) or of **1** (8 μg mL^{-1}). Models were imaged at 24 h to determine wound closure rates. At 0 h the wound diameter was an average of 5971.55 μm (*N* = 2) with a SD of 195.85 (Fig 3.9 and 3.10a). Over the 24 h period the fibroblasts and keratinocytes migrated into the wound centre reducing the area of the wound to 261.54 μm (SD= 19.13) at an average percentage closure of 95.6 % (Fig. 3.10g). In parallel, a further wound model was incubated with sterile MHB which resulted in a faster wound closure rate, which decreased wound size by 97.3 % after 24 h (Fig. 3.10c) measuring 160.11 (SD= 7.37) when compared against the 0 h wound.

When incubated with *P. aeruginosa* strain PAO1 alone the wound following a 24 h incubation the wound had closed to 2742.34 μm (SD= 60.26) closing by 54.1 %.

Ciprofloxacin alone, used as a comparison against **1**, closed by 90.2 % to 586.75 μm following 24 h (SD= 5.97) (Fig. 3.10b) whereas when incubated with *P. aeruginosa* strain PAO1 additionally, at 24 h incubation the wound closure rate was greater than adding ciprofloxacin alone, reducing by 97.2 % after 24 h to an area of 166.99 μm (SD= 11.92).

Following incubation with **1** alone, at 24 h the wound area closed by 69.3 % to 1830.31 μm (SD= 14.75) (Fig. 3.10d). Upon incubation with both **1** and *P. aeruginosa* strain PAO1 after 24 h (Fig. 3.12f) closure area was 746.24 μm (SD= 24.00) closing by 87.5 %.

One-way ANOVA analysis demonstrated a significant difference between the means of wound closure with all conditions and time points meaning that the area of wound closure is significantly affected by the addition of **1** and ciprofloxacin allowing for wound healing to

occur quicker when compared to a non-treated control (p<0.0001). Additionally individual t-tests comparing each condition with the 0 h hole, all conditions had a p value >0.0001 confirming that each individual treatment has a profound effect on the rate of wound healing in the model.

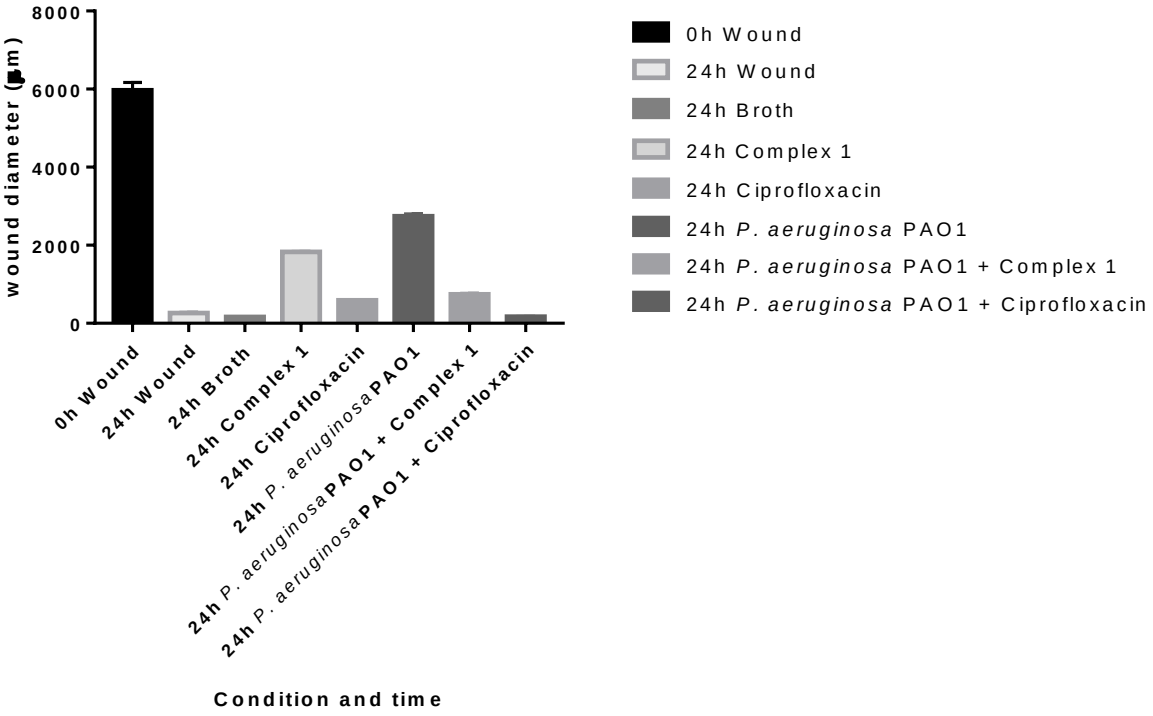

Figure 3. 9: Comparison of the wound diameters in response to 24 h incubation with varying conditions to the 0 h wound diameter (N = 2).

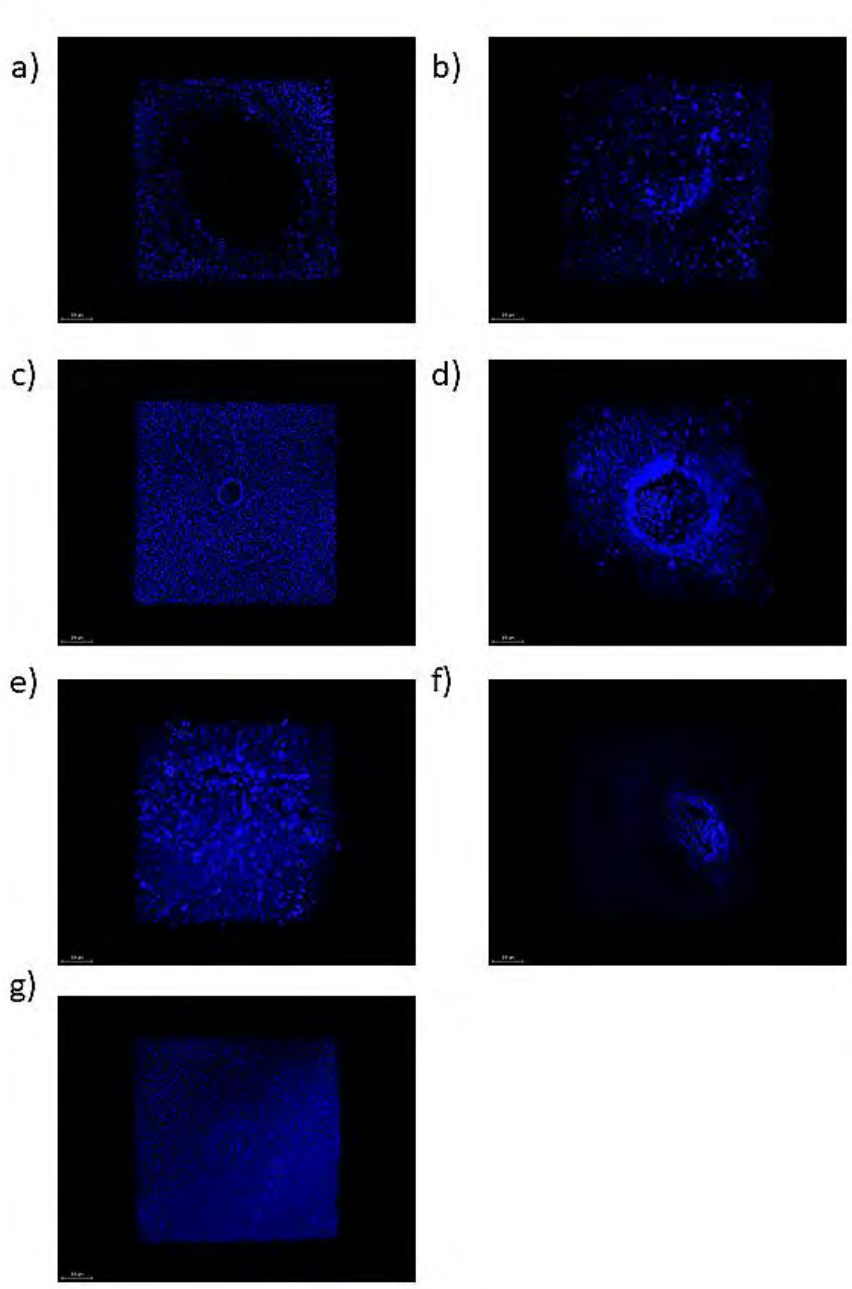

Figure 3. 10: Fluorescence microscopy images looking down from the top at the wound showing wound closure and cell migration using NucBlue as the staining agent for DNA, emitting fluorescence at 460 nm over 24 h (N=2) a) 0 h Wound, b) 24 h wound exposed to ciprofloxacin (64 µg mL^{-1}), c) 24 h wound with Broth, d) 24 h wound exposed to **1** (8 µg mL^{-1}), e) 24 h wound exposed to P. aeruginosa strain PAO1 and Ciprofloxacin (64 µg mL^{-1}), f) 24 h P. aeruginosa strain PAO1 and **1** (8 µg mL^{-1}), g) 24 h Wound (N=2).

In addition to measuring the area of the wound, the NucBlue stain allowed for cell counting in the wound area to determine how many cells had migrated and if the cells were in an apoptotic state following incubation with the different conditions, outlined in Table 3.3. As determined by (Helmy and Azim., 2012), circularity (how round the cells was) was determined, when the circularity of the nuclei was closer to 1 there was higher likelihood of cellular apoptosis. As observed with the study, there is little difference between the circularity values for all conditions with an average of 0.852 μm^2, they are all similar to the wound at 0 h when punctured where the circularity value was 0.839 μm^2. In addition to this Nuclear area factor (NAF) is used as an early indicator of apoptosis, with a lower number indicating apoptosis due to the loss of DNA. Using this as a more accurate indicator, incubation of the wound model for 24 h incubation with both *P. aeruginosa* strain PAO1 and **1** was exhibiting the most apoptosis. Whereas 24 h incubation with broth alone proved the least apoptotic in comparison with the other conditions.

Table 3. 3: Cell count using NucBlue in the wound area for each condition, with average size of the nuclei and circularity, roundness and Nuclear area factor used to determine if cells are in an apoptotic state (*N*=2).

Condition	Nucleus Count	Average Size (μm)	Circularity (μm^2)	Roundness (1/circ)	NAF
0h Wound	2129	82.911	0.839	1.192	210389.6
24h Wound	2848	451.358	0.858	1.166	1498212
24h Broth	3820	168.939	0.733	1.364	880421.2
24h 1	3567	157.309	0.879	1.138	638362.4
24h Ciprofloxacin	2870	61.913	0.887	1.127	200326.5
24h *P. aeruginosa* strain PAO1 + 1	14456	49.994	0.868	1.152	832615
24h *P. aeruginosa* strain PAO1 + Ciprofloxacin	3588	322.016	0.898	1.114	1286630

3.5 Discussion

3.5.1 Cytotoxicity of **1** against multiple cell lines

The MTS assay is adenosine triphosphate (ATP) based and indicates cell metabolism. In damaged or dead cells, ATP degrades rapidly and can be used to determine the number of viable cells present. It is well established that antimicrobial compounds can suppress or increase metabolic activity (Wang *et al*., 2010; Zhu *et al*., 2019). In the present study, **1** caused an increase in metabolic activity in four cells lines, with an increase in concentration being proportional to an increase in cell metabolism.

Ruthenium (II) bis(2,2'-bipyridyl) complexes tested against human keratinocytes HaCaT where cell survival was at 90% at a bacteriostatic concentration of 50 μg mL^{-1}. The cellular morphology remained similar to the non-treated control in comparison to a positive control of doxorubicin which displayed cell shrinkage (Lam *et al*., 2014). **1**, at a lower concentration exhibited higher cellular metabolism at MIC concentration for bacteria which increased with an increase in **1** concentration. Thus demonstrating that at bactericidal concentration, cellular metabolism is increased and the survival of HaCaT cells upon treatment is possible within a wound.

Human skin fibroblasts have additionally been tested for cytotoxicity with ruthenium based complexes. In one study $[RuCl_2(\eta^6\text{-p-cymene})\{\kappa P\text{-}Ph_2P(4\text{-}C_6H_4OSiMe_2{}^tBu)\}]$, $[RuCl_2(\eta^6\text{-p-cymene})\{\kappa P\text{-}Ph_2P(4\text{-}C_6H_4Br)\}]$, $[RuCl_2(\eta^6\text{-p-cymene})\{\kappa P\text{-}Ph_2PO(2\text{-}C_6H_4(SiMe_2{}^tBu))\}]$ and $[Ru(C_2O_4)(\eta^6\text{-p-cymene})\{\kappa P\text{-}Ph_2PO(2\text{-}C_6H_4(SiMe_2{}^tBu))\}]$ all exhibited low IC_{50} values ranging between 7.2-31.9 μM and with the second and third complexes having the capability to stimulate growth in MDA-MB-231 cells at low concentrations. Including $Ph_2P(4\text{-}C_6H_4Br)$ in ruthenium complexes containing an amine group has thus been found to have influence of

the bioactive fragment of the complex through incorporating carboxylic acids within the scaffold (Biancalana *et al*., 2017). Similarly, **1** in the present study at low concentration of 8 µg mL^{-1} allows for increased cellular metabolism and potentially cellular growth, thus stimulating wound healing. Other Ru (II) based complexes with bistriphenylphosphines, bipyridine and *N'*,*N'*-(disubstituted)-*N'*-acylthiourea ligands exhibited low cytotoxicity compared with cisplatin against mouse fibroblast L929 with IC_{50} values ranging between 0.52-1.65 µM and was used to demonstrate selectivity in a cancer study where the prostate tumour cell line DU-145 with cells exhibiting morphological changes indicating apoptosis over a 48 h period (Barolli *et al*., 2017). Additionally no significant cytotoxicity was discovered against the fibroblast cell line HDFa at a concentration of 150 µM of Tetrakis dimethylsulfoxide dichloro ruthenium (II) $[RuCl_2(DMSO)_4]$ (Thankgavel *et al*., 2018). **1** is non-toxic at low concentrations and similar to the study conducted by Binacalana *et al*., 2017 with different Ru complexes, the WS1 fibroblasts were proliferating with an increase in concentration of **1** to 177 % viable.

Polypyridal ruthenium complexes $[Ru(dip)_2(bpy/bpy\text{-}2\text{-}nitroIm)]^{2+}$ where dip is 4,7-diphenyl-1,10-phenanthroline, bpy = 2,2'-bipyridine and bpy-2-nitroIm = 4-[3-(2-nitro-1*H*-imidazol-1-yl)propyl]) proved moderately cytotoxic towards mouse lung endothelial cells MLuMEC FVB due to the cellular uptake of the ruthenium arresting the cell cycle in the S-phase causing apoptosis, additionally cell migration and adhesion are affected through incubation with these complexes (Mazuryk *et al*., 2015). NAMI-A derivatives against human umbilical vein endothelial cells (HUVEC) had moderate cytotoxic effects in a dose-dependent manner, similarly to **1** against EA926 cells. Migration studies confirmed complete closure following a 24 h period with untreated HUVEC cells whereas treated cells had limited closure and

caused a reduction in the quantity of tube structures vital for angiogenesis to occur (Gu *et al*., 2016).

$[Ru(Lap)(PPh_3)_2(phen)]PF_6$ which was used against the malarial parasite *Plasmodium falciparum* with high effectivity, cytotoxicity testing was additionally conducted where the IC_{50} of J774 macrophages was low at 0.33 ± 0.08 µM (Barbosa *et al*., 2014). On the contrary high cytotoxicity was observed with the murine macrophage cell line RAW 264.7 where cytotoxicity was over 200 µM with the ruthenium compound $[RuCl_2(HL_4)(HPTA)_2]Cl_2$ for the treatment of malaria (Sarniguet *et al*., 2014). For the treatment of Leishmaniasis two ruthenium compounds have been tested for both anti-parasitic activity and cytotoxicity against macrophages, with RAW 264.7 and J774 macrophages for both cis-$[RuII(\eta^2\text{-}O_2CR)(dppm)_2]PF_6$, where R = 4-bu-tylben-zoate (bbato) and cis,fac-$[RuCl_2(dmso)_3(tmtp)$ respectively where the cytotoxicity values varied of 8.73 µM and 330.8 µM for each respective complex (Britten and Butler., 2022; Costa *et al*., 2017; Fandzloch *et al*., 2017). **1** appears to have low cytotoxicity against U937 macrophages even at 16 µg mL^{-1} where cell viability remained high at 58 %, significantly higher than the study conducted by Sarniguet *et al*., 2014 suggesting **1** is less cytotoxic at much higher concentrations than other ruthenium complexes tested previously thus other cell lines may be more tolerant, proving a promising treatment for wound infections.

Cytotoxicity in human keratinocytes HaCaT with a *meso*-tetra-ruthenated porphyrin was evaluated and found to be non-toxic, even at the highest concentration of 20 µM however highly toxic to melanoma cells. The specificity is due to the increased cellular uptake of ruthenium by melanoma cells and the uptake of transferrin is an additive factor for ruthenium due to the binding allowing for subsequent entry into the cancer cells (Vizzotto

et al., 2020). Another two ruthenium complexes *mer*/*fac*-$[Ru(hexpytri)_3]^{2+}$ and *mer*/*fac*-$[Ru(octpytri)_3]^{2+}$ exhibited modest cytotoxicity against HaCaT above the MIC value of 8 µg mL^{-1} against MRSA with a reduction of 60-80 % in viability (Kumar *et al*., 2016). Similar to the other cell lines in the present study where **1** exhibited low cytotoxicity against all skin cell lines. This could possibly be due to decreased uptake of ruthenium into human cell lines.

Other cell lines have been explored with Ru complexes, in one study a number of Chiral Pincer-Ru complexes of the type $(^{R2}NNN)RuCl_2$ (PPh_3) (R = 3-methylbutyl and 3,3-dimethylbutyl) was found to supress the growth of both human dermal fibroblasts and human tongue carcinoma cells in a dose-dependent manner with concentrations as low as 5 µg mL^{-1} doxorubicin inhibiting growth by 50 % with untreated SAS cells (Nandi *et al*., 2021). In contrast to **1**, cellular growth and metabolism is not inhibited by incubating cells with 8 µg mL^{-1} but rather increased in response to an increased concentration demonstrating that **1** is non-toxic to wound related cell lines.

An MTT cytotoxicity assay of Ru(II) terpyridine complexes against multiple cell lines including human lung carcinoma cell line A549 and both human and mouse colon carcinoma lines HCT116 and CT26, with the IC_{50}'s ranged between 32.8 µM to 110.8 µM (Lazić *et al*., 2016). Additional ruthenium based complexes with chloride ligands including terpyridine with a general formula of [Ru(Cl-Ph-tpy)(*N*-*N*)Cl][Cl] (where *N*-*N* = en, dach or bpy were tested with two cancer cell lines HeLa and A549. Exhibiting low IC_{50} values of 12.7 µM for HeLa and 4 fold increase to 53.8 µM for A549 cells (Milutinović *et al*., 2017). In comparison to the study with **1** where low concentrations of the complexes had little effect on the viability of cells whereas higher concentrations cause increased viability among skin cell lines. The cause behind the cytotoxicity could be due to the crosslinking to DNA in the cell through

guanine bases, thus halting cellular processes through the cease of DNA replication. The chlorine ligand additionally forms monofunctional adducts and strongly bind to CT-DNA and intercalate the base pairs (Lazić *et al*., 2016). Another reason behind increased cytotoxicity is due to the lipophilicity of the complexes, thus leading to a decreased rate of degradation and allowing longer for the complex to exhibit antimicrobial activity (Lazarević *et al*., 2017). Apoptosis in cells is also induced by the complexes due to ROS mediated dysfunction of mitochondria, thus preventing ATP generation (Han *et al*., 2015). Cell growth in human cell cancer lines (BEL-7402) is inhibited through terminating at the G0/G1 phase of growth and cause arrest of the cycle at the G2 and M phase in cell lines including BEL-7402, protein expression was downregulated upon incubation with ruthenium based complexes such as $[Ru(dmb)_2(DQTT)](ClO_4)_2$ where (DQTT = 12-(1,4-dihydroquinoxalin-6-yl)-4,5,9,14-tetraazabenzo[b]triphenylene, dmb = 4,4′-dimethyl-2,2′-bipyridine), $[Ru(bpy)_2(DQTT)](ClO_4)_2$ where (bpy = 2,2′-bipyridine), $[Ru(phen)_2(DQTT)](ClO_4)_2$ where (phen = 1,10-phenanthroline) and $[Ru(dmp)_2(DQTT)](ClO_4)_2$ where (dmp = 2,9-dimethyl-1,10-phenanthroline) (Zhang *et al*., 2016).

3.5.2 Effect of **1** on *in vitro* wound healing through cell migration assays

Cell migration in this research, was found not to be impeded by the addition of varying concentrations of **1** across multiple cell lines, demonstrating the complexes ability to be used to assist the chronic wound healing process. Rates of cell migration remained similar to the control non-treated cells and with the additional benefit of highly effective antimicrobial activity of **1**, could prove an efficient treatment option for infected wound treatment.

In a contrary study, the migration of MDA-MB-231 or MCF7 breast cancer cells was impeded by the addition of Ru-PIP ($[Ru(dppz)_2(PIP)]^{2+}$ (dppz = dipyrido[3,2-*a*:2′,3′-*c*]phenazine, PIP =

(2-(phenyl)imidazo[4,5-*f*][1,10]phenanthroline) and OLAP (PARP inhibitor) due to the DNA damaging mechanism the complex exhibits on cancer cells (Yusoh *et al*., 2020). Another Ru complex was found to inhibit migration of MDA-MB-231 human metastatic breast carcinoma, $[Ru^{II}(\eta^6\text{-}p\text{-cymene})(PAIDH)(X)]^+$ (where, X = Cl, Br and I) with an IC_{20} dosage, this was indicative of inhibition of epidermal growth factor receptor kinases (Sarkar *et al*., 2019). A study investigating the effect of *trans*-$[Ru(PPh_3)_2(law)(phphen)]PF_6$ against cancer cell line lung A549 at concentrations below 0.09 μM (IC_{50}) additionally showed an inhibition of 85% in cell migration at a concentration of 0.05 μM. This was due to arrest in the cell cycle at the G1 phase and being an apoptosis inducer (Oliveira *et al*., 2017). Overall the effect of Ru complexes against carcinogenic cell lines show an inhibition in cell migration due to the damage caused by DNA. Surprisingly, this does not appear to apply to **1**, where cell migration of a number of cell lines including U937 macrophages and WS1 fibroblasts was not affected by the activity of the complex.

Nowak-Sliwinska *et al*., (2011) examined Ru complexes against endothelial cells which inhibited migration over a course of 6 h with the percentage of wound closure decreasing with an increase in concentration. This is in contrast to the present study where an increase in concentration of **1** had no effect on the rate of wound closure, which could be as a result of **1** exhibiting less of an antiangiogenic activity compared to RAPTA and DAPTA C and T used elsewhere (Nowak-Sliwinska *et al*., 2011). In a study comparing the activity of L929 fibroblasts and HaCaT keratinocytes proved that the fibroblasts migrated quicker than HaCaT and full closure of all replicates closed compared to only half of the HaCaT in serum free conditions. This is in contrast with the present study as the HaCaT migrated faster than the WS1 fibroblasts, however the difference in migration rates could be due to murine carcinogenic fibroblasts being used previously by (Walter *et al*., 2010). Endothelial MLuMEC

FVB cells treated with $[Ru(dip)_2(bpy\text{-}NitroIm)]^{2+}$ demonstrated only a slight inhibition in cell migration over 11 h, similarly to the present study where no change in migration was seen compared between treatments (Mazuryk *et al*., 2015).

In comparison silver complexes have additionally been evaluated for migratory performance, including bovine retinal endothelial cells against silver nanoparticles where VEGF induced migration was inhibited. This was due to silver induced cell mortality in the presence of VEGF (Kalishwaralal *et al*., 2009) which is contradictory to the present study due to **1** being less cytotoxic (Ryder *et al*., unpublished). However another study demonstrated that SVEC4-10 endothelial cell migration was upregulated as a consequence of adding Ag nanoparticles at low concentrations. Over 20 μg mL^1 the nanoparticles were toxic to the cells and induced cell death. The Ag nanoparticles used in this study were smaller than other studies with contrasting results and prepared alternatively (Kang *et al*., 2011). The size of complex may affect the overall migratory rate of cells which may account for the lack of inhibition mediated by **1**, which has a higher molecular weight.

Additionally silver nanoparticles have been used previously in wound dressings (Kalantari *et* al., 2020) and have been assayed against fibroblasts and HaCaT keratinocytes where cell migration was quicker upon additional of nanoparticles compared to the control cells and no difference between the two was reported respectively, which is an advantage for wound dressing applications. The faster migration of the fibroblasts was proven to be due to a transformation into myofibroblasts which are quicker cell migrators than the precursor (You *et al*., 2017). These results showed that HaCaT cells migrated faster compared with control cells, this is in contrast with the study conducted by You *et al* (2017) due to the migratory capacity being affected which could prove positive for wound dressing technologies to

improve rates of wound healing. The similar migratory rates of the fibroblasts suggest the fibroblasts are remaining in their precursor state rather than transforming into myofibroblasts. Macrophages additionally have increased migratory rates with addition of silver nanoparticles especially when combined with chitosan based wound dressing which are readily available on the market. RAW 264.7 macrophages migrated quicker as the concentration of nanoparticles increased with 100 µg mL^{-1} have an 85 % wound closure rate compared to 73% for 75 µg mL^{-1} (Parthasarathy *et al*., 2020). This is similar to **1** where increasing concentrations until 32 µg mL^{-1} appeared to stimulate migration compared to the control cells possibly due to the lack of complex mediated cytotoxicity. This additionally demonstrates that **1** could be beneficial impregnated in wound dressings due to its ability cause rapid cellular migration in response to treatment with the complex at MIC concentration.

3.5.3 Effect of **1** on Host-pathogen interactions with *P. aeruginosa* strain PAO1 and macrophages

Phagocytosis by macrophages rely on the kinase phosphoinositide 3 (PI3K) (Kierbel *et al*., 2007) which converts the cell membrane lipid phosphatidylinositol and bisphosphate into phosphatidylinositol triphosphate needed for Akt recruitment (Lovewell *et al*., 2014). This is required for *P. aeruginosa* invasion and engulfment and increased phagocytosis in the lungs of *P. aeruginosa* occurs due to the loss of murine phosphatase and tensin homolog which converts phosphatidylinositol triphosphate into a diphosphate (Hubbard *et al*., 2011). Phagocytosis is additionally facilitated by host factors serum amyloid A and surfactant protein A which can bind to *P. aeruginosa* (Hari-Dass *et al*., 2005). Perhaps, **1** causes an increase in PI3K allowing for the enhanced phagocytosis of macrophages with an increase in

1 concentration or an increase of serum amyloid A and protein A causing increased binding to *P. aeruginosa* allowing for phagocytosis to occur rapidly.

The bacteria itself has around 100 fold increase in resistance to phagocytic uptake by the hosts immune cells with a loss of flagellar motility independent of the flagellum (Amiel *et al*., 2010) due to the activation of the signalling pathway controlled by PI3K and Akt for motility of swimming. The swimming of the bacteria by the flagella causes Atk activation thus recognition by immune cells and subsequent phagocytosis (Lovewell *et al*., 2014). A deletion in the phosphatase and tensin homolog which has the opposite effect of PI3K causes an increased rate of phagocytosis in alveolar macrophages (Hubbard *et al*., 2011).

Fourier Transform Infrared Spectroscopy (FTIR) spectra of macrophages incubated with *P. aeruginosa* demonstrated distinct peaks in the stretches of O-H, PO_2 symmetric and C-O-H bend suggesting the interaction causes an alteration of hydroxyl groups of the cell wall and composition of the carbohydrate and phospholipid content in macrophage membranes resulting in an elongation in the pseudopodia during the phagocytic process (El Mohtadi *et al*., 2020). As shown by the SEMs taken of the U937 macrophages a similar effect is occurring upon incubation with **1**. The pseudopodia are extended in comparison to a macrophage in media alone suggesting that **1** cause's membrane changes in the macrophages to allow for more efficient pathogen clearance, as demonstrated by a decrease in cell number with an increase in **1** concentration.

OprF additionally may have an impact on macrophages by resisting phagocytosis. An OprF mutant has reduced expression of T3SS genes and the decreased secretion of toxins ExoT and ExoS (Moussouni *et al*., 2021). *P. aeruginosa* is well known for evading phagocytosis and with the OprF mutant, this does not occur due to decreased expression of T3SS (Bernut *et al*., 2019). **1** may be able to prevent the expression of T3SS genes in *P. aeruginosa* or reduce

the secretion of toxins which interfere with phagocytic mechanisms, this combined with extended pseudopodia allows for enhanced clearance of the bacteria within a wound environment. The antibacterial activity of **1** is thought to be due to DNA interaction which can stop the expression of phagocytic evasion genes and membrane perturbation additionally affects the T3SS anchored to the *Pseudomonas* membrane (Galle *et al*., 2012) thus preventing toxin secretion, allowing for phagocytosis to occur more readily.

3.5.4 **1** as a wound healing agent in a 3D application

The epiderm full-thickness tissue, is a novel wound model to demonstrate healing in response to stimuli. This model had not been used in infection studies like the present study before, therefore method development was required. Before the study, two models were used to determine the best approach for microscopy with available technology, concentration of NucBlue needed and incubation period and optimal period of incubation for bacteria.

In order to apply the results to a real-world situation, the 3D wound model involved layers of the dermis and epidermis containing human epidermal keratinocytes and human dermal fibroblasts, vital in the wound healing process. The model itself does not contain hair follicles or sweat glands which limits the available nutrients to the bacterial peptides and lipids (Scharschmidt and Fischabch., 2013). In a model using *P. oleovorans*, nearly 3300 genes were transcribed in comparison to another bacteria *M. luteus*, including two genes regulating β-defensins, DEFB3A and DEFB4A, needed for the host-defence mechanisms (Rademacher *et al*., 2019) and an upregulation of TLR2, involved in immune modulation for promoting regulatory T cells and cytokine secretion (Nawijn *et al*., 2013). Additionally adaptive immunity measures are triggered upon infection due to the secretion of IL-23. Multiple cytokines were found to be elevated in the presence of *P. oleovorans* including IL-1

α and β, IL-6 and IL-10 (Lemoine *et al*., 2020). In the Epiderm full-thickness model, there is a lack of immune cells meaning that the usual immune response associated with infection does not occur. This could contribute to a higher bacterial recovery being found with the model and slower wound healing times. Although wound healing did occur within the model upon incubation with **1**, the wound closure did not occur throughout the depth. The results of wound closure were across the bottom of the model, cells has begun to migrate throughout the model and did close however not fully.

Upon treatment with silver there was no significant re-epithelisation in the wound modelling following a 3 day incubation however platelet-derived growth factor-BB co-loaded scaffold with silver occurred quicker than the former controls (Wan *et al*., 2019).

Dressings treated with nanoAg-impregnated calcium alginate, pre-hydrated polyethylene-nanoAg composite and saturated cotton gauze, polyacrylate–AgCl gel all had significant reduction in the biomass of *P. aeruginosa* PAO1 following 24 h treatment. When implemented onto a porcine model showed similar results with the polyacrylate-AgCl gel caused a 3-log reduction in the biomass after 24 h incubation and was maintained for 72 h. This is due to the wet environment of the wounds and dressings allowing for silver ions to exhibit antimicrobial activity against *P. aeruginosa* (Phillips *et al*., 2015). **1** within the wound model allowed for cell migration to occur throughout the wound, as previously discovered during the scratch assays in the present study. The fibroblasts and keratinocytes in this model exhibited similar behaviour to the individual cell types in the scratch assay, continuing to migrate in the presence of **1**.

It is well established that supernatants of *P. aeruginosa* causes impaired proliferation of keratinocytes in cutaneous models (Jeffery Marano *et al*., 2015), however in the presence of

the *P. aeruginosa* strain PAO1 epidermal cells were found to proliferate due to the induction of the TNF-α inflammatory response (Kanno *et al*., 2013). In scratch assays on keratinocytes, corneal and alveolar epithelial cells, *P. aeruginosa* causes impairment of epithelial repair. It is thought this could be due to LPS, lectin B and LasB elastase which all exhibits a wound healing inhibitory effect (Ruffin and Brochiero., 2019). The *P. aeruginosa* fucose-binding lectin (LecB) binds to cell membrane receptors via the fucosylated residues and causes a dampened signalling of insulin-like growth factor-1 causing cell cycle arrest in keratinocytes, thus impairing wound healing (Landi *et al*., 2019). The wound healing response in the presence of *P. aeruginosa* PAO1 was inhibited, with only 54.1 % closure being exhibited. The correlates with the other studies where the migration of keratinocytes and fibroblasts was impeded, which could be a consequence of the LecB binding to the cell receptors and causing cell cycle arrest, thus migration is not possible. In addition to this, there was no NucBlue fluorescing after 24 h incubation with *P. aeruginosa* PAO1 alone (data not shown) consolidating that the wound model cells had arrested.

A similar effect has been demonstrated on *in vivo* wound in murine, porcine and rabbit models (Chaney *et al*., 2017; Ruffin and Brochiero., 2019). In porcine eye wounds, the presence of *P. aeruginosa* caused accelerated closure of the wound due to the flagellin (Gao *et al*., 2010) and in cutaneous burn wounds the skin covering the infected wound was found to be hyper-proliferative and thicker in comparison with normal wounds (Chaney *et al*., 2017). Reconstructed human epidermis has been used to investigate the role of *Pseudomonas* flagellin, when added on top of the epidermis, the flagellin drives through the *stratum corneum* mimicking the physical barrier (Garcia *et al*., 2018). Thus demonstrating that flagellin delivered to apical epithelial cells across the *stratum corneum* by rhamnolipids which in turn induces the expression in human skin of S100A7 (a calcium-binding protein)

(Meyer-Hoffert *et al*., 2011) this phenomenon is vital to bacterial invasion and persistence in the cutaneous wound (Garcia *et al*., 2018).

The wound model when incubated with *P. aeruginosa* PAO1 is unable to complete cellular migration due to increased expression of the calcium binding protein, however upon treatment with **1** causes bacterial death to allow for the normal wound healing response to occur. This suggests that impregnating wound dressing with **1** could prove beneficial to wound healing with infected wounds due to increased cellular metabolism as suggested by the cellular toxicity assay and increased cellular migration indicated by both the scratch assay and the wound model.

3.5.5 *In vivo Galleria mellonella* modelling of **1** and *Pseudomonas* strains

G. mellonella infected with *P. aeruginosa* strain PAO1 caused complete death of the larvae with $3x10^{1}$ CFU mL^{-1} following 24 h incubation however other strains of *P. aeruginosa* such as ATCC 27853 with an inoculum size of 3×10^{4} CFU mL^{-1} conferring a 46.7 % mortality following 24 h suggesting *P. aeruginosa* is more pathogenic than the other species, similar to this study where mortality is observed following 24 h.

A *P. aeruginosa* strain was injected into *G. mellonella* to determine the role of the type III secretion system upon virulence. The mutant strain *P. aeruginosa* PA14 with an insertion of Tn*phoA* in *pscD* gene decreased the virulence of the bacteria and the PA14 mutant 2B3R attenuated virulence with an LD_{50} higher than 40,000 in comparison to the PA14 mutant (LD_{50} 10) demonstrating that the 2B3R strain was more motile than the PA14 mutant (Miyata *et al*., 2003). When comparing to the study incubating **1** with *P. aeruginosa* PAO1 the *G. mellonella* did not survive following a 24 h incubation. This suggests that the strain *P.*

aeruginosa PAO1 is highly virulent and is therefore more motile, thus causing mortality within the larvae.

Metal-tdda-phen complexes involving manganese, copper and silver were additionally tested for toxicity against *G. mellonella*, with manganese and silver conferring no toxicity at 20.39 µM and 12.5 µM respectively with an increased mortality with concentration. Copper-tdda-phen appeared to be more toxic than the other metals, at 20.15 µM mortality of 53.3 % ± 5.8 % following 72 h incubation with significant melanisation being observed. Following incubation with the compounds it was identified that the expression of the iron-binding protein transferrin was upregulated meaning the compound assist in the immune response initiation in the larvae. Upon a combination of *P. aeruginosa* PAO1 and complexes prolonged survival over 48 h with 26.7 ± 3.3 % survival with manganese and 40 ± 5.8 % with silver compared to the PBS control (66.7 ± 6.7%) (O'Shaughnessy *et al*., 2022).

G. mellonella models have been used with other metallic complexes including cobalt with 100 % of survival at the concentrations of 1 µM, 110 µM and 10 mM following 96 h including $[Co(ATS)(DMAP)_2]NO_3$ (Frei *et al*., 2020)

In one *G. mellonella* model, over 42 concentrations in the range of 1 mg kg^{-1} to 80 mg kg^{-1} had low cytotoxicity after 120 h even at post-MBC concentrations with a maximum of 75% survival. When tested against *P. aeruginosa* strain PA2017 the MIC and MBC levels was 7.8 µM $[Ru_2(Me_4phen)_2(tpphz)]^{4+}$ (Smitten *et al*., 2020).

Copper(II) phenanthroline-oxazine complexes methyl 2-(4-hydroxyphenyl)-2H-[1,4]oxazino[2,3-f][1,10]phenanthroline-3-carboxylate with silver, manganese and copper at the concentrations of 30, 15 and 7.5 µM and all 100 % of the *G. mellonella* survived after 72

h and after 2 weeks all the larvae fully developed without disruption in the life cycle thus non-toxic (Ahmed *et al*., 2022).

A manganese complex $[Mn(CO)_3(tqa\text{-}\kappa^3N)]Br$ was tested against multiple isolates of the Gram-negative pathogen *A. baumannii* and *P. aeruginosa* with *A. baumannii* being more responsive to the complex with MIC values of 100 µM compared to *P. aeruginosa* where the MIC values ranged between 0.2 mM – 0.8 mM. Following this toxicity of the complex was investigated *in vivo* in the range of 20 mg kg^{-1} – 80 mg kg^{-1} with no detrimental effects being observed on *in vivo* growth or survival, upon incubation with additional bacteria, survival decreased to 50 % following 24 h (Güntzel *et al*., 2019). Similar to **1**, however due to the toxic nature of *P. aeruginosa* strain PAO1 no survival was recorded after 24 h with the combination of bacteria.

G. mellonella larvae have been found to increase the immune response including increased hemocyte counts, phagocytic activity, and enzymatic activity including acid and alkaline phosphatase, and phenoloxidase when exposed to low concentrations of chromium and lead. However high concentrations elicited the opposite effect, antioxidant enzyme concentrations increased such as superoxide dismutase, catalase and peroxidase (Wu and Yi., 2015).

Incubation of *G. mellonella* with metal chelates comprised of copper, manganese and silver 1,10-Phenanthroline at 2 µg, 4 µg and 10 µg per larvae with no mortality being detected following 72 h incubation however an increase to 30 µg per larvae resulted in mortality in the range of 80-100 % (Gandra *et al*., 2020). Additionally the less toxic complex $[Ag(phendione)_2]^+$ at concentrations of 5 and 10 µg per larvae was non-toxic and up to 45 mg kg^{-1} was injected into mice and no mortality was discovered (Garanto *et al*., 2021).

Metal complexes involving copper and zinc displayed minimal toxicity in the larvae whereas silver complexes [Ag(2-([3-(1H-imidazol-1-yl)propyl]aminopropyliminomethyl)phenol)$_2$]ClO_4 and [Ag(N-[(E)-1H-Imidazol-5-ylmethylidene]-N-[3-(1H-imidazol-1-yl)propyl]amine)]ClO_4 had higher toxicity (mortality of 40 % at a dose of 0.060 µmol and 0.097 µmol respectively) than $AgNO_3$ where 30 % mortality was observed at a dose of 0.235 µmol. Additionally the MIC_{50} of all the silver complexes tested had antimicrobial activity with *S. aureus*, MRSA, *E. coli* and *P. aeruginosa* within the range of 14.2 µM – 60.9 µM with similar values across species (McGinley *et al*., 2013). Similar to **1** alone, there was limited toxicity within the larvae however the toxicity increases with an increased concentration with only 10 % of larvae surviving following 48 h at 16 µg mL^{-1}.

The antibacterial activity of the Ru complex [{Ru(TMP)$_2$}$_2$(tpphz)]$(PF_6)_4$, [1]$(PF_6)_4$ was tested against *A. baumannii* strains AB12, AB16, AB184 and AB210 and *P. aeruginosa* strains PA1, PA2 and PA2017. The MBC results for *A. baumannii* was found to be lower than *P. aeruginosa* with values ranging between 3.2 µM – 15.9 µM compared with 18 µM - 38.3 µM respectively. *G. mellonella* infection screening was conducted where over the 120 h period, the Ru complex was non-toxic to *G. mellonella* in concentrations ranging up to 80 mg kg^{-1}. When the Ru complex was injected 30 min following infection with *A. baumannii* AB184 at 10^6 CFU mL^{-1} larvae was found to survive due to the complex clearing the infection with a minimum concentration of 40 mg kg^{-1}. Survival remained at 60 % in comparison with the bacterial only control where larvae survival was 10 % (Smitten *et al*., 2022). Upon incubation with both *A. baumannii* and the ruthenium complex which had higher survival than comparing to **1** in the present study. When incubated alone **1** at a lower concentration (8 mg mg^{-1}) has lower survivability, in comparison to the Ru complex with the tppz ligand,

where after 72 h all larvae were deceased. The increased mortality could be due to the toxicity of the ligands present on **1** which have an increased toxic effect.

Ruthenium red dye has additionally been tested for antimicrobial potency against *P. aeruginosa* due to its ability to inhibit the function of the mitochondrial calcium uniporter. Against two strains of *P. aeruginosa* PAO1 and PA14, ruthenium red inhibited growth at 2 μg mL^{-1} and when tested against 22 clinical isolates of *P. aeruginosa* MIC values ranged between 1 μg mL^{-1} and 4 μg mL^{-1}. *G. mellonella* studies conducted with *P. aeruginosa* PAO1 and ruthenium red injected following a 15 minute interval had positive results with 80 % of the larvae surviving after 72 h at the higher concentration of 67 mg kg^{-1} (Weber *et al*., 2022). **1** at a lower concentration of 2 mg kg^{-1} had a survivability over 72 h of 70 % thus suggesting the impact the ligands of the Ru complexes have on increased survivability at higher concentrations.

3.6 Conclusion

1 has proved to be a promising wound healing candidate through *in vitro* studies. Cytotoxicity studies have proven **1** has little cytotoxicity against a plethora of wound healing cells, with proliferation and cellular metabolism taking place additionally. Scratch wounding assays have solidified cell proliferation theory with an increase in the speed of migration of wound closure with epithelial cells at 8 μg mL^{-1}, keratinocytes and macrophages whereas the WS1 fibroblasts had comparable migration compared to an untreated control. The 3D wound model demonstrated that **1** allows for cell migration in a novel application causing increased wound closure rates when infected models was incubated with **1**. However incubation with *P.* aeruginosa PAO1 alone inhibited migration across the model, possibly due to the production of *LecB* causing arrest of the cell cycle, thus stopping migration. When

incorporating bacteria with the cells, migration of macrophages increased by 3 fold as the cells move to perform phagocytosis. Following host-pathogen analysis, the function of the macrophages was not impeded through the addition of **1** and increased phagocytosis occurred proportionally with an increased concentration of **1**. Whereas without addition of **1** macrophages failed to respond as effectively. **1** appeared to cause increased elongation of the pseudopodia leading to a more efficient immune response. The complex may not be able to enter human cells thus the cellular DNA doesn't become damaged and no cell cycle arrest can take place, allowing for antimicrobial specific activity to take place without causing damage. This could prove a promising avenue for wound treatment, by impregnating wound dressings with **1** and applying to infected wounds could allow for treatment of the infections and subsequently allow for the normal wound healing response to occur, thus reducing the number of chronic wounds and reduce impact on health services.

Chapter 4: Evaluating the mechanisms of antimicrobial activity of Hexaammineruthenium (III) chloride ($_1$)

4.1 Introduction

4.1.1 Structure of *Pseudomonas aeruginosa* PAO1 cell membrane

The cell ultrastructure of *P. aeruginosa* is well known for impeding antibiotic diffusion into the cell due to low permeability (Breidenstein *et al*., 2011). The cell envelope is multi-layered and composed of inner and outer membranes containing a periplasmic compartment and cell wall. These components enable Gram-negative bacteria to be protected against environmental stress factors including digestive enzymes, detergents, heavy metals and antibiotics (Kucerka *et al*., 2008). This envelope also regulates the selective passage of waste and nutrients into the cell and enable key biological processes including the oxidation and reduction of substrates entering the cell. The inner membrane of the bacterium is composed of a phospholipid bilayer with molecules vital for cell biogenesis and cellular function including transporters, protein sensors and export machinery (Casabona *et al*., 2013).

The outer membrane has lipopolysaccharide present which is vital for cell survival including causing the inactivation of the complement component C3b, protection against lysis mechanisms and antibiotic binding (Islam *et al*., 2010). The inner leaflet of the outer membrane is composed of cardiolipin, phosphatidylcholine, phosphatidyl-ethanolamine and phosphatidylglycerol lipids (Le Brun *et al*., 2013) in which porin proteins reside to allow for entry of amino acids, nucleotides and nutrients. However, lipopolysaccharide is the main component which protects the bacterial cell from the action of membrane targeting bactericidal agents (Kucerka *et al.,* 2008). Lipopolysaccharide molecules have three units, a lipid A moiety to anchor lipopolysaccharide to the outer membrane hydrophobic domain containing two glucosamine units responsible for the toxicity of lipopolysaccharide, a core oligosaccharide (King *et al*., 2009) comprised of 8-12 monosaccharides connected to lipid A

through 2-keto-3-deoxyoctonoic acid and an O-side chain made of repetitive monosaccharides responsible for the immunospecificity of *P. aeruginosa* (Rice *et al*., 2020; Kucerka *et al*., 2008). The lipid A moiety is additionally known as a pyrogenic endotoxin, promoting interleukin release, fever and hypothalamus stimulation when the moiety is lysed by antibiotics or engulfed by phagocytes.

The O-chain has two glycoforms, the A and B bands with the B band being the dominant antigen on the cell surface (Islam *et al*., 2010). The specificity to antigens are determine primarily by the B-band which is highly diverse in *P. aeruginosa* and has an influence over the binding and killing of antibiotics as well as other surface activities including metal interaction, surface adhesion and colonization and biofilm formation (Kucerka *et al*., 2008).

Sandwiched between the inner and outer membranes, there is a periplasm space consisting of a gel-like matrix (periplasm) with a thin peptidoglycan layer and proteins. There are 395 proteins present in the periplasm of *P. aeruginosa* PAO1 as determined by MALDI-TOF analysis including enzymes such as β-lactamases for degrading the antibiotic and enzymes involved in amino acid and carbohydrate metabolism. Some of the most abundant proteins involve translation factors, chaperonins and ribosomal proteins (Imperi *et al*., 2009)

4.1.2 Bacterial cell membrane as an antimicrobial target

However some classes of antibiotics do have effect on Gram-negative species of bacteria. One of the most common antibiotics are β-lactamases which target the β-lactam ring. These antibiotics do this by disrupting peptidoglycan biogenesis through inhibiting the enzyme penicillin-binding proteins. The transpeptidase is the primary target of β-lactam antibiotics, thus preventing cross-linking glycan strands and subsequently causing cell wall damage (Cho *et al*., 2014).

P. aeruginosa overall has 26 types of porin in which *OprF* is the most abundant (Chevalier *et al*., 2017), making it suitable for antibiotics to target to enter the cell. Antibiotics such as aminoglycosides are able to diffuse through the outer membrane due to interactions occurring electrostatically between LPS and the antibiotic to inhibit protein synthesis within the ribosome (Tomasello *et al*., 2020; Langendonk *et al*., 2021).

A membrane-lytic mechanism of *P.* aeruginosa occurred when incubated with synthesised peptidomimetic antibiotics based on the peptide protegrin I with a low MIC. The outer membrane protein *LptD* is determined to be the target of these antibiotics, the LPS transport function of the protein becomes impaired upon binding to the antibiotics causing a disruption to the outer membrane, disrupting the permeability as demonstrated using a 3,5-dipropylthiacarbocyanine dye ($diSC_3$) (Srinivas *et al*., 2010).

An antibiotic peptide, protonectin, derived from the venom of a wasp *Agelaia pallipes pallipes* was able to maintain an alpha helix conformation and causes membrane perturbation. The MIC value against the multidrug resistant Gram-negative bacteria *E. coli* was discovered to be 32 µM due to the disruption of outer membrane integrity with a similar function occurring to *P. aeruginosa* thus causing destabilisation and the inner membrane was also damaged causing cytoplasmic leakage (Wang *et al*., 2013).

4.1.3 Impact of metallic complexes on bacterial cell membranes

Metal based complexes have been recognised to cause bacterial membrane damage, for example silver nanoparticles have been discovered to interact with the membranes and penetrate to enter the cell thus creating structural damage to the cell, leakage of components following by cell death. Oxidative stress is additionally generated through the production of reactive oxygen species inhibiting cell proliferation (Yan *et al*., 2018). Silver

nanoparticles have been found to induce permeable pits in the bacterial membrane following incorporation consequently resulting in osmotic collapse and intracellular leakage at a concentration of 2.7 μg mL^{-1}. It is hypothesized that binding of silver nanoparticles to the membrane causes physical membrane damage through the cell surface proteins or carbohydrate moieties (Ramalingam *et al*., 2016).

Copper oxide nanoparticles target the cell membrane of bacteria, aggregation occurs of the particle in the cell media and releases copper ions which then remain in the media exhibiting a prolonged effect. The nanoparticles are easily oxidised due to a high oxygen concentration within the cell membrane due to the higher oxygen content than the cell media thus generating hydrogen peroxide by reacting with hydrogen ions causing the membrane damage through oxidative stress (Karlsson *et al*., 2013).

Similar to metallic complexes aggregating in the cellular membrane, the heavy metal terbium is distributed in the spaces both intracellular and extracellular spaces in horseradish following treatment. A decrease in the contents of unsaturated fatty acids within membrane lipids, diameter of proteins and the current of potassium channels additionally occurred however an increase in saturated fatty acids and malondialdehyde was observed. Terbium primarily can be deposited in plant cells in the plasma membranes and cell wall although some ions do enter the cell through a process called plasmodesmata or carriers where they are transported to the mitochondrial and nuclear membranes. The decrease in unsaturated fatty acid content is due to a decreased cis-double bond amount which weakened the membrane lipid molecules thus causing the gaps between molecules decrease and enhance reactions. This causes a decrease in membrane fluidity and reduced function additionally an

increase in the number of free radical reactions occurs similar to other transition metals including cadmium, chromium, lead and iron (Yang *et al*., 2015).

4.1.4 Ruthenium complexes targeting bacterial membranes

Many ruthenium complexes are known to be disruptive to the cell membrane, including $[Ru^{II}L1ClP(Ph_3)]Cl$, (L1 = N,N'-bis(benzimidazol-2-yl-ethyl)ethylenediamine which exhibited bactericidal activity due to the leakage of lactate dehydrogenase when the ruthenium ions enter the cell in bacteria including *S. typhi* and *E. coli* (Hernández-Hernández *et al*., 2020). Two water soluble ruthenium complexes $[Ru(bpy)_2(phendione)](PF_6)_2{\cdot}2H_2O$ and $[Ru(phendione)_3]Cl_2{\cdot}2H_2O$ both exhibited cell membrane damage of *E. coli* and *P. aeruginosa* at concentrations of 10 µM and 20 µM respectively mediated through the production of hydroxyl radicals attacking both the membrane and DNA (Parakh *et al*., 2013).

Ruthenium (II) based complexes have been found to accumulate in the internal membranes after exposure to light in CHO-K1 cells. Modification in the ddpz ligand caused variations in DNA and membrane binding of the complex and further light exposure caused increased damage to the plasma membrane and thus the localisation of ruthenium ions in the intracellular structure occurs (Svensson *et al*., 2010).

Ru nanoparticles demonstrated cellular membrane damage through production of free radicals and singlet oxygen and have increased efficacy when combined with silver nanoparticles with *Arthrobacter sp*. Upon photoirradiation, one of the compounds tested $[Ru(bpy)_3]^{2+}$ oxidises the membrane thus causing increased permeability (An *et al*., 2019). Another ruthenium nanoparticle combination involving ascorbic acid encapsulated in hyaluronic acid and modified with MoS_2 exhibited bactericidal activity. When the combined AA@Ru@HA-MoS_2 system accumulates at the site of injury, the bacteria secrete

hyaluronidase thus causing degradation of the outer capsule of the system. This causes a release of ascorbic acid and subsequent generation of hydroxyl radicals due to MoS_2 catalysis. The nanoparticles can enter the bacterial cell membrane by damaging through oxidation causing intracellular leakage and bacterial cell death. This system has been found to prevent wound site infection and promote the wound healing process in *in vivo* mouse models (Liu *et al*., 2019; Jain *et al*., 2022). Adding hydrophobic groups to Ru complexes causes enhanced cellular uptake, thus allowing for the complexes such as $[\{Ru(DIP)_2\}_2(\mu\text{-tpphz})]^{4+}$ to localise to the hydrophobic regions of bacteria including the membranes, thus causing damage which contrasts other Ru complexes which localise at the nucleus (Gill *et al*., 2013).

Other complexes enter the bacterial cell through an energy independent manner, dinuclear $Rubb_n$ complexes are able to permeabilise the bacterial membranes, however other complexes including $[Ru(Me_4phen)_3]^{2+}$ are proposed to enter the cell and bind preferentially to RNA and accumulate at ribosomes and subsequently condense (Li *et al*., 2014).

A Ru complex RuBP being utilised as a treatment for *Micrococcus tetragenus,* spread throughout the bacterial cells and caused cell wall and membrane damage, resulting in cell death. Flow cytometry confirmed RuBP accumulates within the bacterial cell and DNA affinity studies demonstrated strong binding and damage to DNA and RNA, subsequently reduced fragmentation of DNA, vital for infection of *M. tetragenus.* Intracellular leakage was additionally observed following wrinkling and damage of the cell walls. Similar effects occurred with *S. aureus* where distortions in the membrane structure was also observed, becoming irregular and wrinkled with some perturbations causing cytoplasm leakage when treated with 20 µM of RuBP. Due to the increased permeability of the cell membranes,

electrical conductivity was increased in as little as a 10 minutes incubation with RuBP (Sun *et al*., 2015).

A multifunctional theranostic selenium nanoplatform (Se@PEP) nanoparticles have been found to target cell membranes promoting the interaction of the nanoparticles with the bacteria. Combined with Ru, Se@PEP-Ru_2 increased the bacterial damage to both *S. aureus* and *E. coli* suggesting membrane damage is the predominant mechanism of action (Huang *et al*., 2017). The function of β-galactosidase in *E. coli* involved cleaving lactose to form glucose and galactose vital for glycolysis, its catalyses the transgalactosylation of lactose to allolactose and then further cleaves into monosaccharides (Juers *et al*., 2012). The release of β-galactosidase from the cytoplasm of *E. coli* is increased upon incubation with Se@PEP, thus cytoplasmic leakage occurs due to the enzyme binds to the cell membrane and decreases the integrity. The membrane, through SEM imaging, demonstrated atrophy, wrinkling and damage to the cell walls in comparison with the smooth normal morphology. A high level of ROS is generated through the change in permeability causing oxidative damage to the cell and it was additionally discovered that microbial DNA synthesis is disruption through incubation of the nanoparticle, thus causing leakage of cellular inclusions (Huang *et al*., 2017).

Another multifunctional drug delivery nanoparticle Sph-Ru-MMT@PZ, based on the nanostructured-form of $[Ru(bpy)_2dppz]$ $(PF_6)_2$ (Sph-Ru) is similar to the selenium nanoplatform, causing increased membrane permeability of the cell membrane occurs upon incubation. This is proposed to be due to the ability of the montmorillonite (MMT) portion of the complex adhere to the outer membrane of *E. coli* and interact more readily to cause membrane damage through producing ROS (Yin *et al*., 2021).

Following analysis in the previous chapters, mechanisms of activity of **1** was explored with interaction of the Ru complex and the bacterial membrane of *P. aeruginosa* PAO1 hypothesized to be one of the main mechanisms of action. This chapter investigated potential mechanisms of action against *P. aeruginosa* strain PAO1.

4.2 Aims and Objectives

4.2.1 Aims

This chapter aimed to elucidate the mechanisms of antimicrobial activity of **1** against *P. aeruginosa* strain PAO1 by using physical and biochemical assays, coupled with global molecular analysis of gene expression via RNA sequencing.

4.2.2 Objectives

- To use Scanning electron microscopy to reveal complex **1** mediated alterations in the cellular ultrastructure of *P. aeruginosa* PAO1 and *S. maltophilia* S1.
- To apply membrane depolarization assays to identify perturbations in the cytoplasmic membrane of *P. aeruginosa* PAO1.
- Evaluate intracellular oxidative stress generation mediated by **1** using hydrogen peroxide and ROS generation assays.
- Determine intracellular nucleic acid and protein mobility from *P. aeruginosa* PAO1 by quantifying exogenous release from the bacterial cells.
- Detect global changes in gene expression and regulation in response to **1** using total RNA sequencing of treated *P. aeruginosa* PAO1 in comparison to untreated cells.

4.3 Methods

4.3.1 Scanning Electron Microscopy (SEM)

Following a protocol described in Amin *et* al., 2020, an overnight culture of *P. aeruginosa* strain PAO1 was grown at 37 ℃ in MHB, the following morning the culture was OD to 0.1 and split into two universals, one kept as it is, the other a sub lethal concentration of **1** was added and both incubated for an hour at 37˚C with shaking at 200 rpm. Following this, both were centrifuged at 1721 × *g* for 10 minutes. The supernatant was removed and the pellet washed in 10 mL saline and vortexed for 10 seconds. This washing process was repeated again. The saline was removed from the pellet which was then resuspended in sterile water to achieve an OD of 0.1 at 600 nm. 10 µl of the solution was added to a 10 mm x 10 mm silicon wafer (Amsbio, UK) and dried at room temperature in a class II cabinet for 30 minutes. The wafer was placed in a solution of 4 % glutaraldehyde (1 mL) overnight, after this the wafer was dehydrated in ethanol in concentrations of 30 %, 50 %, 70 %, 90 % and 100 % for 10 minutes each. The sample was then stored in a desiccator with silica beads until analysed. *N* = 3 per condition.

4.3.2 3,3′-Dipropylthiadicarbocyanine iodide ($diSC_3$) inner membrane depolarization assay

To measure the disruption in electrochemical potential across the bacterial cytoplasm the probe 3,3′-dipropylthiadicarbocyanine iodide was used to measure fluorescence at an excitation of 622 nm and emission of 670 nm. Mid-logarithmic phase *P. aeruginosa* strain PAO1 was grown in MHB and washed in a buffer containing 5 mM sodium HEPES (Sigma-Alrich, UK) and 20 mM glucose at a pH pf 7.4. The suspension was adjusted to an OD_{600} of 0.05 in the same buffer and incubated with 0.4 µM $diSC_3$ until equilibrated. A solution on 0.1 M potassium chloride was added to equilibrate the potassium ions in the solution and 2 mL

of the solution was added to a quartz cuvette and fluorescence measured using cary eclipse fluorescence spectrophotometer. Varying concentrations of **1** and the control of 1% Triton-X-100 was added to separate cell suspensions and the fluorescence monitored for changes (Lee *et al*., 2004; Lv *et al*., 2014). *N* = 3 per condition.

4.3.3 Protein and nucleic acid leakage

P. aeruginosa strain PAO1 was grown overnight and adjusted to an OD of 0.1 and centrifuged at 6000 × *g* for 5 minutes. The pellet was re-suspended in 0.85 % sodium chloride (NaCl) and treated with 8 µL mL^{-1} **1** over a 24 h period with 10 µL samples taken regularly at 2 h intervals being taken. The samples were centrifuged at 12,000 × *g* for 10 minutes at 4 ˚C and the supernatant collected. The total protein and nucleic acid content was determined using a nanodrop at a wavelength of 260 nm and 280 nm (Xiang *et al*., 2018). *N* = 3 per condition.

4.3.4 Oxidative stress study

Bacterial cultures of *Pseudomonas aeruginosa* strains PAO1, NCTC 12903 and ATCC 9027 were grown at 37 ˚C and 150 rpm overnight and the OD adjusted to 0.4 at 600 nm 12 h later. MHA plates containing 2.5 mL of the MIC of **1** in the 25 mL MHA which were prepared previously before having 100 µL of each bacteria spread on the agar evenly, the same was done with non-**1** incorporated plates as a control. Sterile filter discs were added to the agar plates in triplicate and 10 µL of hydrogen peroxide was added in order to determine susceptibility to oxidative stress. The plates were incubated at 37 ˚C overnight and the zones measured the following day (Hegazy *et al*., 2020). *N* = 3 per condition.

4.3.5 Reactive oxygen species production

An overnight culture of *P. aeruginosa* strain PAO1 was adjusted to an $OD_{600\ nm}$ of 0.1 and plated in a 96 well plate. Varying concentrations of **1** at 4, 8 and 16 µg mL^{-1} and incubated for 1 h. A ROS detection probe 2',7'-Dichlorofluorescin Diacetate (DCFDA) (Abcam, UK) based on green fluorescence emission was added at a volume of 10 µM to each condition and incubated in the dark for 30 min before being analysed using a fluorescent plate reader (Pan *et al*., 2017). Controls were included, these incorporated no DCFDA to determine a baseline of fluorescence, no cells and a positive colistin control (Yang *et al*., 2013). *N* = 3 per condition.

4.3.6 RNA isolation

An overnight bacterial culture of *P. aeruginosa* strain PAO1 was grown at 37 ˚C and shook at 200 rpm. The culture was then adjusted to an OD_{600} of 0.05 at 600 nm and incubated with agitation at 37 ˚C until the culture reached mid exponential phase (OD ~0.6). The culture was split into 5 mL aliquots and treated with varying concentrations of **1** for 20 minutes again at 37 ˚C and 200 rpm before being transferred to a sterile universal. RNA protect was added to each sample at 10 mL and incubated for 5 minutes at room temperature, then centrifuged at 4200 × *g* for 10 minutes, the supernatant removed and the pellets being stored until extraction of RNA. *N* = 3 per condition.

Following the protocol from Total RNA purification kit (NorgenBiotek, Canada), total RNA was isolated. The bacterial pellet was resuspended in TE buffer containing lysozyme and incubated for 5 minutes. Following this, 300 µL of Buffer RL was added and vortexed for 10 seconds and 200 µL of 96-100% ethanol was added. The 600 µL of cell lysate was added to the spin column and centrifuged at 14000 x *g* for 1 minute with the flowthrough discarded.

The column was washed with 400 µL wash solution A and centrifuged for 1 minute and the supernatant discarded. This was repeated for three times and upon the final wash, the spin column was centrifuged alone to dry for 2 minutes. The RNA was eluted by adding 50 µL of elution solution A and centrifuged for 2 minutes at 200 x *g* and a further 1 minute at 14000 x *g*. The RNA concentration was then determined using a NanoDrop Spectrophotometer with ideal purity being more than 1.8 at A260/A280 ratio, if the value is lower, then this indicated a presence of contaminants including phenols and protein and above 2.0 at A260/A230 if lower, then contaminants of carbohydrate or phenol origin was present.

4.3.7 RNA Sequencing

Following RNA isolation samples are sequenced using a PE150 sequencing strategy on a NovaSeq 6000 S4 at a depth of 6-10 million paired reads per sample. The ribosomal RNA was removed from the total RNA and precipitated with ethanol. Following fragmentation of the sample, the first strand of cDNA was synthesised using hexamer primers and during the second strand of cDNA synthesis dUTP's are replaced with dTTP's in the reaction buffer where end repair, A-tailing, adapter ligation, size selection, USER enzyme digestion, amplification and purification was conducted to create the library. The library was then pooled and sequenced using Illumina platforms. The sequence was compared to the reference genome of *P. aeruginosa* strain PAO1 using Bowtie2 (Langmead and Salzberg., 2012), novel genes were identified using Rockhopper and quantification of gene expression used FeatureCounts to determine FPKM (expected number of Fragments Per Kilobase of transcript sequence per Millions base pairs sequenced) of each gene was calculated based on the reads count mapped and gene length (Novogene).

Samples are then analysed comparing to the whole genome sequencing conducted previously. *N* = 3 per condition.

All results were analysed using Graphpad Prism version 7.0 to determine significant differences between samples, with $p < 0.05$ being considered as statistically significant in all cases. The data was presented as mean, with t-tests and one-way and two-way ANOVA's being used to determine differences between the data.

4.4 Results

4.4.1 Determining the molecular activity of complexes 1, 2 and 3 using scanning electron microscopy (SEM) against *P. aeruginosa* strain PAO1 and *S. maltophilia* strain S1

To identify the role of **1**, **2** and **3** in targeting the bacterial cell ultrastructure, cultures were treated with the respective complexes at a range of concentrations, along with, colistin at 1 mg mL^{-1} and triton X-100 (1%) as controls which are known cellular membrane perturbing agents. Samples were analysed by SEM over a time period.

All bacterial strains subjected to treatment with colistin and Triton X control demonstrated increasing numbers of perturbations over a 24 h period with*, P. aeruginosa* strain PAO1 (Figure 4.2) and *S. maltophilia* S1 (Fig. 4.3) With both bacteria treated with **1**, **2** and **3**, *P. aeruginosa* strain PAO1 (Figure 4.4 and 4.5) and *S. maltophilia* strain S1 (Figure 4.6), cellular morphology changed with perturbations being observed increasingly over the course of 24 h, more prominently in colistin. Untreated bacteria were imaged for comparison normal characteristics of a *P. aeruginosa* were observed such as rod shaped, intact membranes, active cellular division and no evidence of cellular leakage. No perturbations were observed with an increase in bacterial numbers over the course of the 24h period (Figure 4.1).

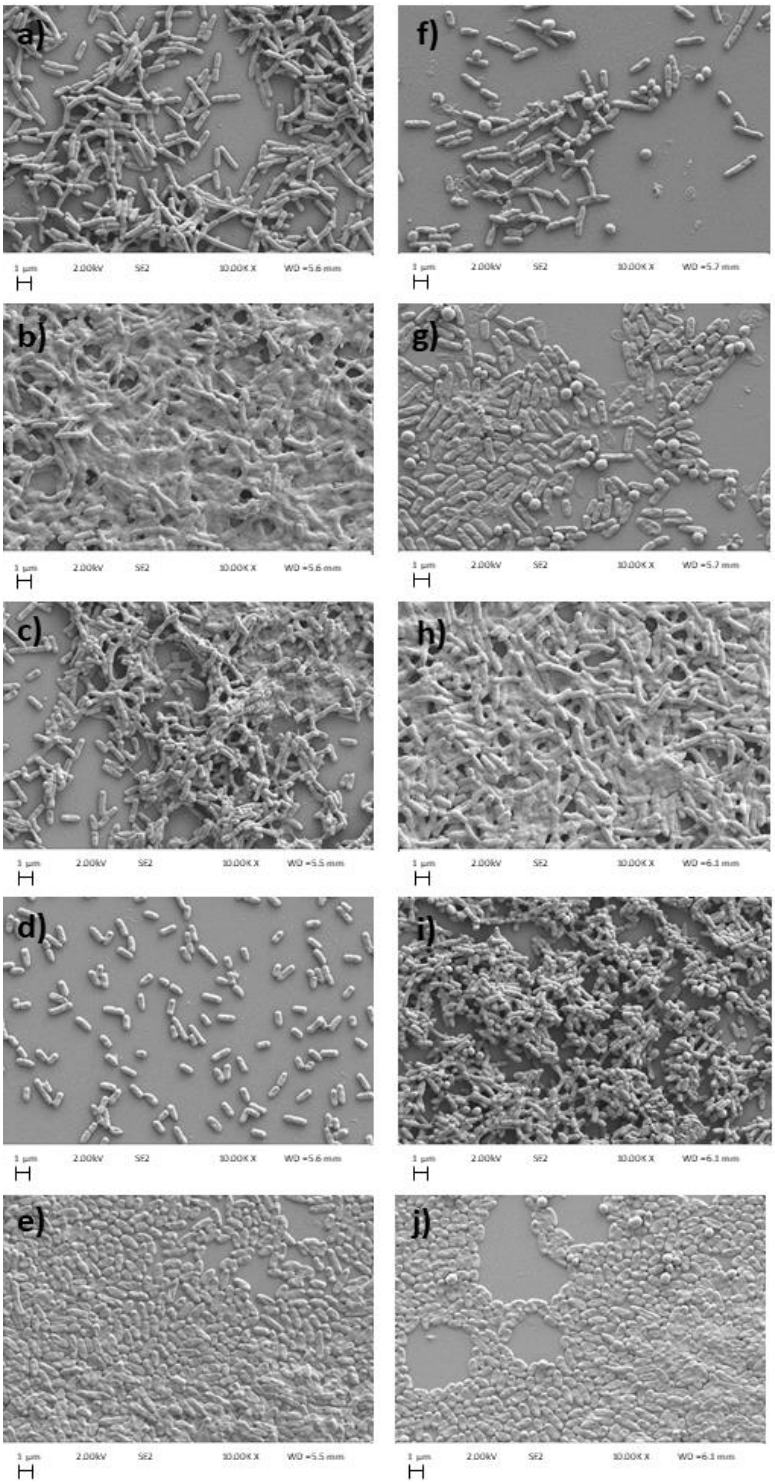

Figure 4. 1: SEM micrographs of *P. aeruginosa* PAO1 (a-e) and *S. maltophilia* S1 (f-j) untreated negative controls at 0 h (a and f), 2 h (b and g), 4 h (c and h), 6 h (d and i) and 24 h (e and i). Images are representative examples of the field of view for 3 biological replicates. Images were captured at the Manchester Metropolitan University SEM central facility at 10,000 times magnification.

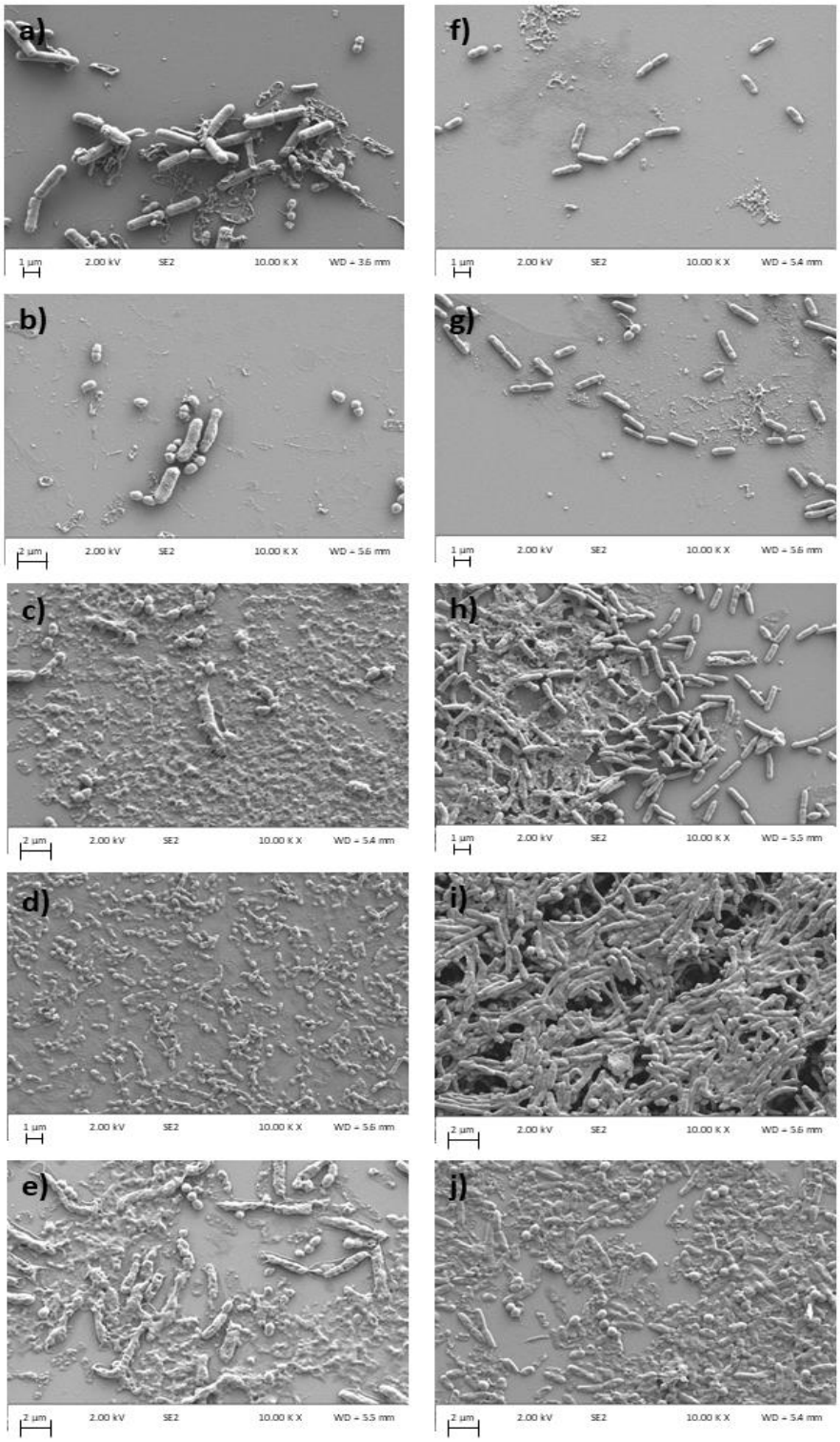

Figure 4. 2: SEM micrographs of *P. aeruginosa* PAO1 treated with colistin (1 mg mL^{-1}) (a-e) and Triton X (1%) (f-j) exposed for 0 h (a and f), 2 h (b and g), 4 h (c and h), 6 h (d and i) and 24 h (e and i). Images are representative examples of the field of view for 3 biological replicates. Images were captured at the Manchester Metropolitan University SEM central facility at 10,000 times magnification.

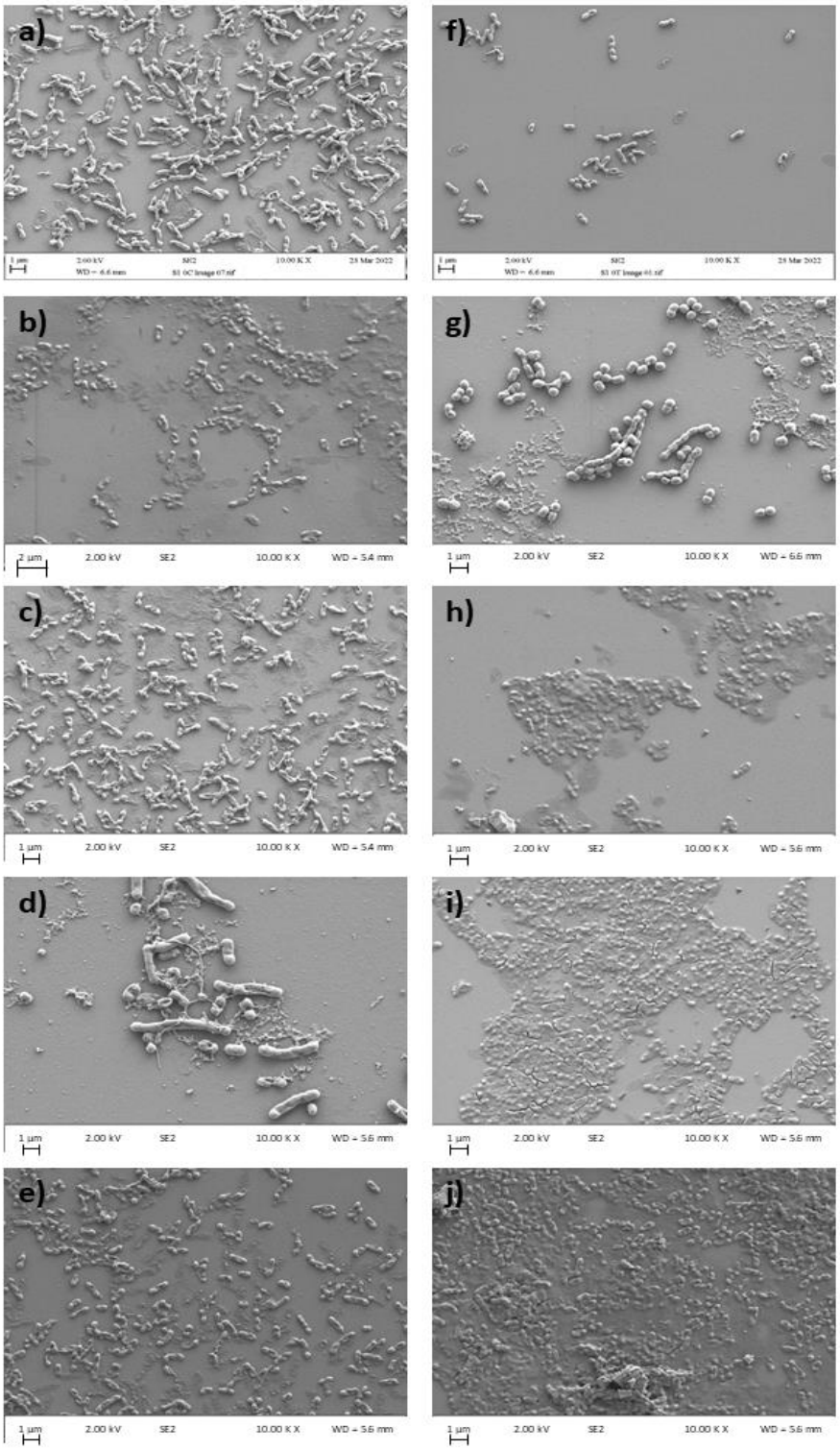

Figure 4. 3: SEM micrographs of *S. maltophilia* S1 treated with colistin (1 mg mL^{-1}) (a-e) and Triton X-100 (1%) (f-j) exposed for 0 h (a and f), 2 h (b and g), 4 h (c and h), 6 h (d and i) and 24 h (e and i). Images are representative examples of the field of view for 3 biological replicates. Images were captured at the Manchester Metropolitan University SEM central facility at 10,000 times magnification.

Incubating *P.* aeruginosa strain PAO1 with **2** and **3** (Fig. 4.4) demonstrate similar perturbation patterns with the other Gram-negative bacteria, with slight membrane changes until 24 h. **2** following 24 h incubation demonstrated membrane damage however no perturbation, however **3** at a high concentration causes perturbations in the bacteria at a lower concentration (Figure 4.4).

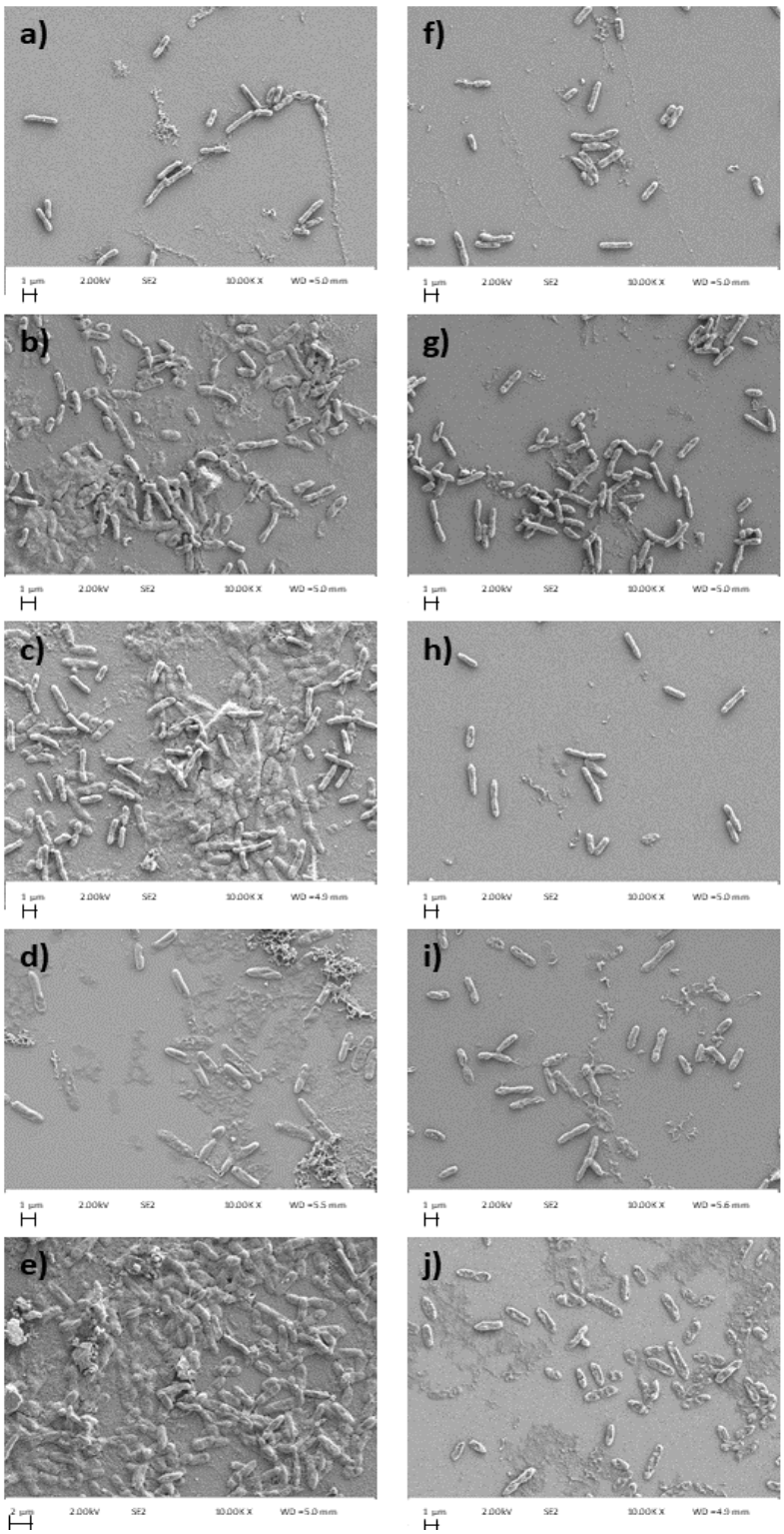

Figure 4. 4: SEM micrographs of *P. aeruginosa* PAO1 with **2** (a-e) and **3** (f-j) exposed for 0 h (a and f), 2 h (b and g), 4 h (c and h), 6 h (d and i) and 24 h (e and j). Images are representative examples of the field of view for 3 biological replicates. Images were captured at the Manchester Metropolitan University SEM central facility at 10,000 times magnification.

Images taken at all concentrations at 0 h show normal *P. aeruginosa* PAO1 morphology, with no signs of cellular perturbations of cellular leakage (Fig. 4.5; Appendix Figure 8.1) however as time increases at 8 μg mL^{-1} of **1** by 6 h some changes in the membrane is observed and by 24 h majority of bacterial cells are damaged and non-viable. At 16 μg mL^{-1} damaging is seen at 4 h with more bacterial cells being damaged at 6 h and by 24 h all cells are completely damaged. At 32 μg mL^{-1} the rate of cellular perturbation occurs quicker as shown at 3 h following incubation with **1**. As the concentration of complex is increased the time taken to damage bacterial membranes increases however at MIC value following 24 h incubation the cells are no longer viable. All images are representative across field of view.

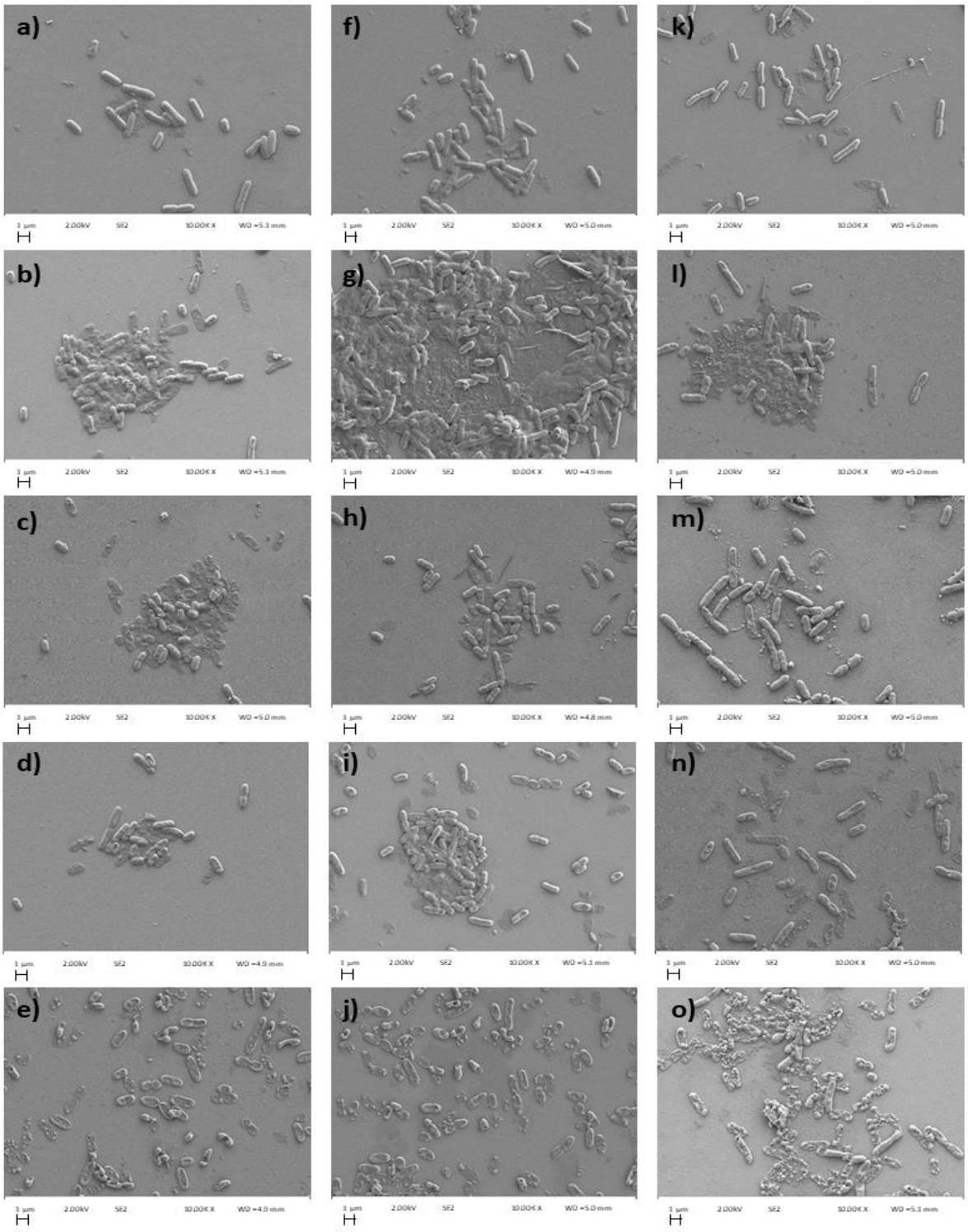

Figure 4. 5: SEM micrographs of *P. aeruginosa* PAO1 with **1** at 8 µg mL^{-1} (a-e), 16 µg mL^{-1} (f-j) and 32 µg mL^{-1} (k-o) exposed for 0 h (a, f, k), 2 h (b, g, l), 4 h (c, h, m), 6 h (d, I, n) and 24 h (e, j, o). Images are representative examples of the field of view for 3 biological replicates. Images were captured at the Manchester Metropolitan University SEM central facility at 10,000 times magnification.

At 0 h with all three complexes *S. maltophilia* S1 are intact as expected (Figure 4.6). However at 2 h membrane damage was beginning to occur with indents forming in the membrane ultrastructure. There no significant changes to membrane ultrastructure between 2 h and 6 h across the complexes with little perturbation. At 24 h more membrane perturbation is seen, **2** causes more perturbation in the bacteria than the other complexes however at a higher concentration than **1** which still demonstrates membrane damage. **3** has less perturbation with the other complexes with 64 μg mL^{-1} meaning its mechanism of activity does not cause membrane damage primarily.

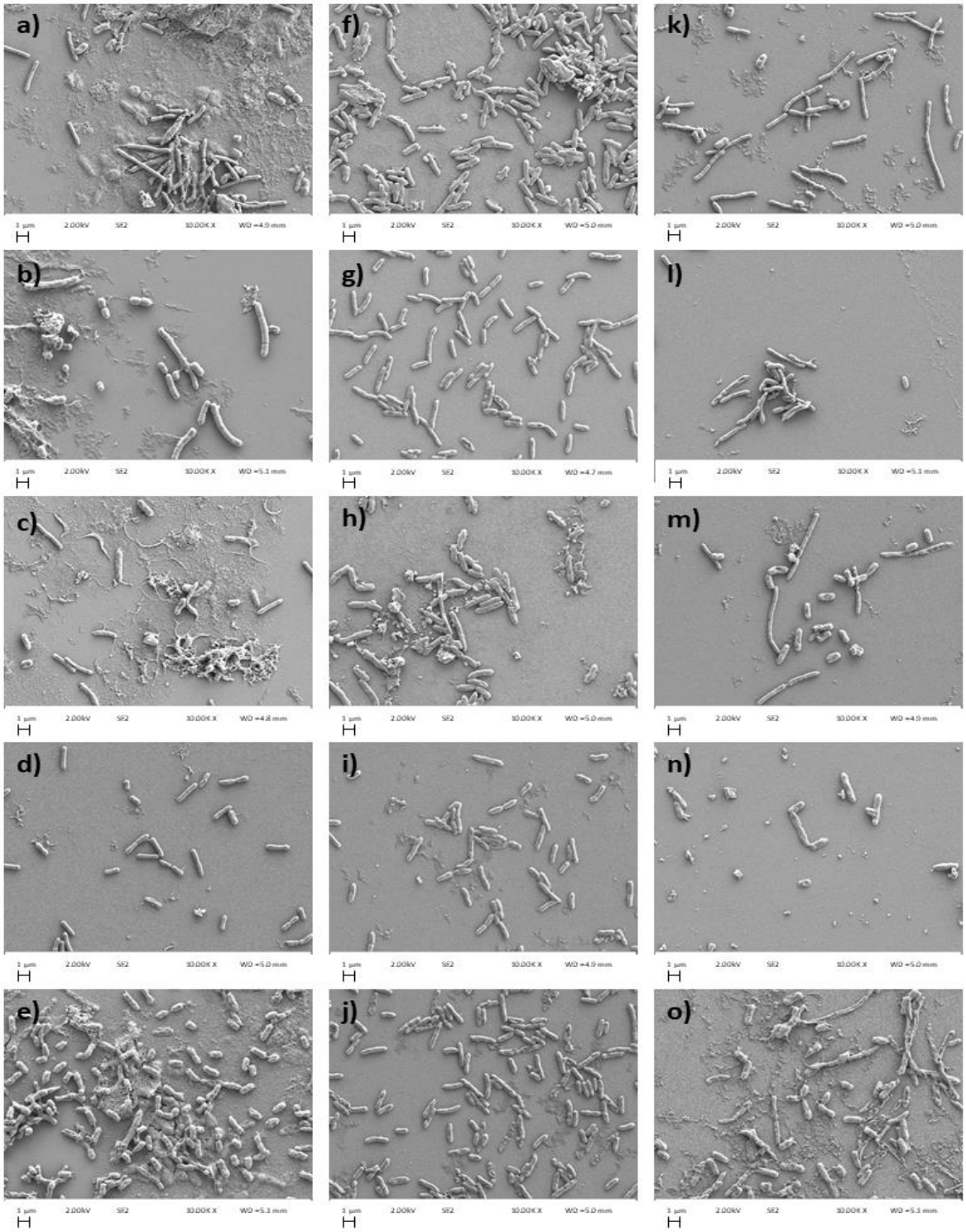

Figure 4. 6: SEM micrographs of *S. maltophilia* S1 with **1** at 8 µg mL^{-1} (a-e), 16 µg mL^{-1} (f-j) and 32 µg mL^{-1} (k-o) exposed for 0 h (a, f, k), 2 h (b, g, l), 4 h (c, h, m), 6 h (d, I, n) and 24 h (e, j, o). Images are representative examples of the field of view for 3 biological replicates. Images were captured at the Manchester Metropolitan University SEM central facility at 10,000 times magnification.

Following observations with all three Gram-negative species and three complexes, it was determined that **1** caused an increased rate of perturbation in the bacteria than the other two complexes on both bacteria. *P. aeruginosa* PAO1 additionally was significantly more effected by the complexes and at lower concentrations than **3**. Varying degrees of perturbation was observed over the time-points with each complex, **3** was overall less effective against the Gram-negative bacteria, causing less structural damage compared to the hexaammineruthenium chloride complexes.

4.4.2 **1** causes increased membrane depolarisation proportional to concentration using diSC_3 Assay

P. aeruginosa strain PAO1 was incubated with 3,3'-dipropylthiadicarbocyanine iodide until equilibrium occurred, then differing concentrations of **1** or Triton-X-100 (1%) was added to determine a change in depolarization of the inner membrane. When **1** was not added to the bacteria, there was little change in the intensity recorded, staying under 50 a.u and was used to zero the results. No fluorescence was present when **1** was tested alone without the presence of diSC_3 at the excitation and emission wavelengths. When **1** was added at 2 µg mL^{-1} a slight increase in intensity was recorded and increased proportionally with an increase in concentration (Figure 4.7). Incubation with Triton-X-100 caused a significant increase in intensity signifying an increase in the perturbations in the bacterial cell membrane and when compared with all concentrations of **1**, there was highly significant correlation (p<0.0001) between the signal intensity and the addition of **1** and Triton-X-100 demonstrating and increase in concentration causes and increase in the perturbations on the inner membrane of the bacteria thus causing an increase in intensity. One way ANOVA analysis also demonstrates **1** does significantly affect the inner membrane of the bacteria, to a similar extent of Triton-X-100 which is a known perturbator with p<0.0001.

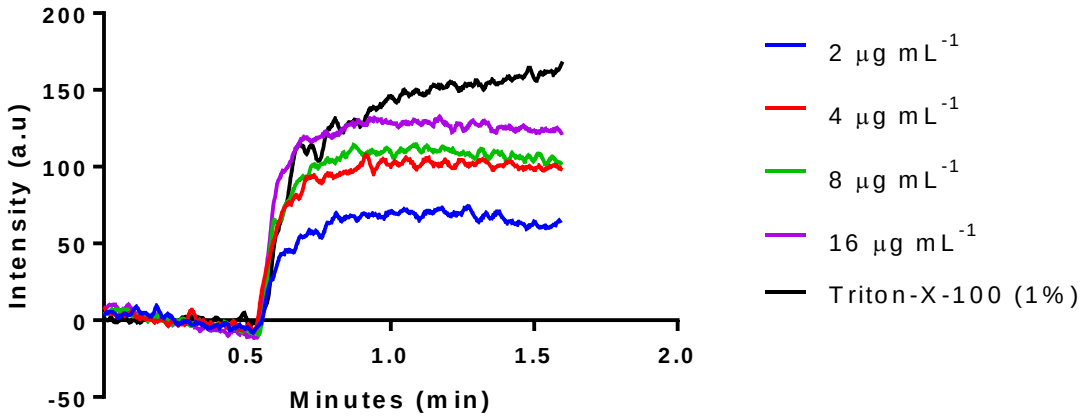

Figure 4. 7: *P. aeruginosa* PAO1 incubated with various concentrations of **1** with intensity observed to determine membrane depolarisation (*N*=3). **1** was added at 0.5 min.

4.4.3 Nucleic acid and Protein leakage from the *P. aeruginosa* strain PAO1 cells in response to the addition of **1**

An overnight bacterial culture of *P. aeruginosa* PAO1 was adjusted to an OD_{600} of 0.1 and incubated with either 4 µg mL^{-1}, 8 µg mL^{-1} or 16 µg mL^{-1} of **1**, Triton X-100 at 1% or not treated. This was recorded over a 24 h period in which the presence of RNA was detected using a nanodrop. With no treatment there was little change in the presence of RNA, at 0 h 49.3±1.55 ng mL^{-1} was detected whereas following incubation for 24 h a recording of 44.48±7.20 ng mL^{-1} was present showing no changes in the presence of RNA (Appendix Table 8.6; Fig 4.8). All other conditions with the exception of Triton-X-100 followed a similar pattern with little change in the presence of RNA over the 24 h period however the presence of 4 and 16 µg mL^{-1} of **1** caused an increase in expression from 93.83±1.42 ng mL^{-1} and 160.13±1.02 ng mL^{-1} respectively at 24 h suggesting the presence of an increased concentration of **1** causes increased leakage of the bacterial cell releasing more RNA. Triton-X-100 however at 0 h was expressing RNA at a concentration of 213.53±0.38 ng mL^{-1}

an increase compared to **1** at 16 µg mL^{-1} and following incubation for 24 h the concentration increased to 236.63±2.50 ng mL^{-1}. The interaction between the conditions and time and the conditions alone both had a highly significant effect on the leakage of the *P. aeruginosa* PAO1 bacteria with *p* values <0.0001 determining that **1** does have an adverse effect on the cell integrity thus causing increasing leakage of components with an increase in concentration whereas the time alone was slightly less significant with a *p* value of 0.0003. Multiple t-tests comparing 0h and 24 h suggests no significant difference with conditions with *p* values ranging between 0.3095-0.8851 with the exception of 16 µg mL^{-1} and Triton-X-100 with *p* values of 0.0025 and 0.0001 respectively.

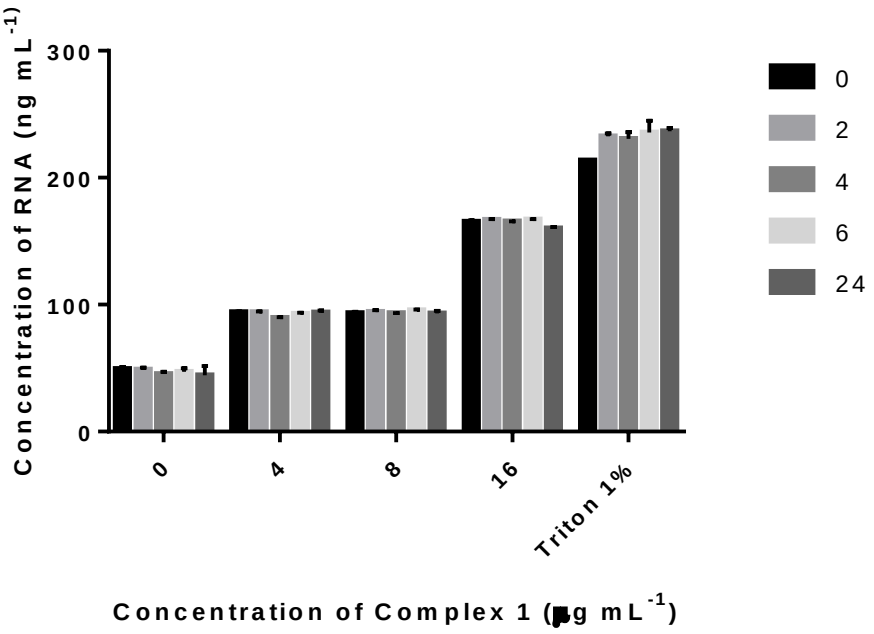

Figure 4. 8: RNA leakage of *P. aeruginosa* strain PAO1 over a 24 h period following incubation with different concentrations of **1** and Triton-X-100 at 1% (*N*=3).

Protein leakage was conducted the same way as the nucleic acid leakage and similar results was discovered with little variation for every concentration of **1** over the course of the 24 h incubation (Appendix Table 8.7; Figure 4.9). Similar to the nucleic acid, there was an increase in the presence of proteins between 4 μg mL^{-1}, 8 μg mL^{-1} and 16 μg mL^{-1} had very similar values, with 1.05±0.021 mg mL^{-1} of protein being present at a concentration of 4 μg mL^{-1} and at 8 μg mL^{-1} an increase was demonstrated to 1.83±0.0095 mg mL^{-1}. Triton-X-100 as expected had an increased leakage of protein of 10.93±0.21 mg mL^{-1} at 24 h. The impact of the conditions alone was highly significant to the leakage of the proteins with a significance $p<0.0001$ whereas time and the interaction between the time and condition were less significant with p values of 0.0458 and 0.0030 respectively demonstrating the cause for leakage of cellular components was a result of the Ru **1** and the time period did not affect the leakage. Multiple t-tests comparing 0 h and 24 h suggests no significant difference for the conditions 4 μg mL^{-1}, colistin and Triton-X-100, however significance over time with no treatment, 8 μg mL^{-1} and 16 μg mL^{-1} of **1** produced p values of 0.0001, 0.0014 and 0.0006 respectively meaning a concentration of at least 8 μg mL^{-1} of **1** is required in order to cause significant leakage of the cell causing a loss of proteins.

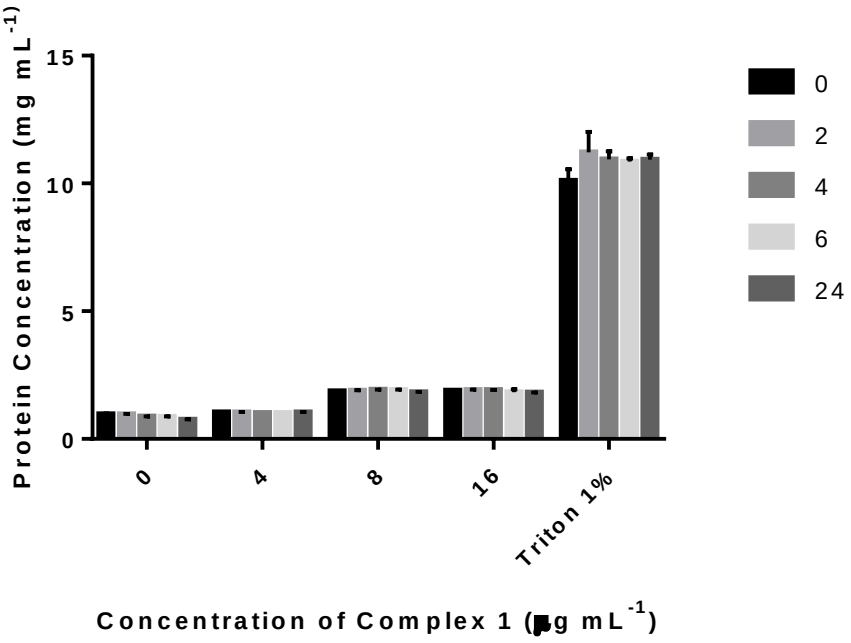

Figure 4. 9: Protein leakage as a result of the addition of **1** at a range of concentrations and Triton-X-100 as a control (*N*=3).

4.4.4 Inhibition of Oxidative stress

Three strains of *P. aeruginosa* were tested with both treated and untreated agar plates to determine if treatment confers a reduced resistance to 3 % hydrogen peroxide. *P. aeruginosa* PAO1 without treatment produced an average zone size of 16.473 mm (SD=0.435) and treated with **1** 15.393 mm (SD=0.611) (Figure 4.10). Non-clinical *P. aeruginosa* ATCC 9027 and NCTC 12903 demonstrated inhibition at of 20.367 mm (0.528) and 20.943 mm (0.542) respectively whereas treated respectively produced 21.103 mm (0.932) and 20.067 mm (0.155). Statistical analysis conducted demonstrated a highly significant difference between the strains on the resistance to oxidative stress ($p<0.0001$) whereas the addition of treatment was non-significant with a p value of 0.1636 suggesting no reduced resistance to **1**. The p value obtained from t-tests for *P. aeruginosa* PAO1

between treatments was *p*=0.0671, *P. aeruginosa* ATCC 9027 *p*=0.2993 and *P. aeruginosa* NCTC 12903 *p*=0.0546 demonstrating non-significance for all testing further proving no reduced hydrogen peroxide resistance thus oxidative stress resistance.

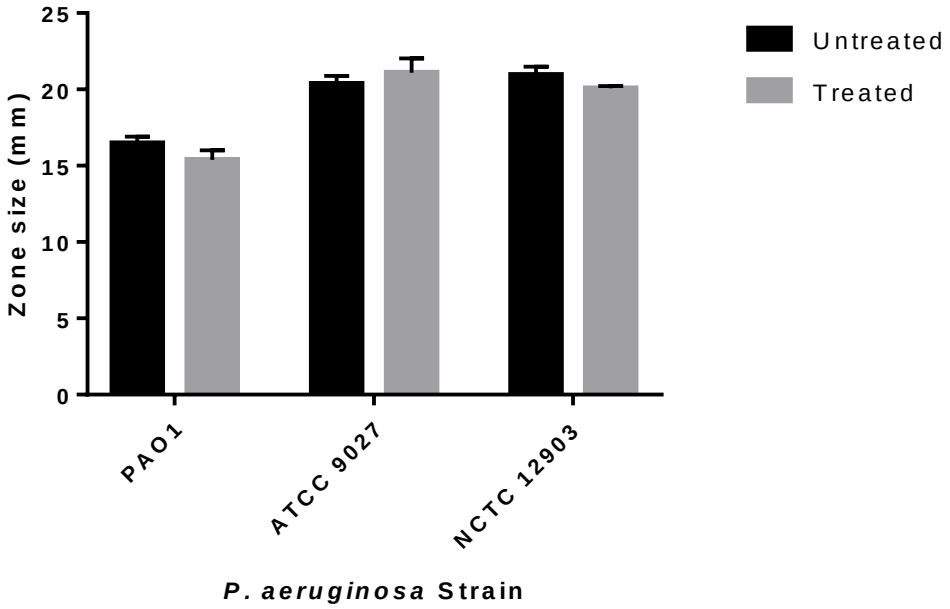

Figure 4. 10: Zone size produced by 3 % hydrogen peroxide on **1** treated and non-treated agar with three strains of *P. aeruginosa* (*N*=3).

4.4.5 Effects of **1** on the generation of Reactive Oxygen Species (ROS) within *P. aeruginosa* strain PAO1

To determine the generation of **1** on reactive oxygen species, a DCFDA assay was performed and analysed using a plate reader at 520 nm to determine the activity of ROS within the cell. In comparison with a bacterial control (Figure 4.11; black bar), when **1** was added at sub inhibitory concentration the ROS generation remained similar with the OD of the two conditions respectively of 13 and 12.667, however when the MIC concentration was added, the ROS activity increased by 1.7 % to 13.222. At post MBC concentration the OD increases

again by 30.7 % to an OD of 17. A colistin control has a similar response with the fluorescence being between 8 µg mL^{-1} and 16 µg mL^{-1} of 16.889. One way ANOVA analysis found no significant difference between the conditions demonstrating concentration of **1** does not affect the production of ROS, as demonstrated by similar absorbances between untreated bacteria and treatment with 4 µg mL^{-1} and 8 µg mL^{-1}.

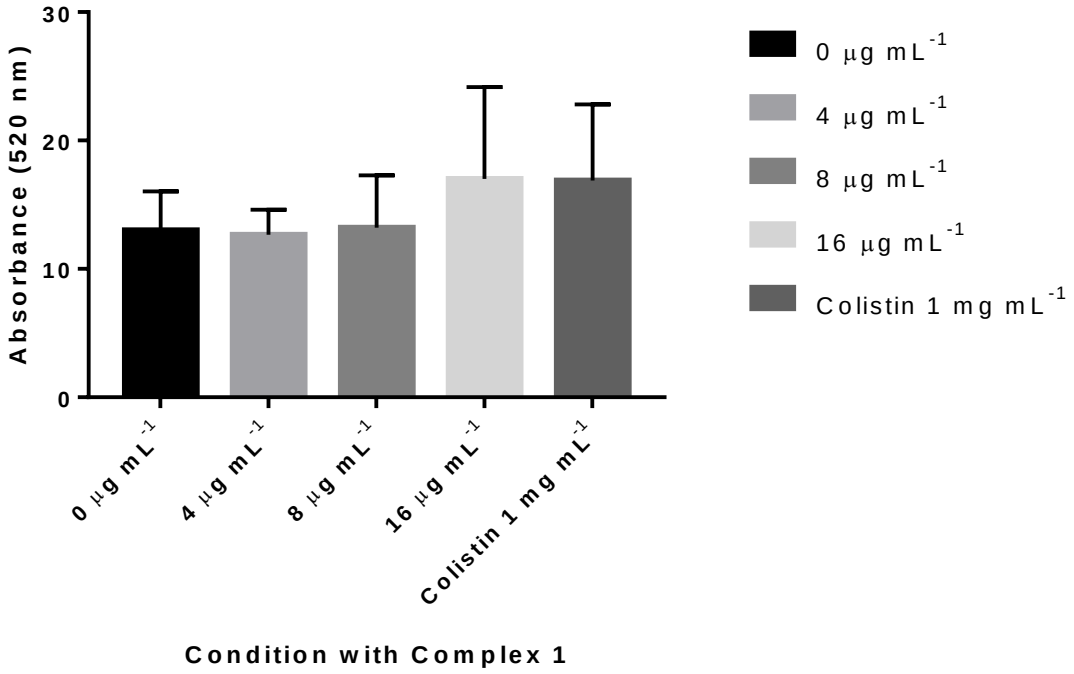

Figure 4. 11: Activity of ROS in *P. aeruginosa* PAO1 cells in response to differing concentrations of **1** (*N*=3).

4.4.6 RNA sequencing

The averaged base error rate of the samples were analysed which demonstrates the effect of the Illumina sequencing machine, reagent and samples, where all 9 samples did not exceed 0.03 % and the AT and GC content distributions were equal across both sets of reads for all 9 samples. The GC content across all 9 samples averaged at 62.9 % (SD=0.33). Data filtering was also conducted where the number of raw reads were analysed to determine the percentage of low quality or reads with adapters. NB1 was 97.3 % clean, NB2 98.5 %,

NB3 98.6 %, NB4 98.7 %, NB5 99.0 %, NB6 98.6 %, NB7 (30) 99.0 %, NB8 96.9 % and NB9 98.9 %. The RNA sequences were then mapped to the reference genome of *P. aeruginosa* strain PAO1 where the total mapping rate on average was 99.2 % (SD= 0.15) demonstrating no contamination and the correct reference gene was chosen.

The RNA sequencing reads were assembled and arranged according to the reference genome where 4 novel genes were predicted. PF02562:*PhoH*-like protein starting at position 4387258 with a length of 1607, PF01676:metalloenzyme superfamily starting at position 5778570 with a length of 1601, another gene starting at position 5020555 with a length of 286 and another with a gene description of PF04349:periplasmic glucan biosynthesis protein, *MdoG* starting at position 5716820 with a length of 1392.

Correlation of samples was conducted to determine similarities between the repeats. Samples NB1, NB4 and NB30_1 which were all control samples at 0 μg mL^{-1} all has a R^2 pearson correlation on average of 0.942 (0.030), samples NB2, NB5 and NB8 all had **1** added at 4 μg mL^{-1} have a R^2 value of 0.962 (0.009) and samples NB3, NB6 and NB9 incubated with **1** at 8 μg mL^{-1} all have a R^2 value of 0.796 (0.131). This demonstrates that all the control samples and samples incubated with 4 μg mL^{-1} are similar due to their R^2 number being closer to 1, however samples incubated with 8 μg mL^{-1} were less similar.

It was identified that 4 protein encoding genes were affected by **1**, with fold changes of 11.90, 9.39, 7.90 and 8.00 between control samples and samples incubated with 4 μg mL^{-1} for genes relating to catalase, ankyrin repeats, barrel-sandwich domain of *CusB* or *HlyD* membrane-fusion and pyridine nucleotide-disulphide oxidoreductase respectively. When a volcano plot (Figure 4.12) was conducted to demonstrate the number of genes up or downregulated with a fold change greater than 0.05. When comparing control samples with

4 µg mL^{-1} samples, 2570 genes remained constant however 1811 genes were upregulated and 1846 was downregulated. In comparison with control samples with 8 µg mL^{-1} 4743 genes remained unchanged, 1015 genes were upregulated and 469 was downregulated (Figure 4.13).

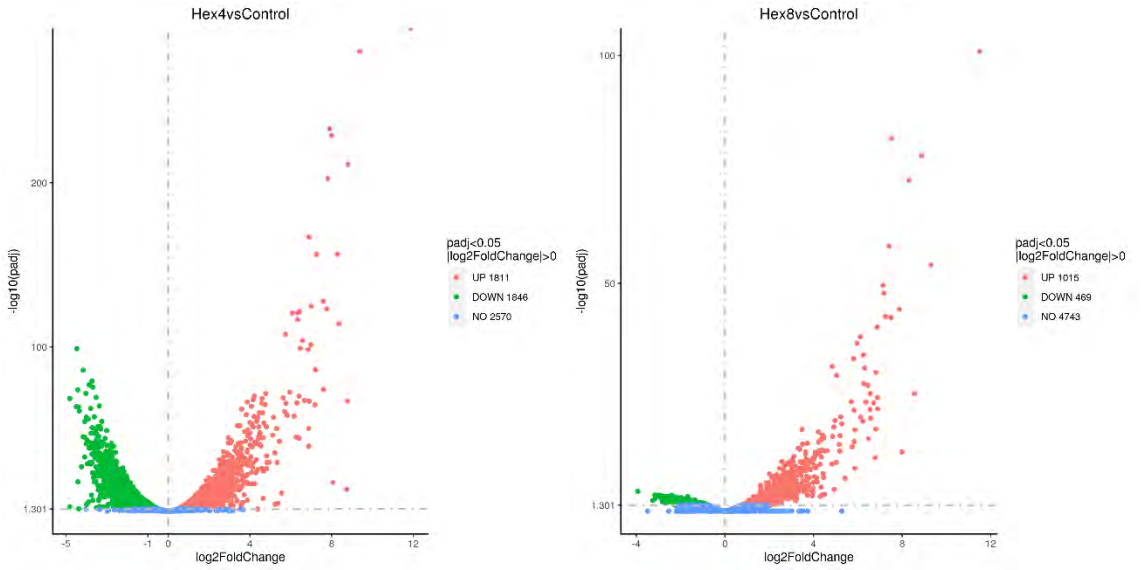

Figure 4. 12: Volcano plot analysis demonstrating the number of genes upregulated (red), downregulated (green) or unchanged (blue) of control samples compared against samples incubated with a) 4 µg mL^{-1} and b) 8 µg mL^{-1}.

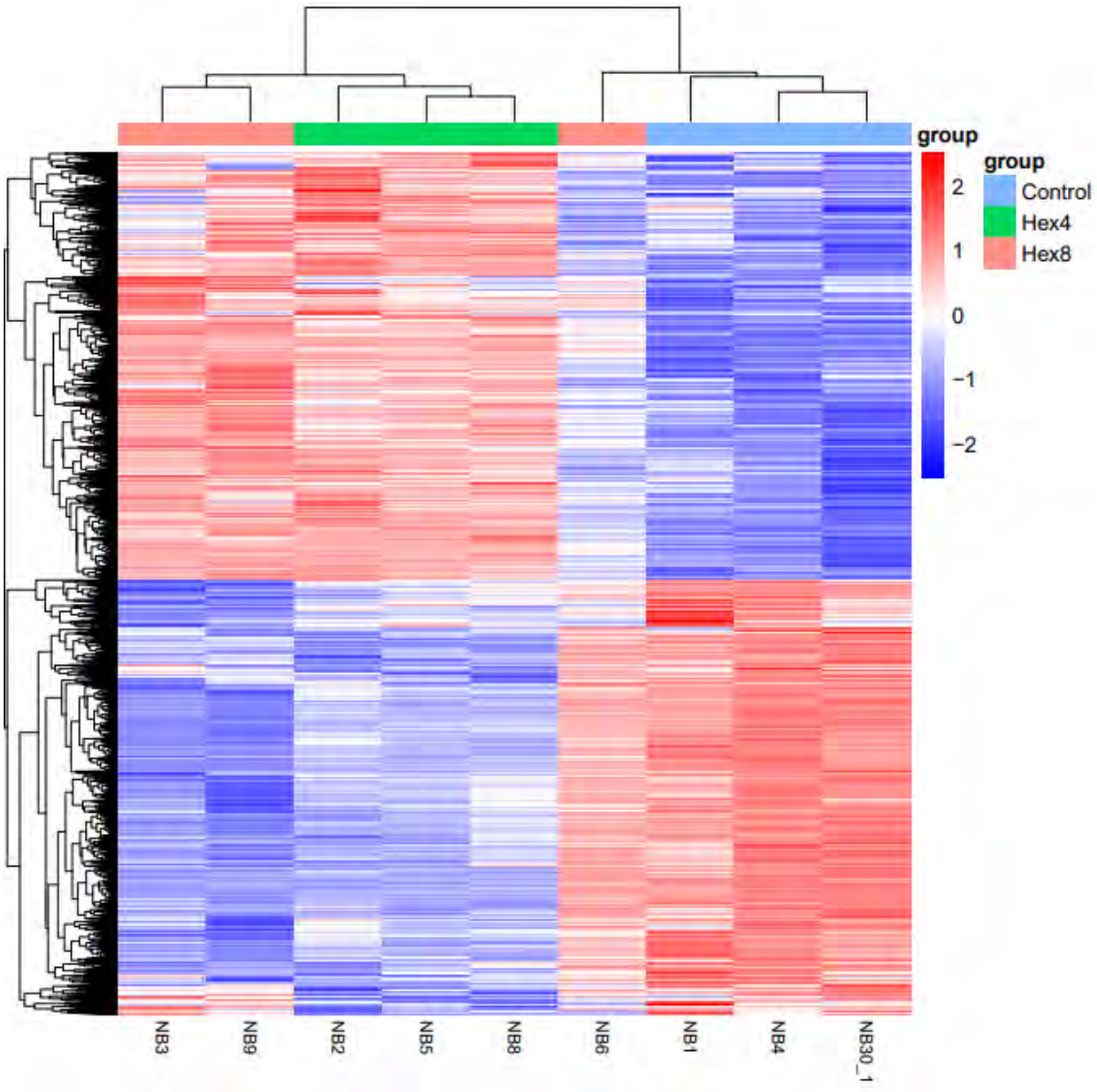

Figure 4. 13: Heatmap of expression values for differentially expressed genes with upregulated genes (red) and down regulated (blue).

Gene ontology was classified to determine what gene category has changed, the four genes identified had the same property of affecting the biological process with functions being translation, amide biosynthetic process, organonitrogen compound biosynthetic process and peptide biosynthetic process. The number of differentially expressed genes for each process was 71, 79, 171 and 71 respectively with an up-regulation of 2, 5, 20 and 2 genes for

each respective process (Figure 4.14). Majority of the genes expressed were downregulated, 97 % of genes identified for translation and peptide biosynthesis were downregulated, as well as 94 % and 88 % of genes associated with amide biosynthesis and organonitrogen compound biosynthesis respectively.

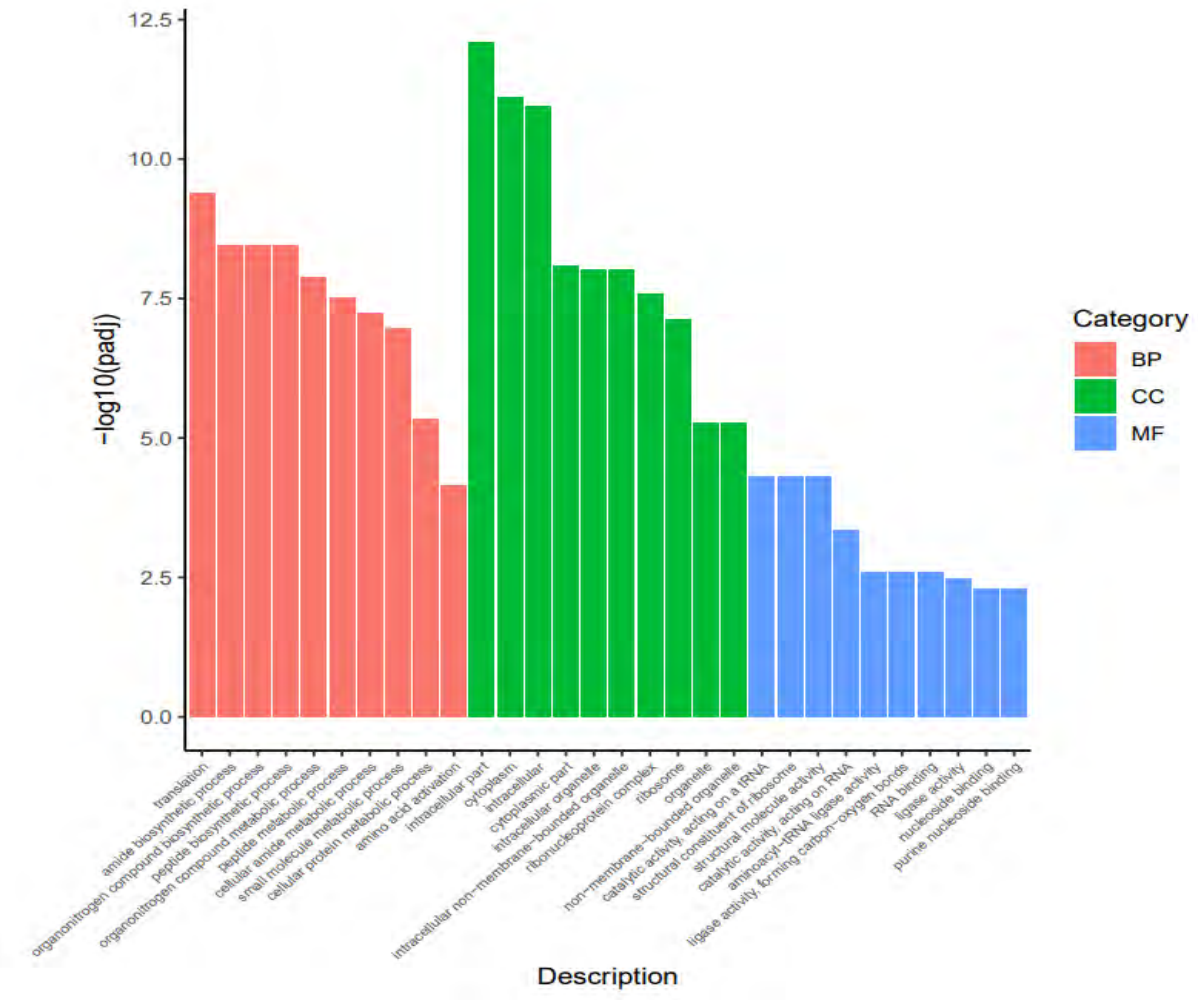

Figure 4. 14: Gene ontology (GO) bar graph demonstrating the top 10 significantly enriched GO terms of differentially expressed gene related to biological process (red), cellular component (green) and molecular function (blue) when *P. aeruginosa* PAO1 was exposed to 4 µg mL^{-1}.

Upon incubation with 4 µg mL^{-1} more genes were downregulated in response to a sub-inhibitory concentration of **1** suggesting *P. aeruginosa* PAO1 protects itself from **1** and slows metabolism (Figure 4.15). Whereas when incubated with MIC concentration at 8 µg mL^{-1} genes associated with metal ion, cofactor and cation binding, oxidation-reduction process and antioxidant activity are increased demonstrating cellular death (Figure 4.16).

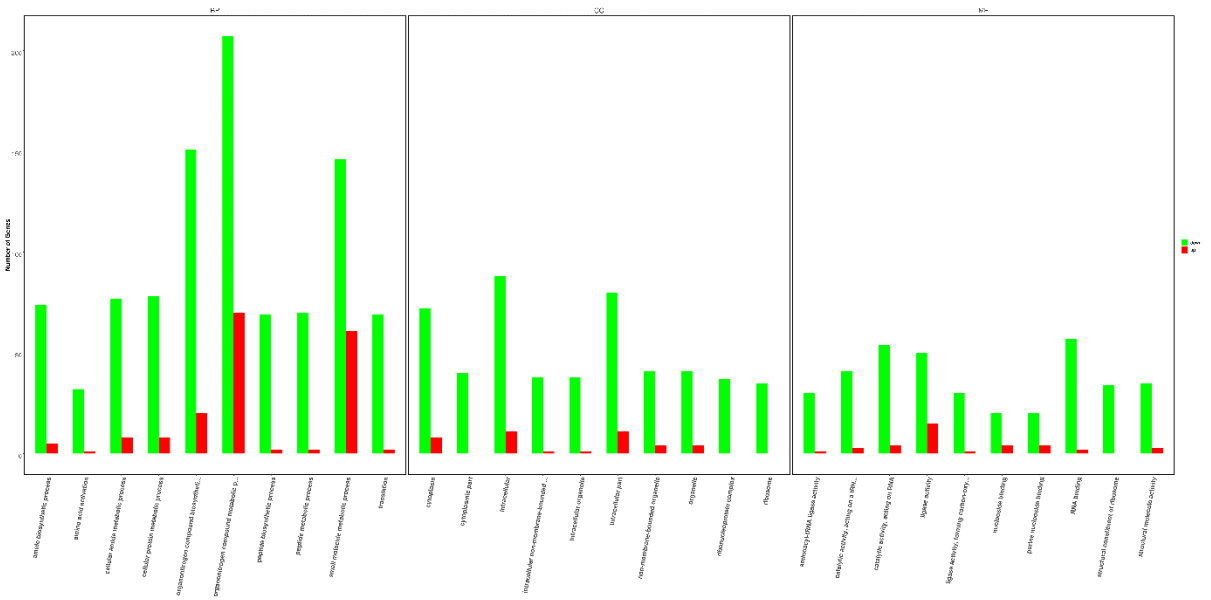

Figure 4. 15: GO ontology of up (red) and downregulation (green) of genes in different categories demonstrating the difference in the number of genes between the control samples and samples treated with 4 µg mL^{-1}.

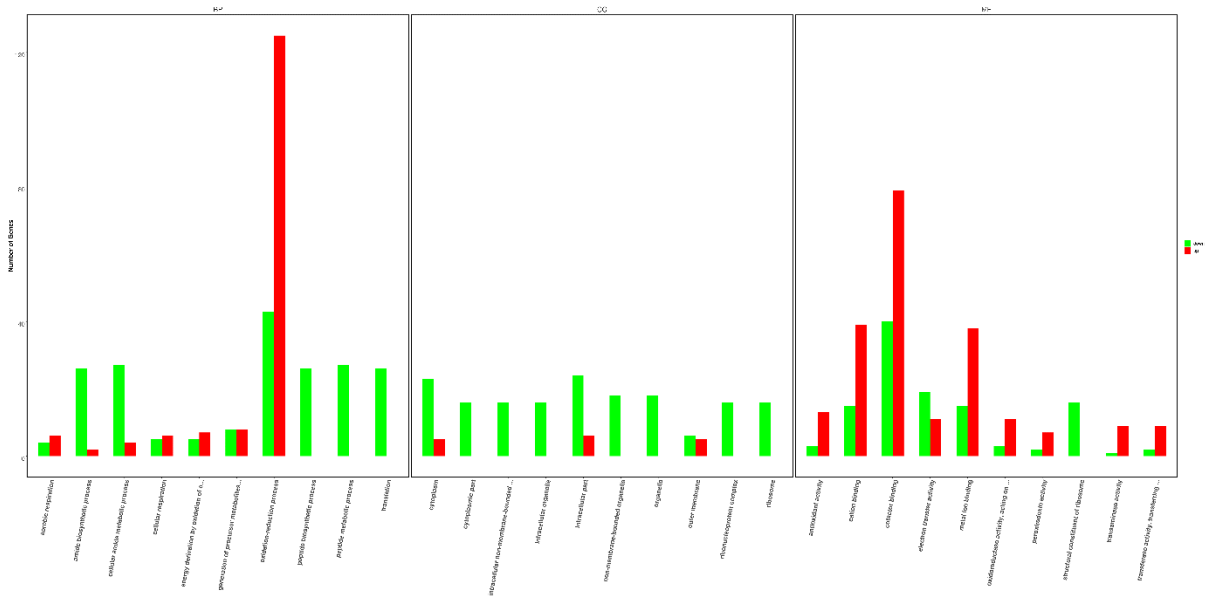

Figure 4. 16: GO ontology of up (red) and downregulation (green) of genes in different categories demonstrating the difference in the number of genes between the control samples and samples treated with 8 µg mL^{-1}.

A number of genes have been found to have fold-changed as a result of incubation with **1**, these included membrane-related genes such as outer membrane porins *OprD*, barrel-sandwich domain of *CusB* or *HlyD* membrane fusion, outer membrane efflux protein, outer membrane protein (*OmpH*-like) and *SecD* export protein N terminal. Other genes involved included ATP synthase, *recA* DNA recombination protein, RNA polymerase, tRNA synthase, genes associated with electron transfer and reverse transcriptase.

In the Kyoto encyclopaedia of genes and genomes (KEGG), four KEGG pathways were identified associated with the ribosome, biosynthesis of cofactors, aminoacyl-tRNA biosynthesis and peptidoglycan biosynthesis where 3.3 %, 27.2 %, 0 % and 47.4 % of genes were upregulated for each respective pathway when *P. aeruginosa* PAO1 is incubated with 4 µg mL^{-1} (Figure 4.17) and 8 µg mL^{-1} (Figure 4.18). Majority of the genes for each pathway

were downregulated with 59, 118, 40 and 10 genes downregulated for each pathway respectively.

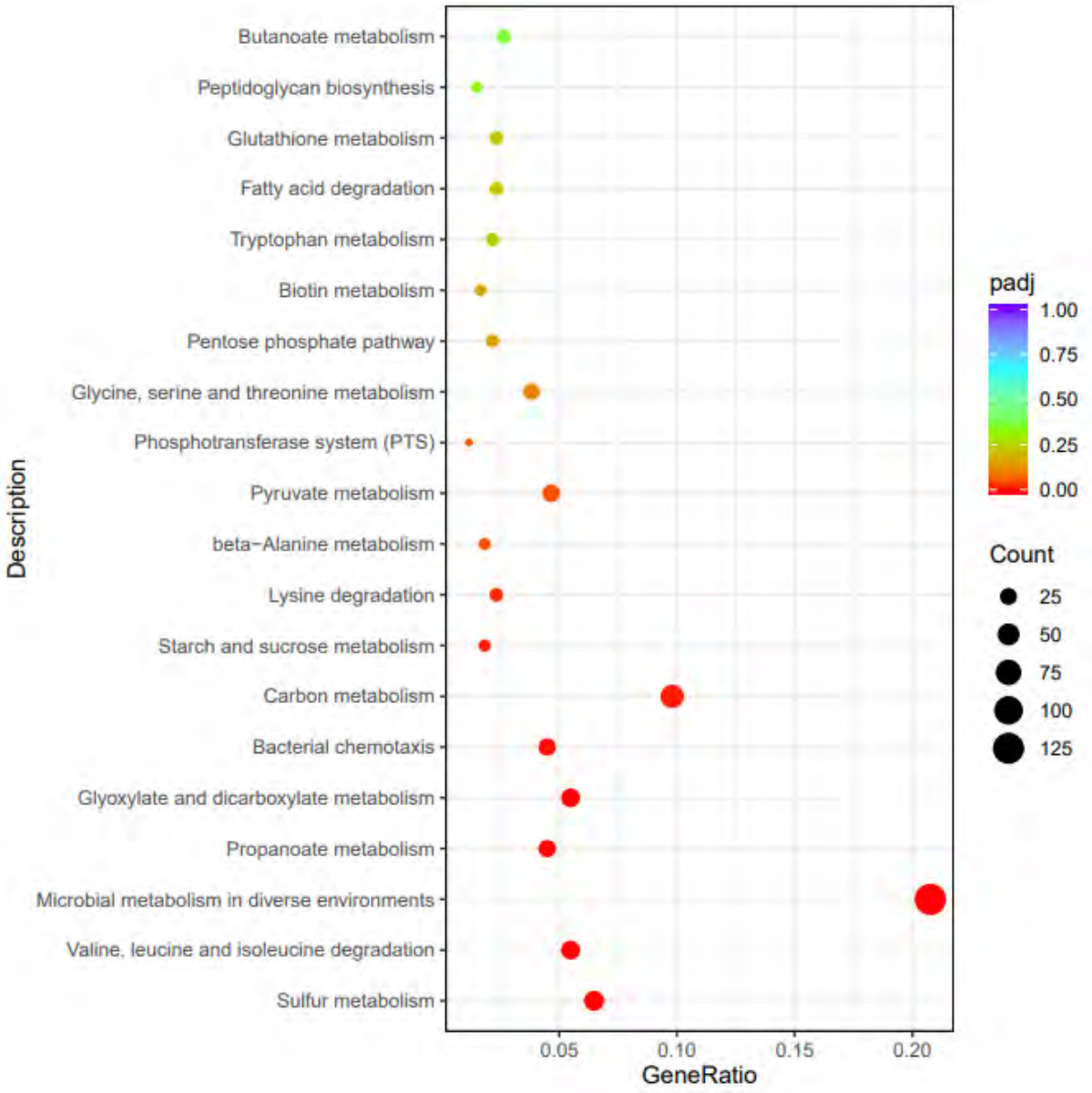

Figure 4. 17: KEGG pathway enrichment analysis of the 20 top enriched pathways of differentially expressed genes upon incubation of *P. aeruginosa* PAO1 following incubation with 4 µg $mL^{-1}$of **1**. The degree of colours represent the *p* adjusted value representing the extent of the enrichment and size related to the number of genes.

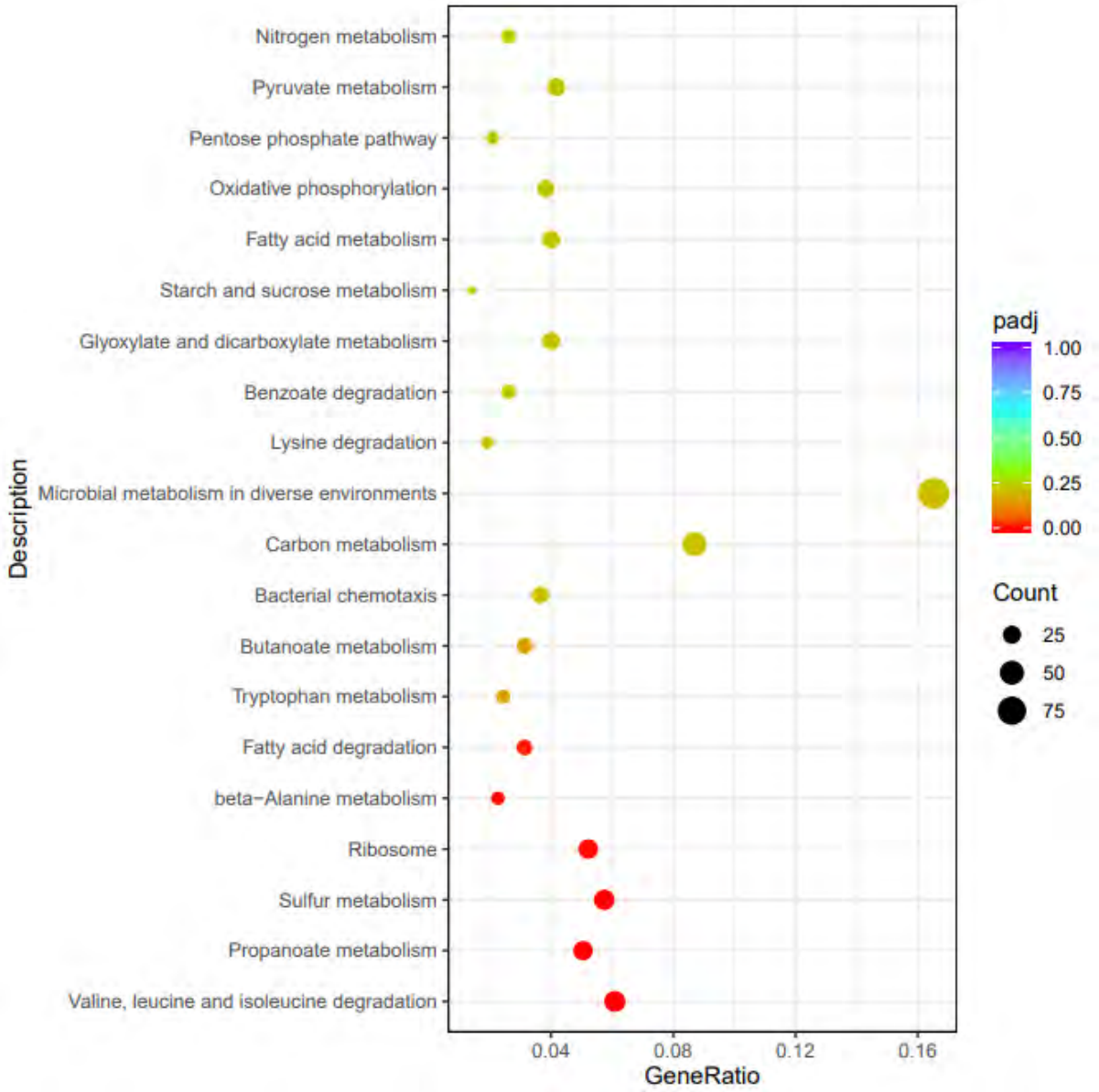

Figure 4. 18: KEGG pathway enrichment analysis of the 20 top enriched pathways of differentially expressed genes upon incubation of *P. aeruginosa* PAO1 following incubation with 8 µg $mL^{-1}$of **1**. The degree of colours represent the extent of the enrichment and size related to the number of genes.

4.5 Discussion

4.5.1 Investigating the effect of complexes 1, 2 and 3 on the cellular membrane of Gram-negative species

Using silver nanoparticles, SEM images using *P. aeruginosa* showed significant membrane damage upon treatment with 50 µg mL^{-1} nanoparticles. This is due to binding with proteins and lipopolysaccharides on the cell surface and causing disorganisation leading to changes in osmotic pressure and cell leakage (Ibraheem *et al*., 2019). Following 2 h incubation with silver nanoparticles, transmission electron microscopy (TEM) demonstrated *P. aeruginosa* membrane integrity loss, vacuole and nucleoplasm agglutination within the bacterial cell. This has been determined to be the cause of the nanoparticles being absorbed initially and then entering the bacterial cytoplasm (Salomoni *et al*., 2017). In comparison to this study, the Ru ions could also be absorbed by the membrane before mediating bactericidal action, thus damaging the membrane. Furthermore, silver nanoparticle studies demonstrate similar findings, with the nanoparticles attaching to the cell wall, entered the cell membrane and resulting in damage to increase the overall permeability of the cell leading to subsequent lysis (Kora *et al*., 2011).

Manganese tricarbonyl based complexes such as $[Mn(CO)_3(tpa\text{-}\kappa^3N)]Br$ where tpa=tris(2-pyridylmethyl)amine was found to cause liposomal damage and leakage of a fluorescent dye carboxyfluorescein due to the oxidation of Mn. In addition to this assay, a membrane permeabilisation assay using $DISC_3$ and *E. coli* where antibacterial activity was exhibited with PhotoCORM activation causing leakage of the bacterial cell membranes. It is hypothesized that the central Mn(tpa) is available to carry three CO ligands for respiratory inhibition of the bacteria as well as inducing membrane damage (Rana *et al*., 2017). Ru complexes cause membrane damage due to the generation of ROS and efflux systems become impaired

allowing for the metal ion to enter the nucleus easily and bind to the N7 region on guanine thus causing cellular mortality. Due to the leakage of the $DISC_3$ dye and membrane perturbations as demonstrated through SEM imaging, this is one of the main mechanisms being exhibited by **1** with increasing damage occurring with an increase in concentration.

Another study investigating the Gram-negative bacteria *E.coli* when treated with bimetallic gold and ruthenium nanoparticles additionally observed membrane damage and ruffling, thus inducing lysis of the bacterial cells. It was induced that the mechanism of action was producing ROS, membrane damage and a decrease in membrane potential (Zhao *et al*., 2020). The same mechanisms could be happening with both Gram-negative bacteria observed in this study. Membrane damage occurs in all complexes and concentrations however at differing rates. This suggests that Ru complexes overall cause membrane disruption and perturbation which is consistent throughout Gram-negative species.

Membrane damage has been observed with Ru complex $[Ru(phen)_2(tip)]$ $(ClO_4)_2$ and the Gram-negative bacteria *E. coli*, the Ru complex is able to enter *E. coli* cells in a time dependent manner and SEM analysis demonstrated membrane disruption and leakage of the cytoplasm. Pores were discovered upon further analysis with AFM. Electrical conductivity of the cell suspension increased after a short incubation period of 10 minutes and gradually increased over time due to the increased presence of electrolytes (Sun *et al*., 2015). Due to the membrane damage, the cellular contents are leaking into the growth medium, similarly to Sun *et al* upon *P. aeruginosa* strain PAO1 incubation with **1** cellular contents have leaked out of the cell. The presence of both protein and RNA increased over time and with concentration in the culture media. Due to the increased presence of RNA,

there will be an overall negative charge of the cell culture media becoming stronger with an increase in concentration, similar to electrolytes.

The images demonstrate an increase in the concentration of **1** and increased time resulted in an increase in membrane perturbation of *P. aeruginosa* PAO1, thus demonstrating the mechanism of action of **1** to be membrane based. The increased perturbations of the cell membrane causes cellular leakage of proteins, nucleic acids and other cellular contents. Additionally a self-quenching dye ($DISC_3$) can detect leakage using fluorescence. Using Ru nanoparticles, an increase in fluorescence was observed with *P. aeruginosa* associated with intracellular leakage over a course of 15 minutes (Huang *et al*., 2016). **1** also caused an increase in fluorescence upon incubation, increasing in a proportional manner with concentration. This is due to an increase in the number of perturbations as demonstrated by the SEM images.

Similarly in a study conducted by Czerwonka *et al* (2019), using a Ru (IV) complex ($(HL_2)_4[RuCl_6]\cdot 2Cl\cdot 4H_2O$) following an overnight culture with *P. aeruginosa* PAO1 showed similar morphological changes as the Ru based complex in this study. This suggests that Ru complexes have a significant effect on the membrane of *P. aeruginosa*. Indeed the Ru ions can interact with the cell wall resulting in bactericidal activity. Results shown by the SEMs in this study show that the Ru ions could disrupt the bacteria cell envelope, leading to distortion. It was additionally concluding within this study that the Ru complex contributes to a change in hydrophobicity causing pyoverdine to be relocated outside of the cell, leaving behind Ru ions in the cell wall to cause disruption (Czerwonka *et al*., 2019). The Ru ions could be responsible for the increase in fluorescence of $DISC_3$ as the plasma membrane is disrupted and an increase in leakage with an increase in concentration is demonstrated. Ru

nanoparticles as a carrier for pro-drugs have been shown to exhibit a similar effect with an increase in fluorescence over a 2 h period and causing cell membrane deformation thus causing cellular leakage in *P. aeruginosa*, some of the nanoparticles were thought to cause ROS accumulation, causing cell mortality (Liu *et al*., 2019).

It is possible this mechanism of action could be occurring with the Ru (III) **1** where higher concentrations resulted in cell membrane damage occurring within a shorter timeframe, possibly due to the accumulation of Ru ions in the membrane. Additionally, the electrostatic interactions between positive Ru ions and negative cell membrane is increased with a high concentration therefore will bind more effectively which could explain the shorter timeframe being required to have the same antimicrobial effect. The protective nature of the outer membrane on *P. aeruginosa* PAO1 and *S. maltophilia* S1 is known to make the bacterium notoriously difficult to treat (Breijyeh *et al*., 2020) therefore having a complex that targets and distorts the membrane, allowing for bactericidal mechanisms to occur is a breakthrough. This could allow for combinations of current antibiotics to be used alongside Ru complexes and have a greater effect, causing a resistance break.

Another Ru complex $Ru(5mp)_2\}_2(tpphz)][PF_6]^{4+}$ showed similar membrane damage to *E. coli* following exposure. After 1 h incubation damage and membrane blebbing was observed and following 2 h the outer membrane detached causing cell lysis. As with this study, **1** could additionally have the ability to bind to other regions within the cell following membrane disruption due to Ru complexes being known for targeting multiple sites, meaning that resistance emergence to this complex is unlikely (Smitten *et al*., 2019). Ruthenium nanoparticles have similar effects on the membrane to this study. Undertaking an experiment using dye to show membrane perturbation, over a period of 15 minutes, Ru

nanoparticles caused significant damage to *P. aeruginosa* PAO1 membranes and increased with the addition of acetylcholine due to membrane targeting and promoting nanoparticle entry. This was demonstrated by SEM that showed porous cell walls and atrophy (Huang *et al*., 2016) similar to the images in this thesis where membrane integrity was also disrupted.

4.5.2 Oxidative stress mechanisms

In a study determining the resistance to oxidative resistance by repurposing anti-diabetic drugs, the zone diameters with the drugs metformin and sitagliptin were increased upon treatment compared with the control thus reducing the tolerance of oxidative stress in *P.* aeruginosa (Hegazy *et al*., 2020). Similarly the industrial strains of *Pseudomonas* where the zone size increased this indicates a reduced resistance to oxidative stress however the medical strain *P. aeruginosa* PAO1 must be more resistant to oxidative stress mechanisms upon incubation with **1**.

A study investigating graphene oxide with *P. aeruginosa* found an increase in ROS production of at least 2.7 fold compared to the negative control and cell death is mediated by this production thus altering redox within the cell (Gurunathan *et al*., 2012). With the gene *ttcA*-deleted mutant of *P. aeruginosa*, there was an observed resistance reduction to hydrogen peroxide compared to *P. aeruginosa* PAO1 by 50 fold suggesting this gene is vital to oxidative stress mechanisms. The detoxification of hydrogen peroxide depends on the enzymes catalase and thiol-peroxidase and haem biosynthesis (Romsang *et al*, 2018), therefore these detoxification mechanisms ore enhanced in the *P. aeruginosa* PAO1 strain thus conferring resistance to oxidative stress mechanisms. Additionally the gene *ttcA* is present in this strain allowing for oxidative stress resistance to be encoded.

RuO_2 nanosheets coated with chitosan enhances ROS generation to target bacterial pathogens and additional hydrogen peroxide affinity especially in *P. aeruginosa* infections (Zhu *et al*., 2021). A Ru complex $[Ru(pip)_3]^{2+}$ was found to increase the generation of ROS in cells upon incubation in a dose and time dependent manner causing apoptosis in A375 melanoma cells, confocal microscopy using a DHE fluorescent probe that is oxidised by ROS where an overproduction was discovered (Luo *et al*., 2014). A similar complex however removing the pip ligand with bpy and modified using ammonium modified ligands to make complexes with a general formula $[Ru(bpy)_{3-n}(bpy\text{-}TMEDA)_n]^{2(n+1)+}$ that increases the cellular uptake and produce ROS causing bactericidal effects with *S. aureus* when photoactivated. The complexes do have an effect on Gram-negative bacteria however less effective due to the presence of the outer membrane (Jain *et al*., 2022). However **1** causes membrane damage allowing for access into the bacterial cell and ROS generation to have more of an effect without the need for photoactivation.

A ruthenium nanoframe core with a physically adsorbed glucose oxidase has been found to exhibit bactericidal effects through the generation of ROS as detected using a laser confocal microscope in *E. coli* and MRSA and the total amount increased over a period of 6 h causing oxidative stress and macromolecular dysfunction (Liu *et al*., 2021). This could be one of the reasons for the effective antimicrobial action of **1**, ROS generation increases with concentration of the complex.

4.5.3 Genomic responses of *P. aeruginosa* PAO1 treated with **1**

A surface coating comprised of micro-galvanic cells formed on a surface layer of both silver microanodes and Ru micro cathodes was used to treat *E. faecalis* 12030 for 24 minutes where a large change in gene expression was observed. The most prevalent category of genes which were differentially expressed were related to inorganic ion transport and metabolism contributing to 17 % of the genes analysed with transcription (11 %) pathways being the second most prevalent upregulated genes. The most down-regulated COG categories involved amino acid transport and metabolism (20 %) and translation, ribosomal structure and biogenesis (15 %). In addition to this, upon exposure a number of SOS-response genes were induced upon damage of the bacterial DNA including *LexA* repressor, *RecA* protein and DNA polymerase IV (Clauss-Lendzian., 2018). Similar to **1** and *P. aeruginosa* PAO1, there were some genes associated with the ribosome that were upregulated 3 % and some of the genes identified additionally included *LexA* DNA binding and *recA* DNA recombination protein which has been modified as a result of incubation with **1**.

One study investigated the use of $[Ru(phen\text{-}PPh_3)_2(dppz)](NO_3)_2$ on the transcriptome of human lung cancer cell line A549 cells at 4, 12 and 25 h following treatment. Indications using gene ontology confirmed the complex mainly effected the metabolic processes, nucleic acid binding transcription factor activity and translation regulator activity with wingless-type MTV integration site signalling pathway, tumour necrosis factor, nuclear factor κ-B and mitogen activated protein kinase affected following treatment of 4 h according to KEGG analysis. In the same study another complex $[Ru(phen)(phen\text{-}PPh_3)(dppz)](NO_3)_2$ exhibited similar cellular uptake behaviours to $[Ru(phen\text{-}PPh_3)_2(dppz)](NO_3)_2$ however is unable to induce the phase separation of DNA with 1188

downregulated genes and 796 upregulated genes. KEGG analysis demonstrated a negative impact on RNA polymerase II transcription due to intercalating into the DNA (Wang *et al*., 2021). KEGG analysis following incubation with **1** demonstrated a significant effect against genes associated with the ribosome, cofactor biosynthesis, aminoacyl-tRNA biosynthesis and peptidoglycan biosynthesis. Therefore metabolism within the bacteria is slowing in response to treatment as a form of preservation however **1** had multiple mechanisms of activity against *P. aeruginosa* PAO1 when incubated. This is in contrast to [Ru(phen-$PPh_3)_2$(dppz)]$(NO_3)_2$ which only significantly affected transcription regulated genes suggesting **1** could confer antimicrobial activity without resistance developing quickly.

When comparing to NAMI-A in MDA-MB-231 cells, the most significantly affected biological processes included the molecular functions and cellular components. These included genes associated with cytoskeletal rearranging, binding to the regulatory subunit of protein kinase A, transcription factor, cell cycle regulator, DNA binding and RNA polymerase II (Bergamo *et al*., 2015). Although incubation with **1** did affect genes associated with the nucleus including translation initiation factor, reverse transcriptase and RNA polymerase, it did affect other GO classifications including genes associated with the membrane and protein coding, including genes such as catalase, ankyrin repeats, barrel-sandwich domain of *CusB* or *HlyD* membrane fusion (responsible for Gram-negative type I secretion systems (Kim *et* al., 2016) and pyridine nucleotide-disulphide oxidoreductase. These are vital for protein coding especially ankyrin repeats which are vital for protein-protein interactions to occur within the bacteria and has the ability to deform the membrane (Kitamata and Suetsugu., 2023). GO terms significantly enriched involved genes related to translation, amide biosynthesis, organonitrogen compound biosynthesis and peptide biosynthesis. Similar to NAMI-A protein binding and synthesis are affected following incubation with **1** and RNA polymerase

demonstrating activity similar to NAMI-A, however genes associated with the membrane are additionally being affected.

Another study investigating the effect of HepG2 cells incubated with two times the IC_{50} concentration of $[Ru(dmbpy)_2(TFBIP)](PF_6)_2$ (50 µM) for 24 h found that systems associated with intracellular signal transduction, multicellular organism development and system development were significantly enriched. In addition to this, pathways associated with cancer including calcium signalling and glutathione metabolism were also affected thus inducing apoptosis (Liu *et al*., 2023).

The anticancer redox organoruthenium complex RDC11 (ruthenium(phenanthroline)(κ-*C,N*-(2-phenyl-pyridine)$(NCMe)_2]PF_6$) at a concentration of 2 µM decreased *HIF1A* (hypoxia inducible factor 1) mRNA levels within 24 h of treatment in cancer U87 cells, as well as the biosynthesis of aminoacyl tRNA and ribosome biogenesis which pathways are known in cancer studies to be deregulated and linked to mTOR signalling to try to allow for cellular survival and proliferation. Due to this it is hypothesized that aminoacyl tRNA biosynthesis could account for anti-cancer activity. In addition to this, RDC11 has been found to regulate ribosome biogenesis and inducing gene changes in oxidative ad ER stress related pathways (Vidimar *et al*., 2019). A similar effect could be why **1** exhibits antibacterial activity, by deregulating 40 genes associated with aminoacyl tRNA biosynthesis and thus inhibit cellular survival mechanisms to occur, ultimately conferring cellular mortality. It is possible **1** induces changes in oxidative and ER stress pathways in addition to affecting the ribosome, similar to RDC11.

One of the main mechanisms of action of **1** is through oxidative stress through the generations of reactive oxygen species with particular increased intracellular levels of

superoxide ($O_2^{\cdot -}$) (Muller., 2006) and hydrogen peroxide (Britigan *et al*., 1999) formed through the cyclic non-enzymatic reduction by NADPH (Hall *et al*., 2016). These ROS cause free radical damage disrupting the cell cycle, DNA damage, NADPH inhibition and depletion and attack of mitochondria (Ran *et al*., 2003; O'Malley *et al*., 2003; Hall *et al*., 2016). *Pseudomonas* sp. infection effects the host cells protective mechanisms including enzymes such as catalase, glutathione peroxidase and superoxide dismutase in which one study found an increase of 8.5 fold in the presence of pyocyanin of superoxide dismutase and a decrease in catalase (Suntres *et al*., 2002; Hall *et al*., 2016).

An alkyl hydroperoxide reductase required in oxidative stress environments. (Kang *et al*., 2007). In response to oxidative stress, activation of *ahpC-lacZ* occurred promoted by *oxyR* (Ochsner *et al*., 2000; Panmanee *et al*., 2017). Any growth inhibition caused by oxidative stress mechanisms is overcome through the expression of *AhpC* due to its property of being a scavenger of hydrogen peroxide (Kang *et al*., 2007). **1** causes a change in the expression of *ahpC* suggesting oxidative stress plays a role in its antimicrobial activity.

Treatment of *S. aureus* ATCC 29213 cells with fosfomycin caused an increase in the number of downregulated genes associated with cofactor biosynthesis in a concentration dependent manner with a maximum concentration of 4 μg mL^{-1} following a 20 min treatment. Genes associated with energy metabolism, amino acid biosynthesis and transport were downregulated in response to incubation whereas upregulated genes included protein synthesis, modification, repair and folding. To validate the results from the sequencing data, qPCR was conducted with 5 genes; *murZ* and *sgtB* associated with peptidoglycan biosynthesis and *ribB* associated with cofactor biosynthesis was upregulated whereas the autolysin *atl* gene and oligopeptide transporter *oppB* were downregulated in response. In

this study, genes were upregulated in response to fosfomycin included ones associated with murein and peptidoglycan biosynthesis and downregulated for surface polysaccharide metabolism. Those upregulated included several *mur* genes involved in the first stage of peptidoglycan biosynthesis, when inhibited, causes an accumulation of phosphoenolpyruvate substrate which acts as a carbon starvation signal. This is responsible for the downregulation of genes associated with central metabolism and nucleic acid biosynthesis (Patek *et al*., 2010). **1** additionally causes downregulation of 118 genes associated with cofactor biosynthesis and 10 peptidoglycan biosynthesis, this could act in a similar way to *S. aureus* and therefore cause an accumulation of phosphoenolpyruvate. Therefore **1** acts in a similar way to *S. aureus* and induces carbon starvation in *P. aeruginosa* PAO1 and is associated with glycogen degradation (Renninger *et al*., 2004) which then effects central metabolism as demonstrated by genes being downregulated during the cofactor biosynthesis process.

OprF is vital in multiple function of *P. aeruginosa*, including cell structure, environmental sensing, membrane permeability and virulence due to its role as the major and most abundant outer membrane protein (Bouffartigues *et al*., 2012). It is a hydrophilic channel (Bazire *et* al., 2010) as well as structural protein to anchor the peptidoglycan and outer membrane layers together (Rawling *et al*., 1998). It is vital in quorum sensing by binding to gamma interferon and causing production of virulence factors phenazine pyocyanin and lectin PA1 to occur (Wu *et al*., 2005)

The ruthenium complex KP1339 (sodium *trans*-[tetrachlorido-bis(1*H*-indazole)ruthenate(III)]) affected ribosomal genes in HCT116 cells upon incubation with 100 µM. This was accompanied with the endoplasmic reticulum unfolded protein response and

mRNA processing genes additionally being upregulated. This subsequently lead to detachment from the endoplasmic reticulum and formed polyribosome clusters which were able to constitute metal detoxification (Neuditschko *et al*., 2021). In contrast to **1**, the genes associated with the ribosome were downregulated, therefore indicating that metal detoxification cannot occur of the Ru ions and antimicrobial activity could continue to cause mortality within *P. aeruginosa* PAO1.

4.6 Conclusion

1 was found to exhibit multiple mechanisms of action with *P. aeruginosa* PAO1. SEM analysis confirmed that a mechanism of action of **1** involves membrane damage, with perturbation being observable at varying concentrations of the complexes against two species of Gram-negative bacteria *P. aeruginosa* PAO1 and *S. maltophilia* S1. In addition to these results, the membrane depolarisation diSC_3 assay additionally demonstrated an increase in membrane leakage upon an increase in concentration of **1** this is also demonstrated with the increase in concentration of nucleic acids and proteins upon incubation with sub-lethal, MIC and post-MBC concentrations of **1** over a 24 h period. This is due to the ability of **1** to decrease the hydrophobicity of the membrane of the bacteria thus causing Ru ion accumulation and membrane perturbations to occur. Oxidative stress is another mechanism in which **1** exhibits upon cells as demonstrated by both the ROS generation study and the hydrogen peroxide assay. These demonstrate an increase in the generation of ROS when entered into *P. aeruginosa* PAO1 and a decreased resistance to oxidative stress thus causing cellular mortality. Finally RNA sequencing provided a comprehensive analysis of gene expression of *P. aeruginosa* PAO1 when incubated with **1**. Genes associated with membrane including peptidoglycan biosynthesis, Barrel-sandwich domain of *CusB* and *HlyD* membrane fusion and periplasmic glucan biosynthesis were

affected including other mechanisms such as genes associated with the ribosome, cofactor biosynthesis and aminoacyl tRNA biogenesis. These are downregulated in response to a sub-inhibitory concentration of **1** due to the attempt at survival, metabolism of the bacteria is reduced meaning removal of Ru ions cannot be detoxified thus ultimately causing cellular death.

Chapter 5: Antimicrobial activity of [Chlorido(η6-p-cymene)(N-(4-chlorophenyl)pyridine-2-carbothioamide) ruthenium(II)] chloride (4) against methicillin-resistant *Staphylococcus aureus.*

5.1 Introduction

5.1.1 Aetiology

Methicillin resistant *S. aureus* evolved in 1960 (Lakhundi and Zhang, 2018), however whole genome sequencing of early MRSA isolates suggested that resistance to methicillin was present in the 1940s. This could be because of *Staphylococcal* cassette chromosome *mec* uptake into multiple *S. aureus* clones via horizontal gene transfer shortly after the introduction of methicillin in the clinical setting (Lee *et al.,* 2018). The acquisition of resistance to antibiotics can account for 25-50 % of hospitalised *S. aureus* infections (Lakhundi and Zhang, 2018) and one study suggested that 81 % of patients hospitalised had chronic skin lesions with a median colonization duration of 282 days (Lucet *et al.*, 2009; Lee *et al.*, 2018).

5.1.2 Epidemiology and global transmission

MRSA is a global issue, predominantly affecting high socioeconomic countries (Figure 5.1). In the USA and Canada, *S. aureus* is the major causative agent of bloodstream infections where MRSA accounts for 60% of the isolates obtained (National nosocomial infections surveillance system, 2004). It was additionally discovered that *S. aureus* strains USA100 (Tsuji *et al*., 2007) and USA 600 were the prevalent strains causing bloodstream infections (Moore *et al*., 2010). In Canada from 2007 and 2009, 24.8 % of 3589 isolates taken from multiple Canadian regions were confirmed as MRSA with 72.4 % (Popovich and Weinstein., 2009) being hospital acquired *S. aureus* strains USA100 and USA 800 (Nichol *et al*., 2011). In 2013-2014 MRSA became the most prominent being associated with 84.5 % of SSIs (Pardos *et al*., 2016) and is now identified as a community acquired endemic pathogen in the USA (D'Agata

et al., 2009; Elston and Barlow., 2009; Otter and French., 2010; Mustafa., 2012; David *et al*., 2012; Nimmo., 2012; Thurlow *et al.,* 2012).

Annually within Europe, 150,000 patients are affected with MRSA costing the EU €380 million (Kock *et al*., 2010). Five clonal complexes are typically involved including CC5, CC8, CC22, CC30 and CC45 (Deurenberg et al., 2007). MRSA was first isolated in 1961 in the United Kingdom, then in 1967 a multidrug resistant phage type 83a was isolated (Jessen et al., 1969; Rountree and Beard., 1968; Benner and Kayser., 1968). In 1982 there was an epidemic of MRSA in London hospitals where the strain is believed to have been bought into the UK from Australia (Pavillard *et al*., 1982; Cookson and Phillips., 1988). Multiple epidemic strains have since been discovered within the UK including EMRSA-15 and EMRSA-16 which for over 20 years have been endemic (Ayliffe *et al*., 1998). In Portugal, MRSA is the most prevalent infection in the EU at 54.3 % (Conceicao *et al*., 2013) and in 2010 it was discovered that the clonal complex CC5 accounted for 20% of MRSA isolated within the country (Espadinha *et al*., 2013). A study conducted in Europe in 2011 demonstrated that the ST22 MRSA clone was the most frequently isolated accounting for 24.5 % of isolates in 350 laboratories (Grundmann *et al*., 2014).

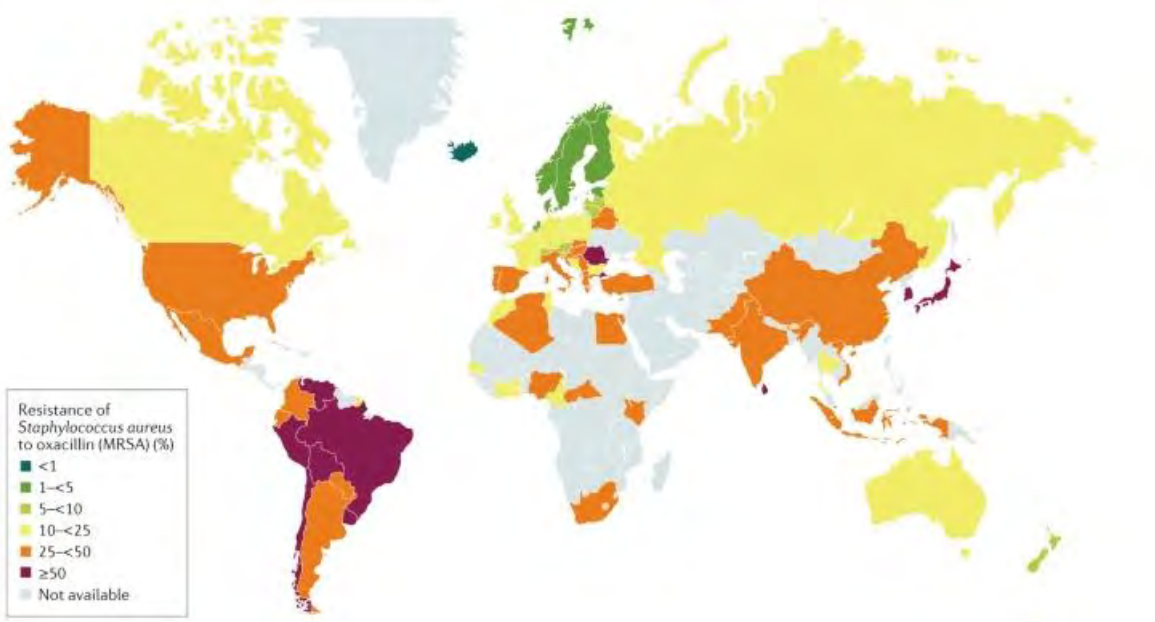

Figure 5. 1: Prevalence of MRSA worldwide (Lee *et al*, 2018).

S. aureus infections can occur on orthopaedic implants, in which one study conducted by Montanaro *et al*, 2011 found that *Staphylococcal* species accounted for 75 % of isolates taken from 242 patients with infections and *S. aureus* was found to be the predominant cause of infections in fixations internal and externals as well as non-implant associated patients.

Risk factors for MRSA infections include the elderly, immunocompromised, having an open fracture, renal failure, being admitted to intensive care units and being a resident within a nursing home (Deny *et al*, 2016; Oliveira *et al*, 2018).

Animals may also be a risk factor for transmitting MRSA such as through direct contact with infected animals, handling contaminated waste and animal product and environmental contamination (Vanderhaeghen *et al*., 2010). In 2005 a study was conducted that showed 760 fold increased risk of Dutch pig farmers being colonised with MRSA (Voss *et al*., 2005) and 12.5 % of veterinarians worldwide were shown to be colonized with MRSA (Huber *et al*.,

2010). People working in such environments have a 77-86 % chance of having their nasal passages colonised by MRSA strains (Cuny *et al*., 2009). There is a hypothesis suggesting that the origin of livestock acquired MRSA was originally from human decent which is both methicillin and tetracycline resistant according to phylogenetic analysis however the phage encoding innate immune modulators in humans was missing (Price *et al*., 2012).

5.1.3 Pathogenesis

Biofilm formation is a vital virulence factor for *S. aureus*, contributing to its pathogenicity (Nassar *et al*., 2020). Adherence through cell wall proteins occurs between abiotic surfaces and eukaryotic cells (Artini *et al*, 2011). A biofilm is formed through surface adhesion mediated by van der waals and steric-electrostatic interactions followed by a formation of a microcolony and bacterial cell detachment. The attached bacterial cells express surface components such as fibronectin and fibrinogen (to stabilize the biofilm) and attach irreversibly to the substrates through hydrophobic, ionic and hydrogen bonding as well as lipopolysaccharides and exopolysaccharides (Oliveira *et al*., 2018). An extracellular polymeric substance (EPS) composed of polysaccharides (primarily polysaccharide intercellular adhesion), lipids, proteins and extracellular DNA, is used for the adhesion of bacteria to a surface and protects the biofilm against chemical and mechanical factors (Hou *et al*., 2018). When in the final stages of biofilm formation, macrocolonies have the presence of channels to distribute signalling molecules and nutrients throughout the biofilm. The presence of a biofilm increases the resistance profile of the bacteria by 1000 fold (Nassar *et al*., 2020), which is due to a decreased penetration of antimicrobial treatment into the depths of the biofilm, an increase in the number of resistant bacterial colonies and dormant cells (Oliveira *et al*, 2018). A number of genes are upregulated in *S.*

aureus during a biofilm, including those regulating amino acid, ammonia, glutamate and glutamine metabolism, superoxide dismutase and quorum sensing regulator genes allowing for continual survival of the biofilm (Nassar *et al*., 2020).

5.1.4 Disease progression and monitoring

Staphylococcal skin infections involve cutaneous abscesses in adults (Tong *et al*, 2009) and impetigo being found more commonly in children (Bangert *et al*., 2012). The infection may be categorised as necrotising fasciiitis with patients who are frequent drug users or immunocompromised. The incidence of soft skin tissue infections increase following surgery with 2-5% of surgeries resulting in infection (Lewis *et al*., 2013).

5.1.5 Current therapeutic options

Infections caused by antibiotic resistant strains can cost an extra £1 billion per annum to the NHS with Methicillin Resistant *Staphylococcus aureus* (MRSA) and *P. aeruginosa* being the leading causes of infection (Public Health England, 2015; Public Health England, 2020). MRSA is a commensal organism but is also the leading cause of many diseases ranging from skin and soft tissue infections to bacteraemia and endocarditis. In 1940, shortly after the discovery of penicillin, bacterial resistance in *Staphylococcus* species emerged which was mediated by the β-lactamase encoding gene *bla2* (Turner *et al.,* 2019). Resistance to antibiotics is largely mediated by *mec* type genes (Chen *et al.*, 2010; Liu *et al.*, 2016). To date, the global mortality rate associated with MRSA infections can vary from 5-60 % depending on the site of infections and patient population.

Current treatment options include oral antibiotics such as trimethoprim, tetracycline, sulfamethoxazole and clindamycin for between 5-14 days (Siddiqui and Koirala, 2019).

Intravenous vancomycin is used for hospitalized patients with the infection or those with endocarditis however these are highly cytotoxic and antibiotic resistance is emerging (Cong *et al.*, 2020). Standard topical and systemic treatment of *S. aureus* infections involve the use of cefazolin, rifampicin, vancomycin, oxacillin, clindamycin, cotrimoxazole, minocycline, linezolid, azithromycin, clarithromycin (Majidpour, *et al*., 2017) doxycycline and daptomycin (David and Daum., 2017).

Current treatments are limited due to allergies within the population. Antibiotic allergies are some of the most common allergies found in hospitals, with penicillin the most common within the United States (King *et al*., 2016) and up to 10 % of the worldwide population have an allergy (Santillo *et al*., 2020). Antibiotics such as rifampicin have concerns with the cytotoxicity when administered orally therefore is only considered as a topical agent (Troeman *et al*., 2018) and other antimicrobials such as cotrimoxazole, rifampicin and vancomycin have adverse side effects associated with use and is therefore discouraged for use (Bratzler *et al*., 2013). Additionally some treatment courses are long, thus the full course is not completed. Standard treatment regimens can range from 3 to 14 days, with longer treatments causing a 5 % increased risk of adverse effects for each additional day exceeding 8 days (Spellberg and Rice., 2019).

5.1.6 Use of Ruthenium complexes against *S. aureus*

In 1960, the first studies of the antimicrobial activity of Ru (II) mononuclear complexes against Gram-negative, Gram-positive and acid-fast bacteria was performed. The initial complex, $[Ru(phen)_3]^{2+}$, exhibited little to no activity against all bacterial strains. However, addition of methyl groups to the bidentate phenanthroline ligands, thus creating $[Ru(Me_4Phen)_3]^{2+}$, caused a significant increase in the antibacterial action, most notably

against Gram-positive bacteria (Dwyer *et al*., 1969). Subsequent studies discovered that the antibacterial effects were due to the complex binding to the major groove of DNA (Metcalfe and Thomas., 2003). More recently, dinuclear poly pyridyl ruthenium(II) compounds have been investigated, mainly due to their higher affinity for DNA, with subsequent increased DNA binding ability. These complex were found to be highly active against a number of bacteria (Li *et al*., 2015).

Various ruthenium based complexes have been investigated for their antimicrobial capability against *S. aureus* species in recent years. For example one study demonstrated effective killing at the low concentration of 6.25 μg mL^{-1} with a bis(2,2'-bipyridine)-ruthenium(ii) complex containing a ligand consisting of *N*-phenyl-substituted diazafluorene (Lam *et al*., 2014) and the chances of resistance evolution are low as demonstrated by (Dwyer *et al*., 1952; Zeng *et al*., 2017). Another study investigating the ruthenium complexes $[Ru(dmb)_2(ETPIP)](ClO_4)_2$ and $[Ru(phen)_2(ETPIP)](ClO_4)_2$ additionally exhibited low MIC values against *S. aureus* at 0.05 and 0.025 mg mL^{-1} respectively. The mode of activity was determined to be thiol depletion as a result of ROS generation (Liao *et al*., 2020). Proposed mechanisms of action of ruthenium complexes against *S. aureus* include the binding of the ruthenium complexes to ribosomal RNA and the bridging of bacterial walls (Weber *et al*., 2016). Ruthenium accumulates in the cells after being transported into the bacterial cells through energy dependent mechanisms depending on the Gram status of the bacteria. Additionally at post MIC concentrations of ruthenium complexes result in damage to the bacterial DNA however this is not the only mechanism of action exhibited by ruthenium complexes (Smitten *et al*., 2020). The cell membranes of the bacteria are also disrupted causing death of the bacteria (Zhang *et al*., 2018). The low MIC values of ruthenium based complexes in many studies demonstrate it's potential at combatting the antibiotic crisis,

including Gram-positive species, thus further testing of **4** must be done to determine its effectivity against *S. aureus*.

3 has the capability to induce cytoplasmic membrane damage (Southam *et al*., 2017) and cause cell cycle arrest (Hartinger and Dyson., 2008) due to targeting the DNA nucleotides, specifically guanine (Hoeschele *et al*., 2007). As demonstrated in the present study in chapter 3, **4** has a range of antimicrobial activity against Gram-positive species of bacteria, with the lowest MIC being at 8 µg mL^{-1} against *S. aureus*. This activity however does not correlate against Gram-negative species, this could be due to **4** lack of ability to cross the cell wall to exhibit its antimicrobial activity and **4** has a DMSO ligand present which exhibits some antimicrobial activity as demonstrated with other Ru complexes (Li *et al*., 2015).

5.2 Aims and Objectives

5.2.1 Aims

The aim was to determine the antimicrobial activity of **4** against a range of clinical isolates of MRSA and to identify the potential for synergy with established antibiotic treatments. *In vivo* activity was also assessed to determine cytotoxicity, coupled with further understanding the role of **4** as a resistance breaker.

5.2.2 Objectives

- To determine the antibiotic resistance profile of MRSA clinical isolates.
- Use checkerboard microbroth dilution assays to identify potential synergy of **4** with established antibiotics.
- To use *Galleria mellonella in vivo* modelling to determine cytotoxicity of **4,** coupled with infection modelling.
- To evaluate the resistance breaking potential of **4** by using a nitrocefin assay to measure the β-lactamase activity of treated MRSA cells.

5.3 Methods

5.3.1 Resistance profiling of *S. aureus*

Similar to 2.3, resistance profiling was completed on every strain of *S. aureus.* Colonies of bacteria was suspended in a saline solution and were inoculated onto MHA using the lawn plating method and left to dry (McFarland). Antibiotic impregnated mast rings (Mast group) were then placed onto the agar and incubated overnight at 37 ˚C. Mast group M13 Mast rings were used for *S. aureus*. M13 antibiotic discs included 25 µg chloramphenicol, 5 µg erythromycin, 10 µg fusidic acid, 5 µg oxacillin, 5 µg novobiocin, 1 unit of penicillin, 10 µg streptomycin and 25 µg tetracycline. The following day results are analysed by measuring the diameter of the zone of inhibition and compared in accordance with CLSI guidelines to determine whether the bacteria are sensitive, resistant or intermediate. *N* = 3 per condition.

5.3.2 Synergy of **4** with antibiotics used to treat *S. aureus* infections

Similar to 2.10 the *Staphylococcal* strain USA300 was tested with **4** and ciprofloxacin (Fluka Analytical, UK), erythromycin (Sigma, UK), penicillin G (Sigma-Aldrich, UK), streptomycin (Sigma-Aldrich, UK) and vancomycin (Sigma, UK) to determine synergistic combinations using the checkerboard method and fractional inhibitory concentrations.

Antibiotic	Concentration (µg mL^{-1})					Reference
Ciprofloxacin	4	8	16	32	64	Sundaramoorthy *et al.,* 2018
Erythromycin	2.5	5	10	20	40	Roudashti *et al*., 2017; Abdolhosseini *et al*., 2019
Penicillin G	0.5	1	2	4	8	
Streptomycin	5	10	20	40	80	
Vancomycin	0.125	0.25	0.5	1	2	Adhikari *et al*., 2017

5.3.3 Nitrocefin Assay

Adjusting the protocol as described by O'Callaghan *et al*., 1972 to detect β-lactamase activity, a stock solution of nitrocefin and DMSO was made using 10 mg of nitrocefin powder (Sigma-Aldrich, UK) and 1 mL DMSO for a stock concentration of 10 mg mL^{-1}. A working solution is made using 1 mL of stock solution and diluting in 9 mL PBS. With bacterial overnight cultures with their respective conditions, 1 mL of cells are lysed using sonification. To confirm complete lysis of cells, a sample of 100 µL of culture was plated onto MHA using the lawn method and incubated at 37 ˚C overnight. Following this 3-5 drops of the working nitrocefin solution was added and incubated at room temperature for 20-30 minutes until a red colour change appears; this was an indication β-lactamase activity. This can then be analysed using a spectrophotometer at 217 nm which detects the 7-acyl group and 386 nm. Over a 24 h period the rate of nitrocefin degradation due to β-lactamase activity was detected at a wavelength of 482 nm.

Controls of MRSA, **4** at 8 µg mL^{-1}, a non β-lactamase producing *S. epidermidis*, DMSO and a β-lactamase inhibitor tazobactam was used to determine baseline OD's. Then combinations of bacteria with **4** was tested to determine the effect of **4** on the production of β-lactamase.

An antibiotic gradient was made to create a standard curve using lactamase enzyme to compare results to. And then test against MRSA, **4** and 0.5 µg mL^{-1} penicillin together to determine the β-lactamase activity. *N* = 3 per condition.

5.3.4 Survival responses to compound treatment

Larvae were inoculated with 10 µL aliquots of either MRSA of OD_{600} nm 0.175, **4** at 10 mg kg^{-1}, DMSO or phosphate buffered saline (PBS) into the rear left proleg. Other sets of larvae were infected with MRSA of OD_{600} nm 0.175 in to the left rear proleg with subsequent administration of **4** (10 mg kg^{-1}) or vancomycin (50 mg kg^{-1}) into the right rear proleg. Larvae were then incubated at 37 ˚C and survival counts were performed at 24 h intervals for a 72 h duration. A control group of untreated larvae was included for reference. Survival was determined by visualising the levels of melanisation and rate of activity. *N* = 10 per condition.

Synergistic combinations of **4** at 0.5 mg kg^{-1} and 4 mg kg^{-1}, penicillin G (Pen) at 128 mg kg^{-1} and streptomycin at a concentration of 10 mg kg^{-1} and 40 mg kg^{-1}. These were made in solution prior to injection and one injection was administered in the right rear proleg. MRSA was additionally added in certain conditions to determine the synergistic effect *in vivo*. The larvae were incubated at 37 ˚C and survival counts were performed at 24 h intervals for a 72 h duration. A control group of untreated larvae was included for reference. Survival was determined by visualising the levels of melanisation and rate of activity. *N* = 10 per condition.

All results were analysed using Graphpad Prism version 7.0 to determine significant differences between samples, with $p < 0.05$ being considered as statistically significant in all cases. The data was presented as mean, standard error of the mean and standard deviation with t-tests, one-way and two-way ANOVA's and log-rank analyses being used to determine differences between the data.

5.4 Results

5.4.1 Resistance profiling

To determine the resistance profiling of twenty multidrug resistant *S. aureus* strains, disc diffusion assays were conducted using M13 mast rings containing chloramphenicol 25 µg, erythromycin 5 µg, fusidic Acid 10 µg, oxacillin 5 µg, novobiocin 5 µg, penicillin G 1 unit, streptomycin 10 µg and tetracycline 25 µg) and incubated overnight with the zones measured the following day. Fusidic acid produced the largest observed zones of inhibition with an average diameter of 30.73 mm (Table 5.1) across all of the species, with all strains identified as sensitive in accordance with EUCAST, with the highest ZOI occurring with the strain *S. aureus* USA200 at 36.10 mm. All of the strains additionally proved to be sensitive to the antibiotic according to EUCAST. Another highly effective antibiotics against all *S. aureus* strains was novobiocin which produced an average zone of inhibition of 26.90 mm and the antibiotic tetracycline had an average zone size of 24.49 mm across all strains however the *S. aureus* strains USA300, 57/92 and E2260 was resistant to this antibiotic with a ZOI of 0.17 mm and 0 mm respectively. Chloramphenicol had a significant affect proving to be sensitive to the bacterial strains apart from E2260 with a ZOI of 10.11 mm however overall the ZOI across all of the strains came to 21.17 mm. Erythromycin and streptomycin had average ZOI across strains of 12.21 mm and 14.47 respectively with erythromycin proving to have mixed sensitivity levels according to EUCAST with 50 % of strains being classed as resistant and 15 % intermediate. Few bacterial strains had an inhibitory zone when exposed to Oxacillin with 95 % of strains identifying as resistant with the exception of strain Btn2299 which was intermediate. Penicillin G only two strains; H65 and Btn2299 had a ZOI of 2.72 mm and 29 mm respectively with all results proving to be resistant to the antibiotic.

The antibiotics used in the present study produced significantly different sizes, thus demonstrating the antibiotic activity is affected by the classes of antibiotics used, one way ANOVA analysis confirmed this with a $p<0.001$. In addition to this, multiple strains of *S. aureus* had similar results demonstrating a similar antibiotic activity across strains of species with no significant difference found ($p=0.974$).

Table 5. 1: Mean zone of inhibitions produced by antibiotics against *S. aureus* strains. EUCAST sensitivity typing is shown as resistant (R), sensitive (S) or intermediate resistance (I).

Strain	Chloramphenicol 25 µg			Erythromycin 5 µg			Fusidic Acid 10 µg			Oxacillin 5 µg			Novobiocin 5 µg		Penicillin G 1 unit			Streptomycin 10 µg		Tetracycline 25 µg		
	Mean ZOI (mm)	SD	RSI	Mean ZOI (mm)	SD	RSI	Mean ZOI (mm)	SD	RSI	Mean ZOI (mm)	SD	RSI	Mean ZOI (mm)	SD	Mean ZOI (mm)	SD	RSI	Mean ZOI (mm)	SD	Mean ZOI (mm)	SD	RSI
H65	20.52	2.09	S	23.04	1.85	S	28.15	1.44	S	12.16	1.87	R	25.03	0.66	2.72	4.71	R	14.25	1.11	25.41	1.65	S
98.4	20.67	0.99	S	0	0	R	29.53	0.85	S	0	0	R	26.02	1.26	0	0	R	16.00	0.60	25.66	0.84	S
99ST	18.90	1.09	S	20.97	1.03	I	24.79	1.72	S	0	0	R	26.50	1.18	0	0	R	16.83	0.53	25.88	3.53	S
ARO	21.45	0.79	S	21.02	1.25	I	29.43	1.26	S	0	0	R	26.72	0.98	0	0	R	17.14	0.93	26.21	1.32	S
H182MRSA	19.52	0.90	S	20.13	0.59	I	28.68	1.28	S	0	0	R	26.45	1.12	0	0	R	16.96	0.78	25.75	0.61	S
UK96	18.83	0.51	S	0	0	R	31.03	0.82	S	0	0	R	25.16	2.31	0	0	R	14.70	0.94	25.01	4.83	S
NottmA2	23.79	1.89	S	0	0	R	30.91	1.62	S	0	0	R	25.60	1.03	0	0	R	13.91	0.89	30.22	1.26	S
ARI12	23.07	1.88	S	0	0	R	30.61	0.53	S	14.42	0.73	R	26.64	0.79	0	0	R	15.11	1.13	26.72	1.16	S
57/92	21.09	1.72	S	23.69	1.50	S	30.73	1.58	S	0	0	R	29.12	1.19	0	0	R	0	0	0	0	R
BK59	18.82	0.68	S	8.65	0.44	R	34.07	0.51	S	0	0	R	25.14	0.67	0	0	R	16.66	0.61	29.63	0.55	S
CDC16	21.69	1.92	S	0	0	R	35.32	0.66	S	0	0	R	27.25	0.30	0	0	R	16.66	0.96	30.92	2.70	S
E2260	10.11	0.19	R	27.75	0.27	S	31.01	0.57	S	12.07	1.46	R	28.57	1.20	0	0	R	0	0	0	0	R
Btn2299	24.31	4.39	S	27.73	0.32	S	29.60	2.29	S	21.48	0.68	I	29.33	0.34	29.00	0.99	R	19.21	0.86	29.83	0.66	S
Btn2289	23.21	0.76	S	21.87	1.12	S	27.83	1.23	S	12.93	0.86	R	27.45	0.81	0	0	R	15.12	0.69	27.92	0.77	S

USA300	22.34	0.49	S	0	0	R	30.82	0.49	S	0	0	R	26.73	1.74	0	0	R	16.24	0.30	9.95	0.17	R
USA800	21.61	2.33	S	25.46	0.91	S	30.88	1.79	S	14.43	1.57	R	25.63	0.88	0	0	R	16.46	0.98	27.63	2.41	S
USA200	23.84	1.37	S	0	0	R	36.10	2.21	S	0	0	R	27.98	1.93	0	0	R	17.69	0.98	35.70	0.85	S
HO	18.50	1.57	S	0	0	R	30.69	1.63	S	0	0	R	27.11	0.98	0	0	R	17.55	0.95	28.73	0.50	S
Sweden	24.57	1.37	S	23.91	0.44	S	29.83	0.98	S	0	0	R	26.29	0.55	0	0	R	13.54	0.37	26.81	0.40	S
NJ992	26.61	1.23	S	0	0	R	34.59	1.24	S	0	0	R	29.22	1.20	0	0	R	15.39	0.75	31.85	0.59	S

5.4.2 Effect of Ru **4** when combined with common antibiotics to determine synergistic status.

To determine synergistic combinations, a checkerboard assay was conducted with commonly used antibiotics and Ru **4** against MRSA. The MIC value for **4** was previously determined as 8 μg mL^{-1} against MRSA, and was the same for when testing the MIC of **4** alone (Table 5.2). All antibiotic combinations proved to be indifferent with FIC values in between 0.5-4 with the exception of **4** and Streptomycin a FIC value 0.375.

Table 5. 2: Synergistic combinations of Ru complex and antibiotics with the overall FIC value and synergistic status.

4 and antibiotic Combination	**MIC of Ru complex (μg mL^{-1})**		**MIC of Antibiotic (μg mL^{-1})**		**MIC Ru complex in combination (μg mL^{-1})**		**MIC of Antibiotic in combination (μg mL^{-1})**		**ΣFIC**	**Synergistic status**
	Mean	SD	Mean	SD	Mean	SD	Mean	SD		
Erythromycin	8	0	40	0	4	0	40	0	1.5	Indifferent
Penicillin G	8	0	8	0	8	0	0.5	0	1.0625	Indifferent
Streptomycin	8	0	80	0	1	0	20	0	0.375	Synergistic
Vancomycin	8	0	2	0	1	0	2	0	1.125	Indifferent
Ciprofloxacin	10.667	4.619	128	0	1	0	128	0	1.104	Indifferent

5.4.3 Determining β-lactamase inhibition mediated by the degradation of Nitrocefin

Following the results from the synergy study, although indifferent additional investigations were carried out to determine the mechanism behind the decreased concentration of penicillin G when incubated with **4**. Nitrocefin changes from a yellow colour to red when degraded by the enzyme β-lactamase at an absorbance of 482 nm. Bacterial cells were treated and sonicated to disrupt the cells, a working concentration of nitrocefin of 1 mg mL^{-1} was added and incubated until a colour change from yellow to red was seen. Due to the yellow colour of **4**, an initial study was done to determine whether a colour change was observed. Varying concentrations of **4** was tested to determine whether a colour change could be observed, in which even at the highest concentration of 8 µg mL^{-1}, a colour change was detected. At concentrations of **4** at 16 µg mL^{-1} and above, any colour change was not able to be detected due to the increased yellow colour of the complex and therefore not used (Data not shown).

No colour change was observed after incubating controls for 0.5 h with nitrocefin demonstrating that the nitrocefin was not being degraded by β-lactamase due to none being present.

Over a 24 h incubation (Appendix Table 8.8; Figure 5.2) the samples containing MRSA (Columns 2,3,4) all experienced a colour change demonstrating β-lactamase activity except row E which contains a known β-lactamase inhibitor tazobactam (1 mg mL^{-1}). Following sonication *S. aureus* does not grow, as determined through plating on agar (Data not shown). A *S. epidermidis* was used as a non-β-lactamase producing control which demonstrated no significant evidence of breakdown of nitrocefin compared to control treatments alone (data not shown) . The control samples all remained yellow with no

activity being present with OD's ranging after 24 h between -0.007 to 0.062 apart from **4** alone which presented an OD of 0.213 due to its yellow colour. Upon incubating **4** and MRSA the OD increased to 0.422 demonstrating an impact on the amount of β-lactamase being produced and with the addition of penicillin the OD increased to 0.449. Compared to MRSA alone and MRSA incubated with penicillin alone (OD's respectively 1.269 and 1.324) the impact of **4** is lower than that of penicillin alone however the addition of penicillin and **4** increased the OD by 6.4 %.

Two way ANOVA analysis confirms significance between the OD values all of the conditions (p<0.0001) demonstrating a difference in β-lactamase production with each condition. Additionally the time for the degradation to occur is highly significant (p<0.0001) over the 24 h and correlation analysis confirming highly significant between the time for the degradation and each condition with all MRSA combinations having significance with an increase in OD occurring with an increase in time due to the increased concentration of β-lactamase with the exception of tazobactam which was not significant (p=0.1455). *S. epidermidis* treated with penicillin, **4** and tazobactam were all highly significant (p<0.0001) and control conditions had significance for media, **4** and **1** alone, (p=0.0002) for penicillin alone, (p=0.0393) for PBS alone and DMSO, water and tazobactam alone with p values of 0.2345, 0.7400 and 0.2282 respectively. All conditions and media alone had a strong positive correlation with an increase in the OD occurring with an increase in time, r values ranging between 0.7832 to 0.9947 with the exception of USA300 and tazobactam which has a weak positive correlation with an r value of 0.2997. The other control conditions has a varying degrees of negative correlation with controls including **4** and **1** with a strong negative correlation of -0.8651 and -0.8563 respectively, penicillin and PBS has correlations of -0.683

and -0.4146 and weak negative correlations of -0.2467, -0.06988 and -0.25 for DMSO, water and tazobactam respectively.

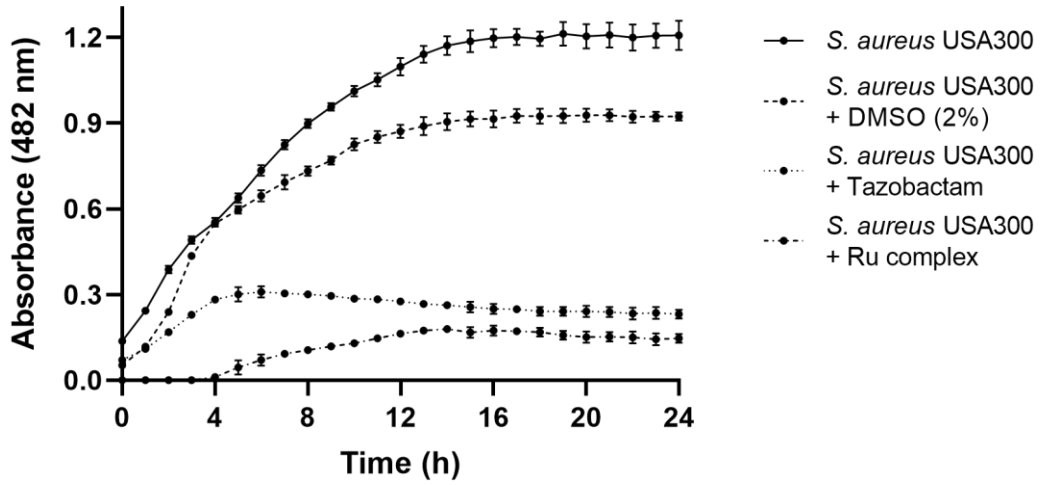

Figure 5. 2: Change in OD over a 24 h period of the degradation of nitrocefin with 24 different conditions.

(A)

MRSA alone	*S. epidermidis* alone	Media
MRSA + **4**	*S. epidermidis* + **4**	**4** alone
MRSA + Penicillin	*S. epidermidis* + Penicillin	Penicillin alone
MRSA + **4** + Penicillin	*S. epidermidis* + **4** + Penicillin	**1** alone
MRSA + Tazobactam	*S. epidermidis* + Tazobactam	DMSO alone
MRSA + DMSO	*S. epidermidis* + DMSO	Water alone
MRSA + Penicillin + DMSO	*S. epidermidis* + Penicillin + DMSO	PBS alone
MRSA + **1**	*S. epidermidis* + **1**	Tazobactam alone

(B)

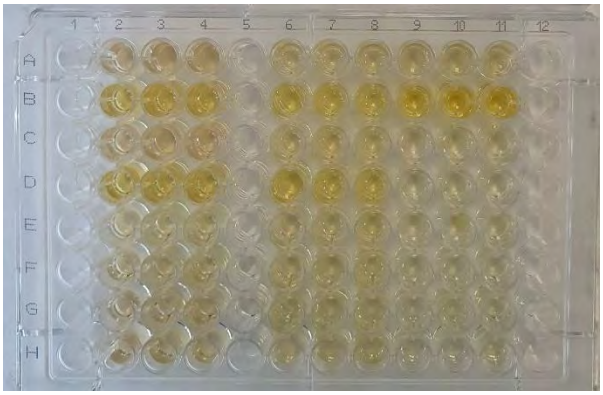

(C)

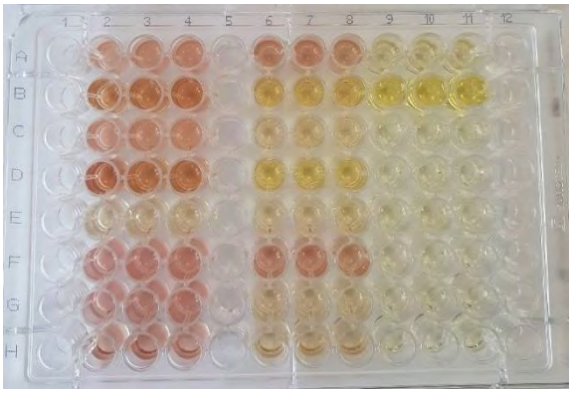

Figure 5. 3: (A) Layout of the 96 well plate with the respective conditions. (B) Image of the 96 well plate following the 20 minute incubation with nitrocefin and analysis at 386 nm. (C) Wells following 24 h incubation with red being the degradation of nitrocefin.

5.4.4 *Galleria mellonella in vivo* modelling

Modelling was carried out to determine the optimum concentration of MRSA which was required to simulate an infection over a 72 h period. Survival was monitored at 24 h intervals over a 72 h period with increased signs of melanisation indicative of larvae mortality as shown in Figure 5.4.

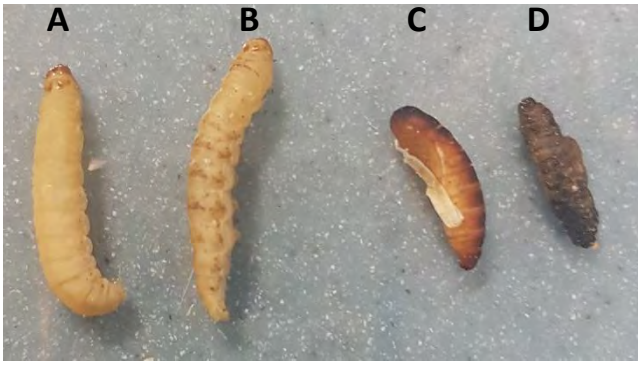

Figure 5. 4**:** Stages of *G. mellonella* survival. Increasing degree of melanisation from **(A)** pale (viable), **(B)** localised melanin accumulation, **(C)** entry to a cocoon state and **(D)** systematic melanisation (non-viable).

Larvae (10 biological repeats, 3 technical) were infected with MRSA at an OD_{600} of 0.175 and the survival phenotype was assessed after subsequent administration of **4** (10 mg kg^{-1}) or vancomycin (50 mg kg^{-1}). *G. mellonella* survival reduced by 3.4% with no injection administered or injection with PBS as a control after 72 h (Appendix Table 8.9; Fig. 5.5). Administration of the DMSO solvent control reduced larvae survival by 13.4 % after 72 h. In the presence of strain MRSA, only 33.3 % of *G. mellonella* survived after 72 h of infection (Fig. 5.5, c). The addition of vancomycin increased this survival rate to 83.3 % (Fig. 5.5, f) but following treatment with **4** only 13.3 % of larvae survived (Fig. 5.5, h). In comparison, 100 % and 76.6 % of larvae survived treatment with vancomycin (Fig. 5.5, g) and **4** alone (Fig. 5.5, d) without infection. This indicated that the addition of **4** to rescue the infection phenotype

was detrimental to the larvae as the mortality rate increased beyond those without treatment. A logrank analysis demonstrated a significant difference in survival compared to the control group of larvae (p<0.0001), where the combination of MRSA with **4** had an overall negative effect on survival.

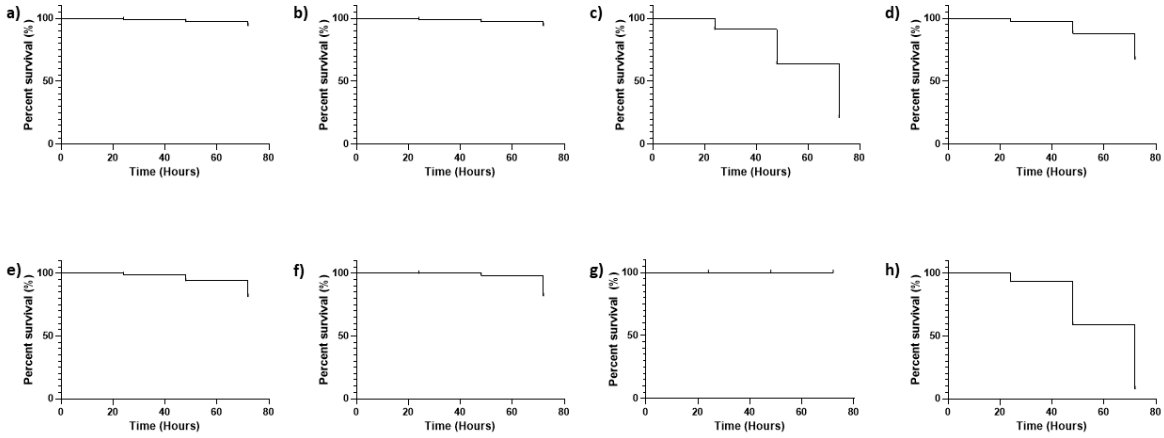

Figure 5. 5**:** Percentage survival of *G. mellonella* after exposure to different conditions. *N* = 10 per condition. a) No injection, b) PBS alone, c) MRSA at an OD_{600} of 0.175, d) **4** at a concentration of 10 mg kg^{-1}, e) 10% DMSO alone, f) Vancomycin (50 mg kg^{-1}) and MRSA, g) Vancomycin alone at a concentration of 50 mg kg^{-1} and h) **4** (10 mg kg^{-1}) and MRSA (*N*=3).

5.4.5 *G. mellonella* modelling with synergistic combinations of **4** with Penicillin G and Streptomycin.

Combinations of **4** and antibiotics (Fig. 5.6) were injected into *G. mellonella* to determine *in vivo* effects larvae were inoculated with **4** at 0.5 mg kg^{-1} and 4 mg kg^{-1}, in addition to penicillin G (Pen) at 128 mg kg^{-1} and streptomycin at a concentration of 10 mg kg^{-1} and 40 mg kg^{-1}.

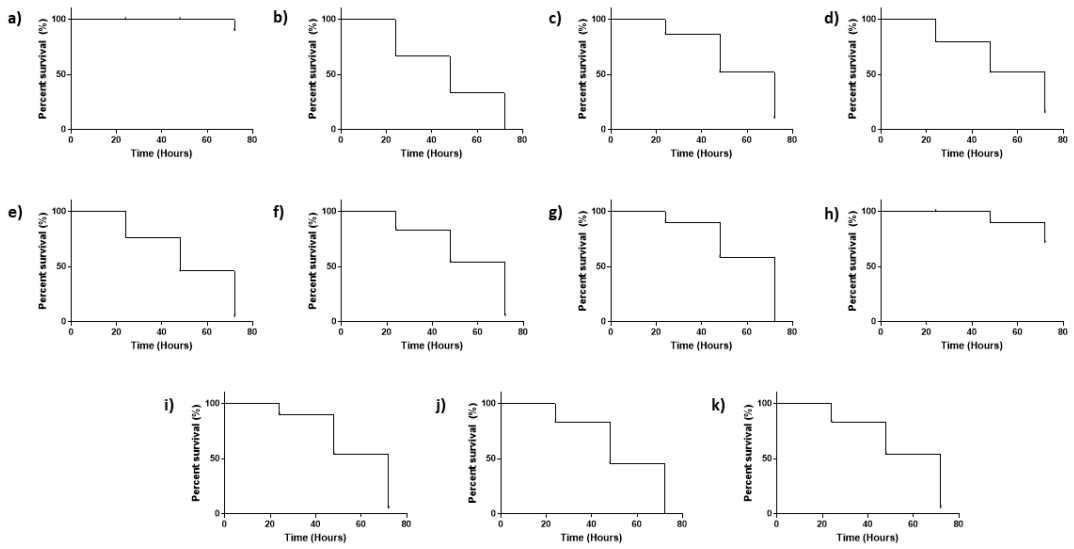

Figure 5. 6**:** *G. mellonella* percentage survival with synergistic combinations. a) Penicillin 128 mg kg^{-1} b) **4** 4 mg kg^{-1} + Penicillin 128 mg kg^{-1} + Bacteria c) Penicillin 128 mg kg^{-1} + Bacteria d) **4** 0.5 mg kg^{-1} e) **4** 0.5 mg kg^{-1} + Bacteria f) Streptomycin 10 mg kg^{-1} g) Streptomycin 10 mg kg^{-1} + Bacteria h) Streptomycin 40 mg kg^{-1} i) Streptomycin 40 mg kg^{-1} + Bacteria j) Streptomycin 10 mg kg^{-1} + **4** 0.5 mg kg^{-1} , k) Streptomycin 10 mg kg^{-1} + **4** 0.5 mg kg^{-1} + Bacteria.

Penicillin alone (Fig.5.6a) maintained survival in *G. mellonella* with an average of 86.6 % survival over the three different concentrations whereas **4** over 72 h had an average survival of 33.3 % (Fig.5.6d). With addition of the synergistic combinations and bacteria to the *G. mellonella* however there was a 100% mortality rate after only 48 h (Appendix Table 8.10).

A logrank Mantel-Cox analysis demonstrated a significant difference in survival compared to the control group of larvae (p <0.0001), where the combination of MRSA, **4** and antibiotic had an overall negative effect on survival.

5.5 Discussion

5.5.1 Susceptibility testing of multiple strains of *P. aeruginosa* with commonly used antibiotics compared with the antimicrobial activity of **4**.

Public health England states that in 2018, 21.3 cases per 100,000 of *S. aureus* infection occurs in England, Wales and Northern Ireland affecting those at both the young and older extremes of age (Public Health England, 2019). Vulnerable groups with susceptibility to wound infections and slow healing could benefit from the development of **4** as a novel antimicrobial. Similar infection rates are observed in other countries. According to a study by Kassam *et al*., (2017), in Tanzania 144 species of pathogenic bacteria were isolated from 93 patient wound sites with *S. aureus* (16 %) and *P. aeruginosa* (10.4 %) being the most commonly isolated pathogens.

The susceptibility profiles for *S. aureus* in the present study proved to be similar to others, one study found resistance in 69 % of 85 clinical samples of *S. aureus* to penicillin, lower than the results found in this work where 100 % of strains proved resistant to penicillin. In contrast oxacillin proved more resistant in the present study with 95 % of strains being resistant compared with 46 % (Wankhade *et al*., 2017). In a second study the resistance profiling with penicillin was 100 % identical to this work, whereas with erythromycin 17.7 % of the 1116 *S. aureus* isolates was resistant (Rağbetli *et al*., 2016).

In a study where 239 MRSA isolates were tested for antimicrobial susceptibility, 100 % of isolates were resistant to both penicillin and oxacillin. Tetracycline and chloramphenicol has high resistance rates of 99.2 % and 83.3 % respectively (Jiang *et al*., 2018), in comparison to the present study where both antibiotics produced resistance rates of 15 % and 5 % respectively for 20 isolates. Two genes responsible for tetracycline resistance are *tet*K and *tet*L in which one study found that out of 121 *S. aureus* isolates 47.9 % were resistant and

the genes were found in 82.8 % and 56.9 % of tetracycline resistant isolates for *tet*K and *tet*M respectively and both genes were present in 39.7 % of the resistant isolates (Khoramrooz *et al*., 2017). The MIC's of **4** remained at 8 µg mL^{-1} with the exception of CDC16 and ARI12 where the MIC's were 4 µg mL^{-1} and 16 µg mL^{-1} respectively, this is consistent with larger ZOI in the presence of fusidic acid and novobiocin. This could be due to the mechanisms of action being similar to **4**. **4** has an increased ionic charge and therefore has a high affinity for negatively charged DNA and proteins (Southam *et al*., 2017) thus this complex may be able to inhibit cell cycle completion (Meier *et al*., 2017). **4** has previously been found to specifically target guanine DNA nucleotides (Hoeschele *et al.*, 2007). Fusidic acid inhibits the synthesis of proteins resulting in peptide translocation and ribosome disassembly not occurring within the cell by binding to EF-G-GDP, as well as causing mutations in the gene *FusA* associated with EF-G (Fernandes., 2016). Novobiocin targets topoisomerases (Shirude and Hameed., 2012) specifically DNA gyrase, competitively inhibiting ATP hydrolysis (Murphy *et al*., 2017) and thus DNA synthesis by preventing DNA supercoiling (Brown., 2017). The similar mechanisms between these antibiotics and **4** explain why the zone sizes were larger compared with other antibiotics and the low MIC value of all strains of *S. aureus* tested in the present study.

5.5.2 Synergistic combinations with metallic based complexes and commonly used antibiotics

The results of the experiment in the present study indicated that the addition of **4** to commonly used antibiotics made little difference to the activity of the antibiotic as shown by the indifferent majority of the FIC readings determining the activity to be indifferent. Antibiotics erythromycin, vancomycin and ciprofloxacin exhibited the same MIC when alone

and in combination with **4** with the checkerboard method. The MIC of penicillin G alone was higher than when in combination however the MIC of **4** remained the same, resulting in an indifferent synergistic effect whereas both **4** and streptomycin MIC values decreased when in combination meaning synergy occurs.

Penicillin and silver nanoparticles were documented by multiple sources as having an increased antibacterial effect against multiple strains of bacteria including *S. aureus* (Panáček *et al*., 2016; Xu *et al*., 2017). The efficacy of silver nanoparticles have been demonstrated with checkerboard assay with Amikacin where a fold change of 2 and 8 occurred for *S. aureus* and *P. aeruginosa* respectively and the nanoparticles combined with ampicillin with a 1 and 32 fold change for each pathogen respectively. Silver nanoparticles have been tested with amoxicillin, cefixime and levofloxacin where synergy was observed with FIC values ranging between 0.12 - 0.25 µg mL^{-1} (Asghar *et al*., 2020).

Similar to a study conducted by Nishanthi *et al*., 2019, the presence of metal particles with antibiotics enhances the antimicrobial effect with *Bacillus* sp. The zones of inhibitions of penicillin and streptomycin increased compared to the antibiotic alone with a 17.9 % fold increase with gold and platinum nanoparticles and 10.7 % increase with silver nanoparticles for penicillin. Streptomycin showed a similar pattern with 23.8 %, 33.3 % and 28.6 % fold increases for gold, silver and platinum nanoparticles respectively. Synergy with ampicillin and kanamycin was observed with multiple metals in one study using nickel and cobalt at half of the MIC concentrations with other metals cadmium and zinc displaying inhibitory effects with ampicillin and low concentrations of zinc (MIC 0.12 mM) additionally exerted synergistic effects with kanamycin (Garza-Cervantes *et al*., 2020).

Zinc and ionophore complex PBT2-Zinc allowed for the sensitisation of MRSA strain USA300 to ampicillin, erythromycin and oxacillin possibly caused by reactive oxygen species being involved in the mechanism of action as a result of the rescue of glutathione (Bohlmann *et al*., 2018). In another study using *S.* aureus Zinc oxide nanoparticles increased the effectiveness of antibiotics such as azithromycin, cefuroxime, cefotazime, chloramphenicol and oxytetracycline and silver nanoparticles additionally caused increased efficacy with ampicillin and fosfomycin (Abo-Shama *et al*., 2020).

Penicillin has previously shown synergism with essential oils, including carvacrol, cinnamaldehyde and thymol against MRSA (Palaniappan and Holley, 2010) Two of the essential oils, carvacrol and thymol have a ring of delocalised electrons which helps to improve the positioning on the cell membrane of bacteria (Langeveld *et al*., 2014) potentially influencing the synergistic reaction (Owen and Laird., 2018). Ciprofloxacin however proved antagonistic with *S. aureus* when combined with essential oils (Van Vuuren *et al*., 2009) which is in contrast to the present study where synergy between *S. aureus* with ciprofloxacin and **4** was indifferent.

Synergistic combinations have been found with different nanoparticles and *S. aureus* and β-lactam antibiotics, including penicillin (Muzammil *et al*., 2018). Silver nanoparticles have been found to exhibit synergistic action with *S. aureus* strain ATCC 6538P with β-lactams 13.5% (Hassan *et al*., 2016) and another combination with cephalothin and cefazolin with an increase of 3.6% when combined with 20 μg mL^{-1} of silver nanoparticles (Hari *et al*., 2014) and ampicillin was synergistic with the same type of nanoparticle against *S. aureus* strain 25923 (Hwang *et al*., 2012). Other metals including iron, gold and titanium nanoparticles have additionally proved synergistic with other antibiotics. Iron oxide nanoparticles in

combination with streptomycin and amoxicillin with increasing zone of inhibition between 14 and 20 mm with an increase in concentration up to 80 mg mL^{-1} of streptomycin (Kooti *et al*., 2015) and an increase in 9.9 % of inhibition with amoxicillin (Khashan *et al*., 2016). Gold nanoparticles combined with a β-lactam cefaclor caused a reduction in MIC to 10 mg mL^{-1} (Rai *et al*., 2010) and ampicillin had a lesser response with a 12 % increase in zone of inhibition in another study (Saha *et al*., 2007). Titanium nanoparticles proved synergistic with penicillin G against MRSA with an increase in 10 mm zone size and significant improvement in antibiotic efficacy (Roy *et al*., 2010).

Other metal complexes have been proven to exhibit synergistic effects with antibiotics previously. Silver nanoparticles have been used against a wide range of antibiotics in multiple studies all outlined by Möhler *et al*., 2018. Streptomycin has been used in synergy studies with silver nanoparticles where a 9.5% fold increase in activity was observed (Baker *et* al., 2017). Similar results were observed with ampicillin and nanoparticle combinations for *S. aureus* with FIC values ranging between 0.46 and 0.48 for 1 % doping with Fe, Mn and Co and a value of 0.44 with 10 % Cu (Sharma *et al*., 2016).

Ruthenium hasn't been found to exhibit synergism with other β-lactam antibiotics, for example cephalexin with a checkerboard assay confirming a FIC index of >0.5 with the ruthenium compolex $[Ru(dmp)_2(CAPIP)](ClO_4)_2$ (Liao *et al*,. 2021). A different complex, cis-$[RuCl_2(dppb)(bqdi)]^{2+}$ (dppb = 1,4-bis(diphenylphosphino)butane and bqdi = o-benzoquinonediimine), was found to be synergistic with a different β-lactam, ampicillin, with a FIC value of 0.187 (Andrade *et al*., 2020). Another ruthenium complex $[Ru(dpa)_2(BTPIP)](PF_6)_2$ however, showed synergism with gentamicin and tobramycin with FIC values of 0.16 and 0.28 respectively against *S. aureus* (Wang *et al*., 2021). Synergism

with gentamicin and $[Ru(dmb)_2(BTPIP)](ClO_4)_2$ was due to the inhibition of the regulatory function of *Sa*CcpA, a catabolite control protein A (b Liao *et al*., 2021) another aminoglycoside, kanamycin was additionally discovered to be synergistic with the ruthenium complex $[Ru(phen)_2(ETPIP)](ClO_4)_2$ however no other antibiotics tested were synergistic including β-lactams (Liao *et al*., 2020).

$[Ru(bpy)_2(BTPIP)]^{2+}$ had high antimicrobial activity against drug-susceptible *S. aureus* with a MIC value of 0.016 mg mL^{-1} and additionally had the capability to disrupt biofilm formation (and was shown to inhibit biofilm formation and, thus, prevent bacteria from developing drug resistance. $[Ru(bpy)_2(BTPIP)]^{2+}$ (Bu *et al*., 2020) and $[Ru(phen)_2(ETPIP)]^{2+}$ were found to have synergistic activity with aminoglycoside antibiotics gentamicin and kanamycin (Liao *et al*., 2020).

Other Ru(III) complexes have been found to have antagonistic activity when combined with trimethoprim (Demirezen *et al*., 2012) however it was found that Ru complexes similar to **4** with the half-sandwich Ru(II)–arene complex [Ru(η^6-p-cymene)] when combined with a ciprofloxacin derivative CipA demonstrated higher activity than ciprofloxacin alone. It was hypothesized that the complex may interfere with DNA repair and efflux mechanisms in cells, causing high cytotoxicity (Ude *et al*., 2016). In comparison with the present study where ciprofloxacin was found to be indifferent, this could be due to the complex targeting human cell lines rather than bacteria.

Ruthenium complexes have been found to be an antimicrobial adjuvant with multiple antibiotics, however little research has been established of ruthenium complexes with β-lactams and even less so with penicillin. This novel research could prove promising, breaking the resistance of penicillin when treating *S. aureus.* As it is one of the most commonly

prescribed antibiotics globally (Yip and Gerriets., 2022), this synergistic mechanism could prove beneficial in the treatment of thousands of people. **4** proved to be synergistic with streptomycin. Acting as a resistance breaker, **4** may be targeting bacterial DNA, perhaps specifically the *mecA* gene. This would prevent the transcription and translation of β-lactamases, thus the degradation of penicillin does not occur, allowing for it to disrupt cell wall synthesis.

5.5.3 Effect of **4** upon the production of β-lactamase in the presence of penicillin through the degradation of nitrocefin in a colorimetric based assay.

Following the results in section 5.4.2, penicillin was chosen as the antibiotic to explore further as one of the first antibiotics affected by antimicrobial resistance. Although the synergistic status was indifferent, there was a notable difference in the MIC. The synergism between **4** and penicillin is intriguing with the hypothesized mechanism involving the decreased production of β-lactamase. This assay confirmed that the presence of **4** causes a reduced concentration of β-lactamase by the MRSA. The nitrocefin protocol is sensitive to the smallest amounts of β-lactamase, making it a perfect assay (Vergis *et al*., 2018).

In a study investigating enteroaggregative *E.coli* isolates, 41.9% of 74 isolates were found to be producers of extended spectrum β-lactamases through a colour change following incubation for 30 minutes and has proved both a sensitive and accurate test for measuring β-lactamase activity (Vergis *et al*., 2018). Similar to the present study, upon investigating *E. coli* that were resistant to β-lactam antibiotics such as ampicillin when analysed in a microplate reader using a dual-enzyme trigger-enabled cascade technology (DETECT), the yielded score of 1.026 was discovered and susceptible samples had a core of 0.2990 (deBoer *et al*., 2018). In the present study *S. aureus* alone had an OD of 1.269 conveying resistance

to our β-lactam penicillin and when incubated with **4** the OD of the nitrocefin decreased to 0.449 potentially allowing penicillin to exhibit its antimicrobial action.

A study using nitrocefin degradation to determine susceptibility to penicillin found the gene *blaZ,* in highly susceptible *S. aureus* isolates, was not detected and therefore not expressed in sensitive strains (Matono *et al*., 2018). Typically, all *S. aureus* strains resistant to penicillin are positive for the gene *BlaZ* through PCR testing, as demonstrated by zones of inhibition of 245 blood culture isolates with penicillin all conferring a zone of greater than 26 mm and all tested positive through PCR for the *BlaZ* gene (Hagstrand Aldman *et al*., 2017). Additionally the *blaZ* gene is found in more than 90% of *S. aureus* isolates derived from humans (Peacock and Paterson., 2015). Ruthenium complexes are well documented to cause DNA damage due to the production of ROS (Jain *et al*., 2022). Certain Ru complexes, including ones tested by Smitten *et al*, enter the bacterial cell and binds to DNA preferentially (Smitten *et* al., 2020) and in *E. coli* cells following an hour incubation, cell length is increased and multi-nucleation occurs (Dwyer *et al*., 2012). In *S. aureus* cells, the ruthenium complex is found to be localised in the centre of bacterial cells, where the DNA is located suggesting preferential binding similar to *E. coli*, in addition to this an Ames fluctuation test confirmed DNA mutagenesis in response to the Ru complex [Ru(3,4,7,8-tetramethyl-1,10-phenanthroline)(tpphz)][PF_6]$_2$ (Smitten *et al*., 2020). Perhaps **4** targets the DNA and causes mutagenesis in the *blaZ* gene, thus preventing expression of β-lactamase, allowing penicillin to exhibit its normal antimicrobial action.

5.5.4 *In vivo Galleria mellonella* modelling with *S. aureus* and metallic based complexes

The *G. mellonella* wax moth larvae was used due to the similarities between their immune response and the mammalian innate immune response (Desbois and Coote, 2011). The larval immune response is categorised into humoral and cellular. Melanisation is the main larval immune mechanism carried out by producing melanin to encapsulate pathogens at the wound site (Tsai *et al*., 2015) and is demonstrated as melanin deposits increased until death is observed. Larvae in response to bacterial infection alone demonstrated 33.3 % survival after 72 h but with the addition of **4** this decreased to 13.3 %, suggesting antagonistic effects within the larval model. In contrast, treatment of larvae with vancomycin cured infected larvae (83.3 % survival). **4** is tolerated well within eukaryotic models (Arshad et al., 2017) where anticancer activity has been explored, although the predicted effective drug concentration is less than would be required for effective antimicrobial therapy. However, in a study conducted by Rochford et al., (2018), the cisplatin anticancer agent was administered to larvae at 100 µg with 90 % mortality of the larvae after 72 h, whereas at 10 µg there was 6 % mortality. **4** however exhibited 76.6 % mortality over 72 h with 10 mg kg^{-1} meaning that a much higher concentration of **4** exhibits a lower mortality to *G. mellonella* at much higher concentrations than cisplatin over the same period of time.

Upon infection with *S. aureus* inoculums of $2x10^4$ – $2x10^6$ cells per larvae where at $2x10^4$ in which 100 % of larvae survived after 72, whereas $2x10^6$ cells decreased in viability to 80 %, 55 % and 10.2 % for 24, 48 and 72 h respectively (Sheehan *et al*., 2019). Injecting *G. mellonella* in this fashion causes nodules to be produced in a similar fashion to skin abscesses in tissue infections in humans (Kobayashi *et al*., 2015). Upon incubation with the

largest number of bacteria, an increase in hemocytes within 4 h of infection (Sheehan *et al*., 2019).

Inoculating larvae with *S. aureus* strain ATCC 11195 had similar results to the present study where an increased inoculum caused a decreased percentage of survival in the larvae in a dose dependant manner. When paired with vancomycin the survival of the bacteria increased significantly. When treated with peptide epidermicin little antimicrobial activity was found *in vivo* this could be due to the distribution within the *G. mellonella* and the bioavailability of the peptide (Gibreel and Upton., 2013).

With *S. aureus* strains ATCC 29213, ATCC 43300, N54, and N9 at a CFU of 10^6 survival rates varied between 20-60 % and at 10^3–10^4 CFU injected per larvae in 5 days survival was between 70-100 %. Thus a concentration of 10^6 cells was used.

The drug candidate 1,3-dibenzyl-4,5-diphenyl-imidazol-2-ylidene silver(I) acetate was tested against *S. aureus* and *G. mellonella* where at a concentration of 25 µg mL^{-1} inhibited bacterial growth by 71.2 ± 1.28 % and increased with concentration. In the *G. mellonella* survival was not affected at a concentration if 250 µg mL^{-1}, however when increased to 500 µg mL^{-1} viability reduced by 40 % following a 24 h incubation. Upon subsequent incubation with *S. aureus* following a 72 h incubation survival was low at 15 %, in combination with the silver complex survival ranged between 36.7 – 46.7 % for the concentrations 10, 100 and 250 µg mL^{-1} (Browne *et al*., 2014). Additionally this compound failed to boost the immune response in the larvae as demonstrated by the hemocyte count not increasing and a number of proteins involved in the immune response had reduced expression thus the immune response within the larvae was non-specific (Tacke., 2017).

Copper complexes with an MIC_{50} value of less than 5 µM against *S. aureus.* When injected into *G. mellonella* at a concentration of 0.25 mg mL^{-1} complexes $[Cu(ES\text{-}5\text{-}phen)(DPQ)]^{2+}$ and $[Cu(EE\text{-}5\text{-}phen)(DPQ)]^{2+}$ reduced the viability of the *G. mellonella* in 72 h by 60 % and 20 % respectively and $[Cu(ES\text{-}5\text{-}phen)(DPPN)]^{2+}$ and $[Cu(EE\text{-}5\text{-}phen))(DPPN)]^{2+}$ by 20 %. At concentrations above 0.5 mg mL^{-1} resulted in complete death following incubation for 72 h. Upon incubation with both *S. aureus* and the copper complexes mortality reduced to 20 – 40 % after 24 h incubation and with incubation with $[Cu(ES\text{-}5\text{-}phen)(DPPN)]^{2+}$ and $[Cu(EE\text{-}5\text{-}phen))(DPPN)]^{2+}$ where 100 % *G. mellonella* survival was observed following 24 h and 80 % after 48 h (Barrett *et al*., 2018).

In one study a Ru complex, (2-([1,1'-biphenyl]-4-yl)-1H-imidazo[4,5-f][1,10]phenanthroline)-bis(4,4'-dimethyl-2,2'-bipyridine)-ruthenium bis(hexafluorophosphate) methanol solvate, significantly improved the survival rates of *G. mellonella* when injected following an hour incubation with *S. aureus* and showed similar results compared with a Gentamicin trial. Additionally when treated with the Ru complex alone, it displayed similar survivability compared with PBS demonstrating low toxicity and high biocompatibility (Chen *et al*., 2022). In contrast, the present study proved **4** detrimental to the survival of infected *G. mellonella* although incubation with **4** alone where 76.6 % of *G. mellonella* survived. There was antagonistic activity when both **4** and *S. aureus* was incubated demonstrating lower biocompatibility in comparison with the complex studies by Chen *et al*.

Another Ru (II) polypyridine complex $Ru(dtbpy)_2Cl_2$ with pyrene ligands was observed over 4 days to determine toxicity *in vivo*. At 16 and 32 mg kg^{-1} the survivability was above 50 % however decreased with an increase in concentration of the complex. When *G. mellonella* was infected, treatment with 8 mg kg^{-1} improved survival to 62.5 % in comparison with a

DMSO control (Ma *et al*., 2022). **4** alone in the present study proved more toxic than a DMSO control in comparison with the study conducted by Ma *et al* and in addition more toxic than pyrene ligands.

When injected with *S. aureus* at a concentration of 10^7 CFU mL^{-1} 50 % of *G. mellonella* survived within 24 h, and when incubated for 30 min and injected with the Ru complex $[Ru(dmb)_2(BPIP)](PF_6)_2$ 75 % survived following incubation for 24 h and dropped to 37.5 % after 48 h at a concentration of 16 µg mL^{-1} (Wang *et al*., 2022). At 72 h in the present study, treatment of *S. aureus* with **4** only had a survival rate of 13.3 % demonstrating higher toxicity *in vivo* than the polypyridine Ru complex tested.

The *G. mellonella* wax moth larvae is used during this experiment due to the similarities the immune response is to the mammal innate immune response (Desbois and Coote, 2011). The larval immune response is categorised into humoral and cellular. The cellular pathway involves eight different cell types including granulocytes involved in the encapsulation and phagocytosis of pathogens (Pereira et al., 2018). Similar to neutrophils, hemocytes express a protein similar to calreticulin and use reactive oxygen species initiated by the NADPH complex in order to fight infection. In one study the use of a ruthenium complex does affect the number of granulocytes present in rats when administered through intraperitoneal injection (Tsai *et al*., 2015). Although the ruthenium complex cis-$(Ru[phen]_2[ImH]_2)^{2+}$ preserved granulocytes more efficiently than cisplatin at 2 mg kg^{-1} (2.68±0.05 $x10^3$ μl^{-1}), there was still a decrease in the number of granulocytes present when administered at 10 mg kg^{-1} (4.42±1.9 $x10^3$ μl^{-1}) (de Souza *et al*., 2017). Thus the decrease in granulocytes in the rat model could explain the antagonistic effect in the *G. mellonella* in the present study upon incubation with both **4** and *S. aureus* strains USA300. Insufficient encapsulation is able

to occur causing reduced bacterial clearance by the *G. mellonella* immune response. In addition to this the cis-$(Ru[phen]_2[ImH]_2)^{2+}$ complex promotes the inhibition of the respiratory chain, generating more lactic acid as a consequence of using glycolysis for energy production. The lactic acid in turn causing Ru(II) to enter a redox state, promoting longer cytotoxic activity in the rat (de Souza *et al*., 2017). This increased cytotoxicity within the *G. mellonella* would also explain the antagonistic activity of incubation with **4** and MRSA as both the infection and the Ru in redox state would be harmful to the larvae.

5.5.6 Synergistic antibiotic combinations with the *in vivo* model

As demonstrated by Betts et al. (2017), synergy with other commonly used antibiotics could induce a synergistic effect such as **4** when in combination with vancomycin within *G. mellonella* in the present study.

Metal-tdda-phen complexes when administered with antibiotics at low doses conferred increased toxicity within the *G. mellonella* model when compared to the individual complexes with gentamicin inoculated with manganese, copper and silver-tdda-phen complexes resulting in mortality of 86.7 %, 100 % and 93.3 % following 72 h incubation. It is suggested that a combination of complexes overstimulates the larval immune system thus causing mortality (O'Shaunghnessy *et al*., 2022).

Pleuromutilins as a natural product antibiotic were tested individually and in combination with tetracycline against *S. aureus* strains ATCC 29213, 43300, MSSA N54 and MRSA N9. As a monotherapy both valnemulin and tetracycline increased survival within *G. mellonella* models compared to infection alone but in combination together survival was significantly increased being 70 % and above for all strains. Similarly the combination of tetracycline with

both tiamulin and retapamulin significantly improved *G. mellonella* survival (Dong *et al*., 2017).

MRSA strain ATCC 33592 inoculated in *G. mellonella* within 5 days without treatment mortality rates reached 89 %, fosfomycin alone conferred 100 % survival and cefazolin alone had a mortality of 65 %. When the two antibiotics were combined, a mortality of 21 %, a decrease from the treatment alone (Kussmann *et al*., 2021).

Biaryl hydroxyketone complexes which are quorum quenching agents have additionally been tested for synergistic action in *G. mellonella* models as AgrA small molecules inhibitors in *S. aureus* thus blocking toxin expression and host cell damage (Greenberg *et al*., 2018). When larvae was infected with $2x10^7$ CFU of MRSA mortality of all *G. mellonella* was observed within 12 h. Similar results were expressed for cephalothin and nafcillin at concentrations of 30 mg kg^{-1}. The small molecule inhibitor F1 alone conferred 100 % mortality within 60 h which increased to 72 h and 78 h with additional treatment with cephalothin and nafcillin respectively, and the same pattern with F19 and F12 although addition of Nafcillin resulted in the same time for mortality of 42 h compared with 84 following additional treatment with cephalothin (Kuo *et al*., 2015).

Individual doses of amphotericin B increased survival within the larvae and pedalitin alone also increased survivability with a dose of 40 mg kg^{-1} resulting in 37 % of larvae alive after 7 days. The synergistic combination of 0.3 mg kg^{-1} amphotericin B and 10 mg kg^{-1} pedalitin was tested both individually and together within the model. After 5 and days, the larvae survivability was 50 % and 18.7 % for amphotericin B respectively and 26 % and 0 % for pedalitin. The combination together after 7 days resulted in survivability of less than 56 %

and decreased the prevalence of the yeast *Cryptococcus neoformans* (Sangalli-Leite *et al*., 2016).

5.6 Conclusion

S. aureus has transformed over the years to a highly resistant bacteria, with many antibiotics no longer effective. Against multiple strains oxacillin and penicillin G were found to be completely resistant across strains of species, with fusidic acid proving the most effective antibiotic out of the eight antibiotics. After observing the effects of **4** in chapter 3 (MIC 8 μg mL^{-1} with all strains), synergism was assessed with commonly used treatment for *S. aureus* infections where penicillin G and streptomycin had a positive result. There are many reasons behind the synergism however it is proposed that **4** targets bacterial DNA, causing a detriment to the transcription of the β-lactamase encoding gene *blaZ*. Thus penicillin can exhibit its normal antimicrobial action, this is plausible due to the lack of colour change of nitrocefin in the presence of the combination of penicillin G and **4**, suggesting lower production of β-lactamase in comparison to cells incubated with penicillin alone suggesting the mechanism of synergism could be regulation modification. *G. mellonella* testing suggested a detriment to the survival of the model following 72 h incubation with **4** and MRSA, with higher mortality compared with an untreated control. The high mortality has proved similar to the anti-cancer agent cisplatin, commonly used in human treatment, with further testing against human cell lines and other *in vivo* models, this potentially could be used in infection treatment.

Chapter 6: Discussion

6.1 Discussion

Antimicrobial resistance is an ever increasing global threat, with the prospect of mortality estimated to reach 10 million people by the year 2050 (Srivastava *et al.*, 2019). *Pseudomonas aeruginosa* is an opportunistic pathogen, highly resistant to multiple antibiotics and biocidal products used in both medical and industrial industries (Blair *et al*., 2015). As one of the WHO's top priority pathogens, investigations into novel antimicrobials or resistance breaking complexes are vital in order to combat infections. The presence of *P. aeruginosa* in wounds is a common phenomenon (Serra *et al*., 2015), due to the virulence factors possessed by the pathogen. *P. aeruginosa* has the ability to from biofilms within wounds due to the activity of pyoverdine enhancing the expression of biofilm associated genes (Brandenburg *et al*., 2019).

Using metals as an antimicrobial have been used for decades with silver being using in medical dressings to prevent infections of surgical sites and coating on medical implements (Mijnendonkx *et al.*, 2013; Gold *et al.*, 2018). Silver exhibits its antimicrobial activity through numerous mechanisms including generation of ROS, targeting DNA, proteins and lipids (Slavin *et al*., 2017). Other metals have additionally been assessed for their antimicrobial activity, as some metals have the capability to disrupt biofilm formation (Hobman and Crossman., 2015). Ruthenium complexes have multiple mechanisms of activity upon bacterial cells (Southam *et al*., 2017) and have the capability to carry ligands to enhance its lipophilicity and solubility (Meier *et al*., 2017).

The activity of ruthenium based complexes can be Gram-status dependent as demonstrated in chapter 2. Testing against a wide variety of Gram-positive and Gram-negative bacteria of each complex conveyed different results, **1** was highly active against Gram-negative

pathogens including *P. aeruginosa* where MIC values ranged between 8 μg mL^{-1} and 32 μg mL^{-1}, whereas little effect was shown against Gram-positive species with MIC values exceeding 32 μg mL^{-1}. The opposite effect was observed with **4**, with less antimicrobial activity being exhibited with Gram-negative species (MIC >256 μg mL^{-1}) in comparison to Gram-positive (MIC range from 8 μg mL^{-1} to 128 μg mL^{-1}). The increased resistance of certain complexes to Gram-negative species is due to the extra defence mechanism of Gram-negative bacteria, the cell wall. This makes treatment harder due to less efficient entry into the cell (Kumar *et al*., 2016) meaning Ru complexes must overcome the barrier before being able to exhibit antimicrobial action. Susceptibility across strains of species of *P.* aeruginosa and *S. aureus* was additionally tested with similar susceptibility profiles being observed with **1** and **4** demonstrating the consistency of each complex with similar action occurring across strains instead of being species specific. Out of all of the complexes tested in the present study, **1** and **4** were the most effective, this has been determined to be due to stability of the complexes and lower oxidation states causing accumulation of Ru ions within the bacterial cell (Southam *et al*., 2017). **4** has additional η^6-p-cymene ligand which provides additional antimicrobial activity as the Ru central ion as demonstrated in studies such as (Obradović *et al*., 2020).

Additionally cell death occurs in a time-dependent manner, thought to be due to the increase in the concentration of Ru ions over a 24 h time period (Chen and Yang., 2020). Previous studies using silver nanoparticles have identified a similar pattern however the Ru complexes achieved this with lower MIC values (Loo *et al*., 2018). Testing was conducted with two Gram-negative species with **1** to determine the effect of time on the growth kinetics of the bacteria. With *P. aeruginosa* strain PAO1 and *S. maltophilia* strain S1, the increase in concentration was proportional to the time taken to cause complete killing of

bacteria, this could be due to the increase in Ru ions present to exhibit a more effective antimicrobial effect (Chen and Yang *et al*., 2020)

As previously described *P. aeruginosa* has a tendency to form biofilms due to the presence of lipopolysaccharide in the cell walls causing persister cells to be more prevalent (Sultana *et al*., 2016). Biofilms are notoriously harder to treat in comparison to singular cells (Azam and Khan., 2019), however Ru complexes have an ability to cause decreased expression of extracellular matrix proteins (Li *et al*., 2013) and prevent initial bacterial adhesion by binding to adhesins on the membrane (Haiko and Westerlund-Wikström., 2013).

The ability to form biofilms is one reason why industrial strains of *Pseudomonas* are difficult to eradicate (Azam and Khan., 2019). Additionally industrial strains have increased expression of genes associated with resistance including quorum sensing (Freschi *et al*., 2019) and Pyocyanin (Grosso-Becerra *et al*., 2016). Due to these mechanisms **1** is not as effective as the medical strain *P. aeruginosa* PAO1, however in an industrial setting the concentration of complex used can be higher in comparison to human treatment without the need to consider cytotoxicity therefore could remain a viable option for industrial treatments. Additionally Ru complexes containing chloride ligands, similar to **1**, have the ability to cause aggregation of *Pseudomonas* cells preventing adhesion for biofilm formation (Jabłońska-Wawrzycka *et al*., 2020).

Resistance profiling identified a tolerance in many classes of antibiotics in both the Gram-negative bacterium *P. aeruginosa* and Gram-Positive bacterium *S. aureus*. This is due to an increased expression of efflux pumps (Kanai and Haldar., 2020), methylation of the N7 region of the bacterial ribosome (Cox *et al*., 2018) and increased expression of resistance genes (Khoramrooz *et al*., 2017).

Due to the increased resistance to antibiotics, using ruthenium as a resistance breaking agent could be vital in re-using formerly resistant antibiotics (Möhler *et al*., 2018). With multiple mechanisms of synergy (Sullivan *et al*., 2020) determining combinations is an exciting prospect. **1** was found to be synergistic with tetracycline with the bacteria *P. aeruginosa* PAO1, this could be due to **1** causing membrane damage to the bacterial cell similar to other Ru complexes (Sun *et al*., 2015), allowing entry of tetracycline to exhibit its usual antimicrobial mechanism of translation disruption (Grossman., 2016). Similarly with MRSA, synergism was discovered with **4** and streptomycin as well as other Ru complexes with aminoglycoside antibiotics (Andrade *et al*., 2020).

Due to the drastic difference between **4** and penicillin G, the mechanism was investigated with **4** in which it was discovered that the concentration of β-lactamase was reduced upon incubation, allowing for penicillin to exhibit antimicrobial action in addition to **4**. Ru complexes are known to cause DNA damage (Jain *et al*., 2022) and β-lactamase is encoded on the *BlaZ* gene (Hagstrand Aldman *et al*., 2017) therefore it is plausible that the transcription of this gene is inhibited by the Ru complex damage therefore the bacteria cannot produce β-lactase thus degradation of penicillin does not occur always for cell wall disruption.

In addition to **1** having antimicrobial activity, cellular cytotoxicity is limited, with an increase in concentration appearing to stimulate cell proliferation similar to MDA-MB-231 cells with the Ru complex $[Ru(C_2O_4)(\eta^6\text{-p-cymene})\{\kappa P\text{-}Ph_2PO(2\text{-}C_6H_4(SiMe_2{}^tBu))\}]$ (Biancalana *et al*., 2017). No significant cytotoxicity was discovered with multiple Ru complexes and cells, this could be due to the Ru complexes affinity to bacteria which could prevent arrest of G2/M phase of the cell cycle (Zhang *et al*., 2016) and crosslinking DNA does not occur (Lazarević *et al*., 2017). The cell proliferation could contribute to the increased speed of cell migration

and tube structures contributing to cell angiogenesis are increasingly present upon incubation of **1** in contrast with (Gu *et al*., 2016). In comparison with other studies where Ru complexes impede cell migration, **1** could prove smaller which has a positive impact (Kang *et al*., 2011). With fibroblasts, addition of **1** could allow for the transformation into myofibroblasts which are quicker cell migrators (You *et al*., 2017) as demonstrated by the results in chapter 3.

In addition to other cell lines, increased migration was discovered in macrophages (Parthasarathy *et al*., 2020). **1** could cause an increase in PI3K thus enhancing phagocytic capability of the macrophages (Amiel *et* al., 2010) and the overall migration of the cells. Perhaps addition of **1** could cause membrane composition to change in particular the carbohydrate and phospholipid content, allowing for macrophage pseudopodia to elongate and capture the bacteria effectively (El Mohtadi *et al*., 2020) as demonstrated by Figure 3.9.

A full thickness wound model with human epidermal keratinocytes and dermal fibroblasts was used as a 3D application of **1** as a wound healing agent. Incubating with *P. aeruginosa* PAO1 alone resulted in a delay in wound healing as expected and well documented (Jeffery Marano *et al*., 2015) due to binding to membrane receptors and inducing cell cycle arrest in the fibroblasts and keratinocytes (Landi *et al*., 2019). However when *P. aeruginosa* PAO1 is treated with **1**, wound healing occurs, reducing wound size by 87.5 % in comparison to the untreated wound at 0 h. Thus indicating **1** has a positive and significant (p>0.0001) effect on the rate of wound healing, potentially due to the transformation of fibroblasts into myofibroblasts as demonstrated with scratch assay studies allowing for migration to occur in a timely manner (You *et al*., 2017). The model does not have immune cells present and therefore could impede full wound closure, with immune cells present such as

macrophages, in a real-world situation, **1** could potentiate antimicrobial activity as shown by increased pseudopodia in host-pathogen interactions. Subsequently, this would lead to an increased rate of bacterial clearance and cellular migration, leading to full closure of the wound site as demonstrated previously with silver nanoparticle impregnated wound dressings (Phillips *et al*., 2015).

To determine the mechanisms of antimicrobial activity of **1**, multiple assays were conducted. Membrane damage appears to be one of the main mechanisms as shown through perturbations in the membrane of SEM imaging in multiple Gram-negative species. **1** might bind to the lipopolysaccharides on the surface of the cells causing disruption (Ibraheem *et al*., 2019) and decreased membrane potential (Zhao *et al*., 2020). Ru ions accumulate in the membrane due to the electrostatic force of the membrane attracting the ions, causing increasing damage (Breijyeh *et al*, 2020). This disruption in turn causes cell leakage as demonstrated by an increase in electrical conductivity of cellular suspension upon incubation with Ru complexes (Sun *et al*., 2015) and the increase in proteins and nucleic acids over time with incubation of **1**.

Additionally Ru complexes cause an increase in ROS which cause membrane damage (Liu *et al*., 2019) with an increase in ROS occurring in a dose and time dependent manner (Luo *et al*., 2014). An increase in ROS has been found to be related to macromolecular dysfunction (Liu *et al*., 2021) thus affecting the phospholipids in the bacterial membrane contributing to the perturbations. An increase in pyocyanin concentration in the *P.* aeruginosa strain PAO1 contributes to oxidative stress (Dong *et al*., 2021) due to the phenol group giving pyocyanin weak acidic properties causing cell membrane penetration (Hall *et al*., 2016) and free radical

production (McDermott *et al*., 2013) which additionally causes DNA and mitochondrial damage (O'Malley *et al*., 2003).

RNA sequencing analysis identified downregulation of genes associated with encoding proteins, including catalase, Ankyrin repeats, Barrel-sandwich domain of *CusB* or *HlyD* membrane-fusion and Pyridine nucleotide-disulphide oxidoreductase, vitally Ankyrin repeats allow for protein-protein interactions to occur within the bacteria ultimately causing membrane alterations (Kitamata and Suetsugu., 2023). In addition to this, genes associated with translation, affecting genes such as RNA polymerase and tRNA synthase causing a halt in the cell cycle, thus resulting in cellular mortality similar to the study using [Ru(phen-$PPh_3)_2$(dppz)]$(NO_3)_2$ where translation regulation was affected upon incubation (Wang *et al*., 2021). Membrane activity was additionally altered, with genes associated with the Barrel-sandwich domain of *CusB* or *HlyD* which is responsible for membrane-fusion via secretion systems (Kim *et al*., 2016) was affected upon **1** incubation, with genes downregulated, thus causing decreased detachment in soft-tissue infections and decreased colonisation (Turner *et al*., 2014). Other membrane associated genes affected by the incubation of **1** includes the outer membrane porin *OprD*, outer membrane efflux protein and the outer-membrane protein (*OmpH*-like), thus causing cellular perturbations as demonstrated by SEM imagery.

6.1.1 Potential for metal resistance

As with all potential bacterial treatments, resistance has the potential to evolve, an example being the rise of mercury resistance through continual use in dental amalgam fillings (Naguib *et al*, 2018). Bacteria have developed a resistance mechanism to reduce the metal ion Hg^{2+} to Hg^{0} which is volatile and leaves the bacterial cytoplasm as a result of low solubility and high vapour pressure. In *Staphylococcus* species resistance can be seen on

Staphylococcal cassette chromosome elements, having already been seen in MRSA present in livestock, with a potential for cross-resistance to occur (Argudín et al, 2019).

Summarised methods of metal resistance have been published by Bruins et al, (1999) identifying six potential mechanisms, including metal exclusion caused by a modification in the bacterial envelope, cell wall and cell membrane, allowing protection of metal sensitive areas of the cell for the prevention of antimicrobial effects. There may be an extracellular polysaccharide coating present which absorbs metal ions or a single gene mutation which may decrease metal ion permeability preventing access to the cell. Intracellular sequestration by protein binding; metal detoxification by enzymatic reaction which reduces metal toxicity; extracellular sequestration where glutathione is excreted adhering to metal particles preventing their antimicrobial action and finally a reduction of metal sensitivity allowing natural selection to eliminate sensitive bacteria.

There is a potential for **1** and **4** to become futile with constant exposure which can generate a mutation within the genome of the bacteria. This can lead to the formation of efflux pumps to remove the Ru ions out of the bacterial cell similar to P-type ATPase ZntA efflux pumps in *E.* coli zinc resistance cases (Takahashi *et al*, 2015). The formation of a 'metal sponge' similar to those that confer silver resistance such as *SilE* (Asiani *et al*, 2016). Additionally proteins may also be formed such as the ones associated with arsenic resistance, ArsC, arsenate reductase which reduces As^{5+} to As^{3+} allowing efflux by the antiporter ArsB (Pal *et al*, 2017). These mechanisms could be passed on to other bacteria and subsequently resistance can emerge to our novel antimicrobials.

6.2 Future work

Investigations into the synergy of **1** and **4** with other antibiotics against both *P. aeruginosa* and *S. aureus* using the checkerboard method as described previously should be carried out to determine whether further resistance breaking mechanisms can be found. In addition to this investigations into the synergy with tetracycline and **1** with *P.* aeruginosa and streptomycin and **4** with *S. aureus* should be explored. Previously synergistic mechanisms with streptomycin have been determined through SEM analysis, ROS generation and thermal injury as described by (Zhao *et al*., 2020). In addition to membrane permeability assays to determine synergistic effect with tetracycline, such as alkaline phosphatase release and propidium iodide uptake, gene expression is used with singular antibiotic treatments and the combination (Qu *et al*., 2019).

Cellular work could be expanded with additional MTS cytotoxicity studies carried out with other cell lines such as lung cells for potential *Pseudomonal* infections in cystic fibrosis applications. Further scratch assays must be conducted using **1** and fibroblasts with additional concentrations including 4, 16 and 32 μg mL^{-1} to complete the data set and compare the effects of an whether an increased concentration is proportional to quicker wound healing. Another avenue is determining the stress response of cell lines which could be analysed using western blotting to determine levels of VACM and ICAM in endothelial cells with antibodies anti-ICAM-1, anti-VCAM-1 and mouse monoclonal anti-GAPDH and analysed using a chemiluminescence kit. By analysing the chemiluminescence following incubation with **1**, determination of cellular stress can be established (Lin *et al*., 2019). Flow cytometry would need to be performed in order to confirm full differentiation of M0 macrophages to M1. Detection of the surface antigen CD_{11c} is detected using FITC-

conjugated antibodies and analysed using a cytometer, to determine the percentage differentiated (Sproston *et al*., 2018).

The wound model assay could be developed further to include histological analysis of the model to determine the impact of **1** on cellular morphology and a bacterial recover assay, to indicate persistence in the model following incubation.

Analysis of gene targets following RNA sequencing will be vital in validating the mechanisms of action of **1**, qrt-PCR as described by Qiagen OneStep RT-PCR protocol will be performed using the targets highlighted by the sequencing. This will include specific analysis of membrane genes *OprD, CusB* and *HlyD* and ribosomal genes such as RNA polymerase.

To determine the effect **1** has on protein-protein interactions, use of the fluorescence kit such as NanoBiT® PPI Starter Systems by Promega, which can quantify protein interactions in real-time. This could be conducted using different concentrations of **1** to determine the impact on protein-protein interactions (Dixon *et al*., 2016).

Subcellular fractionation could be conducted in order to understand the internalisation of **1** within *P. aeruginosa* strain PAO1. Combined with ICP-MS this method could be used to compare the internalisation of **1** in comparison to antibiotics such as tetracycline and be vital in understanding where **1** accumulates (Prochnow *et al*., 2018).

Liposome modelling could additionally re-inforce data that **1** causes membrane damage. This would be done using liposomes consisting of (1,2-dioleoyl-*sn*-glycero-3-phospho-(1'-*rac*-glycerol) (sodium salt) (DOPG) (Avanti Polar Lipids) or 1,2-dioleoyl-*sn*-glycero-3-phosphoethanolamine (DOPE)-DOPG (7:3 mol parts) containing 50 mM 5(6)-carboxyfluorescein (ThermoFisher) extruded through polycarbonate filters and incubated with varying concentrations of **1** with the rate of 5(6)-carboxyfluorescein leakage being observed as described by Balhara *et al*., 2013.

6.3 Conclusion

The purpose of this study was to evaluate the antimicrobial activity of two main Ru complexes against a wide range of bacterial pathogens to determine efficacy as antimicrobial agents. Subsequent cellular studies were conducted to determine the effect of the complexes on the host when skin infection occurs and the mechanisms behind the Ru complexes mechanisms of action established.

Initial screening of a plethora of metallic based complexes demonstrated Ru complexes exhibited potent antimicrobial activity when compared to Cobalt and Platinum complexes. **1** was highly active against multiple Gram-negative species including multiple strains of the high-priority pathogen *Pseudomonas aeruginosa* and **4** exhibits antimicrobial activity against Gram-positive species *Staphylococcus aureus*. These two complexes were selected for further testing due to the broad range of antimicrobial activity against multiple species. **1** was observed to have the ability to promote wound healing in both the 3D wound model and scratch assays, proving the potential for impregnating wound dressings with ruthenium complexes for Gram-negative based wound infections. The mechanisms behind the complexes activity indeed appears to be membrane disruption, thus perturbations and cellular leakage occurs resulting in a loss of cell viability with low concentrations of the complex as demonstrated by SEM imaging and inner membrane permeability assays. Additionally the antimicrobial activity of **1**, causing membrane perturbation potentially disrupts membrane anchored type 3 secretion systems, stopping the secretion of immune evading toxins, allowing for subsequent phagocytosis to occur more readily, compared with a non-treated control. **1** due to this could prove a viable option for wound dressings allowing for the immune response to be optimised and the normal wound healing process to take place. Oxidative stress studies confirmed an increase in oxidative stress within the

bacterial cell similarly to the ROS generation assay which subsequently causes DNA damage of the bacterial cell. RNA sequencing identified four gene ontologies affected by incubation with **1**, including translation, amide biosynthetic process, organonitrogen compound biosynthetic process and peptide biosynthetic process which contributes to cellular death. Due to ruthenium's ability to exhibit multiple mechanisms to cause bacterial cell mortality and assist in the wound healing process, **1** could prove an effective therapeutic option for future treatments of highly resistant bacteria within wound dressings.

7.0 References

Abd-El-Aziz, A.S., Agatemor, C. and Etkin, N. (2017) 'Antimicrobial resistance challenged with metal-based antimicrobial macromolecules.' *Biomaterials*, 118(1), pp.27-50.

Abdolhosseini, M., Zamani, H. and Salehzadeh, A. (2019) 'Synergistic antimicrobial potential of ciprofloxacin with silver nanoparticles conjugated to thiosemicarbazide against ciprofloxacin resistant *Pseudomonas aeruginosa* by attenuation of MexA-B efflux pump genes.' *Biologia*, *74*(9), pp.1191-1196.

Abednejad, A., Ghaee, A., Nourmohammadi, J. and Mehrizi, A.A. (2019) 'Hyaluronic acid/carboxylated Zeolitic Imidazolate Framework film with improved mechanical and antibacterial properties.' *Carbohydrate polymers*, 222(1), pp.115033-115045.

Abo-Shama, U.H., El-Gendy, H., Mousa, W.S., Hamouda, R.A., Yousuf, W.E., Hetta, H.F. and Abdeen, E.E. (2020) 'Synergistic and antagonistic effects of metal nanoparticles in combination with antibiotics against some reference strains of pathogenic microorganisms.' *Infection and Drug Resistance*, 13(1), pp.351-362.

Adeniyi, A.A. and Ajibade, P.A. (2016) 'Exploring the ruthenium-ligands bond and their relative properties at different computational methods.' *Journal of Chemistry*, 2016(1) pp. 1-15.

Adhikari, R., Pant, N.D., Neupane, S., Neupane, M., Bhattarai, R., Bhatta, S., Chaudhary, R. and Lekhak, B. (2017) 'Detection of methicillin resistant Staphylococcus aureus and determination of minimum inhibitory concentration of vancomycin for Staphylococcus aureus isolated from pus/wound swab samples of the patients attending a tertiary care hospital in Kathmandu, Nepal.' *Canadian Journal of Infectious Diseases and Medical Microbiology*, 2017(1), pp.1-7.

Adnan, M., Patel, M., Deshpande, S., Alreshidi, M., Siddiqui, A.J., Reddy, M.N., Emira, N. and De Feo, V. (2020) 'Effect of Adiantum philippense extract on biofilm formation, adhesion with its antibacterial activities against foodborne pathogens, and characterization of bioactive metabolites: an in vitro-in silico approach.' *Frontiers in microbiology*, 11, pp.823-842.

Agana, T., Boakye, Y. and Agyare, C. (2017) 'Antimicrobial Activities and Time-Kill Kinetics of Extracts of Selected Ghanaian Mushrooms.' *Evidence-Based Complementary and Alternative Medicine*, 2017(1), pp. 1-15.

Aguado, S., Quirós, J., Canivet, J., Farrusseng, D., Boltes, K. and Rosal, R. (2014) 'Antimicrobial activity of cobalt imidazolate metal–organic frameworks.' *Chemosphere*, 113(1), pp.188-192.

Aherwar, A., Singh, A.K. and Patnaik, A. (2016) 'Cobalt Based Alloy: A Better Choice Biomaterial for Hip Implants.' *Trends in Biomaterials & Artificial Organs*, 30(1) pp.50-55

Ahmed, M., Ward, S., McCann, M., Kavanagh, K., Heaney, F., Devereux, M., Twamley, B. and Rooney, D. (2022) 'Synthesis and characterisation of phenanthroline-oxazine ligands and their Ag (I), Mn (II) and Cu (II) complexes and their evaluation as antibacterial agents.' *BioMetals*, 35(1), pp.173-185.

Alahmadi, N.S., Betts, J.W., Cheng, F., Francesconi, M.G., Kelly, S.M., Kornherr, A., Prior, T.J. and Wadhawan, J.D. (2017) 'Synthesis and antibacterial effects of cobalt–cellulose magnetic nanocomposites.' *RSC advances*, 7(32), pp.20020-20026.

Alanis, A.J. (2005) 'Resistance to antibiotics: are we in the post-antibiotic era?.' *Archives of Medical Research*, 36(6), pp.697-705.

Alberts, B. (1994) ‘Cell junctions, cell adhesion and the extracellular matrix.’ *Molecular biology of the cell*, pp.949-1009.

Alderden, R.A., Hall, M.D. and Hambley, T.W. (2006) ‘The discovery and development of cisplatin.’ *Journal of chemical education*, 83(5), pp.728-735.

Aldeyab, M.A., Monnet, D.L., López-Lozano, J.M., Hughes, C.M., Scott, M.G., Kearney, M.P., Magee, F.A. and McElnay, J.C. (2008) ‘Modelling the impact of antibiotic use and infection control practices on the incidence of hospital-acquired methicillin-resistant Staphylococcus aureus: a time-series analysis.’ *Journal of Antimicrobial Chemotherapy*, 62(3), pp.593-600.

Alessio, E. (2017) ‘Thirty years of the drug candidate nami-a and the myths in the field of ruthenium anticancer compounds: a personal perspective.’ *European Journal of Inorganic Chemistry*, 2017(12), pp.1549-1560.

Alessio, E. and Messori, L. (2019) 'NAMI-A and KP1019/1339, two iconic ruthenium anticancer drug candidates face-to-face: a case story in medicinal inorganic chemistry.' *Molecules*, 24(10), pp.1995-2015.

Alsharif, G., Ahmad, S., Islam, M.S., Shah, R., Busby, S.J. and Krachler, A.M. (2015) ‘Host attachment and fluid shear are integrated into a mechanical signal regulating virulence in Escherichia coli O157: H7.’ *Proceedings of the National Academy of Sciences*, 112(17), pp.5503-5508.

Amiel, E., Lovewell, R.R., O'Toole, G.A., Hogan, D.A. and Berwin, B. (2010) ‘Pseudomonas aeruginosa evasion of phagocytosis is mediated by loss of swimming motility and is independent of flagellum expression.’ *Infection and immunity*, 78(7), pp.2937-2945.

Amin, M., Rowley-Neale, S., Shalamanova, L., Lynch, S., Wilson-Nieuwenhuis, J.T., El Mohtadi, M., Banks, C.E. and Whitehead, K.A. (2020) ‘Molybdenum disulfide surfaces to

reduce Staphylococcus aureus and Pseudomonas aeruginosa biofilm formation.' *ACS applied materials & interfaces*, 12(18), pp.21057-21069.

An, X., Naowarojna, N., Liu, P. and Reinhard, B.M. (2019) 'Hybrid plasmonic photoreactors as visible light-mediated bactericides.' *ACS Applied Materials & Interfaces*, 12(1), pp.106-116.

Andrade, A.L., de Vasconcelos, M.A., Arruda, F.V.D.S., do Nascimento Neto, L.G., Carvalho, J.M.D.S., Gondim, A.C.S., Lopes, L.G.D.F., Sousa, E.H.S. and Teixeira, E.H. (2020) 'Antimicrobial activity and antibiotic synergy of a biphosphinic ruthenium complex against clinically relevant bacteria.' *Biofouling*, 36(4), pp.442-454.

Ang, W.H., Casini, A., Sava, G. and Dyson, P.J. (2011) 'Organometallic ruthenium-based antitumor compounds with novel modes of action.' *Journal of Organometallic Chemistry*, 696(5), pp.989-998.

Antunes, L., Visca, P. and Towner, K.J. (2014) 'Acinetobacter baumannii: evolution of a global pathogen.' *Pathogens and disease*, 71(3), pp.292-301.

Argudín, M.A., Hoefer, A. and Butaye, P. (2019) 'Heavy metal resistance in bacteria from animals.' *Research in Veterinary Science*, 122(1) pp.132-147.

Arias, L.S., Pessan, J.P., Vieira, A.P.M., Lima, T.M.T.D., Delbem, A.C.B. and Monteiro, D.R. (2018) 'Iron oxide nanoparticles for biomedical applications: A perspective on synthesis, drugs, antimicrobial activity, and toxicity.' *Antibiotics*, 7(2), pp.46-78.

Arias, M., Hassan-Reshat, S. and Newsholme, W. (2019) 'Retrospective analysis of diabetic foot osteomyelitis management and outcome at a tertiary care hospital in the UK.' *PloS one*, 14(5) pp. 1-16.

Arif, N., Yousfi, S. and Vinnard, C. (2016) 'Deaths from necrotizing fasciitis in the United States, 2003–2013.' *Epidemiology & Infection*, 144(6), pp.1338-1344.

Arshad, J., Hanif, M., Movassaghi, S., Kubanik, M., Waseem, A., Söhnel, T., Jamieson, S.M. and Hartinger, C.G. (2017) 'Anticancer Ru (η6-p-cymene) complexes of 2-pyridinecarbothioamides: A structure–activity relationship study.' *Journal of Inorganic Biochemistry*, 177(1), pp.395-401.

Artini, M., Scoarughi, G.L., Papa, R., Cellini, A., Carpentieri, A., Pucci, P., Amoresano, A., Gazzola, S., Cocconcelli, P.S. and Selan, L. (2011) 'A new anti-infective strategy to reduce adhesion-mediated virulence in Staphylococcus aureus affecting surface proteins.' *International journal of immunopathology and pharmacology*, 24(3), pp.661-672.

Arumugam, A.P., Elango, G. and Guhanathan, S. (2018) 'Molecular Docking, Fluorescence, Morphological, and Antimicrobial studies of Novel Schiff Base Ligand Derived from Glutaric Anhydride and its Nickel (II) complex.' *Asian J Appl Res*, 4(12), pp.9-14.

Asghar, M.A., Yousuf, R.I., Shoaib, M.H., Asghar, M.A., Ansar, S., Zehravi, M. and Rehman, A.A. (2020) 'Synergistic Nanocomposites of Different Antibiotics Coupled with Green Synthesized Chitosan-Based Silver Nanoparticles: Characterization, Antibacterial, in vivo Toxicological and Biodistribution Studies.' *International Journal of Nanomedicine*, 15, pp.7841-7859.

Asiani, K.R., Williams, H., Bird, L., Jenner, M., Searle, M.S., Hobman, J.L., Scott, D.J. and Soultanas, P. (2016) 'SilE is an intrinsically disordered periplasmic "molecular sponge" involved in bacterial silver resistance.' *Molecular Microbiology*, 101(5), pp.731-742.

Ayliffe, G.A.J., Buckles, A., Casewell, M.W., Cookson, B.D., Cox, R.A., Duckworth, G.J., French, G.L., Griffiths-Jones, A., Heathcock, R., Humphreys, H., Keane, C.T., Marples, R.R., Shanson, D.C., Slack, R., Tebbs, E. (1998) 'Revised guidelines for the control of methicillin-resistant Staphylococcus aureus infection in hospitals.' British Society for Antimicrobial

Chemotherapy, Hospital Infection Society and the Infection Control Nurses Association.' *J Hosp Infect*, 39(4), pp. 253–290.

Azam, M.W. and Khan, A.U. (2019) 'Updates on the pathogenicity status of Pseudomonas aeruginosa.' *Drug discovery today*, 24(1), pp.350-359.

Bacot-Davis, V.R., Bassenden, A.V. and Berghuis, A.M. (2016) 'Drug-target networks in aminoglycoside resistance: hierarchy of priority in structural drug design.' *MedChemComm*, 7(1), pp.103-113.

Baker, S., Pasha, A. and Satish, S. (2017) 'Biogenic nanoparticles bearing antibacterial activity and their synergistic effect with broad spectrum antibiotics: Emerging strategy to combat drug resistant pathogens. '*Saudi Pharmaceutical Journal*, 25(1), pp.44-51.

Baker, S.J., Payne, D.J., Rappuoli, R. and De Gregorio, E. (2018) 'Technologies to address antimicrobial resistance.' *Proceedings of the National Academy of Sciences*, 115(51), pp.12887-12895.

Bala, R., Sharma, R.P., Venugopalan, P. and Harrison, W.T. (2007) 'Cationic cobaltammine as anion receptor: Synthesis, characterization, single crystal X-ray structure and packing analysis of hexaamminecobalt (III) chloride (R, R)-tartrate monohydrate.' *Journal of molecular structure*, 830(1-3), pp.8-13.

Balakrishnan, S.K., Dass, S.K., Rajendran, H.A.D. and Savrimuthu, I. (2015) 'Cytotoxicity and antimicrobial activity of mono-, di-and trinuclear ruthenium (II) polypyridine complexes.' *Int. J. Pharm. Pharm. Sci*, 7(1), pp.317-321.

Balhara, V., Schmidt, R., Gorr, S.U. and DeWolf, C. (2013) 'Membrane selectivity and biophysical studies of the antimicrobial peptide GL13K.' *Biochimica et Biophysica Acta (BBA)-Biomembranes*, 1828(9), pp.2193-2203.

Bandyopadhyay, B., Fan, J., Guan, S., Li, Y., Chen, M., Woodley, D.T. and Li, W. (2006) 'A "traffic control" role for TGFβ3: orchestrating dermal and epidermal cell motility during wound healing.' *The Journal of cell biology*, 172(7), pp.1093-1105.

Bangert, S., Levy, M. and Hebert, A.A. (2012) 'Bacterial resistance and impetigo treatment trends: a review.' *Pediatric dermatology*, 29(3), pp.243-248.

Barbosa, M.I., Correa, R.S., de Oliveira, K.M., Rodrigues, C., Ellena, J., Nascimento, O.R., Rocha, V.P., Nonato, F.R., Macedo, T.S., Barbosa-Filho, J.M. and Soares, M.B. (2014) 'Antiparasitic activities of novel ruthenium/lapachol complexes.' *Journal of inorganic biochemistry*, 136(1), pp.33-39.

Barolli, J.P., Maia, P.I., Colina-Vegas, L., Moreira, J., Plutin, A.M., Mocelo, R., Deflon, V.M., Cominetti, M.R., Camargo-Mathias, M.I. and Batista, A.A. (2017) 'Heteroleptic tris-chelate ruthenium (II) complexes of N, N-disubstituted-N'-acylthioureas: Synthesis, structural studies, cytotoxic activity and confocal microscopy studies.' *Polyhedron*, 126(1), pp.33-41.

Baron, S.S. and Rowe, J.J. (1981) 'Antibiotic action of pyocyanin.' *Antimicrobial agents and chemotherapy*, 20(6), pp.814-820.

Barrett, S., Delaney, S., Kavanagh, K. and Montagner, D. (2018) 'Evaluation of in vitro and in vivo antibacterial activity of novel Cu (II)-steroid complexes.' *Inorganica Chimica Acta*, 479(1), pp.261-265.

Bashir, R., Afroze, B., Zulfiqar, H.F., Saleem, R., Altaf, I., Saleem, F., Aslam, F. and Naz, S. (2016) 'Microbiological Load of Ethylene Oxide Sterilized Medical Devices and its Elimination by Cobalt 60 Source.' *Journal of the College of Physicians and Surgeons Pakistan*, 26(6), pp.486-489.

Battista, S., Campitelli, P., Carlone, A. and Giansanti, L. (2019) 'Influence of structurally related micelle forming surfactants on the antioxidant activity of natural substances.' *Chemistry and physics of lipids*, 225(1), pp.104818-104827.

Bayot, M.L. and Bragg, B.N. (2019) 'Antimicrobial susceptibility testing.' https://www.ncbi.nlm.nih.gov/books/NBK539714/

Bazire, A., Shioya, K., Soum-Soutéra, E., Bouffartigues, E., Ryder, C., Guentas-Dombrowsky, L., Hémery, G., Linossier, I., Chevalier, S., Wozniak, D.J. and Lesouhaitier, O. (2010) 'The sigma factor AlgU plays a key role in formation of robust biofilms by nonmucoid Pseudomonas aeruginosa.' *Journal of Bacteriology*, 192(12), pp. 3001-3010.

Benner EJ, Kayser FH. (1968) 'Growing clinical significance of methcillin-resistant Staphylococcus aureus.' *Lancet*, 2(7571), pp. 741–744.

Benner, E.J. and Kayser, F.H. (1968) 'Growing clinical significance of methicillin-resistant Staphylococcus aureus.' *The Lancet*, 292(7571), pp.741-744.

Bergamo, A., Gerdol, M., Lucafo, M., Pelillo, C., Battaglia, M., Pallavicini, A. and Sava, G. (2015) 'RNA-seq analysis of the whole transcriptome of MDA-MB-231 mammary carcinoma cells exposed to the antimetastatic drug NAMI-A.' *Metallomics*, 7(10), pp.1439-1450.

Bergen, P.J., Landersdorfer, C.B., Zhang, J., Zhao, M., Lee, H.J., Nation, R.L. and Li, J. (2012) 'Pharmacokinetics and pharmacodynamics of 'old'polymyxins: what is new?.' *Diagnostic microbiology and infectious disease*, *74*(3), pp.213-223.

Bernut, A., Belon, C., Soscia, C., Bleves, S. and Blanc-Potard, A.B. (2015) 'Intracellular phase for an extracellular bacterial pathogen: MgtC shows the way.' *Microbial Cell*, 2(9), pp.353-355.

Bessa, L.J., Fazii, P., Di Giulio, M. and Cellini, L. (2015) 'Bacterial isolates from infected wounds and their antibiotic susceptibility pattern: some remarks about wound infection.' International wound journal, 12(1), pp.47-52.

Betts, J., Nagel, C., Schatzschneider, U., Poole, R. and La Ragione, R.M. (2017) 'Antimicrobial activity of carbon monoxide-releasing molecule [Mn (CO) 3 (tpa-κ3N)] Br versus multidrug-resistant isolates of Avian Pathogenic Escherichia coli and its synergy with colistin.' *PloS one*, 12(10) pp. e0186359-e0186371.

Beyth, N., Houri-Haddad, Y., Domb, A., Khan, W. and Hazan, R. (2015) 'Alternative antimicrobial approach: nano-antimicrobial materials.' *Evidence-Based Complementary and Alternative Medicine*, 2015(1) pp. 1-16

Bhattacharya, R., Xu, F., Dong, G., Li, S., Tian, C., Ponugoti, B. and Graves, D.T. (2014) 'Effect of bacteria on the wound healing behavior of oral epithelial cells.' *PloS one*, 9(2), p.e89475-e89485.

Biancalana, L., Zacchini, S., Ferri, N., Lupo, M.G., Pampaloni, G. and Marchetti, F. (2017) 'Tuning the cytotoxicity of ruthenium (II) para-cymene complexes by mono-substitution at a triphenylphosphine/phenoxydiphenylphosphine ligand.' *Dalton Transactions*, 46(47), pp.16589-16604.

Bielefeld, K.A., Amini-Nik, S. and Alman, B.A. (2013) 'Cutaneous wound healing: recruiting developmental pathways for regeneration.' *Cellular and Molecular Life Sciences*, 70(12), pp.2059-2081.

Bjarnsholt, T. (2013) 'The role of bacterial biofilms in chronic infections.' *Apmis*, *121*, pp.1-58.

Blair, J.M., Webber, M.A., Baylay, A.J., Ogbolu, D.O,. and Piddock, L.J. (2015) 'Molecular mechanisms of antibiotic resistance.' *Nature reviews microbiology*, 13(1), pp.42-51.

Blunden, B.M., Lu, H. and Stenzel, M.H. (2013) 'Enhanced delivery of the RAPTA-C macromolecular chemotherapeutic by conjugation to degradable polymeric micelles.' *Biomacromolecules*, 14(12), pp.4177-4188.

Blunden, B.M., Thomas, D.S. and Stenzel, M.H. (2012) 'Macromolecular ruthenium complexes as anti-cancer agents.' *Polymer Chemistry*, 3(10), pp.2964-2975.

Bodansky, D.M., Begaj, I., Evison, F., Webber, M., Woodman, C.B. and Tucker, O.N. (2020) 'A 16-year longitudinal cohort study of incidence and bacteriology of necrotising fasciitis in England.' *World journal of surgery*, 44(8), pp.2580-2591.

Bohlmann, L., De Oliveira, D.M., El-Deeb, I.M., Brazel, E.B., Harbison-Price, N., Cheryl-lynn, Y.O., Rivera-Hernandez, T., Ferguson, S.A., Cork, A.J., Phan, M.D. and Soderholm, A.T. (2018) 'Chemical synergy between ionophore PBT2 and zinc reverses antibiotic resistance.' *MBio*, 9(6), pp.e02391-18.

Bolard, A., Plésiat, P. and Jeannot, K. (2017) 'Mutations in gene fusA1 as a novel mechanism of aminoglycoside resistance in clinical strains of Pseudomonas aeruginosa.' *Antimicrobial agents and chemotherapy*, 62(2), pp.e01835-17.

Borkow, G. and Gabbay, J. (2009). 'Copper, an ancient remedy returning to fight microbial, fungal and viral infections.' *Current Chemical Biology*, 3(3), pp.272-278.

Borselli, D., Lieutaud, A., Thefenne, H., Garnotel, E., Pagès, J.M., Brunel, J.M. and Bolla, J.M. (2016) 'Polyamino-isoprenic derivatives block intrinsic resistance of P. aeruginosa to doxycycline and chloramphenicol in vitro.' *PloS one*, 11(5), pp.e0154490-e015456.

Bose, D. and Chatterjee, S. (2016) 'Biogenic synthesis of silver nanoparticles using guava (Psidium guajava) leaf extract and its antibacterial activity against Pseudomonas aeruginosa.' *Applied Nanoscience*, 6(6), pp.895-901.

Bouayadi, K., Villani, G. and Salles, B. (1993) 'Resistance to cisplatin in an E. coli B/r NalR mutant.' *Mutation Research/DNA Repair*, 294(1), pp.77-87.

Bouffartigues, E., Gicquel, G., Bazire, A., Bains, M., Maillot, O., Vieillard, J., Feuilloley, M.G., Orange, N., Hancock, R.E.W., Dufour, A. and Chevalier, S. (2012) 'Transcription of the oprF gene of Pseudomonas aeruginosa is dependent mainly on the SigX sigma factor and is sucrose induced.' *Journal of bacteriology*, 194(16), pp.4301-4311.

Boukerb, A.M., Rousset, A., Galanos, N., Méar, J.B., Thépaut, M., Grandjean, T., Gillon, E., Cecioni, S., Abderrahmen, C., Faure, K. and Redelberger, D. (2014) 'Antiadhesive properties of glycoclusters against Pseudomonas aeruginosa lung infection.' *Journal of medicinal chemistry*, 57(24), pp.10275-10289.

Brandenburg, K.S., Weaver Jr, A.J., Qian, L., You, T., Chen, P., Karna, S.R., Fourcaudot, A.B., Sebastian, E.A., Abercrombie, J.J., Pineda, U. and Hong, J. (2019) 'Development of Pseudomonas aeruginosa biofilms in partial-thickness burn wounds using a Sprague-Dawley rat model.' *Journal of Burn Care & Research*, 40(1), pp.44-57.

Bratzler, D.W., Dellinger, E.P., Olsen, K.M., Perl, T.M., Auwaerter, P.G., Bolon, M.K., Fish, D.N., Napolitano, L.M., Sawyer, R.G., Slain, D. and Steinberg, J.P. (2013) 'Clinical practice guidelines for antimicrobial prophylaxis in surgery.' *Surgical Infections*, 14(1), pp. 73-156.

Breidenstein, E.B., de la Fuente-Núñez, C. and Hancock, R.E. (2011) 'Pseudomonas aeruginosa: all roads lead to resistance.' *Trends in microbiology*, 19(8), pp.419-426.

Breijyeh, Z., Jubeh, B. and Karaman, R. (2020) 'Resistance of Gram-negative bacteria to current antibacterial agents and approaches to resolve it.' *Molecules*, *25*(6), pp.1340.

Brennan-Krohn, T., Pironti, A. and Kirby, J.E. (2018) 'Synergistic activity of colistin-containing combinations against colistin-resistant Enterobacteriaceae.' *Antimicrobial agents and chemotherapy*, 62(10), pp.e00873-18.

Britigan, B.E., Railsback, M.A. and Cox, C.D. (1999) 'The Pseudomonas aeruginosa secretory product pyocyanin inactivates α1 protease inhibitor: implications for the pathogenesis of cystic fibrosis lung disease.' *Infection and immunity*, 67(3), pp.1207-1212.

Britten, N.S. and Butler, J.A. (2022) 'Ruthenium Metallotherapeutics: Novel Approaches to Combatting Parasitic Infections.' *Current Medicinal Chemistry*, 29(31), pp.5159-5178.

Brown, D.G. (2017) 'New drugs and emerging leads in antibacterial drug discovery.' *Comprehensive Medicinal Chemistry III*, 2017(1), pp. 682-702.

Browne, N., Hackenberg, F., Streciwilk, W., Tacke, M. and Kavanagh, K. (2014) 'Assessment of in vivo antimicrobial activity of the carbene silver (I) acetate derivative SBC3 using Galleria mellonella larvae.' *Biometals*, 27(4), pp.745-752.

Bruins, M.R., Kapil, S. and Oehme, F.W. (2000) 'Microbial resistance to metals in the environment.' *Ecotoxicology and Environmental Safety*, 45(3) pp.198-207.

Bu, S., Jiang, G., Jiang, G., Liu, J., Lin, X., Shen, J., Xiong, Y., Duan, X., Wang, J. and Liao, X. (2020) 'Antibacterial activity of ruthenium polypyridyl complexes against Staphylococcus aureus and biofilms.' *JBIC Journal of Biological Inorganic Chemistry*, 25(5), pp.747-757.

Bush, K. and Bradford, P.A. (2020) 'Epidemiology of β-lactamase-producing pathogens.' Clinical microbiology reviews, 33(2), pp.e00047-19.

Byrd, M.S., Sadovskaya, I., Vinogradov, E., Lu, H., Sprinkle, A.B., Richardson, S.H., Ma, L., Ralston, B., Parsek, M.R., Anderson, E.M. and Lam, J.S. (2009) 'Genetic and biochemical analyses of the Pseudomonas aeruginosa Psl exopolysaccharide reveal overlapping roles for

polysaccharide synthesis enzymes in Psl and LPS production.' *Molecular microbiology*, 73(4), pp.622-638.

Cai, B., Echols, R., Magee, G., Arjona Ferreira, J.C., Morgan, G., Ariyasu, M., Sawada, T. and Nagata, T. (2017) 'Prevalence of carbapenem-resistant Gram-negative infections in the United States predominated by Acinetobacter baumannii and Pseudomonas aeruginosa.' *Open forum infectious diseases,* 4(3), pp.1-7.

Casabona, M.G., Vandenbrouck, Y., Attree, I. and Couté, Y. (2013) 'Proteomic characterization of Pseudomonas aeruginosa PAO1 inner membrane.' *Proteomics*, 13(16), pp.2419-2423.

Casey, G. (2000) 'Modern wound dressings.' *Nursing Standard (through 2013)*, 15(5), pp.47-51.

Castañeda-Montes, F.J., Avitia, M., Sepúlveda-Robles, O., Cruz-Sánchez, V., Kameyama, L., Guarneros, G. and Escalante, A.E. (2018) 'Population structure of Pseudomonas aeruginosa through a MLST approach and antibiotic resistance profiling of a Mexican clinical collection.' *Infection, Genetics and Evolution*, 65(1), pp.43-54.

Cavinato, L., Genise, E., Luly, F.R., Domenico, E.G.D., Del Porto, P. and Ascenzioni, F. (2020) 'Escaping the Phagocytic Oxidative Burst: The Role of SODB in the Survival of Pseudomonas aeruginosa Within Macrophages.' *Frontiers in microbiology*, 11(1), pp.326-338.

Chambers, C., Stewart, S.B., Su, B., Jenkinson, H.F., Sandy, J.R. and Ireland, A.J. (2017) 'Silver doped titanium dioxide nanoparticles as antimicrobial additives to dental polymers.' *Dental Materials*, 33(3), pp.e115-e123.

Chaney, S.B., Ganesh, K., Mathew-Steiner, S., Stromberg, P., Roy, S., Sen, C.K. and Wozniak, D.J. (2017) 'Histopathological comparisons of S taphylococcus aureus and P seudomonas

aeruginosa experimental infected porcine burn wounds.' *Wound Repair and Regeneration*, 25(3), pp.541-549.

Chebbi, A., Elshikh, M., Haque, F., Ahmed, S., Dobbin, S., Marchant, R., Sayadi, S., Chamkha, M. and Banat, I.M. (2017) 'Rhamnolipids from Pseudomonas aeruginosa strain W10; as antibiofilm/antibiofouling products for metal protection.' *Journal of basic microbiology*, 57(5), pp.364-375.

Chellan, P., Land, K.M., Shokar, A., Au, A., An, S.H., Taylor, D., Smith, P.J., Riedel, T., Dyson, P.J., Chibale, K. and Smith, G.S. (2014) 'Synthesis and evaluation of new polynuclear organometallic Ru (II), Rh (III) and Ir (III) pyridyl ester complexes as in vitro antiparasitic and antitumor agents.' *Dalton Transactions*, 43(2), pp.513-526.

Chen, C. and Yang, K. (2020) 'Ruthenium complexes as prospective inhibitors of metallo-β-lactamases to reverse carbapenem resistance.' *Dalton Transactions*, 49(40), pp.14099-14105.

Chen, S., Lu, J., You, T. and Sun, D. (2021) 'Metal-organic frameworks for improving wound healing.' *Coordination Chemistry Reviews*, 439(1), pp.213929-213957.

Chen, S.Y., Wang, J.T., Chen, T.H.H., Lai, M.S., Chie, W.C., Chien, K.L., Hsueh, P.R., Wang, J.L. and Chang, S.C. (2010) 'Impact of traditional hospital strain of methicillin-resistant Staphylococcus aureus (MRSA) and community strain of MRSA on mortality in patients with community-onset S aureus bacteremia.' *Medicine*, 89(5), pp. 285-294.

Chen, Y., Liu, L., Wang, X., Liao, Z., Wang, R., Xiong, Y., Cheng, J., Jiang, G., Wang, J. and Liao, X. (2022) 'The synthesis and antibacterial activity study of ruthenium-based metallodrugs with a membrane-disruptive mechanism against Staphylococcus aureus.' *Dalton Transactions*, 51(39), pp.14980-14992.

Chevalier, J., Mahamoud, A., Baitiche, M., Adam, E., Viveiros, M., Smarandache, A., Militaru, A., Pascu, M.L., Amaral, L. and Pagès, J.M. (2010) 'Quinazoline derivatives are efficient chemosensitizers of antibiotic activity in Enterobacter aerogenes, Klebsiella pneumoniae and Pseudomonas aeruginosa resistant strains.' *International journal of antimicrobial agents*, 36(2), pp.164-168.

Chevalier, S., Bouffartigues, E., Bodilis, J., Maillot, O., Lesouhaitier, O., Feuilloley, M.G., Orange, N., Dufour, A. and Cornelis, P. (2017) 'Structure, function and regulation of Pseudomonas aeruginosa porins.' *FEMS microbiology reviews*, 41(5), pp.698-722.

Chevereau, G. and Bollenbach, T. (2015) 'Systematic discovery of drug interaction mechanisms.' *Molecular systems biology*, 11(4), pp.807-816.

Chidurala, S.C., Kalagadda, V.R. and Tambur, P. (2016) 'Antimicrobial activity of pure Cu nano particles synthesized by surfactant varied chemical reduction method.' *Environmental Nanotechnology, Monitoring & Management*, 6(1), pp.88-94.

Chiswick, E.L., Duffy, E., Japp, B. and Remick, D. (2012) 'Detection and quantification of cytokines and other biomarkers.' *Leucocytes* 844(1) pp. 15-30.

Cho, H., Uehara, T. and Bernhardt, T.G. (2014) 'Beta-lactam antibiotics induce a lethal malfunctioning of the bacterial cell wall synthesis machinery.' *Cell*, 159(6), pp.1300-1311.

Chopra, I. (2007) 'The increasing use of silver-based products as antimicrobial agents: a useful development or a cause for concern?.' *Journal of Antimicrobial Chemotherapy*, 59(4), pp.587-590.

Choueiri, T.K., Fishman, M.N., Escudier, B., McDermott, D.F., Drake, C.G., Kluger, H., Stadler, W.M., Perez-Gracia, J.L., McNeel, D.G., Curti, B. and Harrison, M.R. (2016)

‘Immunomodulatory activity of nivolumab in metastatic renal cell carcinoma.’ *Clinical Cancer Research*, 22(22), pp.5461-5471.

Chowdhury, N., Wood, T.L., Martínez-Vázquez, M., García-Contreras, R. and Wood, T.K. (2016) ‘DNA-crosslinker cisplatin eradicates bacterial persister cells.’ *Biotechnology and bioengineering*, 113(9), pp.1984-1992.

Christensen, G.D., Simpson, W.A., Younger, J.J., Baddour, L.M., Barrett, F.F., Melton, D.M. and Beachey, E.H. (1985) ‘Adherence of coagulase-negative staphylococci to plastic tissue culture plates: a quantitative model for the adherence of staphylococci to medical devices.’ Journal of clinical microbiology, 22(6), pp.996-1006.

Classes Coates, A.R., Halls, G. and Hu, Y. (2011) ‘Novel classes of antibiotics or more of the same?’ *British journal of pharmacology*, 163(1), pp.184-194.

Clauss-Lendzian, E., Vaishampayan, A., de Jong, A., Landau, U., Meyer, C., Kok, J. and Grohmann, E. (2018) ‘Stress response of a clinical Enterococcus faecalis isolate subjected to a novel antimicrobial surface coating.’ *Microbiological research*, 207(1), pp.53-64.

Cole, S.T. (2014) ‘Who will develop new antibacterial agents?’. *Philosophical Transactions of the Royal Society B: Biological Sciences*, 369(1645), pp.20130430-20130437.

Collington, S.J., Williams, T.J. and Weller, C.L. (2011) ‘Mechanisms underlying the localisation of mast cells in tissues.’ *Trends in immunology*, 32(10), pp.478-485.

Conceicao T, Diamantino F, Coelho C, de Lencastre H, Aires-de-Sousa M. (2013) ‘Contamination of public buses with MRSA in Lisbon, Portugal: a possible transmission route of major MRSA clones within the community.’ *PLoS One,* 8(1), pp. e77812-77818.

Cong, Y., Yang, S. and Rao, X. (2020) 'Vancomycin resistant Staphylococcus aureus infections: A review of case updating and clinical features.' *Journal of Advanced Research*, 21(1), pp.169-176.

Cookson BD, Phillips I. (1988) 'Epidemic methicillin-resistant Staphylococcus aureus.' *J Antimicrob Chemother*, 21(1), pp. 57–65.

Coppola, P.E., Gaibani, P., Sartor, C., Ambretti, S., Lewis, R.E., Sassi, C., Pignatti, M., Paolini, S., Curti, A., Castagnetti, F. and Ursi, M. (2020) 'Ceftolozane-Tazobactam Treatment of Hypervirulent Multidrug Resistant Pseudomonas aeruginosa Infections in Neutropenic Patients.' *Microorganisms*, 8(12), pp.2055-2066.

Cory, G. (2011) 'Scratch-wound assay.' *Cell Migration: Humana Press*, pp. 25-30.

Costa, M.S., Gonçalves, Y.G., Nunes, D.C., Napolitano, D.R., Maia, P.I., Rodrigues, R.S., Rodrigues, V.M., Von Poelhsitz, G. and Yoneyama, K.A. (2017) 'Anti-Leishmania activity of new ruthenium (II) complexes: Effect on parasite-host interaction.' *Journal of inorganic biochemistry*, 175(1), pp.225-231.

Coughlan, L.M., Cotter, P.D., Hill, C. and Alvarez-Ordóñez, A. (2016) 'New weapons to fight old enemies: novel strategies for the (bio) control of bacterial biofilms in the food industry.' *Frontiers in microbiology*, 7(1), pp.1641-1662.

Cox, G. and Wright, G.D. (2013) 'Intrinsic antibiotic resistance: mechanisms, origins, challenges and solutions.' *International Journal of Medical Microbiology*, 303(6-7), pp.287-292.

Cox, G., Ejim, L., Stogios, P.J., Koteva, K., Bordeleau, E., Evdokimova, E., Sieron, A.O., Savchenko, A., Serio, A.W., Krause, K.M. and Wright, G.D. (2018) 'Plazomicin retains

antibiotic activity against most aminoglycoside modifying enzymes.' *ACS infectious diseases*, 4(6), pp.980-987.

Cuny C, Nathaus R, Layer F, Strommenger B, Altmann D, Witte W. (2009) 'Nasal colonization of humans with methicillin-resistant Staphylococcus aureus (MRSA) CC398 with and without exposure to pigs.' *PLoS One,* 4(8), pp. e6800-6806.

Curran, C.S., Bolig, T. and Torabi-Parizi, P. (2018) 'Mechanisms and targeted therapies for Pseudomonas aeruginosa lung infection.' *American Journal of Respiratory and Critical Care Medicine*, 197(6), pp.708-727.

Cuthbertson, L., Rogers, G.B., Walker, A.W., Oliver, A., Green, L.E., Daniels, T.W., Carroll, M.P., Parkhill, J., Bruce, K.D. and Van Der Gast, C.J. (2016) 'Respiratory microbiota resistance and resilience to pulmonary exacerbation and subsequent antimicrobial intervention.' *The ISME Journal*, 10(5), pp.1081-1091.

Czerwonka, G., Gmiter, D., Guzy, A., Rogala, P., Jabłońska-Wawrzycka, A., Borkowski, A., Cłapa, T., Narożna, D., Kowalczyk, P., Syczewski, M. and Drabik, M. (2019) 'A benzimidazole-based ruthenium (IV) complex inhibits Pseudomonas aeruginosa biofilm formation by interacting with siderophores and the cell envelope, and inducing oxidative stress.' *Biofouling*, 35(1), pp.59-74.

D'Agata, E.M., Webb, G.F., Horn, M.A., Moellering, R.C. and Ruan, S. (2009) 'Modeling the invasion of community-acquired methicillin-resistant Staphylococcus aureus into hospitals.' *Clinical Infectious Diseases*, 48(3), pp.274-284.

Das, M.C., Sandhu, P., Gupta, P., Rudrapaul, P., De, U.C., Tribedi, P., Akhter, Y. and Bhattacharjee, S. (2016) 'Attenuation of Pseudomonas aeruginosa biofilm formation by

Vitexin: A combinatorial study with azithromycin and gentamicin.' *Scientific reports*, 6(1), pp.1-13.

Das, T. and Manefield, M. (2012) 'Pyocyanin promotes extracellular DNA release in Pseudomonas aeruginosa.' *PLoS ONE*, 7(10), pp. e46718-46727.

Dasari, S. and Tchounwou, P.B. (2014) 'Cisplatin in cancer therapy: molecular mechanisms of action.' *European journal of pharmacology*, 740(1), pp.364-378.

David MZ, Rudolph KM, Hennessy TW, Zychowski DL, Asthi K, Boyle-Vavra S, Daum RS. (2012) 'MRSA USA300 at Alaska Native Medical Center, Anchorage, Alaska, USA, 2000-2006.' *Emerg Infect Dis*, 18(1), pp.105–108.

David, M.Z. and Daum, R.S. (2017) 'Treatment of Staphylococcus aureus infections.' *Staphylococcus aureus*, 409(1), pp.325-383.

David, M.Z. and Daum, R.S. (2017) 'Treatment of Staphylococcus aureus infections.' *Staphylococcus aureus,* 2017(1), pp. 325-383.

David, M.Z., Rudolph, K.M., Hennessy, T.W., Zychowski, D.L., Asthi, K., Boyle-Vavra, S. and Daum, R.S. (2012) 'MRSA USA300 at Alaska Native Medical Center, Anchorage, Alaska, USA, 2000–2006.' *Emerging infectious diseases*, 18(1), pp.105-108.

de Lima, R.G., Lever, A.B.P., Ito, I.Y. and da Silva, R.S. (2003) 'Antifungal activity of novel catecholamine ruthenium (III) complexes.' Transition metal chemistry, 28(3), pp.272-275.

De Oliveira, D.M., Forde, B.M., Kidd, T.J., Harris, P.N., Schembri, M.A., Beatson, S.A., Paterson, D.L. and Walker, M.J. (2020) 'Antimicrobial resistance in ESKAPE pathogens.' *Clinical microbiology reviews*, *33*(3), pp. 1-49.

de Sousa, A.P., Ellena, J., Gondim, A.C., Lopes, L.G., Sousa, E.H., de Vasconcelos, M.A., Teixeira, E.H., Ford, P.C. and Holanda, A.K. (2018) 'Antimicrobial activity of cis-[Ru (bpy) 2 (L)(L')] n+ complexes, where L= 4-(4-chlorobenzoyl) pyridine or 4-(benzoyl) pyridine and L'= Cl− or CO.' *Polyhedron*, 144(1), pp.88-94.

de Sousa, A.P., Gondim, A.C., Sousa, E.H., de Vasconcelos, M.A., Teixeira, E.H., Bezerra, B.P., Ayala, A.P., Martins, P.H., de França Lopes, L.G. and Holanda, A.K. (2020) 'An unusual bidentate methionine ruthenium (II) complex: photo-uncaging and antimicrobial activity.' *JBIC Journal of Biological Inorganic Chemistry*, 25(3), pp.419-428.

de Souza, C.E.A., de Souza, H.D.M.A., Stipp, M.C., Corso, C.R., Galindo, C.M., Cardoso, C.R., Dittrich, R.L., de Souza Ramos, E.A., Klassen, G., Carlos, R.M. and Cadena, S.M.S.C., (2017) 'Ruthenium complex exerts antineoplastic effects that are mediated by oxidative stress without inducing toxicity in Walker-256 tumor-bearing rats.' *Free Radical Biology and Medicine*, 110(1), pp.228-239.

deBoer, T.R., Tarlton, N.J., Yamaji, R., Adams-Sapper, S., Wu, T.Z., Maity, S., Vesgesna, G.K., Sadlowski, C.M., DePaola IV, P., Riley, L.W. and Murthy, N. (2018) 'An Enzyme-Mediated Amplification Strategy Enables Detection of β-Lactamase Activity Directly in Unprocessed Clinical Samples for Phenotypic Detection of β-Lactam Resistance.' *ChemBioChem*, 19(20), pp.2173-2177.

Dedduwa-Mudalige, G.N. and Chow, C.S. (2015) 'Cisplatin targeting of bacterial ribosomal RNA hairpins.' *International Journal of Molecular Sciences*, 16(9), pp.21392-21409.

Delany, I., Rappuoli, R. and De Gregorio, E. (2014) 'Vaccines for the 21st century.' *EMBO molecular medicine*, 6(6), pp.708-720.

Delcour, A.H. (2009) 'Outer membrane permeability and antibiotic resistance.' Biochimica et Biophysica Acta (BBA)-Proteins and Proteomics, 1794(5), pp.808-816.

Demirezen, N., Tarınç, D., Polat, D., Çeşme, M., Gölcü, A. and Tümer, M. (2012) 'Synthesis of trimethoprim metal complexes: Spectral, electrochemical, thermal, DNA-binding and surface morphology studies.' *Spectrochimica Acta Part A: Molecular and Biomolecular Spectroscopy*, 94(1), pp.243-255.

Deny, A., Loiez, C., Deken, V., Putman, S., Duhamel, A., Girard, J., Pasquier, G., Chantelot, C., Senneville, E. and Migaud, H. (2016) 'Epidemiology of patients with MSSA versus MRSA infections of orthopedic implants: retrospective study of 115 patients.' *Orthopaedics & Traumatology: Surgery & Research*, 102(7), pp.919-923.

Desbois, A.P. and Coote, P.J. (2011) 'Wax moth larva (Galleria mellonella): an in vivo model for assessing the efficacy of antistaphylococcal agents.' *Journal of Antimicrobial Chemotherapy*, 66(8), pp.1785-1790.

Deurenberg RH, Vink C, Kalenic S, Friedrich AW, Bruggeman CA, Stob-beringh EE. (2007) 'The molecular evolution of methicillin-resistant Staphylococcus aureus.' *Clin Microbiol Infect,* 13(1), pp. 222–235.

Deurenberg, R.H. and Stobberingh, E.E. (2009) 'The molecular evolution of hospital-and community-associated methicillin-resistant Staphylococcus aureus.' *Current molecular medicine*, 9(2), pp.100-115.

Devínsky, F., Kopecka-Leitmanová, A., Šeršeň, F. and Balgavý, P. (1990) 'Cut-off effect in antimicrobial activity and in membrane perturbation efficiency of the homologous series of N, N-dimethylalkylamine oxides.' *Journal of pharmacy and pharmacology*, 42(11), pp.790-794.

Diab, J., Bannan, A. and Pollitt, T. (2020) 'Necrotising fasciitis.' *BMJ*, 369(1), pp. 1-6.

Divya, J., Mohandas, A. and Singh, B. (2018) 'A non-pathogenic environmental isolate of Pseudomonas aeruginosa MCCB 123 with biotechnological potential.' International Journal of Current Microbiology Applied Sciences, 7(1), pp.3060-3071.

Dixon, A.S., Schwinn, M.K., Hall, M.P., Zimmerman, K., Otto, P., Lubben, T.H., Butler, B.L., Binkowski, B.F., Machleidt, T., Kirkland, T.A. and Wood, M.G. (2016) 'NanoLuc complementation reporter optimized for accurate measurement of protein interactions in cells.' *ACS chemical biology*, 11(2), pp.400-408.

Doi, Y., Wachino, J.I. and Arakawa, Y. (2016) 'Aminoglycoside resistance: the emergence of acquired 16S ribosomal RNA methyltransferases.' *Infectious Disease Clinics*, 30(2), pp.523-537.

Domínguez, A.V., Algaba, R.A., Canturri, A.M., Villodres, Á.R. and Smani, Y. (2020) 'Antibacterial activity of colloidal silver against Gram-negative and Gram-positive bacteria.' *Antibiotics*, *9*(1), pp. 1-10.

Dong, C.L., Li, L.X., Cui, Z.H., Chen, S.W., Xiong, Y.Q., Lu, J.Q., Liao, X.P., Gao, Y., Sun, J. and Liu, Y.H. (2017) 'Synergistic effect of pleuromutilins with other antimicrobial agents against Staphylococcus aureus in vitro and in an experimental Galleria mellonella model.' *Frontiers in pharmacology*, 8(1), pp.553-561.

Dowd, S.E., Wolcott, R.D., Sun, Y., McKeehan, T., Smith, E. and Rhoads, D. (2008) 'Polymicrobial nature of chronic diabetic foot ulcer biofilm infections determined using bacterial tag encoded FLX amplicon pyrosequencing (bTEFAP).' PloS one, 3(10), pp.e3326-3333.

Dwyer FP, Reid IK, Shulman A, Laycock GM, Dixon S. (1969) 'Biological actions of 1,10-phenanthroline and 2,20-bipyridinehydrochlorides, quaternary salts and metal chelates and related compounds. 1. Bacteriostatic action on selected Gram-positive, Gram-negative and acid-fast bacteria.' *Austral J Exp Bio Med Sci*, 47(1) pp. 203-218.

Dwyer, D.J., Camacho, D.M., Kohanski, M.A., Callura, J.M. and Collins, J.J. (2012) 'Antibiotic-induced bacterial cell death exhibits physiological and biochemical hallmarks of apoptosis.' *Molecular cell*, 46(5), pp.561-572.

Dwyer, F.P., Gyarfas, E.C., Rogers, W.P. and Koch, J.H. (1952) 'Biological activity of complex ions.' *Nature*, 170(4318), pp.190-191.

Dwyer, FP; Reid, IK; Shulman, A; Laycock, GM; Dixson, S. (1969) 'THE BIOLOGICAL ACTIONS OF 1, 10-PHENANTHROLINE AND 2, 2'-BIPYRIDINE HYDROCHLORIDES, QUATERNARY SALTS AND METAL CHELATES AND RELATED COMPOUNDS: 1. BACTERIOSTATIC ACTION ON SELECTED GRAM-POSITIVE, GRAM-NEGATIVE AND ACID-FAST BACTERIA.' *Aust J Exp Biol Med Sci***.** 47(2), pp. 203-18.

Džidić, S., Šušković, J. and Kos, B. (2008) 'Antibiotic resistance mechanisms in bacteria: biochemical and genetic aspects.' *Food Technology & Biotechnology*, 46(1) pp. 11-21.

El Aamri, M., Yammouri, G., Mohammadi, H., Amine, A. and Korri-Youssoufi, H. (2020) 'Electrochemical biosensors for detection of MicroRNA as a cancer biomarker: Pros and Cons.' Biosensors, 10(11), p.186-232.

El Mohtadi, M., Pilkington, L., Liauw, C.M., Ashworth, J.J., Dempsey-Hibbert, N., Belboul, A. and Whitehead, K.A. (2020) 'Differential engulfment of Staphylococcus aureus and

Pseudomonas aeruginosa by monocyte-derived macrophages is associated with altered phagocyte biochemistry and morphology.' *EXCLI journal*, 19(1), p.1372-1384.

El'Garch, F., Jeannot, K., Hocquet, D., Llanes-Barakat, C. and Plésiat, P. (2007) 'Cumulative effects of several nonenzymatic mechanisms on the resistance of Pseudomonas aeruginosa to aminoglycosides.' *Antimicrobial agents and chemotherapy*, 51(3), pp.1016-1021.

El-Shouny, W.A., Ali, S.S., Sun, J., Samy, S.M. and Ali, A. (2018) 'Drug resistance profile and molecular characterization of extended spectrum beta-lactamase (ESβL)-producing Pseudomonas aeruginosa isolated from burn wound infections. Essential oils and their potential for utilization.' Microbial pathogenesis, 116(1), pp.301-312.

Elston, J.W.T. and Barlow, G.D. (2009) 'Community-associated MRSA in the United Kingdom.' *Journal of Infection*, 59(3), pp.149-155.

Endo, Y., Tani, T,. and Kodama, M. (1987) 'Antimicrobial activity of tertiary amine covalently bonded to a polystyrene fiber.' *Applied and environmental microbiology*, 53(9), pp.2050-2055.

Eriksen KR. (1961) *'"Celbenin"-resistant staphylococci.' Ugeskr Laeger* 123(1), pp. 384–386.

Espadinha, D., Faria, N.A., Miragaia, M., Lito, L.M., Melo-Cristino, J., de Lencastre, H. and Médicos Sentinela Network. (2013) 'Extensive dissemination of methicillin-resistant Staphylococcus aureus (MRSA) between the hospital and the community in a country with a high prevalence of nosocomial MRSA.' *PloS one*, 8(4), p.e59960-68.

Fagnani, L., Nazzicone, L., Brisdelli, F., Giansanti, L., Battista, S., Iorio, R., Petricca, S., Amicosante, G., Perilli, M., Celenza, G. and Bellio, P. (2021) 'Cyclic and Acyclic Amine Oxide

Alkyl Derivatives as Potential Adjuvants in Antimicrobial Chemotherapy against Methicillin-Resistant Staphylococcus aureus with an MDR Profile.' *Antibiotics*, 10(8), pp.952-965.

Fagundes, F.D., Reis, J.D., Appelt, P., Cavarzan, D.A., Murakami, F.S., Scopelliti, R., Dyson, P.J. and De Araujo, M.P. (2016) 'p, t-[Ru (CO)(PR3)(tren)] 2+[R= Ph or p-tol; tren= tris (2-aminoethyl) amine], Ru (II) complexes bearing a simple tripodal tetradentate amine: synthesis, characterization, and antimicrobial activity.' *Journal of Coordination Chemistry*, 69(18), pp.2637-2646.

Fandzloch, M., Arriaga, J.M.M., Sánchez-Moreno, M., Wojtczak, A., Jezierska, J., Sitkowski, J., Wiśniewska, J., Salas, J.M. and Łakomska, I. (2017) 'Strategies for overcoming tropical disease by ruthenium complexes with purine analog: Application against Leishmania spp. and Trypanosoma cruzi.' *Journal of Inorganic Biochemistry*, 176(1), pp.144-155.

Fazli, M., Bjarnsholt, T., Kirketerp-Møller, K., Jørgensen, A., Andersen, C.B., Givskov, M. and Tolker-Nielsen, T. (2011) 'Quantitative analysis of the cellular inflammatory response against biofilm bacteria in chronic wounds.' *Wound repair and regeneration*, 19(3), pp.387-391.

Feng, Y., Sun, W.Z., Wang, X.S. and Zhou, Q.X. (2019) 'Selective Photoinactivation of Methicillin-Resistant Staphylococcus aureus by Highly Positively Charged RuII complexes.' *Chemistry–A European Journal*, 25(61), pp.13879-13884.

Fernandes, P. (2016) 'Fusidic acid: a bacterial elongation factor inhibitor for the oral treatment of acute and chronic staphylococcal infections.' *Cold Spring Harbor perspectives in medicine*, 6(1), pp.a025437-54.

Flemming, H.C. and Wingender, J. (2010) 'The biofilm matrix.' Nature reviews microbiology, 8(9), pp.623-633.

Franke, S. (2007). 'Microbiology of the toxic noble metal silver.' *Molecular Microbiology of Heavy Metals*, Microbiology Monographs, vol 6. Springer, Berlin, Heidelberg, pp. 343-355.

Frauhiger, B. (2014). *Hexaammineruthenium(III) chloride.* Available: http://www.colonialmetals.com/product/hexaammineruthe niumiii-chloride/. Last accessed 6th Jan 2020.

Frausin, F., Cocchietto, M., Bergamo, A., Scarcia, V., Furlani, A. and Sava, G. (2002) 'Tumour cell uptake of the metastasis inhibitor ruthenium complex NAMI-A and its in vitro effects on KB cells.' *Cancer chemotherapy and pharmacology*, 50(1), pp.405-411.

Frei, A. (2020) 'Metal complexes, an Untapped Source of Antibiotic Potential?.' *Antibiotics*, *9*(2), pp.90-114.

Frei, A., King, A.P., Lowe, G.J., Cain, A.K., Short, F.L., Dinh, H., Elliott, A.G., Zuegg, J., Wilson, J.J. and Blaskovich, M.A. (2021) 'Nontoxic Cobalt (III) Schiff Base complexes with Broad-Spectrum Antifungal Activity.' *Chemistry–A European Journal*, 27(6), pp.2021-2029.

Frei, A., Ramu, S., Lowe, G.J., Dinh, H., Semenec, L., Elliott, A.G., Zuegg, J., Deckers, A., Jung, N., Bräse, S. and Cain, A.K. (2021) 'Platinum Cyclooctadiene complexes with Activity against Gram-positive Bacteria.' *ChemMedChem*, 16(20), pp.3165-3171.

Gai, P., Gu, C., Li, H., Sun, X. and Li, F. (2017) 'Ultrasensitive ratiometric homogeneous electrochemical microRNA biosensing via target-triggered Ru (III) release and redox recycling.' Analytical chemistry, 89(22), pp.12293-12298.

Gajdács, M., Urbán, E., Stájer, A. and Baráth, Z. (2021) 'Antimicrobial resistance in the context of the sustainable development goals: A brief review.' *European Journal of Investigation in Health, Psychology and Education*, 11(1), pp.71-82.

Gales, A.C., Seifert, H., Gur, D., Castanheira, M., Jones, R.N. and Sader, H.S. (2019) 'Antimicrobial susceptibility of Acinetobacter calcoaceticus–Acinetobacter baumannii complex and Stenotrophomonas maltophilia clinical isolates: results from the SENTRY antimicrobial surveillance proGram (1997–2016).' *Open forum infectious diseases,* 6(1), pp.34-46.

Galle, M., Carpentier, I. and Beyaert, R. (2012) 'Structure and function of the Type III secretion system of Pseudomonas aeruginosa.' *Current protein and peptide science*, 13(8), pp.831-842.

Gandra, R.M., McCarron, P., Viganor, L., Fernandes, M.F., Kavanagh, K., McCann, M., Branquinha, M.H., Santos, A.L., Howe, O. and Devereux, M. (2020) 'In vivo activity of copper (II), manganese (II), and silver (I) 1, 10-phenanthroline chelates against Candida haemulonii using the Galleria mellonella Model.' *Frontiers in Microbiology*, 11(1), pp.470-485.

Gao, N., Kumar, A., Jyot, J. and Yu, F.S. (2010) 'Flagellin-Induced Corneal Antimicrobial Peptide Production and Wound Repair Involve a Novel NF-κB–Independent and EGFR-Dependent Pathway.' *PloS one*, 5(2), pp.e9351-9361.

Garcia, M., Morello, E., Garnier, J., Barrault, C., Garnier, M., Burucoa, C., Lecron, J.C., Si-Tahar, M., Bernard, F.X. and Bodet, C. (2018) 'Pseudomonas aeruginosa flagellum is critical for invasion, cutaneous persistence and induction of inflammatory response of skin epidermis.' Virulence, 9(1), pp.1163-1175.

García, T., Revenga-Parra, M., Sobrino, B., Carracedo, A., Alonso, C., Lorenzo, E. and Pariente, F. (2011) 'Electrochemical DNA base pairs quantification and endonuclease cleavage detection.' Biosensors and Bioelectronics, 27(1), pp.40-45.

Garza-Cervantes, J.A., Meza-Bustillos, J.F., Resendiz-Hernández, H., Suárez-Cantú, I.A., Ortega-Rivera, O.A., Salinas, E., Escárcega-González, C.E. and Morones-Ramírez, J.R. (2020) 'Re-sensitizing ampicillin and kanamycin-resistant E. coli and S. aureus using synergistic metal micronutrients-antibiotic combinations.' *Frontiers in bioengineering and biotechnology*, 8(1), pp.612-633.

Gautam, T. and Gopi, A. (2019) 'PSEUDOMONAS-AN EMERGING NOSOCOMIAL PATHOGEN.' *Journal of Evolution of Medical and Dental Sciences*, 8(1), pp.5-10.

Gessner, R.V., Quigley, G.J., Wang, A.H.J., van der Mare, G.A., Van Boom, J.H. and Rich, A. (1985) 'Structural basis for stabilization of Z-DNA by cobalt hexaammine and magnesium cations.' *The Excitement of Discovery: Selected Papers of Alexander Rich: A Tribute to Alexander Rich,* pp. 196-199.

Ghafoor, A., Hay, I.D. and Rehm, B.H. (2011) 'Role of exopolysaccharides in Pseudomonas aeruginosa biofilm formation and architecture.' *Applied and environmental microbiology*, 77(15), pp.5238-5246.

Ghosh, S. (2019) 'Cisplatin: The first metal based anticancer drug.' *Bioorganic chemistry*, 88(1), pp.102925-102945.

Giachi, G., Pallecchi, P., Romualdi, A., Ribechini, E., Lucejko, J.J., Colombini, M.P. and Lippi, M.M. (2013) 'Ingredients of a 2,000-y-old medicine revealed by chemical, mineralogical, and botanical investigations.' *Proceedings of the National Academy of Sciences*, 110(4), pp.1193-1196.

Gibreel, T.M. and Upton, M. (2013) 'Synthetic epidermicin NI01 can protect Galleria mellonella larvae from infection with Staphylococcus aureus.' *Journal of Antimicrobial Chemotherapy*, 68(10), pp.2269-2273.

Gibson, T.L.B. and Cohen, P. (1999) 'Inflammation-related neutrophil proteases, cathepsin G and elastase, function as insulin-like growth factor binding protein proteases.' *Growth Hormone & IGF Research*, 9(4), pp.241-253.

Giedraitienė, A., Vitkauskienė, A., Naginienė, R. and Pavilonis, A. (2011) 'Antibiotic resistance mechanisms of clinically important bacteria.' *Medicina*, 47(3), pp.19-29.

Gil, M.R. (2019) 'Overview of the coagulation system.' *Transfusion Medicine and Hemostasis*, pp. 559-564.

Gill, M.R., Walker, M.G., Able, S., Tietz, O., Lakshminarayanan, A., Anderson, R., Chalk, R., El-Sagheer, A.H., Brown, T., Thomas, J.A. and Vallis, K.A. (2020) 'An 111 In-labelled bis-ruthenium (II) dipyridophenazine theranostic complex: mismatch DNA binding and selective radiotoxicity towards MMR-deficient cancer cells.' *Chemical science*, 11(33), pp.8936-8944.

Giurato, L., Meloni, M., Izzo, V. and Uccioli, L. (2017) 'Osteomyelitis in diabetic foot: a comprehensive overview.' *World journal of diabetes*, 8(4), pp.135-142.

Glowacka, E., Banasik, M., Lewkowicz, P. and Tchorzewski, H. (2002) 'The effect of LPS on neutrophils from patients with high risk of type 1 diabetes mellitus in relation to IL-8, IL-10 and IL-12 production and apoptosis in vitro.' *Scandinavian journal of immunology*, 55(2), pp.210-217.

Gold, K., Slay, B., Knackstedt, M. and Gaharwar, A.K. (2018). 'Antimicrobial activity of metal and metal-oxide based nanoparticles.' *Advanced Therapeutics*, 1(3), pp.1700033 - 1700048.

Gould, L., Abadir, P., Brem, H., Carter, M., Conner-Kerr, T., Davidson, J., DiPietro, L., Falanga, V., Fife, C., Gardner, S. and Grice, E. (2015) 'Chronic wound repair and healing in older adults: current status and future research.' Journal of the American Geriatrics Society, 63(3), pp.427-438.

Granato, M.Q., Mello, T.P., Nascimento, R.S., Pereira, M.D., Rosa, T.L., Pessolani, M.C., McCann, M., Devereux, M., Branquinha, M.H., Santos, A.L. and Kneipp, L.F. (2021) 'Silver (I) and Copper (II) complexes of 1, 10-Phenanthroline-5, 6-Dione Against: A Focus on the Interaction With Human Macrophages and Larvae.' *Frontiers in Microbiology*, 12(1), pp. 1-12.

Grass, G., Rensing, C. and Solioz, M. (2011) 'Metallic copper as an antimicrobial surface.' *Applied and Environmental Microbiology*, 77(5), pp.1541-1547.

Green, A.E., Amezquita, A., Le Marc, Y., Bull, M.J., Connor, T.R. and Mahenthiralingam, E. (2018) 'The consistent differential expression of genetic pathways following exposure of an industrial Pseudomonas aeruginosa strain to preservatives and a laundry detergent formulation.' *FEMS microbiology letters*, 365(9), pp.1-8.

Greenberg, M., Kuo, D., Jankowsky, E., Long, L., Hager, C., Bandi, K., Ma, D., Manoharan, D., Shoham, Y., Harte, W. and Ghannoum, M.A. (2018) 'Small-molecule AgrA inhibitors F12 and F19 act as antivirulence agents against Gram-positive pathogens.' *Scientific reports*, 8(1), pp.1-12.

Greiling, D. and Clark, R.A. (1997) 'Fibronectin provides a conduit for fibroblast transmigration from collagenous stroma into fibrin clot provisional matrix.' *Journal of cell science*, 110(7), pp.861-870.

Grossman, T.H. (2016) 'Tetracycline antibiotics and resistance.' *Cold Spring Harbor Perspectives in Medicine*, 6(4), pp.1-25.

Grundmann H, Schouls LM, Aanensen DM, Pluister GN, Tami A,Chlebowicz M, Glasner C, Sabat AJ, Weist K, Heuer O, Friedrich AW,ESCMID Study Group on Molecular Epidemiological Markers, Euro-pean Staphylococcal Reference Laboratory Working Group. (2014) 'The

dynamic changes of dominant clones of Staphylococcus aureus causing bloodstream infections in the European region: results of asecond structured survey.' *Euro Surveill*, 19(49), pp. 20987-20997.

Grundmann, H., Glasner, C., Albiger, B., Aanensen, D.M., TomLinson, C.T., Andrasević, A.T., Cantón, R., Carmeli, Y., Friedrich, A.W., Giske, C.G. and Glupczynski, Y. (2017) 'Occurrence of carbapenemase-producing Klebsiella pneumoniae and Escherichia coli in the European survey of carbapenemase-producing Enterobacteriaceae (EuSCAPE): a prospective, multinational study.' *The Lancet infectious diseases*, 17(2), pp.153-163.

Grundmann, H., Schouls, L.M., Aanensen, D.M., Pluister, G.N., Tami, A., Chlebowicz, M., Glasner, C., Sabat, A.J., Weist, K., Heuer, O. and Friedrich, A.W. (2014) 'The dynamic changes of dominant clones of Staphylococcus aureus causing bloodstream infections in the European region: results of a second structured survey.' *Eurosurveillance*, 19(49), pp.20987.

Gu, L., Li, X., Ran, Q., Kang, C., Lee, C. and Shen, J. (2016) 'Antimetastatic activity of novel ruthenium (III) pyridine complexes.' *Cancer Medicine*, 5(10), pp.2850-2860.

Gu, Y.Q., Shen, W.Y., Yang, Q.Y., Chen, Z.F. and Liang, H. (2022) 'Ru (III) complexes with pyrazolopyrimidines as anticancer agents: Bioactivities and the underlying mechanisms.' *Dalton Transactions*, 51(4), pp.1333-1343.

Guilbaud, M., Bruzaud, J., Bouffartigues, E., Orange, N., Guillot, A., Aubert-Frambourg, A., Monnet, V., Herry, J.M., Chevalier, S. and Bellon-Fontaine, M.N. (2017) 'Proteomic response of Pseudomonas aeruginosa PAO1 adhering to solid surfaces.' *Frontiers in Microbiology*, 8(1), pp.1465-1480.

Güntzel, P., Nagel, C., Weigelt, J., Betts, J.W., Pattrick, C.A., Southam, H.M., La Ragione, R.M., Poole, R.K. and Schatzschneider, U. (2019) 'Biological activity of manganese (i)

tricarbonyl complexes on multidrug-resistant Gram-negative bacteria: From functional studies to in vivo activity in Galleria mellonella.' *Metallomics*, 11(12), pp.2033-2042.

Guo, S.A. and DiPietro, L.A. (2010) 'Factors affecting wound healing.' *Journal of dental research*, 89(3), pp.219-229.

Gupta, P., Sarkar, A., Sandhu, P., Daware, A., Das, M.C., Akhter, Y. and Bhattacharjee, S. (2017) 'Potentiation of antibiotic against Pseudomonas aeruginosa biofilm: a study with plumbagin and gentamicin.' *Journal of applied microbiology*, 123(1), pp.246-261.

Gupta, S.C., Hevia, D., Patchva, S., Park, B., Koh, W. and Aggarwal, B.B. (2012) 'Upsides and downsides of reactive oxygen species for cancer: the roles of reactive oxygen species in tumorigenesis, prevention, and therapy.' *Antioxidants & redox signaling*, *16*(11), pp.1295-1322.

Gupta, V. and Datta, P. (2019) 'Next-generation strategy for treating drug resistant bacteria: Antibiotic hybrids.' *The Indian journal of medical research*, 149(2), pp.97-106.

Gurunathan, S., Han, J.W., Dayem, A.A., Eppakayala, V. and Kim, J.H. (2012) 'Oxidative stress-mediated antibacterial activity of graphene oxide and reduced graphene oxide in Pseudomonas aeruginosa.' *International journal of nanomedicine*, 7(1), pp.5901-5914.

Haaber, J., Friberg, C., McCreary, M., Lin, R., Cohen, S.N. and Ingmer, H. (2015) 'Reversible antibiotic tolerance induced in Staphylococcus aureus by concurrent drug exposure.' *MBio*, 6(1), pp. e02268-14.

Hagstrand Aldman, M., Skovby, A. and I. Påhlman, L. (2017) 'Penicillin-susceptible Staphylococcus aureus: susceptibility testing, resistance rates and outcome of infection.' *Infectious Diseases*, 49(6), pp.454-460.

Haiko, J. and Westerlund-Wikström, B. (2013) 'The role of the bacterial flagellum in adhesion and virulence.' Biology, 2(4), pp.1242-1267.

Hall, S., McDermott, C., Anoopkumar-Dukie, S., McFarland, A.J., Forbes, A., Perkins, A.V., Davey, A.K., Chess-Williams, R., Kiefel, M.J., Arora, D. and Grant, G.D. (2016) 'Cellular effects of pyocyanin, a secreted virulence factor of Pseudomonas aeruginosa.' *Toxins*, 8(8), pp.236-250.

Hambley, T.W., Keyte, P., Lay, P.A. and Paddon-Row, M.N. (1991) 'Structure of pentaamminechlororuthenium (III) sesquichloride hemi (tetrafluoroborate).' *Acta Crystallographica Section C: Crystal Structure Communications*, 47(5), pp.941-943.

Han, B.J., Jiang, G.B., Yao, J.H., Li, W., Wang, J., Huang, H.L. and Liu, Y.J. (2015) 'DNA interaction, antioxidant activity, and bioactivity studies of two ruthenium (II) complexes.' *Spectrochimica Acta Part A: Molecular and Biomolecular Spectroscopy*, 135(1), pp.840-849.

Haney, E.F., Straus, S.K. and Hancock, R.E. (2019) 'Reassessing the host defense peptide landscape.' *Frontiers in chemistry*, 7(1), pp.43-65.

Hardie, K.R. (2020) 'Antimicrobial resistance: the good, the bad, and the ugly.' *Emerging Topics in Life Sciences*, *4*(2), pp.129-136.

Hari, N., Thomas, T.K. and Nair, A.J. (2014) 'Comparative study on the synergistic action of differentially synthesized silver nanoparticles with β-cephem antibiotics and chloramphenicol.' *Journal of Nanoscience*, 2014(1), pp.1-9.

Hari-Dass, R., Shah, C., Meyer, D.J. and Raynes, J.G. (2005) 'Serum amyloid A protein binds to outer membrane protein A of Gram-negative bacteria.' *Journal of Biological Chemistry*, 280(19), pp.18562-18567.

Harika, K., Shenoy, V.P., Narasimhaswamy, N. and Chawla, K. (2020) 'Detection of biofilm production and its impact on antibiotic resistance profile of bacterial isolates from chronic wound infections.' *Journal of Global Infectious Diseases*, 12(3), p.129-134.

Harms, J.M., Schlünzen, F., Fucini, P., Bartels, H. and Yonath, A. (2004) 'Alterations at the peptidyl transferase centre of the ribosome induced by the synergistic action of the streptoGramins dalfopristin and quinupristin.' *BMC biology*, 2(1), pp.4-14.

Harrison, J.J., Ceri, H. and Turner, R.J. (2007) 'Multimetal resistance and tolerance in microbial biofilms.' *Nature Reviews Microbiology*, 5(12), pp.928-938.

Hartinger, C.G. and Dyson, P.J. (2009) 'Bioorganometallic chemistry—from teaching paradigms to medicinal applications.' *Chemical Society Reviews*, 38(2), pp.391-401.

Hassan, M.H.A., Ismail, M.A., Moharram, A.M. and Shoreit, A. (2016) 'Synergistic Effect of Biogenic Silver-nanoparticles with β lactam Cefotaxime against Resistant Staphylococcus arlettae AUMC b-163 Isolated from T3A Pharmaceutical Cleanroom, Assiut, Egypt.' *Am. J. Microbiol. Res*, 4(1), pp.132-137.

Hatamie, S., Ahadian, M.M., Zomorod, M.S., Torabi, S., Babaie, A., Hosseinzadeh, S., Soleimani, M., Hatami, N. and Wei, Z.H. (2019) 'Antibacterial properties of nanoporous graphene oxide/cobalt metal organic framework.' *Materials Science and Engineering: C*, 104(1), pp.109862-109872.

Hay, I.D., Rehman, Z.U., Moradali, M.F., Wang, Y. and Rehm, B.H. (2013) 'Microbial alginate production, modification and its applications.' *Microbial biotechnology*, 6(6), pp.637-650.

Hegazy, W.A., Khayat, M.T., Ibrahim, T.S., Nassar, M.S., Bakhrebah, M.A., Abdulaal, W.H., Alhakamy, N.A. and Bendary, M.M. (2020) 'Repurposing anti-diabetic drugs to cripple quorum sensing in Pseudomonas aeruginosa.' *Microorganisms*, 8(9), pp.1285-1304.

Heidari, A. (2016) 'A Chemotherapeutic and Biospectroscopic Investigation of the Interaction of Double–Standard DNA/RNA–Binding Molecules with Cadmium Oxide (CdO) and Rhodium (III) Oxide (Rh2O3) Nanoparticles as Anti–Cancer Drugs for Cancer Cells' Treatment.' *Chemo Open Access*, 5(2), p.e129-131.

Helmy, I.M. and Abdel Azim, A.M. (2012) 'Efficacy of ImageJ in the assessment of apoptosis.' *Diagnostic pathology*, 7(1), pp.1-6.

Hempel, F., Finke, B., Zietz, C., Bader, R., Weltmann, K.D. and Polak, M. (2014) 'Antimicrobial surface modification of titanium substrates by means of plasma immersion ion implantation and deposition of copper.' *Surface and Coatings Technology*, 256, pp.52-58.

Hernández-Hernández, J.G., Aguilar, C.A.H., Thangarasu, P. and Hernández-Trujillo, J. (2020) 'Photochemical and antibacterial properties of ruthenium complex of N, N'-bis (benzimidazole-2yl-ethyl) ethylenediamine under visible light: Experimental and theoretical studies.' *Journal of Molecular Structure*, 1203(1), pp.127377-127390.

Hesketh, M., Sahin, K.B., West, Z.E. and Murray, R.Z. (2017) 'Macrophage phenotypes regulate scar formation and chronic wound healing.' *International journal of molecular sciences*, 18(7), pp.1545-1555.

Hobman, J. L. & Silver, S. (2007). 'Mercury microbiology: resistance systems, environmental aspects, methylation and human health.' *Molecular Microbiology of Heavy Metals*, pp. 358–370.

Hobman, J.L. and Crossman, L.C. (2015). 'Bacterial antimicrobial metal ion resistance.' *Journal of Medical Microbiology*, 64*(5), pp*. 471–497.

Hoeschele, J.D., Habtemariam, A., Muir, J. and Sadler, P.J. (2007) '^{106}Ru radiolabelling of the antitumour complex [(η 6-fluorene) Ru (en) Cl] PF 6'. *Dalton Transactions*, 43, pp.4974-4979.

Hong, C.Y., Chen, X., Liu, T., Li, J., Yang, H.H., Chen, J.H. and Chen, G.N. (2013) 'Ultrasensitive electrochemical detection of cancer-associated circulating microRNA in serum samples based on DNA concatamers.' *Biosensors and Bioelectronics*, 50(1), pp.132-136.

Hostetter, A.A., Miranda, M.L., DeRose, V.J. and McFarlane Holman, K.L. (2011) 'Ru binding to RNA following treatment with the antimetastatic prodrug NAMI-A in Saccharomyces cerevisiae and in vitro.' *JBIC Journal of Biological Inorganic Chemistry*, 16(1), pp.1177-1185.

Hou, J., Veeregowda, D.H., van de Belt-Gritter, B., Busscher, H.J. and van der Mei, H.C. (2018) 'Extracellular polymeric matrix production and relaxation under fluid shear and mechanical pressure in Staphylococcus aureus biofilms.' *Applied and environmental microbiology*, 84(1), pp.e01516-17.

Huang, N., Chen, X., Zhu, X., Xu, M. and Liu, J. (2017) 'Ruthenium complexes/polypeptide self-assembled nanoparticles for identification of bacterial infection and targeted antibacterial research.' *Biomaterials*, 141(1), pp.296-313.

Huang, X., Chen, G., Pan, J., Chen, X., Huang, N., Wang, X. and Liu, J. (2016) 'Effective PDT/PTT dual-modal phototherapeutic killing of pathogenic bacteria by using ruthenium nanoparticles.' *Journal of Materials Chemistry B*, 4(37), pp.6258-6270.

Hubbard, L.L., Wilke, C.A., White, E.S. and Moore, B.B. (2011) 'PTEN limits alveolar macrophage function against Pseudomonas aeruginosa after bone marrow transplantation.' *American journal of respiratory cell and molecular biology*, 45(5), pp.1050-1058.

Huber, H., Koller, S., Giezendanner, N., Stephan, R. and Zweifel, C. (2010) 'Prevalence and characteristics of meticillin-resistant Staphylococcus aureus in humans in contact with farm

animals, in livestock, and in food of animal origin, Switzerland, 2009.' *Eurosurveillance*, 15(16), pp.19542.

Hudzicki, J. (2009) 'Kirby-Bauer Disk Diffusion Susceptibility Test Protocol.' *American Society for Microbiology*. 1 (1), pp. 1-23.

Hutchings, M., Truman, A. and Wilkinson, B. (2019) 'Antibiotics: past, present and future.' *Current Opinion in Microbiology*, 51(1), pp.72-80.

Hwang, I.S., Hwang, J.H., Choi, H., Kim, K.J. and Lee, D.G. (2012) 'Synergistic effects between silver nanoparticles and antibiotics and the mechanisms involved.' *Journal of medical microbiology*, 61(12), pp.1719-1726.

Ibraheem, S.A., Kadhem, H.A., Hadeethi, S.A., Jabir, M.S., Grigore, R., Popa, M., Gheorghe, I. and Florin, M.D. (2019) 'Effects of silver nanoparticles on nosocomial Pseudomonas aeruginosa strains–an alternative approach for antimicrobial therapy.' *Romanlan Biotechnological Letters*, 24(1), pp.286-293.

Idowu, T., Arthur, G., Zhanel, G.G. and Schweizer, F. (2019) 'Heterodimeric rifampicin–tobramycin conjugates break intrinsic resistance of Pseudomonas aeruginosa to doxycycline and chloramphenicol in vitro and in a Galleria mellonella in vivo model.' *European journal of medicinal chemistry*, 174(1), pp.16-32.

Imperi, F., Ciccosanti, F., Perdomo, A.B., Tiburzi, F., Mancone, C., Alonzi, T., Ascenzi, P., Piacentini, M., Visca, P. and Fimia, G.M. (2009) 'Analysis of the periplasmic proteome of Pseudomonas aeruginosa, a metabolically versatile opportunistic pathogen.' *Proteomics*, 9(7), pp.1901-1915.

Ip, M., Lui, S.L., Poon, V.K., Lung, I. and Burd, A. (2006) 'Antimicrobial activities of silver dressings: an in vitro comparison.' *Journal of Medical Microbiology*, 55(1), pp.59-63.

Ishida, S., Lee, J., Thiele, D.J. and Herskowitz, I. (2002) 'Uptake of the anticancer drug cisplatin mediated by the copper transporter Ctr1 in yeast and mammals.' *Proceedings of the National Academy of Sciences*, 99(22), pp.14298-14302.

Islam, S.T., Taylor, V.L., Qi, M. and Lam, J.S. (2010) 'Membrane topology mapping of the O-antigen flippase (Wzx), polymerase (Wzy), and ligase (WaaL) from Pseudomonas aeruginosa PAO1 reveals novel domain architectures.' *MBio*, 1(3), pp.e00189-10.

Jabłońska-Wawrzycka, A., Rogala, P., Czerwonka, G., Michałkiewicz, S., Hodorowicz, M. and Kowalczyk, P. (2020) 'Ruthenium (IV) complexes as potential inhibitors of bacterial biofilm formation.' *Molecules*, 25(21), pp.4938-4957.

Jäger, M., Jennissen, H.P., Dittrich, F., Fischer, A. and Köhling, H.L. (2017) 'Antimicrobial and osseointegration properties of nanostructured titanium orthopaedic implants.' *Materials*, 10(11), pp.1302-1330.

Jahromi, M.A.M., Zangabad, P.S., Basri, S.M.M., Zangabad, K.S., Ghamarypour, A., Aref, A.R., Karimi, M. and Hamblin, M.R. (2018) 'Nanomedicine and advanced technologies for burns: preventing infection and facilitating wound healing.' *Advanced drug delivery reviews*, 123(1), pp.33-64.

Jain, A., Garrett, N.T. and Malone, Z.P. (2022) 'Ruthenium-based Photoactive Metalloantibiotics.' *Photochemistry and Photobiology*, 98(1), pp.6-16.

Jain, A., Winkel, B.S. and Brewer, K.J. (2022) 'Photodynamic antimicrobial studies on a Ruthenium-based metal complex.' *Inorganica Chimica Acta*, 538(1), pp.120996-121001.

Jain, S.N., Vishwanatha, T., Reena, V., Divyashree, B.C., Sampath, A., Siddhalingeshwara, K.G., Venugopal, N. and Ramesh, I. (2011) 'Antibiotic synergy test: Checkerboard method on multidrug resistant Pseudomonas aeruginosa.' *Int. Res. J. Pharm*, 2(12), pp.196-198.

James, G.A., Swogger, E., Wolcott, R., Pulcini, E.D., Secor, P., Sestrich, J., Costerton, J.W. and Stewart, P.S. (2008) 'Biofilms in chronic wounds.' *Wound Repair and regeneration*, 16(1), pp.37-44.

Jeffery Marano, R., Jane Wallace, H., Wijeratne, D., William Fear, M., San Wong, H. and O'Handley, R. (2015) 'Secreted biofilm factors adversely affect cellular wound healing responses in vitro.' *Scientific reports*, 5(1), pp.1-11.

Jennings, L.K., Storek, K.M., Ledvina, H.E., Coulon, C., Marmont, L.S., Sadovskaya, I., Secor, P.R., Tseng, B.S., Scian, M., Filloux, A. and Wozniak, D.J. (2015) 'Pel is a cationic exopolysaccharide that cross-links extracellular DNA in the Pseudomonas aeruginosa biofilm matrix.' *Proceedings of the National Academy of Sciences*, 112(36), pp.11353-11358.

Jesline, A., John, N.P., Narayanan, P.M., Vani, C. and Murugan, S. (2015) 'Antimicrobial activity of zinc and titanium dioxide nanoparticles against biofilm-producing methicillin-resistant Staphylococcus aureus.' *Applied Nanoscience*, 5(2), pp.157-162.

Jessen, O., Rosendal, K., Bülow, P., Faber, V. and Eriksen, K.R. (1969) 'Changing staphylococci and staphylococcal infections: a ten-year study of bacteria and cases of bacteremia.' *New England Journal of Medicine*, 281(12), pp.627-635.

Jiang, B., Yin, S., You, B., Gong, Y., Huang, G., Yang, Z., Zhang, Y., Chen, Y., Chen, J., Yuan, Z. and Hu, X. (2018) 'Antimicrobial resistance and virulence genes profiling of methicillin-resistant Staphylococcus aureus isolates in a burn center: a 5-year study.' *Microbial pathogenesis*, 114(1), pp.176-179.

Jin, M., Liu, L., Wang, D.N., Yang, D., Liu, W.L., Yin, J., Yang, Z.W., Wang, H.R., Qiu, Z.G., Shen, Z.Q. and Shi, D.Y. (2020) 'Chlorine disinfection promotes the exchange of antibiotic resistance genes across bacterial genera by natural transformation.' *The ISME journal*, 14(7), pp.1847-1856.

Johnstone, T.C., Alexander, S.M., Lin, W. and Lippard, S.J. (2014) 'Effects of monofunctional platinum agents on bacterial growth: a retrospective study.' *Journal of the American Chemical Society*, 136(1), pp.116-118.

Jones, C.J. and Wozniak, D.J. (2017) 'Psl produced by mucoid Pseudomonas aeruginosa contributes to the establishment of biofilms and immune evasion.' *MBio*, 8(3), pp.e00864-17.

Joyce, K., Saxena, S., Williams, A., Damurjian, C., Auricchio, N., Aluotto, S., Tynan, H. and Demain, A.L. (2010) 'Antimicrobial spectrum of the antitumor agent, cisplatin.' *The Journal of Antibiotics*, 63(8), pp.530-532.

Juers, D.H., Matthews, B.W. and Huber, R.E. (2012) 'LacZ β-galactosidase: structure and function of an enzyme of historical and molecular biological importance.' *Protein Science*, 21(12), pp.1792-1807.

Kalantari, K., Mostafavi, E., Afifi, A.M., Izadiyan, Z., Jahangirian, H., Rafiee-Moghaddam, R. and Webster, T.J. (2020) 'Wound dressings functionalized with silver nanoparticles: promises and pitfalls.' *Nanoscale*, *12*(4), pp.2268-2291.

Kalishwaralal, K., Banumathi, E., Pandian, S.R.K., Deepak, V., Muniyandi, J., Eom, S.H. and Gurunathan, S. (2009) 'Silver nanoparticles inhibit VEGF induced cell proliferation and migration in bovine retinal endothelial cells.' *Colloids and Surfaces B: Biointerfaces*, 73(1), pp.51-57.

Kang, K., Lim, D.H., Choi, I.H., Kang, T., Lee, K., Moon, E.Y., Yang, Y., Lee, M.S. and Lim, J.S. (2011) 'Vascular tube formation and angiogenesis induced by polyvinylpyrrolidone-coated silver nanoparticles.' *Toxicology letters*, 205(3), pp.227-234.

Kang, Y.S., Lee, Y., Jung, H., Jeon, C.O., Madsen, E.L. and Park, W. (2007) 'Overexpressing antioxidant enzymes enhances naphthalene biodegradation in Pseudomonas sp. strain As1.' *Microbiology*, 153(10), pp.3246-3254.

Kannan, P., Maiyalagan, T., Lin, B., Lei, W., Jie, C., Guo, L., Jiang, Z., Mao, S. and Subramanian, P. (2020) 'Nickel-phosphate pompon flowers nanostructured network enables the sensitive detection of microRNA.' Talanta, 209(1), pp.120511-120519.

Kanno, E., Kawakami, K., Miyairi, S., Tanno, H., Otomaru, H., Hatanaka, A., Sato, S., Ishii, K., Hayashi, D., Shibuya, N. and Imai, Y. (2013) 'Neutrophil-derived tumor necrosis factor-α contributes to acute wound healing promoted by N-(3-oxododecanoyl)-l-homoserine lactone from Pseudomonas aeruginosa.' *Journal of dermatological science*, 70(2), pp.130-138.

Kapitza, S., Pongratz, M., Jakupec, M.A., Heffeter, P., Berger, W., Lackinger, L., Keppler, B.K. and Marian, B. (2005) 'Heterocyclic complexes of ruthenium (III) induce apoptosis in colorectal carcinoma cells.' *Journal of cancer research and clinical oncology*, 131(1), pp.101-110.

Karimi, K., Odhav, A., Kollipara, R., Fike, J., Stanford, C. and Hall, J.C. (2017) 'Acute cutaneous necrosis: A guide to early diagnosis and treatment.' *Journal of Cutaneous Medicine and Surgery*, 21(5), pp.425-437.

Karlsson, H.L., Cronholm, P., Hedberg, Y., Tornberg, M., De Battice, L., Svedhem, S. and Wallinder, I.O. (2013) 'Cell membrane damage and protein interaction induced by copper containing nanoparticles—Importance of the metal release process.' *Toxicology*, 313(1), pp.59-69.

Kassam, N.A., Damian, D.J., Kajeguka, D., Nyombi, B. and Kibiki, G.S. (2017 'Spectrum and antibioGram of bacteria isolated from patients presenting with infected wounds in a Tertiary Hospital, northern Tanzania.' *BMC Research Notes*, 10(1), pp.757-763.

Katner, S.J., Johnson, W.E., Peterson, E.J., Page, P. and Farrell, N.P. (2018) 'Comparison of metal–ammine complexes binding to DNA and Heparin. Glycans as ligands in bioinorganic chemistry.' *Inorganic chemistry*, 57(6), pp.3116-3125.

Kavanagh, K.T., Abusalem, S. and Calderon, L.E. (2018) 'View point: gaps in the current guidelines for the prevention of Methicillin-resistant Staphylococcus aureus surgical site infections.' *Antimicrobial Resistance & Infection Control*, 7(1), pp.1-6.

Kelley, S.O. (2017) 'New technologies for rapid bacterial identification and antibiotic resistance profiling.' *SLAS TECHNOLOGY: Translating Life Sciences Innovation*, 22(2), pp.113-121.

Kengen, R., Thoonen, E., Daveson, K., Loong, B., Rodgers, H., Beckingham, W., Kennedy, K., Suwandarathne, R. and van Haren, F. (2018) 'Chlorhexidine washing in intensive care does not reduce bloodstream infections, blood culture contamination and drug-resistant microorganism acquisition: an interrupted time series analysis.' *Critical Care and Resuscitation*, 20(3), pp.231-240.

Khaledi, A., Schniederjans, M., Pohl, S., Rainer, R., Bodenhofer, U., Xia, B., Klawonn, F., Bruchmann, S., Preusse, M., Eckweiler, D. and Dötsch, A. (2016) 'Transcriptome profiling of

antimicrobial resistance in Pseudomonas aeruginosa.' *Antimicrobial agents and chemotherapy*, 60(8), pp.4722-4733.

Khalid, A., Ahmad, P., Alharthi, A.I., Muhammad, S., Khandaker, M.U., Rehman, M., Faruque, M.R.I., Din, I.U., Alotaibi, M.A., Alzimami, K. and Bradley, D.A. (2021) 'Structural, optical and antibacterial efficacy of pure and zinc-doped copper oxide against pathogenic bacteria.' *Nanomaterials*, 11(2), pp.451-464.

Khan TM, Kok YL, Bukhsh A, Lee LH, Chan KG, Goh BH. (2018) 'Incidence of methicillin resistant Staphylococcus aureus (MRSA) in isolates in a burn center: a 5-year study.' *Microbial pathogenesis*, *114*, pp.176-179.

Khan, F., Lee, J.W., Pham, D.T.N., Lee, J.H., Kim, H.W., Kim, Y.K. and Kim, Y.M. (2020) 'Streptomycin mediated biofilm inhibition and suppression of virulence properties in Pseudomonas aeruginosa PAO1.' *Applied microbiology and biotechnology*, 104(2), pp.799-816.

Khashan, K.S., Sulaiman, G.M. and Abdulameer, F.A. (2016) 'Synthesis and antibacterial activity of CuO nanoparticles suspension induced by laser ablation in liquid.' *Arabian journal for science and Engineering*, 41(1), pp.301-310.

Khoramrooz, S.S., Dolatabad, S.A., Dolatabad, F.M., Marashifard, M., Mirzaii, M., Dabiri, H., Haddadi, A., Rabani, S.M., Shirazi, H.R.G. and Darban-Sarokhalil, D. (2017) 'Detection of tetracycline resistance genes, aminoglycoside modifying enzymes, and coagulase gene typing of clinical isolates of Staphylococcus aureus in the Southwest of Iran.' *Iranian journal of basic medical sciences*, 20(8), pp.912-920.

Kierbel, A., Gassama-Diagne, A., Rocha, C., Radoshevich, L., Olson, J., Mostov, K. and Engel, J. (2007) 'Pseudomonas aeruginosa exploits a PIP3-dependent pathway to transform apical into basolateral membrane.' *The Journal of cell biology*, 177(1), pp.21-27.

Kim, J.S., Song, S., Lee, M., Lee, S., Lee, K. and Ha, N.C. (2016) 'Crystal structure of a soluble fragment of the membrane fusion protein HlyD in a type I secretion system of Gram-negative bacteria.' *Structure*, 24(3), pp.477-485.

Kim, P.Y., Kim, Y.S., Koo, I.G., Jung, J.C., Kim, G.J., Choi, M.Y., Yu, Z. and Collins, G.J. (2011) 'Bacterial inactivation of wound infection in a human skin model by liquid-phase discharge plasma.' PloS one, 6(8) pp. e24104-24110.

Kim, Y., Bae, I.K., Lee, H., Jeong, S.H., Yong, D. and Lee, K. (2014) 'In vivo emergence of colistin resistance in Acinetobacter baumannii clinical isolates of sequence type 357 during colistin treatment.' *Diagnostic microbiology and infectious disease*, *79*(3), pp.362-366.

King, E.A., Challa, S., Curtin, P. and Bielory, L. (2016) 'Penicillin skin testing in hospitalized patients with β-lactam allergies: effect on antibiotic selection and cost.' *Annals of Allergy, Asthma & Immunology*, 117(1), pp.67-71.

King, J.D., Kocíncová, D., Westman, E.L. and Lam, J.S. (2009) 'Lipopolysaccharide biosynthesis in Pseudomonas aeruginosa.' *Innate immunity*, 15(5), pp.261-312.

Kitamata, M. and Suetsugu, S. (2023) 'Ankyrin repeat domains with an amphipathic helix for membrane deformation.' In *Plasma Membrane Shaping* (pp. 65-75). Academic Press.

Knight, G.M., Glover, R.E., McQuaid, C.F., Olaru, I.D., Gallandat, K., Leclerc, Q.J., Fuller, N.M., Willcocks, S.J., Hasan, R., van Kleef, E. and Chandler, C.I. (2021) 'Antimicrobial resistance and COVID-19: intersections and implications.' *Elife*, 10(1), pp.e64139.

Kobayashi, S.D., Malachowa, N. and DeLeo, F.R. (2015) 'Pathogenesis of Staphylococcus aureus abscesses.' *The American journal of pathology*, 185(6), pp.1518-1527.

Köck, R., Becker, K., Cookson, B., van Gemert-Pijnen, J.E., Harbarth, S., Kluytmans, J.A.J.W., Mielke, M., Peters, G., Skov, R.L., Struelens, M.J. and Tacconelli, E. (2010) 'Methicillin-

resistant Staphylococcus aureus (MRSA): burden of disease and control challenges in Europe.' *Eurosurveillance*, 15(41), pp.19688.

Koechler, S., Farasin, J., Cleiss-Arnold, J. and Arsène-Ploetze, F. (2015) 'Toxic metal resistance in biofilms: diversity of microbial responses and their evolution.' *Research in Microbiology*, 166(10), pp.764-773.

Konai, M.M. and Haldar, J. (2019) 'Lysine-based small molecule sensitizes rifampicin and tetracycline against multidrug-resistant Acinetobacter baumannii and Pseudomonas aeruginosa.' *ACS infectious diseases*, 6(1), pp.91-99.

Konwar, A., Kalita, S., Kotoky, J. and Chowdhury, D. (2016) 'Chitosan–iron oxide coated graphene oxide nanocomposite hydrogel: a robust and soft antimicrobial biofilm.' *ACS Applied Materials & Interfaces*, 8(32), pp.20625-20634.

Kooti, M., Gharineh, S., Mehrkhah, M., Shaker, A. and Motamedi, H. (2015) 'Preparation and antibacterial activity of CoFe2O4/SiO2/Ag composite impregnated with streptomycin. '*Chemical Engineering Journal*, 259(1), pp.34-42.

Kora, A.J. and Arunachalam, J. (2011) 'Assessment of antibacterial activity of silver nanoparticles on Pseudomonas aeruginosa and its mechanism of action.' *World Journal of Microbiology and Biotechnology*, *27*(5), pp.1209-1216.

Krapp, F., Morris, A.R., Ozer, E.A. and Hauser, A.R. (2017) 'Virulence characteristics of carbapenem-resistant Klebsiella pneumoniae strains from patients with necrotizing skin and soft tissue infections.' *Scientific reports*, 7(1), pp.1-14.

Krishnamurthi, V.R., Niyonshuti, I.I., Chen, J. and Wang, Y. (2021) 'A new analysis method for evaluating bacterial growth with microplate readers.' *PLoS One*, *16*(1), p.e0245205-024524.

Kruczek, C., Wachtel, M., Alabady, M.S., Payton, P.R., Colmer-Hamood, J.A. and Hamood, A.N. (2012) 'Serum albumin alters the expression of iron-controlled genes in Pseudomonas aeruginosa.' *Microbiology*, 158(2), pp.353-367.

Krzyszczyk, P., Schloss, R., Palmer, A. and Berthiaume, F. (2018) 'The role of macrophages in acute and chronic wound healing and interventions to promote pro-wound healing phenotypes.' *Frontiers in physiology*, 9(1), pp.419-441.

Kucerka, N., Papp-Szabo, E., Nieh, M.P., Harroun, T.A., Schooling, S.R., Pencer, J., Nicholson, E.A., Beveridge, T.J. and Katsaras, J. (2008) 'Effect of cations on the structure of bilayers formed by lipopolysaccharides isolated from Pseudomonas aeruginosa PAO1.' *The Journal of Physical Chemistry B*, 112(27), pp.8057-8062.

Kumar, M., Jaiswal, S., Sodhi, K.K., Shree, P., Singh, D.K., Agrawal, P.K. and Shukla, P. (2019) 'Antibiotics bioremediation: perspectives on its ecotoxicity and resistance.' Environment international, 124(1), pp.448-461.

Kumar, S.V., Scottwell, S.Ø., Waugh, E., McAdam, C.J., Hanton, L.R., Brooks, H.J. and Crowley, J.D. (2016) 'Antimicrobial properties of tris (homoleptic) ruthenium (II) 2-Pyridyl-1, 2, 3-triazole "click" complexes against pathogenic bacteria, including methicillin-resistant staphylococcus aureus (MRSA).' *Inorganic Chemistry*, 55(19), pp.9767-9777.

Kuo, D., Yu, G., Hoch, W., Gabay, D., Long, L., Ghannoum, M., Nagy, N., Harding, C.V., Viswanathan, R. and Shoham, M. (2015) 'Novel quorum-quenching agents promote methicillin-resistant Staphylococcus aureus (MRSA) wound healing and sensitize MRSA to β-lactam antibiotics.' *Antimicrobial Agents and Chemotherapy*, 59(3), pp.1512-1518.

Kussmann, M., Obermueller, M., Karer, M., Kriz, R., Chen, R.Y., Hohl, L., Schneider, L., Burgmann, H., Traby, L. and Vossen, M.G. (2021) 'Synergistic Effect of Cefazolin Plus Fosfomycin Against Staphylococcus aureus in vitro and in vivo in an Experimental Galleria mellonella Model.' *Frontiers in pharmacology*, 12(1), pp.1095-1101.

Kwasny, S.M. and Opperman, T.J. (2010) 'Static biofilm cultures of Gram-positive pathogens grown in a microtiter format used for anti-biofilm drug discovery.' *Current protocols in pharmacology*, *50*(1), pp.13A-8.

Kwun, M.S. and Lee, D.G. (2020) 'Quercetin-induced yeast apoptosis through mitochondrial dysfunction under the accumulation of magnesium in Candida albicans.' *Fungal Biology*, 124(2), pp.83-90.

Lakhundi, S. and Zhang, K. (2018) 'Methicillin-resistant Staphylococcus aureus: molecular characterization, evolution, and epidemiology.' *Clinical microbiology reviews*, 31(4), pp. 1-103.

Lakhundi, S. and Zhang, K. (2018) 'Methicillin-resistant Staphylococcus aureus: molecular characterization, evolution, and epidemiology.' *Clinical microbiology reviews*, 31(4), pp. e00020-18.

Lam, P.L., Lu, G.L., Hon, K.M., Lee, K.W., Ho, C.L., Wang, X., Tang, J.O., Lam, K.H., Wong, R.M., Kok, S.L. and Bian, Z.X. (2014) 'Development of ruthenium (II) complexes as topical antibiotics against methicillin resistant Staphylococcus aureus. *Dalton Transactions*, 43(10), pp.3949-3957.

Lamb, A.L. (2015) 'Breaking a pathogen's iron will: Inhibiting siderophore production as an antimicrobial strategy.' *Biochimica et Biophysica Acta (BBA)-Proteins and Proteomics*, 1854(8), pp.1054-1070.

Landi, A., Mari, M., Kleiser, S., Wolf, T., Gretzmeier, C., Wilhelm, I., Kiritsi, D., Thünauer, R., Geiger, R., Nyström, A. and Reggiori, F. (2019) 'Pseudomonas aeruginosa lectin LecB impairs keratinocyte fitness by abrogating growth factor signalling.' *Life science alliance*, 2(6), pp. 1-15.

Langendonk, R.F., Neill, D.R. and Fothergill, J.L. (2021) 'The building blocks of antimicrobial resistance in Pseudomonas aeruginosa: implications for current resistance-breaking therapies.' *Frontiers in Cellular and Infection Microbiology*, 11(1), pp.665759-665781.

Langeveld, W.T., Veldhuizen, E.J. and Burt, S.A. (2014) 'Synergy between essential oil components and antibiotics: a review.' *Critical reviews in microbiology*, 40(1), pp.76-94.

Langeveld, W.T., Veldhuizen, E.J. and Burt, S.A. (2014) 'Synergy between essential oil components and antibiotics: a review.' *Critical reviews in microbiology*, 40(1), pp.76-94.

Langmead, B. and Salzberg, S.L. (2012) 'Fast gapped-read alignment with Bowtie 2.' *Nature methods*, 9(4), pp.357-359.

Lapasam, A., Banothu, V., Addepally, U. and Kollipara, M.R. (2020) 'Half-sandwich arene ruthenium, rhodium and iridium thiosemicarbazone complexes: synthesis, characterization and biological evaluation.' *Journal of Chemical Sciences*, 132(1), pp.1-10.

Lazarević, T., Rilak, A. and Bugarčić, Ž.D. (2017) 'Platinum, palladium, gold and ruthenium complexes as anticancer agents: Current clinical uses, cytotoxicity studies and future perspectives.' *European journal of medicinal chemistry*, 142(1), pp.8-31.

Lazić, D., Arsenijević, A., Puchta, R., Bugarčić, Ž.D. and Rilak, A. (2016) 'DNA binding properties, histidine interaction and cytotoxicity studies of water soluble ruthenium (II) terpyridine complexes.' *Dalton Transactions*, 45(11), pp.4633-4646.

Le Brun, A.P., Clifton, L.A., Halbert, C.E., Lin, B., Meron, M., Holden, P.J., Lakey, J.H. and Holt, S.A. (2013) 'Structural characterization of a model Gram-negative bacterial surface using

lipopolysaccharides from rough strains of Escherichia coli.' *Biomacromolecules*, 14(6), pp.2014-2022.

Lee, A.S., de Lencastre, H., Garau, J., Kluytmans, J., Malhotra-Kumar, S., Peschel, A. and Harbarth, S. (2018) 'Methicillin-resistant Staphylococcus aureus.' *Nature reviews Disease primers*, 4(1), pp.1-23.

Lee, D.L., Powers, J.P.S., Pflegerl, K., Vasil, M.L., Hancock, R.E.W. and Hodges, R.S. (2004) 'Effects of single d-amino acid substitutions on disruption of β-sheet structure and hydrophobicity in cyclic 14-residue antimicrobial peptide analogs related to Gramicidin S.' *The Journal of peptide research*, 63(2), pp.69-84.

Lee, K.Y. and Mooney, D.J. (2012) 'Alginate: properties and biomedical applications.' *Progress in polymer science*, 37(1), pp.106-126.

Leiblein, M., Marzi, I., Sander, A.L., Barker, J.H., Ebert, F. and Frank, J. (2018) 'Necrotizing fasciitis: treatment concepts and clinical results.' *European Journal of Trauma and Emergency Surgery*, 44(2), pp.279-290.

Leijen, S.; Burgers, S. A.; Baas, P.; Pluim, D.; Tibben, M.; van Werkhoven, E.; Alessio, E.; Sava, G.; Beijnen, J. H.; Schellens, J. H. M. *Invest. New Drugs* 2015, *33* (1), pp. 201– 214.

Lemire, J.A., Harrison, J.J. and Turner, R.J. (2013). 'Antimicrobial activity of metals: mechanisms, molecular targets and applications.' *Nature Reviews Microbiology*, 11(6), pp.371-384.

Lemoine, L., Dieckmann, R., Al Dahouk, S., Vincze, S., Luch, A. and Tralau, T. (2020) 'Microbially competent 3D Skin: a test system that reveals insight into host–microbe interactions and their potential toxicological impact.' *Archives of toxicology*, 94(10), pp.3487-3502.

Lenselink, E.A. (2015) 'Role of fibronectin in normal wound healing.' *International wound journal*, 12(3), pp.313-316.

Lewis, S.S., Moehring, R.W., Chen, L.F., Sexton, D.J. and Anderson, D.J. (2013) 'Assessing the relative burden of hospital-acquired infections in a network of community hospitals.' *Infection Control & Hospital Epidemiology*, 34(11), pp.1229-1230.

Li, F., Collins, J.G. and Keene, F.R. (2015) 'Ruthenium complexes as antimicrobial agents.' *Chemical Society Reviews*, 44(8), pp.2529-2542.

Li, F., Feterl, M., Mulyana, Y., Warner, J.M., Collins, J.G. and Keene, F.R. (2012) 'In vitro susceptibility and cellular uptake for a new class of antimicrobial agents: dinuclear ruthenium (II) complexes.' *Journal of antimicrobial chemotherapy*, 67(11), pp.2686-2695.

Li, F., Harry, E.J., Bottomley, A.L., Edstein, M.D., Birrell, G.W., Woodward, C.E., Keene, F.R. and Collins, J.G. (2014) 'Dinuclear ruthenium (II) antimicrobial agents that selectively target polysomes in vivo.' *Chemical Science*, 5(2), pp.685-693.

Li, F., Mulyana, Y., Feterl, M., Warner, J.M., Collins, J.G. and Keene, F.R. (2011) 'The antimicrobial activity of inert oligonuclear polypyridylruthenium (II) complexes against pathogenic bacteria, including MRSA.' *Dalton Transactions*, 40(18), pp.5032-5038.

Li, F; Collins, JG; Keene, FR. (2015) 'Ruthenium complexes as antimicrobial agents.' *Chem Soc Rev*, 44(8), pp. 2529-42.

Li, J., Chen, J. and Kirsner, R. (2007) 'Pathophysiology of acute wound healing.' *Clinics in dermatology*, *25*(1), pp.9-18.

Li, S., Wu, C., Tang, X., Gao, S., Zhao, X., Yan, H. and Wang, X. (2013) 'New strategy for reversing biofilm-associated antibiotic resistance through ferrocene-substituted carborane ruthenium (II)-arene complex.' *Science China Chemistry*, *56*(5), pp.595-603.

Li, X., Gorle, A.K., Sundaraneedi, M.K., Keene, F.R. and Collins, J.G. (2018) 'Kinetically-inert polypyridylruthenium (II) complexes as therapeutic agents.' *Coordination Chemistry Reviews*, 375(1), pp.134-147.

Li, X.Z., Plésiat, P. and Nikaido, H. (2015) 'The challenge of efflux-mediated antibiotic resistance in Gram-negative bacteria.' *Clinical Microbiology Reviews*, 28(2), pp.337-418.

Li, Y., Wang, Z., Ma, X., Shao, B., Gao, X., Zhang, B., Xu, G. and Wei, Y. (2014) 'Low-dose cisplatin administration to septic mice improves bacterial clearance and proGrams peritoneal macrophage polarization to M1 phenotype.' *Pathogens and Disease*, 72(2), pp.111-123.

Li, Z., Xiao, G., Lyu, M., Wang, Y., He, S., Du, H., Wang, X., Feng, Y. and Zhu, Y. (2020) 'Shuxuening injection facilitates neurofunctional recovery via down-regulation of G-CSF-mediated granulocyte adhesion and diapedesis pathway in a subacute stroke mouse model.' *Biomedicine & Pharmacotherapy*, 127(1), pp.110213-110227.

Li, Z., Zhang, Y., Huang, D., Huang, L., Zhang, H., Li, N. and Wang, M. (2021) 'Through quorum sensing, Pseudomonas aeruginosa resists noble metal-based nanomaterials toxicity.' *Environmental Pollution*, 269(1), pp.116138-116147.

Liang, C.C., Park, A.Y. and Guan, J.L. (2007) 'In vitro scratch assay: a convenient and inexpensive method for analysis of cell migration in vitro.' *Nature protocols*, 2(2), p.329-333.

Liao, X., Jiang, G., Wang, J., Duan, X., Liao, Z., Lin, X., Shen, J., Xiong, Y. and Jiang, G. (2020) 'Two ruthenium polypyridyl complexes functionalized with thiophen: synthesis and antibacterial activity against Staphylococcus aureus.' *New Journal of Chemistry*. 44(40), pp. 17215-17221.

Liao, X., Liu, L., Tan, Y., Jiang, G., Fang, H., Xiong, Y., Duan, X., Jiang, G. and Wang, J. (2021) 'Synthesis of ruthenium complexes functionalized with benzothiophene and their antibacterial activity against Staphylococcus aureus.' *Dalton Transactions*, 50(16), pp.5607-5616. (b)

Liao, X., Wang, J., Jiang, G., Lingyu, M., Jiang, G., Wang, J. and Huang, B. (2021) 'Identification of ruthenium (II) complexes with furan-substituted ligands as possible antibacterial agents against Staphylococcus aureus.' *Chemical Biology & Drug Design*, 98(5), pp.885-893.

Licona, C., Spaety, M.E., Capuozzo, A., Ali, M., Santamaria, R., Armant, O., Delalande, F., Van Dorsselaer, A., Cianferani, S., Spencer, J. and Pfeffer, M. (2017) 'A ruthenium anticancer compound interacts with histones and impacts differently on epigenetic and death pathways compared to cisplatin.' *Oncotarget*, 8(2), pp.2568-2584.

Lin, J., Xu, P., Peng, Y., Lin, D., Ou, Q., Zhang, T., Bai, C., Ye, X., Zhou, J. and Yao, Z. (2017) 'Prevalence and characteristics of Staphylococcus aureus and methicillin-resistant Staphylococcus aureus nasal colonization among a community-based diabetes population in Foshan, China.' *Journal of diabetes investigation*, 8(3), pp.383-391.

Lin, Y.T., Chen, L.K., Jian, D.Y., Hsu, T.C., Huang, W.C., Kuan, T.T., Wu, S.Y., Kwok, C.F., Ho, L.T. and Juan, C.C., 2019. Visfatin Promotes Monocyte Adhesion by Upregulating ICAM-1 and VCAM-1 Expression in Endothelial Cells via Activation of p38-PI3K-Akt Signaling and Subsequent ROS Production and IKK/NF-κB Activation. *Cellular Physiology and Biochemistry: International Journal of Experimental Cellular Physiology, Biochemistry, and Pharmacology*, *52*(6), pp.1398-1411.

Lipus, D., Vikram, A., Gulliver, D. and Bibby, K. (2019) 'Upregulation of peroxide scavenging enzymes and multidrug efflux proteins highlight an active sodium hypochlorite response in Pseudomonas fluorescens biofilms.' *Biofouling*, 35(3), pp.329-339.

Liu, J., Chen, D., Peters, B.M., Li, L., Li, B., Xu, Z. and Shirliff, M.E. (2016) 'Staphylococcal chromosomal cassettes mec (SCCmec): a mobile genetic element in methicillin-resistant Staphylococcus aureus.' *Microbial Pathogenesis*, 101, pp.56-67.

Liu, J., Lu, Y., Wu, Q., Goyer, R.A. and Waalkes, M.P. (2008). 'Mineral arsenicals in traditional medicines: orpiment, realgar, and arsenolite.' *Journal of Pharmacology and Experimental Therapeutics*, 326(2), pp.363-368.

Liu, T., Zhu, W., Yang, X., Chen, L., Yang, R., Hua, Z. and Li, G. (2009) 'Detection of apoptosis based on the interaction between annexin V and phosphatidylserine.' Analytical chemistry, 81(6), pp.2410-2413.

Liu, W., Ye, A., Han, F. and Han, J. (2019) 'Advances and challenges in liposome digestion: Surface interaction, biological fate, and GIT modeling.' *Advances in Colloid and Interface Science*, 263, pp.52-67.

Liu, Y., Hu, H., Zhang, H., Zhong, R., Huang, C., Chen, J., Liang, L., Wang, Y. and Chen, Y. (2023) 'Synthesis, RNA-Sequence and Evaluation of Anticancer Efficacy of Ruthenium (II) Polypyridyl complexes Towards HepG2 Cells.' *Available at SSRN 4355495*. Pp. 1-44.

Liu, Y., Huo, D., Zhu, X., Chen, X., Lin, A., Jia, Z. and Liu, J. (2021) 'A ruthenium nanoframe/enzyme composite system as a self-activating cascade agent for the treatment of bacterial infections.' *Nanoscale*, 13(35), pp.14900-14914.

Liu, Y., Lin, A., Liu, J., Chen, X., Zhu, X., Gong, Y., Yuan, G., Chen, L. and Liu, J. (2019) 'Enzyme-responsive mesoporous ruthenium for combined chemo-photothermal therapy of drug-resistant bacteria.' *ACS applied materials & interfaces*, 11(30), pp.26590-26606.

Liu, Y., Lin, A., Liu, J., Chen, X., Zhu, X., Gong, Y., Yuan, G., Chen, L. and Liu, J. (2019) 'Enzyme-responsive mesoporous ruthenium for combined chemo-photothermal therapy of drug-resistant bacteria.' *ACS applied materials & interfaces*, 11(30), pp.26590-26606.

Loo, Y.Y., Rukayadi, Y., Nor-Khaizura, M.A.R., Kuan, C.H., Chieng, B.W., Nishibuchi, M. and Radu, S. (2018) 'In vitro antimicrobial activity of green synthesized silver nanoparticles against selected Gram-negative foodborne pathogens.' *Frontiers in microbiology*, 9(1), p.1555-1562.

Lopes, L. M. F., Garcia, A. R., Brogueira, P., & Ilharco, L. M. (2010). Interactions between DNA Purines and Ruthenium Ammine complexes within Nanostructured Sol–Gel Silica Matrixes.*' The Journal of Physical Chemistry B,* 114(11), pp.3987–3998.

Lopez Quezada, L., Silve, S., Kelinske, M., Liba, A., Diaz Gonzalez, C., Kotev, M., Goullieux, L., Sans, S., Roubert, C., Lagrange, S. and Bacqué, E. (2019) 'Bactericidal disruption of magnesium metallostasis in Mycobacterium tuberculosis is counteracted by mutations in the metal ion transporter CorA.' *MBio*, 10(4), pp.e01405-19.

Lopez-Carrizales, M., Velasco, K.I., Castillo, C., Flores, A., Magaña, M., Martinez-Castanon, G.A. and Martinez-Gutierrez, F. (2018) 'In vitro synergism of silver nanoparticles with antibiotics as an alternative treatment in multiresistant uropathogens.' *Antibiotics*, 7(2), pp.50-63.

Lorca, G.L., Barabote, R.D., Zlotopolski, V., Tran, C., Winnen, B., Hvorup, R.N., Stonestrom, A.J., Nguyen, E., Huang, L.W., Kim, D.S. and Saier Jr, M.H. (2007) 'Transport capabilities of

eleven Gram-positive bacteria: comparative genomic analyses.' *Biochimica et Biophysica Acta (BBA)-Biomembranes*, 1768(6), pp.1342-1366.

Lovewell, R.R., Patankar, Y.R. and Berwin, B. (2014) 'Mechanisms of phagocytosis and host clearance of Pseudomonas aeruginosa.' *American Journal of Physiology-Lung Cellular and Molecular Physiology*, 306(7), pp.591-603.

Lowy, F.D. (2003) 'Antimicrobial resistance: the example of Staphylococcus aureus.' *The Journal of Clinical Investigation*, 111(9), pp.1265-1273.

Lu, H., Blunden, B.M., Scarano, W., Lu, M. and Stenzel, M.H. (2016) 'Anti-metastatic effects of RAPTA-C conjugated polymeric micelles on two-dimensional (2D) breast tumor cells and three-dimensional (3D) multicellular tumor spheroids.' *Acta Biomaterialia*, 32(1), pp.68-76.

Lu, H., Butler, J.A., Britten, N.S., Venkatraman, P.D. and Rahatekar, S.S. (2021) 'Natural antimicrobial nano composite fibres manufactured from a combination of alginate and oregano essential oil.' *Nanomaterials*, 11(8), pp.2062-2078.

Lu, M., Chen, F., Noy, J.M., Lu, H. and Stenzel, M.H. (2017) 'Enhanced Antimetastatic Activity of the Ruthenium Anticancer Drug RAPTA-C Delivered in Fructose-Coated Micelles.' *Macromolecular Bioscience*, 17(10), pp.1600513-1600524.

Lucet, J.C., Paoletti, X., Demontpion, C., Degrave, M., Vanjak, D., Vincent, C., Andremont, A., Jarlier, V., Mentré, F. and Nicolas-Chanoine, M.H. (2009) 'Carriage of methicillin-resistant Staphylococcus aureus in home care settings: prevalence, duration, and transmission to household members.' *Archives of internal medicine*, 169(15), pp.1372-1378.

Luft, J.H. (1971) 'Ruthenium red and violet. I. Chemistry, purification, methods of use for electron microscopy and mechanism of action.' *The Anatomical Record*, 171(3), pp.347-368.

Lundov, M.D., Moesby, L., Zachariae, C. and Johansen, J.D. (2009) 'Contamination versus preservation of cosmetics: a review on legislation, usage, infections, and contact allergy.' *Contact Dermatitis*, 60(2), pp.70-78.

Luo, Z., Yu, L., Yang, F., Zhao, Z., Yu, B., Lai, H., Wong, K.H., Ngai, S.M., Zheng, W. and Chen, T. (2014) 'Ruthenium polypyridyl complexes as inducer of ROS-mediated apoptosis in cancer cells by targeting thioredoxin reductase.' *Metallomics*, 6(8), pp.1480-1490.

Lv, Y., Wang, J., Gao, H., Wang, Z., Dong, N., Ma, Q. and Shan, A. (2014) 'Antimicrobial properties and membrane-active mechanism of a potential α-helical antimicrobial derived from cathelicidin PMAP-36.' *PloS one*, 9(1), p.e86364-86376.

Ma, Y., Rajkumar, M., Zhang, C. and Freitas, H. (2016) 'Beneficial role of bacterial endophytes in heavy metal phytoremediation.' *Journal of environmental management*, 174(1), pp.14-25.

Ma, Y., Wei, M., Wang, X., Jiang, L., Xiong, Y., Cheng, J., Tan, Y., Liao, X. and Wang, J. (2022) 'Synthesis and antibacterial against Staphylococcus aureus of new ruthenium (II) polypyridine complexes containing pyrene groups.' *Applied Organometallic Chemistry*, 36(11), pp.e6858-6870.

Madsen, D.H., Leonard, D., Masedunskas, A., Moyer, A., Jürgensen, H.J., Peters, D.E., Amornphimoltham, P., Selvaraj, A., Yamada, S.S., Brenner, D.A. and Burgdorf, S. (2013) 'M2-like macrophages are responsible for collagen degradation through a mannose receptor–mediated pathway.' *Journal of Cell Biology*, 202(6), pp.951-966.

Maifiah, M.H.M., Creek, D.J., Nation, R.L., Forrest, A., Tsuji, B.T., Velkov, T. and Li, J. (2017) 'Untargeted metabolomics analysis reveals key pathways responsible for the synergistic killing of colistin and doripenem combination against Acinetobacter baumannii.' *Scientific reports*, 7(1), pp.1-12.

Majidpour, A., Fathizadeh, S., Afshar, M., Rahbar, M., Boustanshenas, M., Heidarzadeh, M., Arbabi, L. and Moghadam, S.S. (2017) 'Dose-dependent effects of common antibiotics used to treat Staphylococcus aureus on biofilm formation.' *Iranian journal of pathology*, 12(4), pp.362-370.

Maksoud, M.A., El-Sayyad, G.S., Ashour, A.H., El-Batal, A.I., Elsayed, M.A., Gobara, M., El-Khawaga, A.M., Abdel-Khalek, E.K. and El-Okr, M.M. (2019) 'Antibacterial, antibiofilm, and photocatalytic activities of metals-substituted spinel cobalt ferrite nanoparticles.' *Microbial pathogenesis*, 127(1), pp.144-158.

Malarkodi, C., Rajeshkumar, S., Paulkumar, K., Vanaja, M., Gnanajobitha, G. and Annadurai, G. (2014) 'Biosynthesis and antimicrobial activity of semiconductor nanoparticles against oral pathogens.' *Bioinorganic Chemistry and Applications*, 2014(1) pp.1-10

Manchester, J. I., Buurman, E. T., Bisacchi, G. S. and McLaughlin, R. E. (2012) 'Molecular Determinants of AcrB-Mediated Bacterial Efflux Implications for Drug Discovery.' *Journal of Medicinal Chemistry*, 55(6) pp. 2532–2537.

Mandsberg, L.F., Ciofu, O., Kirkby, N., Christiansen, L.E., Poulsen, H.E. and Høiby, N., 2009. Antibiotic resistance in Pseudomonas aeruginosa strains with increased mutation frequency due to inactivation of the DNA oxidative repair system. Antimicrobial agents and chemotherapy, 53(6), pp.2483-2491.

Marks, B., Fasih, T., Amonkar, S. and Pervaz, M. (2019) 'Necrotising fasciitis of the breast: a rare but deadly disease.' *International journal of surgery case reports*, 65(1), pp.10-14.

Maryam, L. and Khan, A.U. (2017) 'Synergistic effect of doripenem and cefotaxime to inhibit CTX-M-15 type β-lactamases: Biophysical and microbiological views.' *Frontiers in pharmacology*, 8(1), pp.449-472.

Maryam, L. and Khan, A.U. (2018) 'Combination of aztreonam and cefotaxime against CTX-M-15 type β-lactamases: A mechanism based effective therapeutic approach.' *International journal of biological macromolecules*, 116(1), pp.1186-1195.

Mast Group Ltd. (2020). *Antibiotic Susceptibility Testing Rings.* Available: https://mast-group.com/uk/products/ast/antibiotic-susceptibility-testing-rings/. Last accessed 13th Oct 2020.

Masters, P.A., O'Bryan, T.A., Zurlo, J., Miller, D.Q. and Joshi, N. (2003) 'Trimethoprim-sulfamethoxazole revisited.' *Archives of Internal Medicine*, 163(4), pp.402-410.

Matono, T., Nagashima, M., Mezaki, K., Motohashi, A., Kutsuna, S., Hayakawa, K., Ohmagari, N. and Kaku, M. (2018) 'Molecular epidemiology of β-lactamase production in penicillin-susceptible Staphylococcus aureus under high-susceptibility conditions.' *Journal of Infection and Chemotherapy*, 24(2), pp.153-155.

Matshwele, J.T., Nareetsile, F., Mapolelo, D., Matshameko, P., Leteane, M., Nkwe, D.O. and Odisitse, S. (2020) 'Synthesis of mixed ligand ruthenium (II/III) complexes and their antibacterial evaluation on drug-resistant bacterial organisms.' *Journal of Chemistry*, 2020(1), pp.1-10.

Mazuryk, O., Suzenet, F., Kieda, C. and Brindell, M. (2015) 'The biological effect of the nitroimidazole derivative of a polypyridyl ruthenium complex on cancer and endothelial cells.' *Metallomics*, 7(3), pp.553-566.

McCallum, R. I. (1977). ‘Observations upon antimony.’ *Proceedings of the Royal Society of Medicine*, 70(1), pp. 756–763.

McGinley, J., McCann, M., Ni, K., Tallon, T., Kavanagh, K., Devereux, M., Ma, X. and McKee, V. (2013) ‘Imidazole Schiff base ligands: Synthesis, coordination complexes and biological activities.’ *Polyhedron*, 55(1), pp.169-178.

Meier, S.M., Kreutz, D., Winter, L., Klose, M.H., Cseh, K., Weiss, T., Bileck, A., Alte, B., Mader, J.C., Jana, S. and Chatterjee, A. (2017) ‘An organoruthenium anticancer agent shows unexpected target selectivity for plectin.’ *Angewandte Chemie International Edition*, 56(28), pp.8267-8271.

Mercer, D.K., Torres, M.D., Duay, S.S., Lovie, E., Simpson, L., von Köckritz-Blickwede, M., de la Fuente-Nunez, C., O'Neil, D.A. and Angeles-Boza, A.M. (2020) ‘Antimicrobial susceptibility testing of antimicrobial peptides to better predict efficacy.’ *Frontiers in Cellular and Infection Microbiology*, 10(1), pp.326-360.

Metcalfe, C; Thomas, JA. (2003) ‘Kinetically inert transition metal complexes that reversibly bind to DNA.’ *Chem Soc Rev*, 32(4), pp.215-24.

Meyer-Hoffert, U., Zimmermann, A., Czapp, M., Bartels, J., Koblyakova, Y., Gläser, R., Schröder, J.M. and Gerstel, U. (2011) ‘Flagellin delivery by Pseudomonas aeruginosa rhamnolipids induces the antimicrobial protein psoriasin in human skin.’ *PLoS One*, 6(1), pp.e16433-16444.

Mijnendonckx, K., Leys, N., Mahillon, J., Silver, S. and Van Houdt, R. (2013) ‘Antimicrobial silver: uses, toxicity and potential for resistance.’ *Biometals*, 26(4), pp.609-621.

Miles, A.A., Misra, S.S. and Irwin, J.O. (1938) ‘The estimation of the bactericidal power of the blood.’ *Epidemiology & Infection*, 38(6), pp.732-749.

Milutinović, M.M., Elmroth, S.K., Davidović, G., Rilak, A., Klisurić, O.R., Bratsos, I. and Bugarčić, Ž.D. (2017) 'Kinetic and mechanistic study on the reactions of ruthenium (II) chlorophenyl terpyridine complexes with nucleobases, oligonucleotides and DNA.' *Dalton Transactions*, 46(7), pp.2360-2369.

Minandri, F., Imperi, F., Frangipani, E., Bonchi, C., Visaggio, D., Facchini, M., Pasquali, P., Bragonzi, A. and Visca, P. (2016) 'Role of iron uptake systems in Pseudomonas aeruginosa virulence and airway infection.' *Infection and Immunity*, 84(8), pp.2324-2335.

Minato, Y., Dawadi, S., Kordus, S.L., Sivanandam, A., Aldrich, C.C. and Baughn, A.D. (2018) 'Mutual potentiation drives synergy between trimethoprim and sulfamethoxazole.' *Nature communications*, 9(1), pp.1-7.

Misiakos, E.P., Bagias, G., Patapis, P., Sotiropoulos, D., Kanavidis, P. and Machairas, A. (2014) 'Current concepts in the management of necrotizing fasciitis.' *Frontiers in surgery*, 1(1), pp.36-46.

Mital, M. and Ziora, Z. (2018). 'Biological applications of Ru (II) polypyridyl complexes.' *Coordination Chemistry Reviews*, 375(1), pp.434-458.

Miyata, S., Casey, M., Frank, D.W., Ausubel, F.M. and Drenkard, E. (2003) 'Use of the Galleria mellonella caterpillar as a model host to study the role of the type III secretion system in Pseudomonas aeruginosa pathogenesis.' *Infection and immunity*, 71(5), pp. 2404-2413.

Mjos, K.D. and Orvig, C. (2014) 'Metallodrugs in medicinal inorganic chemistry.' *Chemical Reviews*, 114(8), pp.4540-4563.

Möhler, J.S., Sim, W., Blaskovich, M.A., Cooper, M.A. and Ziora, Z.M. (2018) 'Silver bullets: A new lustre on an old antimicrobial agent.' *Biotechnology advances*, 36(5), pp.1391-1411.

Monro, S., Colon, K.L., Yin, H., Roque III, J., Konda, P., Gujar, S., Thummel, R.P., Lilge, L., Cameron, C.G. and McFarland, S.A. (2018) 'Transition metal complexes and photodynamic therapy from a tumor-centered approach: challenges, opportunities, and highlights from the development of TLD1433.' *Chemical reviews*, 119(2), pp.797-828.

Montanaro, L., Speziale, P., Campoccia, D., Ravaioli, S., Cangini, I., Pietrocola, G., Giannini, S. and Arciola, C.R. (2011) 'Scenery of Staphylococcus implant infections in orthopedics.' *Future microbiology*, 6(11), pp.1329-1349.

Moore CL, Osaki-Kiyan P, Perri M, Donabedian S, Haque NZ, Chen A,Zervos MJ. (2010) 'USA600 (ST45) methicillin-resistant Staphylococcus aureus bloodstream infections in urban Detroit.' *J Clin Microbiol,* 48(1), pp. 2307–2310.

Moore, D.L., MacDonald, N.E., Canadian Paediatric Society and Infectious Diseases and Immunization Committee, (2015) 'Preventing ophthalmia neonatorum.' *Paediatrics & child health*, 20(2), pp.93-96.

Morones, J.R., Elechiguerra, J.L., Camacho, A., Holt, K., Kouri, J.B., Ramírez, J.T. and Yacaman, M.J. (2005).' The bactericidal effect of silver nanoparticles.' *Nanotechnology*, 16(10), pp.2346-2355.

Mouritzen, M.V. and Jenssen, H. (2018) 'Optimized scratch assay for in vitro testing of cell migration with an automated optical camera.' *Journal of visualized experiments: JoVE*, 138(1), pp.e57691.

Moussouni, M., Berry, L., Sipka, T., Nguyen-Chi, M. and Blanc-Potard, A.B. (2021) 'Pseudomonas aeruginosa OprF plays a role in resistance to macrophage clearance during acute infection.' Scientific reports, 11(1), pp.1-11.

Moyá, B., Beceiro, A., Cabot, G., Juan, C., Zamorano, L., Alberti, S. and Oliver, A. (2012) 'Pan-β-lactam resistance development in Pseudomonas aeruginosa clinical strains: molecular mechanisms, penicillin-binding protein profiles, and binding affinities.' *Antimicrobial agents and chemotherapy*, 56(9), pp.4771-4778.

Mulani, M.S., Kamble, E.E., Kumkar, S.N., Tawre, M.S. and Pardesi, K.R. (2019) 'Emerging strategies to combat ESKAPE pathogens in the era of antimicrobial resistance: a review.' *Frontiers in microbiology*, 10(1), pp.539-563.

Muller, M. (2006) 'Premature cellular senescence induced by pyocyanin, a redox-active Pseudomonas aeruginosa toxin.' *Free Radical Biology and Medicine*, 41(11), pp.1670-1677.

Munita, J.M. and Arias, C.A. (2016) 'Mechanisms of antibiotic resistance.' *Virulence Mechanisms of Bacterial Pathogens*, 4(2) pp.481-511.

Munteanu, A.C. and Uivarosi, V. (2021) 'Ruthenium complexes in the fight against pathogenic microorganisms. an extensive review.' *Pharmaceutics*, 13(6), pp.874-925.

Murphy, M.B., Mercer, S.L. and Deweese, J.E. (2017) 'Inhibitors and poisons of mammalian type II topoisomerases.' *Advances in molecular toxicology,* 11(1), pp. 203-240.

Murray, T.S., Okegbe, C., Gao, Y., Kazmierczak, B.I., Motterlini, R., Dietrich, L.E. and Bruscia, E.M. (2012) 'The carbon monoxide releasing molecule CORM-2 attenuates Pseudomonas aeruginosa biofilm formation.' *PLoS One*, *7*(4), pp.e35499.

Mustafa M. (2012) 'A review on community acquired methicillin resistantStaphylococcus aureusan emerging infectious disease.' *IOSR J PharmBiol Sci,* 3(1).

Musthafa, M., Konakanchi, R., Ganguly, R., Pandikumar, P. and Sreekanth, A. (2020) 'Synthesis, characterization, in silico and in vitro biological activity studies of Ru (II)(η 6-p-cymene) complexes with novel N-dibenzosuberene substituted aroyl selenourea exhibiting Se type coordination.' *Research on Chemical Intermediates*, 46(1), pp.3853-3877.

Muzammil, S., Hayat, S., Fakhar-E-Alam, M., Aslam, B., Siddique, M.H., Nisar, M.A., Saqalein, M., Atif, M., Sarwar, A., Khurshid, A. and Amin, N. (2018) 'Nanoantibiotics: Future nanotechnologies to combat antibiotic resistance.' *Frontiers in Bioscience-Elite*, 10(2), pp.352-374.

Naguib, M.M., El-Gendy, A.O. and Khairalla, A.S. (2018) 'Microbial diversity of mer operon genes and their potential rules in mercury bioremediation and resistance.' *The Open Biotechnology Journal*, 12(1), pp.56-77.

Naik, M.M., Naik, H.B., Nagaraju, G., Vinuth, M., Vinu, K. and Viswanath, R. (2019) 'Green synthesis of zinc doped cobalt ferrite nanoparticles: Structural, optical, photocatalytic and antibacterial studies.' *Nano-Structures & Nano-Objects*, 19(1), pp.100322-100335.

Nandi, P.G., Jadi, P.K., Das, K., Prathapa, S.J., Mandal, B.B. and Kumar, A. (2021) 'Synthesis of NNN Chiral Ruthenium complexes and Their Cytotoxicity Studies.' *Inorganic Chemistry*, 60(10), pp.7422-7432.

Nassar, R., Hachim, M.Y., Nassar, M., Kaklamanos, E.G., Jamal, M., Williams, D. and Senok, A. (2020) 'Microbial metabolic genes crucial for S. aureus biofilms: an insight from re-analysis of publicly available microarray datasets.' *Frontiers in microbiology*, 11(1), pp.3598-3605.

Nathan, C. (2004) 'Antibiotics at the crossroads.' *Nature*, 431(7011), pp.899-902.

Nathan, C. and Cars, O. (2014) 'Antibiotic resistance—problems, progress, and prospects. *New England Journal of Medicine'*, 371(19), pp.1761-1763.

Nathan, C. and Cunningham-Bussel, A. (2013). 'Beyond oxidative stress: an immunologist's guide to reactive oxygen species.' *Nature Reviews Immunology*, 13(5), pp.349-361.

National Nosocomial Infections Surveillance System. (2004) 'National Nosocomial Infections Surveillance (NNIS) System report, data sum-mary from January 1992 through June 2004, issued October 2004.' *AmJ Infect Control,* 32(1), pp. 470–485.

Nawijn, M.C., Motta, A.C., Gras, R., Shirinbak, S., Maazi, H. and van Oosterhout, A.J. (2013) 'TLR-2 activation induces regulatory T cells and long-term suppression of asthma manifestations in mice.' *PloS one*, 8(2), p.e55307-16.

Nessa, F., Khan, S.A. and Shawish, K.A. (2016) 'Lead, cadmium and nickel contents of some medicinal agents.' *Indian Journal of Pharmaceutical Sciences*, 78(1), pp.111-119.

Neuditschko, B., Legin, A.A., Baier, D., Schintlmeister, A., Reipert, S., Wagner, M., Keppler, B.K., Berger, W., Meier-Menches, S.M. and Gerner, C. (2021) 'Interaction with Ribosomal Proteins Accompanies Stress Induction of the Anticancer Metallodrug BOLD-100/KP1339 in the Endoplasmic Reticulum.' *Angewandte Chemie International Edition*, 60(10), pp.5063-5068.

Ng, S., Goodson, B., Ehrhardt, A., Moos, W.H., Siani, M. and Winter, J. (1999) 'Combinatorial discovery process yields antimicrobial peptoids.' *Bioorganic & medicinal chemistry*, 7(9), pp.1781-1785.

Nice. (2021) 'Chronic wounds: Advanced wound dressings and antimicrobial dressings. National Institute of Health and Care Excellence.' https://www.nice.org.uk/guidance/esmpb2.

Nichol, K.A., Adam, H.J., Hussain, Z., Mulvey, M.R., McCracken, M., Mataseje, L.F., Thompson, K., Kost, S., Lagacé-Wiens, P.R., Hoban, D.J. and Zhanel, G.G. (2011) 'Comparison of community-associated and health care-associated methicillin-resistant Staphylococcus

aureus in Canada: results of the CANWARD 2007–2009 study.' *Diagnostic microbiology and infectious disease*, 69(3), pp.320-325.

Nimmo, G.R. (2012) 'USA300 abroad: global spread of a virulent strain of community-associated methicillin-resistant Staphylococcus aureus.' *Clinical microbiology and infection*, 18(8), pp.725-734.

Nishanthi, R., Malathi, S. and Palani, P. (2019) 'Green synthesis and characterization of bioinspired silver, gold and platinum nanoparticles and evaluation of their synergistic antibacterial activity after combining with different classes of antibiotics.' *Materials Science and Engineering: C*, 96(1), pp.693-707.

Nobre, L.S., Jeremias, H., Romão, C.C. and Saraiva, L.M. (2016) 'Examining the antimicrobial activity and toxicity to animal cells of different types of CO-releasing molecules.' *Dalton Transactions*, *45*(4), pp.1455-1466.

Nordmann, P. and Poirel, L. (2019) 'Epidemiology and diagnostics of carbapenem resistance in Gram-negative bacteria.' *Clinical Infectious Diseases*, 69(7), pp.521-528.

Nowak-Sliwinska, P., van Beijnum, J.R., Casini, A., Nazarov, A.A., Wagnieres, G., van den Bergh, H., Dyson, P.J. and Griffioen, A.W. (2011) 'Organometallic ruthenium (II) arene complexs with antiangiogenic activity.' *Journal of medicinal chemistry*, 54(11), pp.3895-3902.

O'Shaughnessy, M., Piatek, M., McCarron, P., McCann, M., Devereux, M., Kavanagh, K. and Howe, O. (2022) 'In Vivo Activity of Metal complexes Containing 1, 10-Phenanthroline and 3, 6, 9-Trioxaundecanedioate Ligands against Pseudomonas aeruginosa Infection in Galleria mellonella Larvae.' *Biomedicines*, 10(2), pp.222-243.

Obradović, D., Nikolić, S., Milenković, I., Milenković, M., Jovanović, P., Savić, V., Roller, A., Crnogorac, M.Đ., Stanojković, T. and Grgurić-Šipka, S. (2020) 'Synthesis, characterization, antimicrobial and cytotoxic activity of novel half-sandwich Ru (II) arene complexes with benzoylthiourea derivatives.' *Journal of Inorganic Biochemistry*, 210(1), pp.111164-111173.

O'Callaghan, C.H., Morris, A., Kirby, S.M. and Shingler, A.H. (1972) 'Novel method for detection of β-lactamases by using a chromogenic cephalosporin substrate.' *Antimicrobial agents and chemotherapy*, 1(4), pp.283-288.

Ochsner, U.A., Vasil, M.L., Alsabbagh, E., Parvatiyar, K. and Hassett, D.J. (2000) 'Role of the Pseudomonas aeruginosa oxyR-recG operon in oxidative stress defense and DNA repair: OxyR-dependent regulation of katB-ankB, ahpB, andahpC-ahpF.' *Journal of bacteriology*, 182(16), pp.4533-4544.

Ogle, M.E., Segar, C.E., Sridhar, S. and Botchwey, E.A. (2016) 'Monocytes and macrophages in tissue repair: Implications for immunoregenerative biomaterial design.' *Experimental Biology and Medicine*, 241(10), pp.1084-1097.

Oliveira, K.M., Liany, L.D., Corrêa, R.S., Deflon, V.M., Cominetti, M.R. and Batista, A.A. (2017) 'Selective Ru (II)/lawsone complexes inhibiting tumor cell growth by apoptosis.' *Journal of inorganic biochemistry*, 176(1), pp.66-76.

Oliveira, W.F., Silva, P.M.S., Silva, R.C.S., Silva, G.M.M., Machado, G., Coelho, L.C.B.B. and Correia, M.T.S. (2018) 'Staphylococcus aureus and Staphylococcus epidermidis infections on implants.' *Journal of Hospital Infection*, 98(2), pp.111-117.

Oluyombo, O., Penfold, C.N. and Diggle, S.P. (2019) 'Competition in biofilms between cystic fibrosis isolates of Pseudomonas aeruginosa is shaped by R-pyocins.' *MBio*, 10(1), pp.e01828-18.

O'Malley, Y.Q. (2003) 'Abdalla MY, McCormick ML, Reszka KJ, Denning GM, and Britigan BE. *Subcellular localization of Pseudomonas pyocyanin cytotoxicity in human lung epithelial cells.' Am J Physiol Lung Cell Mol Physiol*, 284(1), pp.420-430.

O'Malley, Y.Q., Reszka, K.J., Spitz, D.R., Denning, G.M. and Britigan, B.E. (2004) 'Pseudomonas aeruginosa pyocyanin directly oxidizes glutathione and decreases its levels in airway epithelial cells.' *American Journal of Physiology-Lung Cellular and Molecular Physiology*, 287(1), pp.94-103.

Omar, A., Wright, J.B., Schultz, G., Burrell, R. and Nadworny, P. (2017) 'Microbial biofilms and chronic wounds.' *Microorganisms*, *5*(1), pp.9-24.

O'Reilly, C., Blasco, S., Parekh, B., Collins, H., Cooke, G., Gunnlaugsson, T. and Byrne, J.P. (2021) 'Ruthenium-centred btp glycoclusters as inhibitors for Pseudomonas aeruginosa biofilm formation.' *RSC Advances*, 11(27), pp.16318-16325.

Otter, J.A. and French, G.L. (2010) 'Molecular epidemiology of community-associated meticillin-resistant Staphylococcus aureus in Europe.' *The Lancet infectious diseases*, 10(4), pp.227-239.

Owen, L. and Laird, K. (2018) 'Synchronous application of antibiotics and essential oils: dual mechanisms of action as a potential solution to antibiotic resistance.' *Critical Reviews in Microbiology*, 44(4), pp.414-435.

Özdemir, D.S., Kaçar, C., Dalkıran, B., Küçükkolbaşı, S., Erden, P.E. and Kılıç, E. (2019) 'Effect of hexaammineruthenium chloride and/or horseradish peroxidase on the performance of hydrogen peroxide (bio) sensors: a comparative study.' Journal of Materials Science, 54(7), pp.5381-5398.

Pachori, P., Gothalwal, R. and Gandhi, P. (2019) 'Emergence of antibiotic resistance Pseudomonas aeruginosa in intensive care unit; a critical review.' *Genes & Diseases*, 6(2), pp.109-119.

Páez, P.L., Bazán, C.M., Bongiovanni, M.E., Toneatto, J., Albesa, I., Becerra, M.C. and Argüello, G.A. (2013) 'Oxidative stress and antimicrobial activity of chromium (III) and ruthenium (II) complexes on Staphylococcus aureus and Escherichia coli.' *BioMed Research International*, 2013(1), pp. 1-8.

Pal, C., Asiani, K., Arya, S., Rensing, C., Stekel, D.J., Larsson, D.J. and Hobman, J.L. (2017) 'Metal resistance and its association with antibiotic resistance.' *Advances in Microbial Physiology,* 70(1) pp. 261-313.

Palaniappan, K. and Holley, R.A. (2010) 'Use of natural antimicrobials to increase antibiotic susceptibility of drug resistant bacteria.' *International journal of food microbiology*, 140(2-3), pp.164-168.

Pallister, C.J and Watson, M.S. (2011). *Haematology*. 2nd ed. Banbury: Scion Publishing Limited. pp. 336-347.

Pan, C.L., Chen, M.H., Tung, F.I. and Liu, T.Y. (2017) 'A nanovehicle developed for treating deep-seated bacteria using low-dose X-ray.' *Acta Biomaterialia*, 47(1), pp.159-169.

Pan, X., Redding, J.E., Wiley, P.A., Wen, L., McConnell, J.S. and Zhang, B. (2010). 'Mutagenicity evaluation of metal oxide nanoparticles by the bacterial reverse mutation assay.' *Chemosphere*, 79(1), pp.113-116.

Panáček, A., Smékalová, M., Kilianová, M., Prucek, R., Bogdanová, K., Večeřová, R., Kolář, M., Havrdová, M., Płaza, G.A., Chojniak, J. and Zbořil, R. (2016) 'Strong and nonspecific

synergistic antibacterial efficiency of antibiotics combined with silver nanoparticles at very low concentrations showing no cytotoxic effect.' *Molecules*, 21(1), pp.26-43.

Pandrala, M., Li, F., Feterl, M., Mulyana, Y., Warner, J.M., Wallace, L., Keene, F.R. and Collins, J.G. (2013) 'Chlorido-containing ruthenium (II) and iridium (III) complexes as antimicrobial agents.' *Dalton Transactions*, 42(13), pp.4686-4694.

Pang, Z., Raudonis, R., Glick, B.R., Lin, T.J. and Cheng, Z. (2019) 'Antibiotic resistance in Pseudomonas aeruginosa: mechanisms and alternative therapeutic strategies.' *Biotechnology Advances*, 37(1), pp.177-192.

Panmanee, W., Charoenlap, N., Atichartpongkul, S., Mahavihakanont, A., Whiteside, M.D., Winsor, G., Brinkman, F.S., Mongkolsuk, S. and Hassett, D.J. (2017) 'The OxyR-regulated phnW gene encoding 2-aminoethylphosphonate: pyruvate aminotransferase helps protect Pseudomonas aeruginosa from tert-butyl hydroperoxide.' *PLoS One*, 12(12), pp.e0189066-e0189085.

Parakh, P., Gokulakrishnan, S. and Prakash, H. (2013) 'Visible light water disinfection using [Ru (bpy) 2 (phendione)](PF6) 2· 2H2O and [Ru (phendione) 3] Cl2· 2H2O complexes and their effective adsorption onto activated carbon.' *Separation and Purification Technology*, 109(1), pp.9-17.

Pardos de la Gandara, M., Curry, M., Berger, J., Burstein, D., Della-Latta, P., Kopetz, V., Quale, J., Spitzer, E., Tan, R., Urban, C. and Wang, G. (2016) 'MRSA causing infections in hospitals in greater metropolitan New York: major shift in the dominant clonal type between 1996 and 2014.' *PLoS One*, 11(6), pp.e0156924-37.

Parthasarathy, A., Vijayakumar, S., Malaikozhundan, B., Thangaraj, M.P., Ekambaram, P., Murugan, T., Velusamy, P., Anbu, P. and Vaseeharan, B. (2020) 'Chitosan-coated silver

nanoparticles promoted antibacterial, antibiofilm, wound-healing of murine macrophages and antiproliferation of human breast cancer MCF 7 cells.' *Polymer Testing*, 90(1), pp.106675-106686.

Partridge, S.R., Kwong, S.M., Firth, N. and Jensen, S.O. (2018) 'Mobile genetic elements associated with antimicrobial resistance.' *Clinical microbiology reviews*, 31(4), pp.e00088-17.

Pastar, I., Nusbaum, A.G., Gil, J., Patel, S.B., Chen, J., Valdes, J., Stojadinovic, O., Plano, L.R., Tomic-Canic, M. and Davis, S.C. (2013) 'Interactions of methicillin resistant Staphylococcus aureus USA300 and Pseudomonas aeruginosa in polymicrobial wound infection.' *PloS one*, *8*(2) pp. e56846.

Paul, M., Andreassen, S., Nielsen, A.D., Tacconelli, E., Almanasreh, N., Fraser, A., Yahav, D., Ram, R. and Leibovici, L. (2006) 'Prediction of bacteremia using TREAT, a computerized decision-support system.' *Clinical Infectious Diseases*, 42(9), pp.1274-1282.

Pavillard, R., Harvey, K., Douglas, D., Hewstone, A., Andrew, J., Collopy, B., Asche, V., Carson, P., Davidson, A., Gilbert, G. and Spicer, J. (1982) 'Epidemie of hospital-acquired infection due to methicillin-resistant Staphylococcus aureus in major Victorian hospitals.' *Medical Journal of Australia*, 1(11), pp.451-454.

Peacock, S.J. and Paterson, G.K. (2015) 'Mechanisms of methicillin resistance in Staphylococcus aureus.' *Annu Rev Biochem*, 84(1), pp.577-601.

Pereira, T.C., De Barros, P.P., Fugisaki, L.R.D.O., Rossoni, R.D., Ribeiro, F.D.C., De Menezes, R.T., Junqueira, J.C. and Scorzoni, L. (2018) 'Recent advances in the use of Galleria mellonella model to study immune responses against human pathogens.' *Journal of Fungi*, 4(4) pp.128-147.

Periayah, M.H., Halim, A.S. and Saad, A.Z.M. (2017) 'Mechanism action of platelets and crucial blood coagulation pathways in hemostasis.' *International journal of hematology-oncology and stem cell research*, 11(4), pp.319-237.

Persat, A., Nadell, C.D., Kim, M.K., Ingremeau, F., Siryaporn, A., Drescher, K., Wingreen, N.S., Bassler, B.L., Gitai, Z. and Stone, H.A. (2015) 'The mechanical world of bacteria.' *Cell*, 161(5), pp.988-997.

Petek, M., Baebler, Š., Kuzman, D., Rotter, A., Podlesek, Z., Gruden, K., Ravnikar, M. and Urleb, U. (2010) 'Revealing fosfomycin primary effect on Staphylococcus aureus transcriptome: modulation of cell envelope biosynthesis and phosphoenolpyruvate induced starvation.' *BMC microbiology*, 10(1), pp.1-12.

Phillips, P.L., Yang, Q., Davis, S., Sampson, E.M., Azeke, J.I., Hamad, A. and Schultz, G.S. (2015) 'Antimicrobial dressing efficacy against mature Pseudomonas aeruginosa biofilm on porcine skin explants.' *International wound journal*, 12(4), pp.469-483.

Pitt, T.L., Sparrow, M., Warner, M. and Stefanidou, M., 2003. Survey of resistance of Pseudomonas aeruginosa from UK patients with cystic fibrosis to six commonly prescribed antimicrobial agents. *Thorax*, *58*(9), pp.794-796.

Pletzer, D., Wolfmeier, H., Bains, M. and Hancock, R.E. (2017) 'Synthetic peptides to target stringent response-controlled virulence in a Pseudomonas aeruginosa murine cutaneous infection model.' *Frontiers in microbiology*, 8(1), pp.1867-1882.

Popovich KJ, Weinstein RA. (2009) 'The graying of methicillin-resistantStaphylococcus aureus.' *Infect Control Hosp Epidemiol*, 30(1), pp.9–12.

Popovich, K.J. and Weinstein, R.A. (2009) 'The graying of methicillin-resistant Staphylococcus aureus.' *Infection Control & Hospital Epidemiology*, 30(1), pp.9-12.

Posnett, J. and Franks, P. (2008) 'The burden of chronic wounds in the UK.' *Nursing times*, 104(3), pp.44-45.

Prabhakara, R., Harro, J.M., Leid, J.G., Harris, M. and Shirtliff, M.E. (2011) 'Murine immune response to a chronic Staphylococcus aureus biofilm infection.' *Infection and immunity*, 79(4), pp.1789-1796.

Price LB, Stegger M, Hasman H, Aziz M, Larsen J, Andersen PS, PearsonT, Waters AE, Foster JT, Schupp J, Gillece J, Driebe E, Liu CM, SpringerB, Zdovc I, Battisti A, Franco A, Zmudzki J, Schwarz S, Butaye P, Jouy E,Pomba C, Porrero MC, Ruimy R, Smith TC, Robinson DA, Weese JS,Arriola CS, Yu F, Laurent F, Keim P, Skov R, Aarestrup FM. (2012) 'Staphylococcus aureusCC398: host adaptation and emergence of methicillin resistance in livestock.' *mBio*, 4(1), pp. e00305-11.

Prochnow, H., Fetz, V., Hotop, S.K., García-Rivera, M.A., Heumann, A. and Brönstrup, M. (2018) 'Subcellular quantification of uptake in Gram-negative bacteria.' *Analytical chemistry*, 91(3), pp.1863-1872.

Public Health England (2015) Health matters: antimicrobial resistance - GOV.UK. Gov.uk. [Online] [Accessed 11th April 2018] https://www.gov.uk/government/publications/health-matters-antimicrobial-resistance/health-matters-antimicrobial-resistance.

Public Health England. (2019). *Laboratory surveillance of Staphylococcus aureusbloodstream infections in England, Wales and Northern Ireland: 2018.* Available: https://assets.publishing.service.gov.uk/government/uploads/system/uploads/attachment_data/file/825679/hpr2919_staph-aureus.pdf. [Accessed 23rd Apr 2020].

Public Health England. (2020). 'Laboratory surveillance of Pseudomonas and Stenotrophomonas spp bacteraemia in England, Wales and Northern Ireland: 2018.' *Health Protection Report*. 14(3), pp.1-19. [Online]. Available at: https://assets.publishing.service.gov.uk/government/uploads/system/uploads/attachment_data/file/8641 [Accessed 27 August 2022].

Public Health England. English surveillance proGramme for antimicrobial utilisation and resistance (ESPAUR) report. (2019) https://www.gov.uk/government/publications/english-surveillance-proGramme-antimicrobial-utilisation-and-resistance-espaur-report. Accessed 21 Oct 2021.

Qing, C. (2017) 'The molecular biology in wound healing & non-healing wound.' *Chinese Journal of Traumatology*, 20(4), pp.189-193.

Qu, S., Dai, C., Shen, Z., Tang, Q., Wang, H., Zhai, B., Zhao, L. and Hao, Z., 2019. Mechanism of synergy between tetracycline and quercetin against antibiotic resistant Escherichia coli. *Frontiers in Microbiology*, *10*, p.2536.

Rademacher, F., Simanski, M., Hesse, B., Dombrowsky, G., Vent, N., Gläser, R. and Harder, J. (2019) 'Staphylococcus epidermidis activates aryl hydrocarbon receptor signaling in human keratinocytes: implications for cutaneous defense.' *Journal of innate immunity*, 11(2), pp.125-135.

Rağbetli, C., Parlak, M., Bayram, Y., Guducuoglu, H. and Ceylan, N. (2016) 'Evaluation of antimicrobial resistance in Staphylococcus aureus isolates by years.' *Interdisciplinary Perspectives on Infectious Diseases*, 2016(1), pp.1-4

Raghunath, A. and Perumal, E. (2017) 'Metal oxide nanoparticles as antimicrobial agents: a promise for the future.' *International Journal of Antimicrobial Agents*, 49(2), pp.137-152.

Rahim, K., Saleha, S., Zhu, X., Huo, L., Basit, A. and Franco, O.L. (2017) 'Bacterial contribution in chronicity of wounds.' Microbial ecology, 73(3), pp.710-721.

Rahnamoun, A., Kim, K., Pedersen, J.A. and Hernandez, R. (2020) 'Ionic environment affects bacterial lipopolysaccharide packing and function.' *Langmuir*, 36(12), pp.3149-3158.

Rai, A., Prabhune, A. and Perry, C.C. (2010) 'Antibiotic mediated synthesis of gold nanoparticles with potent antimicrobial activity and their application in antimicrobial coatings.' *Journal of Materials Chemistry*, 20(32), pp.6789-6798.

Rai, A., Prabhune, A. and Perry, C.C. (2010) 'Antibiotic mediated synthesis of gold nanoparticles with potent antimicrobial activity and their application in antimicrobial coatings.' *Journal of Materials Chemistry*, 20(32), pp.6789-6798.

Raja, S.K., Garcia, M.S. and Isseroff, R.R. (2007) 'Wound re-epithelialization: modulating keratinocyte migration in wound healing.' *Front Biosci*, 12(3), pp.2849-2868.

Ramalingam, B., Parandhaman, T. and Das, S.K. (2016) 'Antibacterial effects of biosynthesized silver nanoparticles on surface ultrastructure and nanomechanical properties of Gram-negative bacteria viz. Escherichia coli and Pseudomonas aeruginosa.' *ACS applied materials & interfaces*, 8(7), pp.4963-4976.

Ramirez, M.C., Marchessault, M., Govednik-Horny, C., Jupiter, D. and Papaconstantinou, H.T. (2013) 'The impact of MRSA colonization on surgical site infection following major gastrointestinal surgery.' *Journal of Gastrointestinal Surgery*, 17(1), pp.144-152.

Rana, N., Jesse, H.E., Tinajero-Trejo, M., Butler, J.A., Tarlit, J.D., Milena, L., Nagel, C., Schatzschneider, U. and Poole, R.K. (2017) 'A manganese photosensitive tricarbonyl molecule [Mn (CO) 3 (tpa-κ3N)] Br enhances antibiotic efficacy in a multi-drug-resistant Escherichia coli.' *Microbiology*, 163(10), pp.1477-1489.

Rappuoli, R., Bloom, D.E. and Black, S. (2017) 'Deploy vaccines to fight superbugs.' *Nature*, 552(7684), pp.165-167.

Rasamiravaka, T., Labtani, Q., Duez, P. and El Jaziri, M. (2015) 'The formation of biofilms by Pseudomonas aeruginosa: a review of the natural and synthetic compounds interfering with control mechanisms.' *BioMed research international*, 2015(1), pp. 1-17.

Rawling, E.G., Brinkman, F.S. and Hancock, R.E. (1998) 'Roles of the carboxy-terminal half of Pseudomonas aeruginosa major outer membrane protein OprF in cell shape, growth in low-osmolarity medium, and peptidoglycan association.' *Journal of bacteriology*, 180(14), pp.3556-3562.

Rawson, T.M., Ming, D., Ahmad, R., Moore, L.S. and Holmes, A.H. (2020) 'Antimicrobial use, drug-resistant infections and COVID-19.' *Nature Reviews Microbiology*, 18(8), pp.409-410.

Rawson, T.M., Moore, L.S., Castro-Sanchez, E., Charani, E., Davies, F., Satta, G., Ellington, M.J. and Holmes, A.H. (2020) 'COVID-19 and the potential long-term impact on antimicrobial resistance.' *Journal of antimicrobial chemotherapy*, 75(7), pp.1681-1684.

Renninger, N., Knopp, R., Nitsche, H., Clark, D.S. and Keasling, J.D. (2004) 'Uranyl precipitation by Pseudomonas aeruginosa via controlled polyphosphate metabolism.' *Applied and environmental microbiology*, 70(12), pp.7404-7412.

Rice, A., Rooney, M.T., Greenwood, A.I., Cotten, M.L. and Wereszczynski, J. (2020) 'Lipopolysaccharide simulations are sensitive to phosphate charge and ion parameterization.' *Journal of chemical theory and computation*, 16(3), pp.1806-1815.

Rios de la Rosa, J.M., Tirella, A., Gennari, A., Stratford, I.J. and Tirelli, N. (2017) 'The CD44-mediated uptake of hyaluronic acid-based carriers in macrophages.' *Advanced healthcare materials*, 6(4), pp.1601012-1601023.

Rivera, S.L., Vargas, E., Ramírez-Díaz, M.I., Campos-García, J. and Cervantes, C. (2008) 'Genes related to chromate resistance by Pseudomonas aeruginosa PAO1.' *Antonie Van Leeuwenhoek*, 94(2), pp.299-305.

Rochford, G., Molphy, Z., Browne, N., Surlis, C., Devereux, M., McCann, M., Kellett, A., Howe, O. and Kavanagh, K. (2018) 'In-vivo evaluation of the response of Galleria mellonella larvae to novel copper (II) phenanthroline-phenazine complexes.' *Journal of Inorganic Biochemistry*, 186(1), pp.135-146.

Rogala, P., Czerwonka, G., Michałkiewicz, S., Hodorowicz, M., Barszcz, B. and Jabłońska-Wawrzycka, A. (2019) 'Synthesis, structural characterization and antimicrobial evaluation of ruthenium complexes with heteroaromatic carboxylic acids.' *Chemistry & Biodiversity*, 16(11), pp.e1900403-24.

Romanowska, J., Reuter, N. and Trylska, J. (2013) 'Comparing aminoglycoside binding sites in bacterial ribosomal RNA and aminoglycoside modifying enzymes.' *Proteins: Structure, Function, and Bioinformatics*, 81(1), pp.63-80.

Romsang, A., Duang-Nkern, J., Khemsom, K., Wongsaroj, L., Saninjuk, K., Fuangthong, M., Vattanaviboon, P. and Mongkolsuk, S. (2018) 'Pseudomonas aeruginosa ttcA encoding tRNA-thiolating protein requires an iron-sulfur cluster to participate in hydrogen peroxide-mediated stress protection and pathogenicity.' *Scientific reports*, 8(1), pp.1-15.

Ronfard, V. and Barrandon, Y. (2001) 'Migration of keratinocytes through tunnels of digested fibrin.' *Proceedings of the National Academy of Sciences*, 98(8), pp.4504-4509.

Rosenberg, B., Van Camp, L. and Krigas, T. (1965) 'Inhibition of cell division in Escherichia coli by electrolysis products from a platinum electrode.' *Nature*, 205(4972), pp.698-699.

Roudashti, S., Zeighami, H., Mirshahabi, H., Bahari, S., Soltani, A. and Haghi, F. (2017) 'Synergistic activity of sub-inhibitory concentrations of curcumin with ceftazidime and ciprofloxacin against Pseudomonas aeruginosa quorum sensing related genes and virulence traits.' *World Journal of Microbiology and Biotechnology*, 33(3), pp.1-8.

Rountree, P.M. and Beard, M.A. (1968) 'Hospital strains of Staphylococcus aureus, with particular reference to methicillin-resistant strains.' *Medical Journal of Australia*, 2(26), pp.1163-8.

Rousselle, P. and Beck, K. (2013) 'Laminin 332 processing impacts cellular behaviour.' *Cell adhesion & migration*, 7(1), pp.122-134.

Rousselle, P., Montmasson, M. and Garnier, C. (2019) 'Extracellular matrix contribution to skin wound re-epithelialization.' *Matrix Biology*, 75(1), pp.12-26.

Rowinska-Zyrek, M., Skilandat, M. and Sigel, R.K. (2013) 'Hexaamminecobalt (III)–Probing metal ion binding sites in nucleic acids by NMR spectroscopy.' *Zeitschrift für anorganische und allgemeine Chemie*, 639(8-9), pp.1313-1320.

Roy, A.S., Parveen, A., Koppalkar, A.R. and Prasad, M.A. (2010) 'Effect of nano-titanium dioxide with different antibiotics against methicillin-resistant Staphylococcus aureus.' *Journal of Biomaterials and Nanobiotechnology*, 1(1), pp.37-42.

Ruffin, M. and Brochiero, E. (2019) 'Repair process impairment by Pseudomonas aeruginosa in epithelial tissues: major features and potential therapeutic avenues.' *Frontiers in cellular and infection microbiology*, 9(1), pp.182-200.

Russell, C.D., Fairfield, C.J., Drake, T.M., Turtle, L., Seaton, R.A., Wootton, D.G., Sigfrid, L., Harrison, E.M., Docherty, A.B., de Silva, T.I. and Egan, C. (2021) 'Co-infections, secondary infections, and antimicrobial use in patients hospitalised with COVID-19 during the first pandemic wave from the ISARIC WHO CCP-UK study: a multicentre, prospective cohort study.' *The Lancet Microbe*, 2(8), pp.e354-e365.

Saha, B., Bhattacharya, J., Mukherjee, A., Ghosh, A., Santra, C., Dasgupta, A.K. and Karmakar, P. (2007) 'In vitro structural and functional evaluation of gold nanoparticles conjugated antibiotics.' *Nanoscale Research Letters*, 2(12), pp.614-622.

Salomoni, R., Léo, P., Montemor, A.F., Rinaldi, B.G. and Rodrigues, M.F.A. (2017) 'Antibacterial effect of silver nanoparticles in Pseudomonas aeruginosa.' *Nanotechnology, science and applications*, 10(1), pp.115-121.

Sanchez, D.A. and Martinez, L.R. (2019) 'Underscoring interstrain variability and the impact of growth conditions on associated antimicrobial susceptibilities in preclinical testing of novel antimicrobial drugs.' *Critical Reviews in Microbiology*, 45(1), pp.51-64.

Sangalli-Leite, F., Scorzoni, L., da Silva, J.D.F., de Oliveira, H.C., de Lacorte Singulani, J., Gullo, F.P., da Silva, R.M., Regasini, L.O., da Silva, D.H.S., da Silva Bolzani, V. and Fusco-Almeida, A.M. (2016) 'Synergistic effect of pedalitin and amphotericin B against Cryptococcus neoformans by in vitro and in vivo evaluation.' *International journal of antimicrobial agents*, 48(5), pp.504-511.

Sangalli-Leite, F., Scorzoni, L., da Silva, J.D.F., de Oliveira, H.C., de Lacorte Singulani, J., Gullo, F.P., da Silva, R.M., Regasini, L.O., da Silva, D.H.S., da Silva Bolzani, V. and Fusco-Almeida, A.M. (2016) 'Synergistic effect of pedalitin and amphotericin B against Cryptococcus

neoformans by in vitro and in vivo evaluation.' *International journal of antimicrobial agents*, 48(5), pp.504-511.

Sanna, B., Debidda, M., Pintus, G., Tadolini, B., Posadino, A.M., Bennardini, F., Sava, G. and Ventura, C. (2002) 'The anti-metastatic agent imidazolium trans-imidazoledimethylsulfoxide-tetrachlororuthenate induces endothelial cell apoptosis by inhibiting the mitogen-activated protein kinase/extracellular signal-regulated kinase signaling pathway.' *Archives of Biochemistry and Biophysics*, 403(2), pp.209-218.

Santillo, M., Wanat, M., Davoudianfar, M., Bongard, E., Savic, S., Savic, L., Porter, C., Fielding, J., Butler, C.C., Pavitt, S. and Sandoe, J. (2020) 'Developing a behavioural intervention package to identify and amend incorrect penicillin allergy records in UK general practice and subsequently change antibiotic use.' *BMJ open*, 10(10), pp.e035793-035803.

Saravanan, M., Ramachandran, B. and Barabadi, H. (2018) 'The prevalence and drug resistance pattern of extended spectrum β–lactamases (ESBLs) producing Enterobacteriaceae in Africa.' Microbial pathogenesis, 114(1), pp.180-192.

Sarkar, A., Acharya, S., Khushvant, K., Purkait, K. and Mukherjee, A. (2019) 'Cytotoxic Ru II-pcymene complexes of an anthraimidazoledione: halide dependent solution stability, reactivity and resistance to hypoxia deactivation.' Dalton Transactions, 48(21), pp.7187-7197.

Sarker, S.D., Nahar, L. and Kumarasamy, Y. (2007) 'Microtitre plate-based antibacterial assay incorporating resazurin as an indicator of cell growth, and its application in the in vitro antibacterial screening of phytochemicals.' *Methods*, 42(4), pp.321-324.

Sarniguet, C., Toloza, J., Cipriani, M., Lapier, M., Vieites, M., Toledano-Magaña, Y., García-Ramos, J.C., Ruiz-Azuara, L., Moreno, V., Maya, J.D. and Azar, C.O. (2014) 'Water-soluble ruthenium complexes bearing activity against protozoan parasites.' *Biological trace element research*, 159(1), pp.379-392.

Sawatzky, P., Liu, G., Dillon, J.A.R., Allen, V., Lefebvre, B., Hoang, L., Tyrrell, G., Van Caeseele, P., Levett, P. and Martin, I. (2015) 'Quality assurance for antimicrobial susceptibility testing of Neisseria gonorrhoeae in Canada, 2003 to 2012.' *Journal of clinical microbiology*, 53(11), pp.3646-3649.

Scharschmidt, T.C. and Fischbach, M.A. (2013) 'What lives on our skin: ecology, genomics and therapeutic opportunities of the skin microbiome.' *Drug Discovery Today: Disease Mechanisms*, 10(3-4), pp.83-89.

Schreml, S., Szeimies, R.M., Prantl, L., Landthaler, M. and Babilas, P. (2010) 'Wound healing in the 21st century.' *Journal of the American Academy of Dermatology*, 63(5), pp.866-881.

Seixas, J.D., Santos, M.F., Mukhopadhyay, A., Coelho, A.C., Reis, P.M., Veiros, L.F., Marques, A.R., Penacho, N., Gonçalves, A.M., Romão, M.J. and Bernardes, G.J. (2015) 'A contribution to the rational design of Ru (CO) 3 Cl 2 L complexes for in vivo delivery of CO.' *Dalton Transactions*, 44(11), pp.5058-5075.

Serafim, M.S., Lavorato, S.N., Kronenberger, T., Sousa, Y.V., Oliveira, G.P., Dos Santos, S.G., Kroon, E.G., Maltarollo, V.G., Alves, R.J. and Mota, B.E. (2019) 'Antibacterial activity of synthetic 1, 3-bis (aryloxy) propan-2-amines against Gram-positive bacteria.' *Microbiologyopen*, 8(11), pp.e814-829.

Serra, R., Grande, R., Butrico, L., Rossi, A., Settimio, U.F., Caroleo, B., Amato, B., Gallelli, L. and de Franciscis, S. (2015) 'Chronic wound infections: the role of Pseudomonas aeruginosa and Staphylococcus aureus.' *Expert Review of Anti-infective Therapy*, 13(5), pp.605-613.

Shakya, S., He, Y., Ren, X., Guo, T., Maharjan, A., Luo, T., Wang, T., Dhakhwa, R., Regmi, B., Li, H. and Gref, R. (2019) 'Ultrafine silver nanoparticles embedded in cyclodextrin metal-organic frameworks with GRGDS functionalization to promote antibacterial and wound healing application.' *Small*, 15(27), pp.1901065-1901078.

Shao, X., Zhang, X., Zhang, Y., Zhu, M., Yang, P., Yuan, J., Xie, Y., Zhou, T., Wang, W., Chen, S. and Liang, H. (2018) 'RpoN-dependent direct regulation of quorum sensing and the Type VI secretion system in Pseudomonas aeruginosa PAO1.' *Journal of bacteriology*, 200(16), pp.e00205-18.

Sharma, N., Jandaik, S. and Kumar, S. (2016) 'Synergistic activity of doped zinc oxide nanoparticles with antibiotics: ciprofloxacin, ampicillin, fluconazole and amphotericin B against pathogenic microorganisms.' *Anais Da Academia Brasileira De Ciências*, 88(3), pp.1689-1698.

Sheehan, G., Dixon, A. and Kavanagh, K. (2019) 'Utilization of Galleria mellonella larvae to characterize the development of Staphylococcus aureus infection.' *Microbiology*, 165(8), pp.863-875.

Shettigar, K. and Murali, T.S. (2020) 'Virulence factors and clonal diversity of Staphylococcus aureus in colonization and wound infection with emphasis on diabetic foot infection.' *European Journal of Clinical Microbiology & Infectious Diseases*, 39(1), pp.2235-2246.

Shirude, P.S. and Hameed, S. (2012) 'Nonfluoroquinolone-based inhibitors of mycobacterial type II topoisomerase as potential therapeutic agents for TB.' *Annual reports in medicinal chemistry*, 47(1), pp. 319-330.

Shrivastava, S.R., Shrivastava, P.S. and Ramasamy, J. (2018) 'World health organization releases global priority list of antibiotic-resistant bacteria to guide research, discovery, and development of new antibiotics.' *Journal of Medical Society*, 32(1), pp.76-77.

Siddiqui, A.H. and Koirala, J. (2018) 'Methicillin resistant Staphylococcus aureus (MRSA).' StatPearls [Internet]. Treasure Island (FL), StatPearls Publishing (2018) https://www.ncbi.nlm.nih.gov/books/NBK482221/ [Accessed 4th June 2020].

Silver, S. (2003). 'Bacterial silver resistance: molecular biology and uses and misuses of silver compounds.' *FEMS Microbiology Reviews*, 27(2-3), pp.341-353.

Silver, S., Phung, L.T. and Silver, G. (2006) 'Silver as biocides in burn and wound dressings and bacterial resistance to silver compounds.' *Journal of Industrial Microbiology and Biotechnology*, 33(7), pp.627-634.

Sim, W., Barnard, R.T., Blaskovich, M.A.T. and Ziora, Z.M. (2018).' Antimicrobial silver in medicinal and consumer applications: A patent review of the past decade (2007–2017).' *Antibiotics*, 7(4), pp.93-108.

Singh, S., Navale, G.R., Mahale, M., Chaudhary, V.K., Kodam, K. and Ghosh, K. (2022) 'Photodissociation of nitric oxide from designed ruthenium nitrosyl complex: Studies on wound healing and antibacterial activity.' *Nitric Oxide*, 129(1), pp.30-40.

Singh, S., Young, A. and McNaught, C.E. (2017) 'The physiology of wound healing.' *Surgery (Oxford)*, 35(9), pp.473-477.

Siripatrawan, U. and Kaewklin, P. (2018) 'Fabrication and characterization of chitosan-titanium dioxide nanocomposite film as ethylene scavenging and antimicrobial active food packaging.' *Food hydrocolloids*, 84, pp.125-134.

Siriyong, T., Srimanote, P., Chusri, S., Yingyongnarongkul, B.E., Suaisom, C., Tipmanee, V. and Voravuthikunchai, S.P. (2017) 'Conessine as a novel inhibitor of multidrug efflux pump

systems in Pseudomonas aeruginosa.' *BMC complementary and alternative medicine*, 17(1), pp.1-7.

Sivitz, W.I. and Yorek, M.A. (2010) 'Mitochondrial dysfunction in diabetes: from molecular mechanisms to functional significance and therapeutic opportunities.' *Antioxidants & redox signaling*, 12(4), pp.537-577.

Slate, A.J., Wickens, D.J., El Mohtadi, M., Dempsey-Hibbert, N., West, G., Banks, C.E. and Whitehead, K.A. (2018) 'Antimicrobial activity of Ti-ZrN/Ag coatings for use in biomaterial applications.' *Scientific Reports*, 8(1), pp.1-12.

Slavin, Y.N., Asnis, J., Häfeli, U.O. and Bach, H. (2017). 'Metal nanoparticles: understanding the mechanisms behind antibacterial activity.' *Journal of Nanobiotechnology*, 15(1), pp.65-85.

Smitten, K., Southam, H.M., Fairbanks, S., Graf, A., Chauvet, A. and Thomas, J.A. (2022) 'Clearing an ESKAPE Pathogen in a Model Organism; A Polypyridyl Ruthenium (II) complex Theranostic that Treats a Resistant Acinetobacter baumannii Infection in Galleria mellonella.' *Chemistry–A European Journal*, 29(11), pp.e202203555-63.

Smitten, K.L., Fairbanks, S.D., Robertson, C.C., de la Serna, J.B., Foster, S.J. and Thomas, J.A. (2020) 'Ruthenium based antimicrobial theranostics–using nanoscopy to identify therapeutic targets and resistance mechanisms in Staphylococcus aureus.' *Chemical science*, 11(1), pp.70-79.

Smitten, K.L., Southam, H.M., de la Serna, J.B., Gill, M.R., Jarman, P.J., Smythe, C.G., Poole, R.K. and Thomas, J.A. (2019) 'Using nanoscopy to probe the biological activity of antimicrobial leads that display potent activity against pathogenic, multidrug resistant, Gram-negative bacteria.' *ACS nano*, *13*(5), pp.5133-5146.

Smitten, K.L., Thick, E.J., Southam, H.M., de la Serna, J.B., Foster, S.J. and Thomas, J.A. (2020) 'Mononuclear ruthenium (ii) theranostic complexes that function as broad-spectrum antimicrobials in therapeutically resistant pathogens through interaction with DNA.' *Chemical science*, 11(33), pp.8828-8838.

Sobha, S., Mahalakshmi, R. and Raman, N. (2012) 'Studies on DNA binding behaviour of biologically active transition metal complexes of new tetradentate N2O2 donor Schiff bases: Inhibitory activity against bacteria.' *Spectrochimica Acta Part A: Molecular and Biomolecular Spectroscopy*, 92, pp.175-183.

Sondi, I. and Salopek-Sondi, B. (2004). 'Silver nanoparticles as antimicrobial agent: a case study on E. coli as a model for Gram-negative bacteria.' *Journal of Colloid and Interface Science*, 275(1), pp.177-182.

Southam, H.M., Butler, J.A., Chapman, J.A. and Poole, R.K. (2017) 'The microbiology of ruthenium complexes.' *Advances in Microbial Physiology*, 71(1) pp. 1-96.

Southam, H.M., Smith, T.W., Lyon, R.L., Liao, C., Trevitt, C.R., Middlemiss, L.A., Cox, F.L., Chapman, J.A., El-Khamisy, S.F., Hippler, M. and Williamson, M.P. (2018) 'A thiol-reactive Ru (II) ion, not CO release, underlies the potent antimicrobial and cytotoxic properties of CO-releasing molecule-3.' *Redox biology*, 18(1), pp.114-123.

Spellberg, B. and Rice, L.B. (2019) 'Duration of antibiotic therapy: shorter is better.' *Annals of internal medicine*, 171(3), pp.210-211.

Spoorthi, N.J., Vishwanatha, T., Reena, V., Divyashree, B.C., Aishwarya, S., Siddhalingeshwara, K.G., Venugopal, N. and Ramesh, I. (2011) 'Antibiotic synergy test: Checkerboard method on multidrug resistant Pseudomonas aeruginosa.' *International Research Journal of Pharmacy*, 2(12), pp.196-198.

Sproston, N.R., El Mohtadi, M., Slevin, M., Gilmore, W. and Ashworth, J.J., 2018. The effect of C-reactive protein isoforms on nitric oxide production by U937 monocytes/macrophages. *Frontiers in immunology*, *9*, p.1500.

Srinivas, N., Jetter, P., Ueberbacher, B.J., Werneburg, M., Zerbe, K., Steinmann, J., Van der Meijden, B., Bernardini, F., Lederer, A., Dias, R.L. and Misson, P.E. (2010) 'Peptidomimetic antibiotics target outer-membrane biogenesis in Pseudomonas aeruginosa.' *Science*, 327(5968), pp.1010-1013.

Srivastava, P., Shukla, M., Kaul, G., Chopra, S. and Patra, A.K. (2019) 'Rationally designed curcumin based ruthenium (II) antimicrobials effective against drug-resistant Staphylococcus aureus.' *Dalton Transactions*, 31(1) pp. 196-198.

Stefanopoulou, M., Kokoschka, M., Sheldrick, W.S. and Wolters, D.A. (2011) 'Cell response of Escherichia coli to cisplatin-induced stress.' *Proteomics*, 11(21), pp.4174-4188.

Steinberg, D.C., (2010) 'Frequency of preservative use.' *Cosmetics and toiletries*, 125(11), pp. 46-51.

Stetsenko, A. and Guskov, A. (2020) 'Cation permeability in CorA family of proteins.' *Scientific reports*, 10(1), pp.1-9.

Strempel, N., Neidig, A., Nusser, M., Geffers, R., Vieillard, J., Lesouhaitier, O., Brenner-Weiss, G. and Overhage, J. (2013) 'Human host defense peptide LL-37 stimulates virulence factor production and adaptive resistance in Pseudomonas aeruginosa.' *PloS one*, 8(12), pp.e82240-82252.

Stringer, T., Quintero, M.A.S., Wiesner, L., Smith, G.S. and Nordlander, E. (2019) 'Evaluation of PTA-derived ruthenium (II) and iridium (III) quinoline complexes against chloroquine-

sensitive and resistant strains of the Plasmodium falciparum malaria parasite.' *Journal of Inorganic Biochemistry*, 191(1), pp.164-173.

Sudhindra, P., Sharma, S.A., Roy, N., Moharana, P. and Paira, P. (2020) 'Recent advances in cytotoxicity, cellular uptake and mechanism of action of ruthenium metallodrugs: A review.' *Polyhedron*, 192(1), pp.114827.

Sullivan, G.J., Delgado, N.N., Maharjan, R. and Cain, A.K. (2020) 'How antibiotics work together: Molecular mechanisms behind combination therapy.' *Current Opinion in Microbiology*, 57(1), pp.31-40.

Sultana, S.T., Babauta, J.T. and Beyenal, H. (2015) 'Electrochemical biofilm control: a review.' *Biofouling*, 31(9-10), pp.745-758.

Sultana, S.T., Call, D.R. and Beyenal, H. (2016) 'Eradication of Pseudomonas aeruginosa biofilms and persister cells using an electrochemical scaffold and enhanced antibiotic susceptibility.' *NPJ biofilms and microbiomes*, 2(1), pp.1-8.

Sun, B., Musgrave, I.F., Day, A.I., Heimann, K., Keene, F.R. and Collins, J.G. (2018) 'Eukaryotic Cell Toxicity and HSA Binding of [Ru (Me4phen)(bb7)] 2+ and the Effect of Encapsulation in Cucurbit.' *Frontiers in Chemistry*, 6(1), pp. 1-12.

(a) Sun, W., Sanderson, P.E. and Zheng, W. (2016) 'Drug combination therapy increases successful drug repositioning.' *Drug discovery today*, 21(7), pp.1189-1195.

(b) Sun, W., Weingarten, R.A., Xu, M., Southall, N., Dai, S., Shinn, P., Sanderson, P.E., Williamson, P.R., Frank, K.M. and Zheng, W. (2016) 'Rapid antimicrobial susceptibility test for identification of new therapeutics and drug combinations against multidrug-resistant bacteria.' *Emerging microbes & infections*, 5(1), pp.1-11.

Sun, D., Zhang, W., Lv, M., Yang, E., Zhao, Q. and Wang, W. (2015) 'Antibacterial activity of ruthenium (II) polypyridyl complex manipulated by membrane permeability and cell morphology.' *Bioorganic & Medicinal Chemistry Letters*, 25(10), pp.2068-2073.

Sun, D., Zhang, W., Yang, E., Li, N., Liu, H. and Wang, W. (2015) 'Investigation of antibacterial activity and related mechanism of a ruthenium (II) polypyridyl complex.' *Inorganic Chemistry Communications*, 56(1), pp.17-21.

Sundaramoorthy, N.S., Mitra, K., Ganesh, J.S., Makala, H., Lotha, R., Bhanuvalli, S.R., Ulaganathan, V., Tiru, V., Sivasubramanian, A. and Nagarajan, S. (2018) 'Ferulic acid derivative inhibits NorA efflux and in combination with ciprofloxacin curtails growth of MRSA in vitro and in vivo.' *Microbial pathogenesis*, 124(1), pp.54-62.

Suntres, Z.E., Omri, A. and Shek, P.N. (2002) 'Pseudomonas aeruginosa-induced lung injury: role of oxidative stress.' *Microbial pathogenesis*, 32(1), pp.27-34.

Sur, V.P., Mazumdar, A., Kopel, P., Mukherjee, S., Vítek, P., Michalkova, H., Vaculovičová, M. and Moulick, A. (2020) 'A novel ruthenium based coordination compound against pathogenic bacteria.' *International Journal of Molecular Sciences*, 21(7), pp.2656-2674.

Suresh, M., Nithya, N., Jayasree, P.R., Vimal, K.P. and Kumar, P.M. (2018) 'Mutational analyses of regulatory genes, mexR, nalC, nalD and mexZ of mexAB-oprM and mexXY operons, in efflux pump hyperexpressing multidrug-resistant clinical isolates of Pseudomonas aeruginosa.' *World Journal of Microbiology and Biotechnology*, 34(6), pp.1-11.

Svensson, F.R., Matson, M., Li, M. and Lincoln, P. (2010) 'Lipophilic ruthenium complexes with tuned cell membrane affinity and photoactivated uptake'. *Biophysical chemistry*, 149(3), pp.102-106.

Tacke, M. (2017) June. Coinage Metal NHC complexes as Novel Antibiotics and Anticancer Drugs. In *The 26th International Conference on Coordination Chemistry (26th ICCBiC), Smolenice, Slovakia, 4-9 June 2017*. Slovak University of Technology Publishing House.

Taherlo, R. and Salehi, M. (2014) 'Synthesis, crystal structures, electrochemically studies and antibacterial properties of three new mono-nuclear and one very rare bi-nuclear cobalt (III) Schiff base complexes.' *Inorganica Chimica Acta*, 418(1), pp.180-186.

Takahashi, H., Oshima, T., Hobman, J.L., Doherty, N., Clayton, S.R., Iqbal, M., Hill, P.J., Tobe, T., Ogasawara, N., Kanaya, S. and Stekel, D.J. (2015) 'The dynamic balance of import and export of zinc in Escherichia coli suggests a heterogeneous population response to stress.' *Journal of the Royal Society Interface*, 12(106), pp. 1-12.

Talukder, A., Rahman, M., Chowdhury, M.M.H., Mobashshera, T.A. and Islam, N.N. (2021) 'Plasmid profiling of multiple antibiotic-resistant Pseudomonas aeruginosa isolated from soil of the industrial area in Chittagong, Bangladesh.' Beni-Suef University Journal of Basic and Applied Sciences, 10(1), pp.1-7.

Taneja, N., Sethi, S., Tahlan, A.K. and Kumar, Y. (2019) 'Introductory Chapter: Stepping into the Post-Antibiotic Era—Challenges and Solutions.' *Antimicrobial Resistance-A Global Threat*. IntechOpen 2019(1), pp.1-13.

Thangavel, P., Viswanath, B. and Kim, S. (2018) 'Synthesis and characterization of kaempferol-based ruthenium (II) complex: A facile approach for superior anticancer application.' *Materials Science and Engineering: C*, 89(1), pp.87-94.

Thi, M.T.T., Wibowo, D. and Rehm, B.H. (2020) 'Pseudomonas aeruginosa biofilms.' *International journal of molecular sciences*, 21(22), pp.8671-8696.

Thomaz, L., Gustavo de Almeida, L., Silva, F.R., Cortez, M., Taborda, C.P. and Spira, B. (2020) 'In vivo activity of silver nanoparticles against Pseudomonas aeruginosa infection in Galleria mellonella.' *Frontiers in Microbiology*, 11(1) pp.1-14.

Thompson, D.S., Weiss, G.J., Jones, S.F., Burris, H.A., Ramanathan, R.K., Infante, J.R., Bendell, J.C., Ogden, A. and Von Hoff, D.D. (2012) 'NKP-1339: Maximum tolerated dose defined for first-in-human GRP78 targeted agent.' *Invest New Drugs,* 2016(1), pp. 261-268.

Thurlow, L.R., Joshi, G.S. and Richardson, A.R. (2012) 'Virulence strategies of the dominant USA300 lineage of community-associated methicillin-resistant Staphylococcus aureus (CA-MRSA).' *FEMS Immunology & Medical Microbiology*, 65(1), pp.5-22.

Tian, M., Qing, C., Niu, Y., Dong, J., Cao, X., Song, F., Ji, X. and Lu, S. (2016) 'Aminoguanidine cream ameliorates skin tissue microenvironment in diabetic rats.' *Archives of medical science: AMS*, 12(1), pp.179-187.

Tiwana, H., Gupta, S., Prakash, D.N., Panda, N., Chetan, B., Angrup, A., Ray, P., Bakshi, J., Mohindra, S., Gupta, R. and Virk, R. (2020) 'Current trends in pathogenesis, management, bacteriology, and antibiotic resistance in deep neck space infections: An institutional review.' *Annals of Indian Academy of Otorhinolaryngology Head and Neck Surgery*, 4(1), pp.5-9.

Tjahjono, E., McAnena, A.P. and Kirienko, N.V. (2020) 'The evolutionarily conserved ESRE stress response network is activated by ROS and mitochondrial damage.' *BMC biology*, 18(1), pp.1-17.

To, W.S. and Midwood, K.S. (2011) 'Plasma and cellular fibronectin: distinct and independent functions during tissue repair.' *Fibrogenesis & tissue repair*, 4(1), pp.1-17.

Todd, B.A. and Rau, D.C. (2008) 'Interplay of ion binding and attraction in DNA condensed by multivalent cations.' *Nucleic acids research*, 36(2), pp.501-510.

Tomasello, G., Armenia, I. and Molla, G. (2020) 'The Protein Imager: a full-featured online molecular viewer interface with server-side HQ-rendering capabilities.' *Bioinformatics*, 36(9), pp.2909-2911.

Tong, S.Y., Bishop, E.J., Lilliebridge, R.A., Cheng, A.C., Spasova-Penkova, Z., Holt, D.C., Giffard, P.M., McDonald, M.I., Currie, B.J. and Boutlis, C.S. (2009) 'Community-associated strains of methicillin-resistant Staphylococcus aureus and methicillin-susceptible S. aureus in indigenous Northern Australia: epidemiology and outcomes.' *The Journal of infectious diseases*, 199(10), pp.1461-1470.

Torres, M.R., Slate, A.J., Ryder, S.F., Akram, M., Iruzubieta, C.J.C. and Whitehead, K.A. (2021) 'Ionic gold demonstrates antimicrobial activity against Pseudomonas aeruginosa strains due to cellular ultrastructure damage.' *Archives of Microbiology*, 203(6), pp.1-10.

Tottoli, E.M., Dorati, R., Genta, I., Chiesa, E., Pisani, S. and Conti, B. (2020) 'Skin wound healing process and new emerging technologies for skin wound care and regeneration.' *Pharmaceutics*, 12(8), pp.735-765.

Troeman, D.P.R., Van Hout, D. and Kluytmans, J.A.J.W. (2019) 'Antimicrobial approaches in the prevention of Staphylococcus aureus infections: a review.' *Journal of Antimicrobial Chemotherapy*, 74(2), pp.281-294.

Trunk, K., Benkert, B., Quäck, N., Münch, R., Scheer, M., Garbe, J., Jänsch, L., Trost, M., Wehland, J., Buer, J. and Jahn, M. (2010) 'Anaerobic adaptation in Pseudomonas aeruginosa: definition of the Anr and Dnr regulons.' *Environmental microbiology*, 12(6), pp.1719-1733.

Tsai, C.J.Y., Loh, J.M.S. and Proft, T. (2016) 'Galleria mellonella infection models for the study of bacterial diseases and for antimicrobial drug testing.' *Virulence*, 7(3), pp.214-229.

Tsuji, B.T., Rybak, M.J., Cheung, C.M., Amjad, M. and Kaatz, G.W. (2007) 'Community-and health care-associated methicillin-resistant Staphylococcus aureus: a comparison of molecular epidemiology and antimicrobial activities of various agents.' *Diagnostic microbiology and infectious disease*, 58(1), pp.41-47.

Tumbarello, M., Raffaelli, F., Peghin, M., Losito, A.R., Chirico, L., Giuliano, G., Spanu, T., Sartor, A., Fiori, B. and Bassetti, M. (2020) 'Characterisation and risk factor profiling of Pseudomonas aeruginosa urinary tract infections: pinpointing those likely to be caused by multidrug-resistant strains.' *International journal of antimicrobial agents*, *55*(4), pp.105900.

Turner, K.H., Everett, J., Trivedi, U., Rumbaugh, K.P. and Whiteley, M. (2014) 'Requirements for Pseudomonas aeruginosa acute burn and chronic surgical wound infection.' *PLoS Genetics*, 1*0*(7), pp. 1-12.

Turner, N.A., Sharma-Kuinkel, B.K., Maskarinec, S.A., Eichenberger, E.M., Shah, P.P., Carugati, M., Holland, T.L. and Fowler, V.G. (2019) 'Methicillin-resistant Staphylococcus aureus: an overview of basic and clinical research.' *Nature Reviews Microbiology*, 17(4), pp.203-218.

Ude, Z., Romero-Canelón, I., Twamley, B., Hughes, D.F., Sadler, P.J. and Marmion, C.J. (2016) 'A novel dual-functioning ruthenium (II)–arene complex of an anti-microbial ciprofloxacin derivative—Anti-proliferative and anti-microbial activity.' *Journal of inorganic biochemistry*, 160(1), pp.210-217.

Uivarosi, V., Olar, R., Badea, M. and CARMEN, M. (2017) 'Antimicrobial activity of some new Ru (III) complexes with quinolone derivatives.' Farmacia, 65(6), pp.972-977.

Vaidya, M., McBain, A.J., Banks, C.E. and Whitehead, K.A. (2019) 'Single and combined antimicrobial efficacies for nine metal ion solutions against Klebsiella pneumoniae,

Acinetobacter baumannii and Enterococcus faecium.' *International Biodeterioration & Biodegradation*, 141(1), pp.39-43.

Valko, M., Jomova, K., Rhodes, C.J., Kuča, K. and Musílek, K. (2016) 'Redox-and non-redox-metal-induced formation of free radicals and their role in human disease.' *Archives of Toxicology*, 90(1), pp.1-37.

van Belkum, A., Bachmann, T.T., Lüdke, G., Lisby, J.G., Kahlmeter, G., Mohess, A., Becker, K., Hays, J.P., Woodford, N., Mitsakakis, K. and Moran-Gilad, J. (2019) 'Developmental roadmap for antimicrobial susceptibility testing systems.' *Nature Reviews Microbiology*, 17(1), pp.51-62.

Van Vuuren, S.F., Suliman, S. and Viljoen, A.M. (2009) 'The antimicrobial activity of four commercial essential oils in combination with conventional antimicrobials.' *Letters in applied microbiology*, 48(4), pp.440-446.

Vanderhaeghen, W., Hermans, K., Haesebrouck, F. and Butaye, P. (2010) 'Methicillin-resistant Staphylococcus aureus (MRSA) in food production animals.' *Epidemiology & Infection*, 138(5), pp.606-625.

Venkatraman, P.D., Butler, J.A. and Britten, N.S. (2023) 'Advances in medical textiles.' *Functional and Technical Textiles*, pp.31-70.

Vannella, K.M. and Wynn, T.A. (2017) 'Mechanisms of organ injury and repair by macrophages.' *Annual review of physiology*, 79(1), pp.593-617.

Ventola, C.L. (2015) 'The antibiotic resistance crisis: part 1: causes and threats.' *Pharmacy and Therapeutics*, 40(4), p.277-283.

Vergis, J., Pathak, R., Kumar, M., Sunitha, R., Malik, S.V.S., Barbuddhe, S.B. and Rawool, D.B. (2018) 'A comparative study for detection of extended spectrum β-lactamase (ESBL)

production by Enteroaggregative Escherichia coli (EAEC) strains using double disc, nitrocefin and PCR assays.' *Journal of microbiological methods*, 151(1), pp.57-61.

Vidimar, V., Licona, C., Cerón-Camacho, R., Guérin, E., Coliat, P., Venkatasamy, A., Ali, M., Guenot, D., Le Lagadec, R., Jung, A.C. and Freund, J.N. (2019) 'A redox ruthenium compound directly targets PHD2 and inhibits the HIF1 pathway to reduce tumor angiogenesis independently of p53.' *Cancer Letters*, 440(1), pp.145-155.

Vizzotto, B.S., Dias, R.S., Iglesias, B.A., Krause, L.F., Viana, A.R. and Schuch, A.P. (2020) 'DNA photocleavage and melanoma cells cytotoxicity induced by a meso-tetra-ruthenated porphyrin under visible light irradiation.' *Journal of Photochemistry and Photobiology B: Biology*, 209(1), pp.111922-111928.

Voss, A., Loeffen, F., Bakker, J., Klaassen, C. and Wulf, M. (2005) 'Methicillin-resistant Staphylococcus aureus in pig farming.' *Emerging infectious diseases*, 11(12), pp.1965-1966.

Walker, T.S., Tomlin, K.L., Worthen, G.S., Poch, K.R., Lieber, J.G., Saavedra, M.T., Fessler, M.B., Malcolm, K.C., Vasil, M.L. and Nick, J.A. (2005) 'Enhanced Pseudomonas aeruginosa biofilm development mediated by human neutrophils.' *Infection and immunity*, 73(6), pp.3693-3701.

Walter, M.N., Wright, K.T., Fuller, H.R., MacNeil, S. and Johnson, W.E.B. (2010) 'Mesenchymal stem cell-conditioned medium accelerates skin wound healing: an in vitro study of fibroblast and keratinocyte scratch assays.' *Experimental cell research*, 316(7), pp.1271-1281.

Wan, W., Cai, F., Huang, J., Chen, S. and Liao, Q. (2019) 'A skin-inspired 3D bilayer scaffold enhances granulation tissue formation and anti-infection for diabetic wound healing.' *Journal of Materials Chemistry B*, 7(18), pp.2954-2961.

Wang, K., Dang, W., Yan, J., Chen, R., Liu, X., Yan, W., Zhang, B., Xie, J., Zhang, J. and Wang, R. (2013) 'Membrane perturbation action mode and structure-activity relationships of Protonectin, a novel antimicrobial peptide from the venom of the neotropical social wasp Agelaia pallipes pallipes.' *Antimicrobial agents and chemotherapy*, 57(10), pp.4632-4639.

Wang, L., Huang, B., Duan, X., Jiang, G., Xiong, Y., Zhong, S., Wang, J. and Liao, X. (2021) 'The development of three ruthenium-based antimicrobial metallodrugs: Design, synthesis, and activity evaluation against Staphylococcus aureus.' *Journal of Chemical Research*, 45(11-12), pp.1059-1067.

Wang, P., Henning, S.M. and Heber, D. (2010) 'Limitations of MTT and MTS-based assays for measurement of antiproliferative activity of green tea polyphenols.' *PloS one*, 5(4), p.e10202-10212.

Wang, R., Wei, M., Wang, X., Chen, Y., Xiong, Y., Cheng, J., Tan, Y., Liao, X. and Wang, J. (2022) 'Synthesis of ruthenium polypyridine complexes with benzyloxyl groups and their antibacterial activities against Staphylococcus aureus.' *Journal of Inorganic Biochemistry*, 236(1), pp.111954-111966.

Wang, S., Yan, F., Ren, P., Li, Y., Wu, Q., Fang, X., Chen, F. and Wang, C. (2020).' Incorporation of metal-organic frameworks into electrospun chitosan/poly (vinyl alcohol) nanofibrous membrane with enhanced antibacterial activity for wound dressing application.' *International journal of biological macromolecules*, 158(1), pp.9-17.

Wang, W.J., Li, J.J., Rui, K., Gai, P.P., Zhang, J.R. and Zhu, J.J. (2015) 'Sensitive electrochemical detection of telomerase activity using spherical nucleic acids gold nanoparticles triggered mimic-hybridization chain reaction enzyme-free dual signal amplification.' Analytical chemistry, 87(5), pp.3019-3026.

Wang, W.J., Mu, X., Tan, C.P., Wang, Y.J., Zhang, Y., Li, G. and Mao, Z.W. (2021) 'Induction and monitoring of DNA phase separation in living cells by a light-switching ruthenium complex.' *Journal of the American Chemical Society*, 143(30), pp.11370-11381.

Wang, Y., Limon-Petersen, J.G. and Compton, R.G. (2011) 'Measurement of the diffusion coefficients of [Ru (NH3) 6] 3+ and [Ru (NH3) 6] 2+ in aqueous solution using microelectrode double potential step chronoamperometry.' Journal of Electroanalytical Chemistry, 652(1-2), pp.13-17.

Wang, Y., Wang, Z. and Wang, J. (2018) 'Lab-scale and pilot-scale fabrication of amine-functional reverse osmosis membrane with improved chlorine resistance and antimicrobial property.' *Journal of Membrane Science*, 554(1), pp.221-231.

Wankhade, A.B., Panda, S., Hathiwala, R. and Keche, Y. (2017) 'Study of antibiotic resistance profiling of Staphylococcus aureus isolated from clinical specimens of the patients attending a tertiary teaching hospital from Chhattisgarh.' *International Journal of Research in Medical Sciences*, 5(11), pp.4808-4812.

Webb, M.I. and Walsby, C.J. (2013) 'EPR as a probe of the intracellular speciation of ruthenium (III) anticancer compounds.' *Metallomics*, 5(12), pp.1624-1633.

Weber, B.S., Carfrae, L.A., Woods, J.J., Klobucar, K., Bigham, N.P., MacNair, C.R., Raivio, T.L., Wilson, J.J. and Brown, E.D. (2022) 'Polynuclear ruthenium complexes are effective antibiotics against Pseudomonas aeruginosa.' *bioRxiv*, pp.2022-08.

Weber, D.K., Sani, M.A., Downton, M.T., Separovic, F., Keene, F.R. and Collins, J.G. (2016) 'Membrane insertion of a dinuclear polypyridylruthenium (II) complex revealed by solid-

state NMR and molecular dynamics simulation: Implications for selective antibacterial activity.' *Journal of the American Chemical Society*, 138(46), pp.15267-15277.

Weinstein, Z.B., Bender, A. and Cokol, M. (2017) 'Prediction of synergistic drug combinations.' *Current Opinion in Systems Biology*, 4(1), pp.24-28.

Weiser, R., Green, A.E., Bull, M.J., Cunningham-Oakes, E., Jolley, K.A., Maiden, M.C., Hall, A.J., Winstanley, C., Weightman, A.J., Donoghue, D. and Amezquita, A. (2019). 'Not all Pseudomonas aeruginosa are equal: strains from industrial sources possess uniquely large multireplicon genomes.' *Microbial genomics*, *5*(7), pp.1-15.

Weiss, A., Berndsen, R.H., Dubois, M., Müller, C., Schibli, R., Griffioen, A.W., Dyson, P.J. and Nowak-Sliwinska, P. (2014) 'In vivo anti-tumor activity of the organometallic ruthenium (II)-arene complex [Ru (η 6-p-cymene) Cl 2 (pta)](RAPTA-C) in human ovarian and colorectal carcinomas.' *Chemical Science*, 5(12), pp.4742-4748.

Wheeler, K.M., Cárcamo-Oyarce, G., Turner, B.S., Dellos-Nolan, S., Co, J.Y., Lehoux, S., Cummings, R.D., Wozniak, D.J. and Ribbeck, K. (2019) 'Mucin glycans attenuate the virulence of Pseudomonas aeruginosa in infection.' *Nature microbiology*, 4(12), pp.2146-2154.

Wilkinson, H.N., Iveson, S., Catherall, P. and Hardman, M.J. (2018) 'A novel silver bioactive glass elicits antimicrobial efficacy against Pseudomonas aeruginosa and Staphylococcus aureus in an ex vivo skin wound biofilm model.' Frontiers in microbiology, 9(1), pp.1450-1466.

Wilson, J.L., Wareham, L.K., McLean, S., Begg, R., Greaves, S., Mann, B.E., Sanguinetti, G. and Poole, R.K. (2015) 'CO-releasing molecules have nonheme targets in bacteria: transcriptomic, mathematical modeling and biochemical analyses of CORM-3 [Ru (CO) 3Cl

(glycinate)] actions on a heme-deficient mutant of Escherichia coli.' *Antioxidants & redox signaling*, 23(2), pp.148-162.

Wolcott, R.D., Hanson, J.D., Rees, E.J., Koenig, L.D., Phillips, C.D., Wolcott, R.A., Cox, S.B. and White, J.S. (2016) 'Analysis of the chronic wound microbiota of 2,963 patients by 16S rDNA pyrosequencing.' Wound repair and regeneration, 24(1), pp.163-174.

Wong, E.L.M., Sun, R.W.Y., Chung, N.P.Y., Lin, C.L.S., Zhu, N. and Che, C.M. (2006) 'A mixed-valent ruthenium− oxo oxalato cluster Na7 [Ru4 (μ 3-O) 4 (C2O4) 6] with potent anti-HIV activities.' *Journal of the American Chemical Society*, 128(15), pp.4938-4939.

Wong, S.Y., Manikam, R. and Muniandy, S. (2015) 'Prevalence and antibiotic susceptibility of bacteria from acute and chronic wounds in Malaysian subjects.' The Journal of Infection in Developing Countries, 9(09), pp.936-944.

Wright, G.D. (2011) 'Molecular mechanisms of antibiotic resistance.' *Chemical Communications*, 47(14), pp.4055-4061.

Wright, G.D. (2016) 'Antibiotic adjuvants: rescuing antibiotics from resistance.' *Trends in microbiology*, 24(11), pp.862-871.

Wu, G. and Yi, Y. (2015) 'Effects of dietary heavy metals on the immune and antioxidant systems of Galleria mellonella larvae.' *Comparative Biochemistry and Physiology Part C: Toxicology & Pharmacology*, 167(1), pp.131-139.

Wu, L., Estrada, O., Zaborina, O., Bains, M., Shen, L., Kohler, J.E., Patel, N., Musch, M.W., Chang, E.B., Fu, Y.X. and Jacobs, M.A. (2005) 'Recognition of host immune activation by Pseudomonas aeruginosa.' *Science*, 309(5735), pp.774-777.

Wu, Y.K., Cheng, N.C. and Cheng, C.M. (2019) 'Biofilms in chronic wounds: pathogenesis and diagnosis.' *Trends in biotechnology*, *37*(5), pp.505-517.

Wypij, M., Czarnecka, J., Świecimska, M., Dahm, H., Rai, M. and Golinska, P. (2018) 'Synthesis, characterization and evaluation of antimicrobial and cytotoxic activities of biogenic silver nanoparticles synthesized from Streptomyces xinghaiensis OF1 strain.' *World Journal of Microbiology and Biotechnology*, 34(2), pp.1-13.

Xia, Q., Yang, L., Hu, K., Li, K., Xiang, J., Liu, G. and Wang, Y. (2018) 'Chromium Cross-Linking Based Immobilization of Silver Nanoparticle Coating on Leather Surface with Broad-Spectrum Antimicrobial Activity and Durability.' *ACS Applied Materials & Interfaces*, 11(2), pp.2352-2363.

Xiang, Q., Liu, X., Li, J., Liu, S., Zhang, H. and Bai, Y. (2018) 'Effects of dielectric barrier discharge plasma on the inactivation of Zygosaccharomyces rouxii and quality of apple juice.' *Food chemistry*, 254(1), pp.201-207.

Xiao, J., Chen, S., Yi, J., Zhang, H.F. and Ameer, G.A. (2017) 'A cooperative copper metal–organic framework-hydrogel system improves wound healing in diabetes.' *Advanced functional materials*, 27(1), pp.1604872-93.

Xu, F., Kang, Y., Zhang, H., Piao, Z., Yin, H., Diao, R., Xia, J. and Shi, L. (2013) 'Akt1-mediated regulation of macrophage polarization in a murine model of Staphylococcus aureus pulmonary infection.' *The Journal of infectious diseases*, 208(3), pp.528-538.

Xu, N., Cheng, H., Xu, J., Li, F., Gao, B., Li, Z., Gao, C., Huo, K., Fu, J. and Xiong, W. (2017) 'Silver-loaded nanotubular structures enhanced bactericidal efficiency of antibiotics with synergistic effect in vitro and in vivo.' *International journal of nanomedicine*, 12(1), pp.731-743.

Yahav, D., Duskin-Bitan, H., Eliakim-Raz, N., Ben-Zvi, H., Shaked, H., Goldberg, E. and Bishara, J. (2014) 'Monomicrobial necrotizing fasciitis in a single center: the emergence of Gram-negative bacteria as a common pathogen.' *International Journal of Infectious Diseases*, 28(1), pp.13-16.

Yan, X., He, B., Liu, L., Qu, G., Shi, J., Hu, L. and Jiang, G. (2018) 'Antibacterial mechanism of silver nanoparticles in Pseudomonas aeruginosa: proteomics approach.' *Metallomics*, 10(4), pp.557-564.

Yang, Q., Wang, L., Zhou, Q. and Huang, X. (2015) 'Toxic effects of heavy metal terbium ion on the composition and functions of cell membrane in horseradish roots.' *Ecotoxicology and Environmental Safety*, 111(1), pp.48-58.

Yang, Y., Wang, J., Xiu, Z. and Alvarez, P.J. (2013) 'Impacts of silver nanoparticles on cellular and transcriptional activity of nitrogen-cycling bacteria.' *Environmental toxicology and chemistry*, 32(7), pp.1488-1494.

Yasir, M., Dutta, D. and Willcox, M.D. (2019) 'Comparative mode of action of the antimicrobial peptide melimine and its derivative Mel4 against Pseudomonas aeruginosa.' *Scientific reports*, 9(1), pp.1-12.

Yasuyuki, M., Kunihiro, K., Kurissery, S., Kanavillil, N., Sato, Y. and Kikuchi, Y. (2010). 'Antibacterial properties of nine pure metals: a laboratory study using Staphylococcus aureus and Escherichia coli.' *Biofouling*, 26(7), pp.851-858.

Yin, C., Wang, Z., Ding, X., Chen, X., Wang, J., Yang, E., Wang, W., Martin, L.L. and Sun, D. (2021) 'Crystalline ruthenium polypyridine nanoparticles: a targeted treatment of bacterial infection with multifunctional antibacterial, adhesion and surface-anchoring photosensitizer properties.' *Journal of Materials Chemistry B*, 9(18), pp.3808-3825.

Yin, J., Zheng, W., Gao, Y., Jiang, C., Shi, H., Diao, X., Li, S., Chen, H., Wang, H., Li, R. and Li, A. (2019) 'Single-stranded DNA-binding protein and exogenous RecBCD inhibitors enhance phage-derived homologous recombination in Pseudomonas.' *Iscience*, 14(1), pp.1-14.

Yip DW, Gerriets V. Penicillin. 2022 Apr 30. In: StatPearls [Internet]. Treasure Island (FL): StatPearls Publishing; 2022 Jan–. PMID: 32119447.

You, C., Li, Q., Wang, X., Wu, P., Ho, J.K., Jin, R., Zhang, L., Shao, H. and Han, C. (2017) 'Silver nanoparticle loaded collagen/chitosan scaffolds promote wound healing via regulating fibroblast migration and macrophage activation.' *Scientific reports*, 7(1), pp.1-11.

Yu, G., Vicini, A.C. and Pieters, R.J. (2019) 'Assembly of divalent ligands and their effect on divalent binding to Pseudomonas aeruginosa lectin LecA.' *The Journal of organic chemistry*, 84(5), pp.2470-2488.

Yuan, M., Chua, S.L., Liu, Y., Drautz-Moses, D.I., Yam, J.K.H., Aung, T.T., Beuerman, R.W., Salido, M.M.S., Schuster, S.C., Tan, C.H. and Givskov, M. (2018) 'Repurposing the anticancer drug cisplatin with the aim of developing novel Pseudomonas aeruginosa infection control agents.' *Beilstein journal of organic chemistry*, 14(1), pp.3059-3069.

Yuan, Y., Wu, H., Lu, H., Zheng, Y., Ying, J.Y. and Zhang, Y. (2019) 'ZIF nano-dagger coated gauze for antibiotic-free wound dressing.' *Chemical communications*, 55(5), pp.699-702.

Yusoh, N.A., Leong, S.W., Chia, S.L., Harun, S.N., Rahman, M.B.A., Vallis, K.A., Gill, M.R. and Ahmad, H. (2020) 'Metallointercalator [Ru (dppz) 2 (PIP)] 2+ renders BRCA wild-type triple-negative breast cancer cells hypersensitive to PARP inhibition.' *ACS chemical biology*, *15*(2), pp.378-387.

Zeng, L., Gupta, P., Chen, Y., Wang, E., Ji, L., Chao, H. and Chen, Z.S. (2017) 'The development of anticancer ruthenium (II) complexes: from single molecule compounds to nanomaterials.' *Chemical Society Reviews*, 46(19), pp.5771-5804.

Zhang, C., Han, B.J., Zeng, C.C., Lai, S.H., Li, W., Tang, B., Wan, D., Jiang, G.B. and Liu, Y.J. (2016) 'Synthesis, characterization, in vitro cytotoxicity and anticancer effects of ruthenium (II) complexes on BEL-7402 cells.' *Journal of Inorganic Biochemistry*, 157(1), pp.62-72.

Zhang, C., Zhu, X., Li, F., Gao, F., Tu, J. and Zhang, D. (2019) 'Enhanced eradication of Pseudomonas aeruginosa bio-films by using ultrasound combined with neutrophil and antibiotics.' *Applied Acoustics*, 152(1), pp.101-109.

Zhang, L., Zhao, S.Q., Zhang, J., Sun, Y., Xie, Y.L., Liu, Y.B., Ma, C.C., Jiang, B.G., Liao, X.Y., Li, W.F. and Cheng, X.J. (2020) 'Proteomic Analysis of Vesicle-Producing Pseudomonas aeruginosa PAO1 Exposed to X-Ray Irradiation.' *Frontiers in microbiology*, 11(1), pp. 558233-558247.

Zhang, Y., Chen, X., Gueydan, C. and Han, J. (2018) 'Plasma membrane changes during proGrammed cell deaths.' *Cell research*, 28(1), pp.9-21.

Zhao, R., Liang, H., Clarke, E., Jackson, C. and Xue, M. (2016) 'Inflammation in chronic wounds.' *International journal of molecular sciences*, 17(12), pp.2085-2099.

Zhao, X., Chen, M., Wang, H., Xia, L., Guo, M., Jiang, S., Wang, Q., Li, X. and Yang, X., 2020. Synergistic antibacterial activity of streptomycin sulfate loaded PEG-MoS2/rGO nanoflakes assisted with near-infrared. *Materials Science and Engineering: C*, *116*, p.111221.

Zhao, X., Jia, Y., Dong, R., Deng, J., Tang, H., Hu, F., Liu, S. and Jiang, X. (2020) 'Bimetallic nanoparticles against multi-drug resistant bacteria.' *Chemical Communications*, 56(74), pp.10918-10921.

Zhao, Z., Li, H., Tao, X., Xie, Y., Yang, L., Mao, Z.W. and Xia, W. (2021) 'Light-Triggered Nitric Oxide Release by a Photosensitizer to Combat Bacterial Biofilm Infections.' *Chemistry–A European Journal*, *27*(17), pp.5453-5460.

Zheng, K., Setyawati, M.I., Leong, D.T. and Xie, J. (2017). 'Antimicrobial gold nanoclusters.' *ACS Nano*, 11(7), pp.6904-6910.

Zheng, W., Sun, W. and Simeonov, A. (2018) 'Drug repurposing screens and synergistic drug-combinations for infectious diseases.' *British journal of pharmacology*, 175(2), pp.181-191.

Zhou, Y., Gao, B., Zimmerman, A.R. and Cao, X. (2014) 'Biochar-supported zerovalent iron reclaims silver from aqueous solution to form antimicrobial nanocomposite.' *Chemosphere*, 117(1), pp.801-805.

Zhu, J. and Thompson, C. B. (2019) 'Metabolic regulation of cell growth and proliferation.' *Nature Reviews. Molecular Cell Biology*, 20(7) pp. 436–450.

Zhu, J.M., Hosseini, M., Fakhri, A., Rad, S.S., Hadadi, T. and Nobakht, N. (2019) 'Highly efficient of molybdenum trioxide-cadmium titanate nanocomposites for ultraviolet light photocatalytic and antimicrobial application: Influence of reactive oxygen species.' *Journal of Photochemistry and Photobiology B: Biology*, 191(1), pp.75-82.

Zhu, X., Chen, X., Jia, Z., Huo, D., Liu, Y. and Liu, J. (2021) 'Cationic chitosan@ Ruthenium dioxide hybrid nanozymes for photothermal therapy enhancing ROS-mediated eradicating multidrug resistant bacterial infection.' *Journal of Colloid and Interface Science*, 603(1), pp.615-632.

Zhuang, W., Yuan, D., Li, J.R., Luo, Z., Zhou, H.C., Bashir, S. and Liu, J. (2012) 'Highly potent bactericidal activity of porous metal-organic frameworks.' *Advanced healthcare materials*, 1(2), pp.225-238.

Zou, L., Wang, J., Gao, Y., Ren, X., Rottenberg, M.E., Lu, J. and Holmgren, A. (2018) 'Synergistic antibacterial activity of silver with antibiotics correlating with the upregulation of the ROS production.' *Scientific reports*, 8(1), pp.1-11.

8.0 Appendix

Table 8. 1: Luminescence of ATP in *P. aeruginosa* PAO1 in RLU over a 2 hour time period following incubation with **1** at varying concentrations and colistin and triton controls.

	0		30		60		90		120	
0 μg mL^{-1}	190.67	19.40	222	25.23	434.67	48.90	546.67	32.78	698.67	66.87
8 μg mL^{-1}	223.11	23.91	205	45.52	137.56	22.38	153.22	26.08	123.56	23.05
16 μg mL^{-1}	128.22	26.42	160.89	33.92	172.89	27.15	177.89	23.59	146.33	26.98
32 μg mL^{-1}	170.22	18.55	148.22	30.66	160.22	21.22	109.56	15.08	77.78	13.59
Colistin	477	40.84	103.56	26.16	90.44	14.58	71.89	15.91	79.33	15.82

Table 8. 2**:** Average absorbance values for *P. aeruginosa* PAO1 biofilms following treatment with varying concentrations and time incubations with **1**.

Time (H)	Concentration (µg/mL)	0	4	8	16	32	64	128
1	Average OD	0.460	0.361	0.349	0.337	0.329	0.287	0.248
	SD	0.049	0.076	0.026	0.028	0.055	0.057	0.042
	% Reduction	0	21.5	24.1	26.7	28.5	39.6	46.1
2	Average OD	0.418	0.283	0.283	0.375	0.323	0.320	0.238
	SD	0.097	0.064	0.098	0.060	0.077	0.049	0.021
	% Reduction	0	32.3	32.3	10.3	22.7	23.4	43.1
3	Average OD	0.409	0.263	0.258	0.262	0.258	0.246	0.246
	SD	0.048	0.007	0.008	0.016	0.016	0.012	0.012
	% Reduction	0	35.7	36.9	35.9	36.9	39.9	39.9
4	Average OD	0.333	0.282	0.273	0.261	0.240	0.237	0.229
	SD	0.023	0.012	0.045	0.033	0.014	0.023	0.014
	% Reduction	0	15.3	18.0	21.6	27.9	28.8	31.2
6	Average OD	0.485	0.362	0.353	0.300	0.297	0.269	0.260
	SD	0.047	0.038	0.062	0.039	0.062	0.037	0.060
	% Reduction	0	25.4	27.2	38.1	38.8	44.5	46.4
24	Average OD	0.425	0.420	0.255	0.255	0.225	0.223	0.222
	SD	0.126	0.035	0.010	0.023	0.014	0.015	0.017
	% Reduction	0	1.2	40.0	40.0	47.1	47.5	47.8

Table 8. 3: Absorbance readings of non-clinical strains of *P. aeruginosa* biomass stained with crystal violet with varying concentrations of **1** over a 24h period.

	0		64		128		256	
P. aeruginosa ATCC 9027								
0	0.503	0.085	0.524	0.027	0.574	0.041	0.560	0.109
2	0.548	0.292	0.442	0.096	0.433	0.060	0.422	0.195
4	0.565	0.123	0.302	0.089	0.268	0.013	0.397	0.130
6	0.573	0.213	0.299	0.007	0.267	0.041	0.303	0.085
24	0.798	0.285	0.282	0.046	0.258	0.022	0.277	0.064

P. aeruginosa NCTC 12903								
0	0.711	0.052	0.793	0.388	0.737	0.026	0.671	0.312
2	0.698	0.118	0.771	0.041	0.675	0.139	0.645	0.122
4	0.957	0.158	0.572	0.509	0.432	0.246	0.509	0.108
6	1.158	0.320	0.423	0.086	0.385	0.079	0.444	0.152
24	2.780	0.217	0.354	0.049	0.286	0.098	0.295	0.148

Table 8. 4: Percentage closure of EA.hy926 cells following treatment with 8 μg mL^{-1}, 16 μg mL^{-1} and 32 μg mL^{-1} **1** over a period of an hour.

Time (min)	0			10			20			30			40			50			60		
	Width (μm)	SD	%	Width (μm)	SD	%	Width (μm)	SD	%	Width (μm)	SD	%	Width (μm)	SD	%	Width (μm)	SD	%	Width (μm)	SD	%
0 μg mL^{-1}	1.668	0.037	0	1.218	0.235	26.98	0.893	0.124	46.46	0.513	0.120	59.24	0	0	100	0	0	100	0	0	100
8 μg mL^{-1}	1.635	0.128	0	1.056	0.193	35.41	0.926	0.114	43.36	0.728	0.125	55.47	0	0	100	0	0	100	0	0	100
16 μg mL^{-1}	1.747	0.279	0	0.987	0.211	43.50	0.692	0.156	60.39	0.529	0.126	69.72	0	0	100	0	0	100	0	0	100
32 μg mL^{-1}	1.551	0.071	0	1.399	0.078	9.80	0.776	0.030	49.97	0.538	0.046	65.31	0	0	100	0	0	100	0	0	100

Table 8. 5**:** Percentage closure of WS1 cells following treatment with 8 μg mL^{-1} **1** over 6 h.

Time (h)	T = 0			T = 1			T = 2			T = 3			T = 4			T = 5			T = 6		
	Width (μm)	SD	%	Width (μm)	SD	%	Width (μm)	SD	%	Width (μm)	SD	%	Width (μm)	SD	%	Width (μm)	SD	%	Width (μm)	SD	%
WS1	1.373	0.384	0	1.121	0.207	18.35	1.064	0.214	22.50	0.992	0.358	27.75	0.745	0.192	45.74	0.537	0.270	60.90	0.427	0.134	68.90
WS1 + **1**	1.374	0.324	0	1.309	0.203	4.73	1.104	0.225	19.65	0.997	0.258	27.44	0.806	0.242	41.34	0.658	0.175	52.11	0.494	0.250	64.05

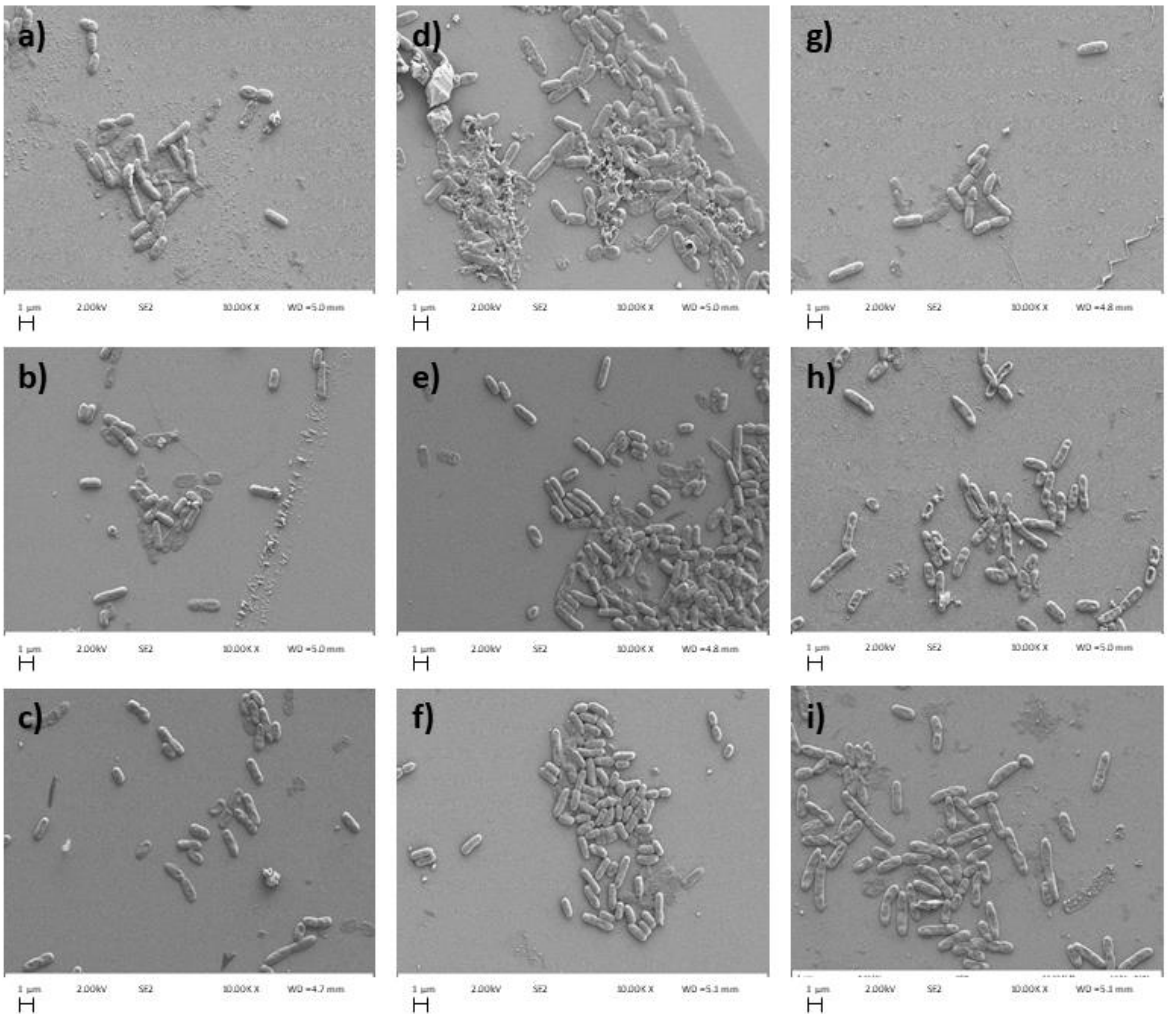

Figure 8. 1: SEM micrographs of *P. aeruginosa* PAO1 with **1** at 8 µg mL^{-1} (a-c), 16 µg mL^{-1} (d-f) and 32 µg mL^{-1} (g-i) exposed for 1 h (a, d, g), 3 h (b, e, h) and 5 h (c, f, i). Images are representative examples of the field of view for 3 biological replicates. Images were captured at the Manchester Metropolitan University SEM central facility at 10,000 times magnification.

Table 8. 6: Average quantity of RNA being released from *P. aeruginosa* PAO1 following incubation with **1** at varying concentrations, Triton X-100 (1%) and Colistin at 1 mg ,mL^{-1}.

	0		2		4		6		24	
	Average	SD	Average	SD	Average	SD	Average	SD	Average	SD
0 μgmL^{-1}	49.43	1.55	48.97	1.34	45.39	1.79	47.09	2.85	44.48	7.20
4 μgmL^{-1}	94.17	0.55	94.10	0.44	89.70	0.36	92.97	0.55	93.83	1.42
8 μgmL^{-1}	93.37	0.93	94.43	1.07	93.30	0.17	95.53	0.71	93.17	2.05
16 μgmL^{-1}	165.40	0.87	166.80	0.66	165.53	0.21	167.07	0.38	160.13	1.02
Colistin	51.67	0.99	50.30	0.35	50.17	1.85	50.40	0.95	50.93	2.66
Triton 1%	213.53	0.38	232.73	2.26	230.70	5.20	235.73	9.25	236.63	2.50

Table 8. 7: Average quantity of protein being released from *P. aeruginosa* PAO1 following incubation with **1** at varying concentrations, Triton X-100 (1%) and Colistin at 1 mg ,mL^{-1}.

	0		2		4		6		24	
	Average	SD	Average	SD	Average	SD	Average	SD	Average	SD
0 μgmL^{-1}	0.97	0.016	0.97	0.012	0.88	0.0025	0.86	0.013	0.75	0.021
4 μgmL^{-1}	1.05	0.0091	1.05	0.0072	1.02	0.0021	1.02	0.0017	1.05	0.0097
8 μgmL^{-1}	1.87	0.0032	1.90	0.011	1.93	0.0047	1.92	0.0042	1.83	0.0095
16 μgmL^{-1}	1.90	0.015	1.92	0.0093	1.91	0.0065	1.83	0.11	1.82	0.0036
Colistin	0.42	0.0036	0.46	0.019	0.46	0.010	0.40	0.015	0.40	0.016
Triton 1%	10.10	0.46	11.22	0.81	10.95	0.31	10.86	0.13	10.93	0.21

Table 8. 8**:** OD at 0 and 24 h following the degradation of nitrocefin by β-lactamase of *S. aureus* USA 300 and *S. epidermidis* NCTC 11047 upon incubation with **4**.

Condition	**0h**		**24h**	
	Average OD	**SD**	**Average OD**	**SD**
USA300	0.185	0.013	1.269	0.089
USA300 + **4**	0.199	0.005	0.422	0.027
USA300 + Pen	0.200	0.013	1.324	0.026
USA300 + **4** + Pen	0.185	0.012	0.449	0.054
USA300 + Taz	0.129	0.007	0.296	0.043
USA300 + DMSO	0.121	0.006	0.997	0.025
USA300 + Pen + DMSO	0.139	0.017	0.956	0.038
USA300 + **1**	0.154	0.023	0.421	0.063
S. epidermidis	0.115	0.010	0.346	0.036
S. epidermidis + **4**	0.136	0.008	0.180	0.007
S. epidermidis + Pen	0.112	0.016	0.230	0.037
S. epidermidis + **4** + Pen	0.119	0.011	0.204	0.043
S. epidermidis + Taz	0.108	0.020	0.222	0.023
S. epidermidis + DMSO	0.090	0.007	0.263	0.027
S. epidermidis + Pen + DMSO	0.085	0.006	0.152	0.006
S. epidermidis + **1**	0.094	0.018	0.146	0.025
Media Only	0.047	0.003	0.062	0.009
4 Only	0.232	0.037	0.213	0.013
Pen Only	0.016	0.003	0.006	0.003
1 Only	0.009	0.002	-0.007	0.002
DMSO Only	0.020	0.004	0.012	0.006
Water Only	0.012	0.002	0.004	0.001
PBS Only	0.017	0.004	0.008	0.005

Table 8. 9**:** Percentage survival of *G. mellonella* in response to different conditions over a 72 h period.

Condition	24 h			48 h			72 h		
	Mean	SD	SE	Mean	SD	SE	Mean	SD	SE
No Injection	96.6	5.77	3.33	96.6	5.77	3.33	96.6	5.77	3.33
PBS	96.6	5.77	3.33	96.6	5.77	3.33	96.6	5.77	3.33
S. aureus	73.3	11.5	6.67	40	26.5	15.3	33.3	23.1	13.3
4	93.3	5.77	3.33	80	10	5.77	76.6	11.5	6.66
DMSO	96.6	5.77	3.33	90	17.3	10	86.6	15.3	8.82
***S. aureus* + Vancomycin**	100	0	0	96.6	5.77	3.33	83.3	11.5	6.66
Vancomycin	100	0	0	100	0	0	100	0	0
***S. aureus* + 4**	80	10	5.77	26.6	5.77	3.33	13.3	5.77	3.33

Table 8. 10**:** Initial testing of percentage survival of *G. mellonella* subject to synergistic combinations of **4** and Penicillin.

Condition	*24 h*	*48 h*	*72 h*
No Injection	90	70	70
PBS	20	20	10
DMSO	30	30	30
Bacteria only	60	30	20
4 4 µg mL^{-1}	60	50	50
4 8 µg mL^{-1}	50	30	30
4 16 µg mL^{-1}	50	50	20
Pen128	100	100	80
Pen256	100	100	90
Pen512	100	100	90
4 4 µg mL^{-1} Pen128	10	0	0
4 4 µg mL^{-1} Pen256	0	0	0
4 4 µg mL^{-1} Pen512	10	0	0
4 8 µg mL^{-1} Pen128	30	0	0
4 8 µg mL^{-1} Pen256	0	0	0
4 8 µg mL^{-1} Pen512	10	0	0
4 16 µg mL^{-1} Pen128	0	0	0
4 16 µg mL^{-1} Pen256	20	0	0
4 16 µg mL^{-1} Pen512	30	0	0